The circadian clock protein BMAL1 regulates IL-1β in macrophages via NRF2

Thesis submitted to the University of Dublin
for the
Degree of Doctor of Philosophy

by

James Early

School of Biochemistry and Immunology
Trinity Biomedical Sciences Institute
Trinity College Dublin
Ireland

March 2018

Declaration

I declare that this thesis has not been submitted as an exercise for a degree at this or any other university and is entirely my own work with the exception of the following figures:

Figure 3.5
This work was performed by Daniel O' Connell

Figure 3.14
This work was carried out in collaboration with Sarah Geiger and Karsten Hokamp

Figure 3.17
Figure 3.18
Figure 3.25
This work was carried out in collaboration with Cathy Wyse

Figure 3.22
Figure 3.23
This work was carried out in collaboration with Dylan Ryan

Figure 4.21
Figure 4.22
Figure 4.24
Figure 4.25
Figure 4.26
This work was carried out in collaboration with Deepthi Menon

Figure 4.32

Figure 4.33

This work was carried out in collaboration with James O' Siorain

I agree to deposit this thesis in the University's open access institutional repository, or allow the library to do so on my behalf, subject to Irish Copyright Legislation and Trinity College Library conditions of use and acknowledgement.

_____

James Early

Acknowledgements

First of all I would like to say a huge thank you to my two supervisors, Annie and Luke. Annie, I could not have made it this far without you, namely because I needed you to hire me. In all seriousness though, you have been a wonderful supervisor, understanding of personal constraints, supportive in allowing me to follow my own ideas, and last but not least, ever positive. Whenever a question needed answering or support was required you were never far away. I have no doubt the many future Ph.D. students you mentor will be lucky to have you. Luke, you have been a wonderful source of support and advice over the last number of years, not to mention a good source for electric picnic tickets. You have a great way of instilling positivity in people when they need it and in providing the key idea at the right moment. I thank both of you for the hard work and dedication in keeping me on the right path and for providing me with this opportunity.

From day one I felt welcome in this lab. It is a wonderful and fostering environment for someone to enter when starting the daunting prospect of being a poor student for another 4 years. This is 100 % down to the people who work here and I hope none of you ever change. If given the opportunity I could write a small thesis on each one of you, but a few words will have to do. First of all to Richie and Z, the two older brothers I already have. The many lunches, long coffee breaks, political debates and random facts made every day a lot more interesting. Kathy and Eva, proof that life doesn't slow down after kids, always up for a laugh and to provide a sympathetic ear when needed. Anne, I don't know a single other person as effective at providing the subtle support you do to those around you, thank you for bringing us home from Sitges in one piece! Corkie and tiny Niamh, thank you for keeping a roof over my head when I had a few too many. Corkie, you had a rough deal having me as your reading room buddy, but I appreciate all of the proof reading of emails and keeping my sense of humour in check. You can keep the hairbrush. Niamh, I've

never had a better gym buddy and probably never will again! Mossy, Danny and Jay, the lads, good pints with good pals, keep her lit. Mark, Marah and Ciana, A.K.A., the gossip girls, thanks for the laughs, and remember, it's how you use it that counts. Alex, Dylan and Stevie, great friends with great banter. Keep up the footie and you might get good at that too in a few years. The RCSI crew, Cathy, George and Mariana, it was a pleasure to work with each of you, and Mariana, I hope you picked up a cupla focail from me. To each and every one of you, I give a sincere thank you.

To my friends, be it from Kilkenny, Donegal, Dublin or further afield, thank you for the laughs. Special mention to my closest pals and roomies, JJ, Billy, Sean, and Jeff (yes boy), it was great living with you all.

To my parents Christy and Joanne. This is the one section in which I will make a conscious effort to avoid joking. The biggest thank you of all has to go to you both. Nothing I have ever achieved would have been possible without all you have done for me. I don't much believe in luck, but I recognize that I could not have gotten any luckier than having both of you as my parents. I believe it is the role of most parents to be the unsung hero of their children's lives, but I want you to both know that I recognise all you have done for me and appreciate every last bit of it. Thank you and I love you both.

My numerous siblings of ill repute. You are all wonderful. Bob, our family would have drifted apart if you'd stayed in Australia. Yourself and Pigsy made me realise how easy being in the lab could be when there was renovation work that needed doing at home. From the weekly lunches to the sporadic attempts to get me to do cardio, you have been my greatest confidant and of great help in getting me through the Ph.D. Peck and Tracey, you similarly sheltered me at various points, but I'm pretty sure that 50 euro sushi voucher I bought you 4 years ago more than covers it. Chris, you are a grumpy bugger, but you have a great ability to find the humour in

any situation, you can make anyone laugh, and I know there will always be life in our family as long as you are around. The boisterous whisky goblin Tom, you may have three young children with Sheila, but I guarantee you're younger than all of them. You are one of the most genuinely kind people I know, willing to lend a hand to anyone that asks, and I hope you never lose that spark. Last but not least, the oracle, Kate. While you may know everything about everyone, I don't believe I know a more natural born mother. Jack could not possibly have been given to a more giving or caring person. Thank you for making me that wonderful boys godfather.

While I am approaching the end of my final thesis procrastinations, there is one more person that must be mentioned. Erin. I have never met a more beautiful person inside and out. You have been one of the most positive influences on my life and never have a bad word to say about anyone. You have been with me from start to finish and I thank you for your unyielding support. I am proud of the person you have become and cannot wait to see what else you will achieve. It will of course be awkward if we ever break up as this message will be hardbound in leather, but my contingency is to simply find another girl called Erin (luckily in this country a rock thrown out my window will probably hit such a candidate). I am willing to take that risk, as in all seriousness, and to sum it all up, I love you.

I have learned a lot over the last 3 and a half years, but the most important thing I picked up was to slow down, relax, and appreciate everything as it comes. Nothing is ever as stressful as you perceive it to be.

Awards, presentations and publications related to thesis

Awards

- Irish Society for Immunology Conference Prize 2017, awarded for the best flash oral presentation
- Irish Immunology Forum Prize 2017, awarded for best oral presentation
- Irish Society for Immunology Conference Prize 2016, awarded for the best oral presentation

Presentations

- Irish Society for Immunology conference, flash 3 minute presentation, 2017
- Irish Immunology Forum, 40 minute presentation, 2017
- Keystone Immunometabolism Conference, Dublin, poster presentation, 2017
- British society for Immunology conference, Liverpool, poster presentation, 2016
- Irish Society for Immunology conference, 15 minute presentation, 2016
- Oxford Chronobiology and Sleep Medicine Meeting, poster and oral presentation, 2016
- Molecular and Cell Therapeutics research talk, RCSI, 30 minute presentation. 2017
- Immunology Research Forum, Trinity College Dublin, 20 minute presentation- 2016

Publications

- **Loss of the molecular clock in myeloid cells exacerbates T cell-mediated CNS autoimmune disease**
  Nature Communications 2017

Caroline E. Sutton, Conor M.Finlay, Mathilde Raverdeau, **James O. Early**, Joseph de Courcey Zbigniew Zaslona Luke A.J. O'Neill Kingston H. G. Mills and Annie M.Curtis
Significance: High impact study demonstrating the importance of the innate immune circadian clock in priming and dictating action of the adaptive immune response.

- **The circadian protein BMAL1 in myeloid cells is a negative regulator of allergic asthma**
  Am J Physiol Lung Cell Mol Physiol. 2017 Jun 1;312(6):L855-L860.
  Zbigniew Zaslona, Sarah Case, **James O. Early**, Stephen J. Lalor, Rachel M. McLoughlin, Anne M Curtis, Luke A. O'Neill

  Significance: Asthma has long been known to display circadian rhythmicity. This is one of the first publications to describe a molecular mechanism for circadian control of allergic asthma.

- **Immunometabolism: Is it under the eye of the clock?**
  Semin Immunol. 2016 Oct;28(5):478-490. **Review**
  James O. Early, Anne M. Curtis

  Significance: First review to explore the emerging field of circadian immunometabolism.

- **Circadian control of innate immunity in macrophages by miR-155 targeting Bmal1.**
  PNAS. 2015 Jun 9;112(23):7231-6
  Anne M. Curtis, Caio T. Fagundes, Guangrui Yang, Eva M. Palsson-McDermott, Paulina Wochal, Anne F. McGettrick, Niamh H. Foley, **James O. Early**, Lihong Chen, Hanrui Zhang , Chenyi Xue, Sarah S. Geiger, Karsten Hokamp, Muredach P. Reilly, Andrew N. Coogan, Elena Vigorito, Garret A. FitzGerald and Luke A. J. O'Neill

  Significance: This is the first study to provide a mechanism by which inflammation inhibits clock function by the miRNA MiR-155 targeting the core clock protein BMAL1.

Table of Contents

Declaration ii
Acknowledgements iv
Awards, Presentations and Publications related to thesis vii
Table of Contents ix
List of Figures xiii
List of tables xv
Abbreviations xvi
Abstract xx

Chapter 1: Introduction 1
1.1 The circadian cycle 2
1.1.1 Circadian rhythms 3
1.1.2 Regulation of circadian rhythms 5
1.1.3 The molecular clock 8
1.1.4 Models of clock study 11
1.1.5 Circadian disruption in health and disease 14
1.2 Innate immunity 16
1.2.1 Pattern recognition receptors and TLR signalling 19
1.2.2 Clock proteins in immunity 23
1.2.3 Inflammasomes 26
1.2.4 Macrophages 29
1.2.5 Metabolic alterations in macrophages 29
1.2.6 Circadian regulation of metabolism 33
1.3 Oxidative stress 36
1.3.1 ROS production 36
1.3.2 Mitochondrial ROS 37
1.3.3 Circadian regulation of ROS 40
1.4 Antioxidants 41
1.4.1 NRF2 antioxidant defence pathway 41
1.4.2 NRF2 in inflammation 44
1.5 Aims 46

Chapter 2: Materials and methods 47
2.1 Materials 47
2.1.1 Buffers 47
2.1.2 Reagents for cell culture 48
2.1.3 Animals 48
2.1.4 Primary cells and cell lines 49

2.1.5 Laboratory chemicals 49
2.1.6 Western blotting reagents 49
2.1.7 Antibodies 50
2.1.8 PCR 50
2.1.9 Enzyme-lined-immunoabsorbant assays (ELISA) 51
2.1.10 GSH kit 51
2.1.11 FACs and confocal reagents 51
2.1.12 Seahorse reagents 51
2.1.13 LDH assay kit 52
2.1.14 BCA assay 52
2.1.15 Subcellular frationation 52
2.2 Methods 53
2.2.1 Culture of L929 cells 53
2.2.2 BMDM isolation 53
2.2.3 Peritoneal cell isolation 54
2.2.4 siRNA transfection 54
2.2.5 Western blotting 55
2.2.6 RNA extraction and analysis 57
2.2.7 ELISA 60
2.2.8 FACs analysis of cellular reactive oxygen species 61
2.2.9 Confocal imaging 61
2.2.10 Seahorse analysis 62
2.2.11 Quantification of oxidative stress genes. 63
2.2.12 Transcription factor sequencing 64
2.2.13 Glutathione assay 65
2.2.14 LDH assay 65
2.2.15 Inflammasome assays 65
2.2.16 Subcellular fractionation 66
2.2.17 BCA assay 66
2.2.18 Graphing of rhythms in peritoneal cells and serum shock 66
2.2.19 Statistical analysis 67

Chapter 3: Results 68
3.1 Introduction 68
3.2 Examining circadian mediated regulation of NRF2 in myeloid cells 69
3.2.1 *Nrf2* displays diurnal rhythms in myeloid cells 69
3.2.2 Basal and induced levels of NRF2 are lower in *Bmal1 d*eficient macrophages . 71
3.3 Analysis of BMAL1 mediated regulation of NRF2 activity 76
3.3.1 Transcription factor sequencing uncovers decrease in NRF2 activity with deletion of *Bmal1* 76
3.3.2 Induction of NRF2 target antioxidant genes is decreased in *Bmal1* deficient macrophages 76
3.4 Examination of NRF2 mediated regulation of the circadian clock 85
3.5 Analysis of BMAL1 mediated regulation of oxidative stress 88
3.5.1 ROS regulation displays diurnal rhythms 88
3.5.2 ROS accumulation is increased in *Bmal1* deficient macrophages 89
3.5.3 HIF-1α protein and activity increased in *Bmal1*$^{-/-}$ macrophages 89

3.6 Investigation into the effect of the circadian cycle on metabolism in macrophages 98
3.6.1 Glycolytic genes increased in *Bmal1*$^{-/-}$ macrophages 98
3.6.2 Glycolysis and oxidative phosphorylation are increased in *Bmal1*$^{-/-}$ BMDMs 98
3.6.3 *Irg1* expression is decreased in *Bmal1*$^{-/-}$ macrophages 99
3.6.4 Investigation of circadian rhythms in mitochondrial regulation 100
3.7 Discussion 107
3.7.1 Regulation of NRF2 by BMAL1 107
3.7.2 Regulation of oxidative stress by BMAL1 via NRF2 109
3.7.3 Regulation of metabolism by BMAL1 111
3.7.4 Final conclusions 113

Chapter 4: Results 115
4.1 Introduction 115
4.2 BMAL1 localisation is dynamic following LPS stimulation 116
4.3 *Bmal1* and *Nrf2* deficiency enhances IL-1β production 118
4.4 BMAL1 mediated regulation of pro-inflammatory cytokines 124
4.5 Examination of molecular clock agonists and antagonist on inflammatory cytokine production 128
4.5.1 GSK4112 enhances production of pro-inflammatory cytokines 128
4.5.2 SR9009 decreases production of IL-10 128
4.5.3 SR8278 decreases production of pro-IL-1β 129
4.5.4 KL001 decreases production of pro-IL-1β 129
4.6 Investigation of BMAL1 mediated regulation of IL-1β processing 134
4.6.1 Increased IL-1β processing with deletion of *Bmal1* 134
4.6.2 Caspase 1, but not NLRP3 is increased in *Bmal1*$^{-/-}$ macrophages 134
4.6.3 Increased IL-1β processing in *Bmal1*$^{-/-}$ macrophages is not specific to NLRP3 inflammasome 135
4.7 Examination of *Keap1* knockdown in *Bmal1*$^{-/-}$ macrophages 141
4.7.1 *Keap1* knockdown decreases pro-inflammatory cytokine production in macrophages 141
4.7.2 *Keap1* knockdown rescues NRF2 levels and activity in *Bmal1*$^{-/-}$ macrophages 141
4.7.3 *Keap1* knockdown rescues IL-1β phenotype of *Bmal1*$^{-/-}$ macrophages 142
4.8 Investigation into the effects of pharamcological activation of NRF2 and ROS scavenging on *Bmal1*$^{-/-}$ macrophages 152
4.8.1 NAC and DEM treatment decreases pro-inflammatory cytokine production in macrophages 152
4.8.2 DEM but not NAC rescues NRF2 activity in *Bmal1*$^{-/-}$ macrophages 153
4.8.3 DEM and NAC rescue IL-1β activity in *Bmal1*$^{-/-}$ macrophages 153
4.8.4 OI decreases pro-IL-1β in *Bmal1*$^{-/-}$ macrophages 154
4.8.5 NAC and DEM partially rescue cleaved IL-1β phenotype in *Bmal1*$^{-/-}$ macrophages 154
4.9 Discussion 162
4.9.1 Regulation of BMAL1 during inflammation 162
4.9.2 BMAL1 mediated regulation of IL-1β 163
4.9.3 Pharmacological manipulation of the clock regulates IL-1β 165

4.9.4 Boosting NRF2 activity and limiting ROS confirms role of BMAL1 in IL-1β production 166
4.9.5 BMAL1 regulates inflammasome activation 168
4.9.6 Final conclusions 171

Chapter 5: General Discussion 173
5.1 Circadian rhythms: Linking metabolism and immunity 173
5.2 Circadian misalignment: A malady of modern society 174
5.3 IL-1β: The missing link 175
5.4 Clinical relevance 176
5.5 Thesis conclusions 179
5.6 Closing remarks 181

Chapter 6: References 182

Chapter 7: Appendix 197

List of figures

Figure 1.1 Properties of a circadian gene **4**
Figure 1.2 Regulation of mammalian circadian rhythms **7**
Figure 1.3 The oscillation of circadian clock proteins **10**
Figure 1.4 Light/Dark and activity **13**
Figure 1.5 Circadian regulation of immune function **18**
Figure 1.6 TLR4 signalling **22**
Figure 1.7 Activation of the NLRP3 and AIM2 inflammasomes **28**
Figure 1.8 Metabolic reprogramming of macrophages **32**
Figure 1.9 BMAL1 in cellular metabolism **35**
Figure 1.10 Mitochondrial ROS in immunity **39**
Figure 1.11 The NRF2 pathway **43**
Figure 3.1. Dirunal rhythms are present in clock genes and *Nrf2* expression **72**
Figure 3.2 Rhythms in Nrf2 transcription are ablated with *Bmal1* deletion **73**
Figure 3.3 NRF2 transcript and protein is decreased in *Bmal1*$^{-/-}$ BMDMs **74**
Figure 3.4 NRF2 transcript and protein is decreased in *Bmal*1 knockdown BMDMs **75**
Figure 3.5 NRF2 activity is decreased in *Bmal1*$^{-/-}$ BMDMs determined by TF-seq **78**
Figure 3.6 Antioxidant genes are decreased with LPS stimulation in *Nrf2* knockdown BMDMs **80**
Figure 3.7 Antioxidant genes are decreased in *Bmal1*$^{-/-}$ BMDMs with LPS stimulation **81**
Figure 3.8 Antioxidant genes are decreased in *Bmal1-/-* BMDMs with H_2O_2 stimulation **82**
Figure 3.9 Antioxidant genes are decreased with LPS stimulation in *Bmal1* knockdown BMDMs **83**
Figure 3.10 GSH is decreased in *Bmal1-/-* BMDMs **84**
Figure 3.11 NRF2 activation alters expression of circadian clock genes **86**
Figure 3.12 LPS stimulation alters expression of circadian clock genes **87**
Figure 3.13 ROS displays variation in peritoneal myeloid cells **90**
Figure 3.14 Diurnal regulation of oxidative stress genes is present in peritoneal cells **91**
Figure 3.15 ROS levels are increased in *Bmal1*$^{-/-}$ BMDMs **93**
Figure 3.16 ROS levels are increased in *Bmal1* silenced BMDMs **94**
Figure 3.17 ROS levels are increased in *Bmal1*$^{-/-}$ BMDMs view by confocal **95**
Figure 3.18 Quantification of ROS levels viewed by confocal **96**
Figure 3.19 HIF-1α levels and activity are increased in *Bmal1*$^{-/-}$ BMDMs **97**
Figure 3.20 Glycolytic gene expression is increased in *Bmal1*$^{-/-}$ BMDMs following LPS stimulation **101**

Figure 3.21 Initial glycolytic burst is increased in *Bmal1*$^{-/-}$ BMDMs following LPS stimulation 102
Figure 3.22 Glycolysis is increased in *Bmal1*$^{-/-}$ BMDMs..... 103
Figure 3.23 Oxidative phosphorylation is increased in *Bmal1*$^{-/-}$ BMDMs 104
Figure 3.24 LPS induced *Irg1* transcription is decreased in both *Bmal1*$^{-/-}$ and *Bmal1* knockdown BMDMs 105
Figure 3.25 Mitochondrial membrane potential displays circadian rhythmicity 106
Figure 3.26 Current hypothesis for the role of BMAL1 in oxidative stress regulation..... 114
Figure 4.1 Localisation of BMAL1 is dynamic following LPS treatment..... 117
Figure 4.2 IL-1β transcript and protein are increased with *Nrf2* knockdown 119
Figure 4.3 Increased *Il1b* transcription in *Bmal1*$^{-/-}$ BMDMs 120
Figure 4.4 Increased Pro-IL-1β protein in *Bmal1*$^{-/-}$ BMDMs 121
Figure 4.5 Increased IL-1β transcript and protein with *Bmal1* knockdown . 122
Figure 4.6 Increased Pro-IL-1β protein in *Bmal1*$^{-/-}$ PECs..... 123
Figure 4.7 IL-6 increased, IL-10 decreased and no change in TNFα in *Bmal1*$^{-/-}$ BMDMs 125
Figure 4.8 IL-6 increased, IL-10 decreased and no change in TNFα in *Bmal1* knockdown BMDMs 126
Figure 4.9 No change in IL-6, IL-10 decreased and TNFa increased in *Bmal1*$^{-/-}$ peritoneal cells..... 127
Figure 4.10 GSK4112 increases LPS induced Pro-IL-1B and IL-6, decreased IL-10 and has no effect on TNFα 130
Figure 4.11 SR9009 decreases LPS induced IL-10 but has no effect on Pro-IL-1β, IL-6 or TNFα 131
Figure 4.12 SR8278 decreases LPS induced Pro-IL-1β..... 132
Figure 4.13 KL001 decreases LPS induced Pro-IL-1β..... 133
Figure 4.14 Increased IL-1β processing in *Bmal1*$^{-/-}$ BMDMs..... 136
Figure 4.15 Increased cell death in *Bmal1*$^{-/-}$ BMDMs 137
Figure 4.16 NLRP3 transcript and protein not increased in *Bmal1*$^{-/-}$ BMDMs138
Figure 4.17 Caspase 1 levels increased in *Bmal1*$^{-/-}$ BMDMs 139
Figure 4.18 Increased IL-1β with AIM2 inflammasome activation in *Bmal1*$^{-/-}$ BMDMs 140
Figure 4.19 *Keap1* knockdown decreases Pro-IL-1β 144
Figure 4.20 *Keap1* knockdown decreases IL-6 but has no effect on IL-10 and TNFα..... 145
Figure 4.21 *Keap1* knockdown depletes KEAP1 protein in *Bmal1*$^{+/+}$ and *Bmal1*$^{-/-}$ BMDMs 146
Figure 4.22 *Keap1* knockdown has no effect on *Nrf2* transcription but increases NRF2 protein in *Bmal1*$^{-/-}$ BMDMs..... 147
Figure 4.23 *Nqo1* transcription is increased with *Keap1* knockdown in *Bmal1*$^{+/+}$ and *Bmal1*$^{-/-}$ BMDMs 148

Figure 4.24 Increased HIF-1α levels *in Bmal1*$^{-/-}$ BMDMs decreased with *Keap1* knockdown 149
Figure 4.25 Keap1 knockdown decreases IL-1B transcription and protein in *Bmal1*$^{-/-}$ BMDMs 150
Figure 4.26 *Keap1* knockdown decreases IL-1β activation in *Bmal1*$^{-/-}$ BMDMs 151
Figure 4.27 NAC and DEM decrease Pro-IL-1β levels 155
Figure 4.28 NAC and DEM affect inflammatory cytokine levels in *Bmal1*$^{+/+}$ and *Bmal1*$^{-/-}$ BMDMs 156
Figure 4.29 DEM but not NAC increases Nqo1 expression in *Bmal1*$^{+/+}$ and *Bmal1*$^{-/-}$ BMDMs 157
Figure 4.30 DEM and NAC decrease IL-1β transcript and protein in *Bmal1*$^{+/+}$ and *Bmal1*$^{-/-}$ BMDMs 158
Figure 4.31 OI decreases Pro-IL-1β protein in *Bmal1*$^{-/-}$ BMDMs 159
Figure 4.32 NAC and DEM decrease IL-1β activation in *Bmal1*$^{-/-}$ BMDMs 160
Figure 4.33 NAC but not DEM decreases NLRP3 induced cell death in *Bmal1*$^{-/-}$ BMDMs 161
Figure 4.34 Current hypothesis for BMAL1 mediated regulation of IL-1β 172

List of tables

Table 2.1 Buffer compositions 47
Table 2.2 Antibodies 50
Table 2.3 siRNA used 55
Table 2.4 Gel compositions 56
Table 2.5 RT-PCR Reaction mix 58
Table 2.6 SYBR primer sequences 59
Table 2.7 Taqman primer list 59
Table 2.8 SYBR PCR reaction mix 60
Table 2.9 Taqman PCR reaction mix 60
Table 3.1 Table of transcription factors and pathways analysed in TF-seq screen 79
Table 3.2 Oxidative stress genes analysed and their Log2 ratios (ZT12/ZT0) 92

Abbreviations

2DG	2-Deoxyglucose
ACTH	Adrenocorticotropic hormone
ADP	Adenosine diphosphate
AMP	Adenosine monophosphate
AMPK	AMP activated kinase
ANS	Autonomic nervous system
ARE	Antioxidant response element
ASC	Apoptosis-associated speck-like protein containing a CARD
ATP	Adenosine triphosphate
bHLH	Basic helix-loop-helix
BMAL1	Brain muscle Arnt-like protein 1
BMDM	Bone marrow derived macrophage
BSA	Bovine serum albumin
CARD	Caspase associated recruitment domain
CLOCK	Circadian Locomotor Output Cycles Kaput
COX	Cyclicoxygenase
CRY	Cryptochrome
CXCR4	C-X-C chemokine receptor type 4
DAMP	Danger associated molecular pattern
DEM	Diethyl Maleate
DMEM	Dulbecco's modified Eagle's medium
DMF	Dimethyl fumurate
DMSO	Dimethyl sulfoxide
DNA	Deoxyribonucleic acid
DS	Double stranded
EAE	Experimental autoimmune encephalomyelitis

EDTA	Ethylenediaminetetracetic acid
ELISA	Enzyme-linked immunosorbent assay
FCS	Fetal calf serum
GAPDH	Glyceraldehyde-3-phosphate dehydrogenase
GCLC	Glutamate-cysteine ligase catalytic
GCLM	Glutamate-cysteine ligase regulatory
GSH	Reduced glutathione
GSR	Glutathione reductase
GSSG	Glutathione disulphide
H_20_2	Hydrogen peroxide
HIF-1α	Hypoxia inducible factor-1α
Hk2	Hexokinase 2
HMOX1	Heme oxygenease-1
Hour	hr
HPA	Hypothalamic-pituitary-adrenal axis.
IL	Interleukin
iNOS	Inducible nitric oxide synthase
IRF	Interferon regulatory factor
Irg1	Immunoresponsive gene 1
JNK	c-JUN N-terminal kinase
kDa	KiloDalton
KEAP1	Kelch-like ECH-associated protein 1
KO	Knock out
LDHa	Lactate dehydrogenase A
LPS	Lipopolysaccharide
MAL	MyD88 adapter-like
MAPK	Mitogen-activated protein kinase
MCSF	Macrophage colony stimulating factor
MFI	Mean fluorescence intensity

mRNA	messenger ribonucleic acid
mTOR	Mammalian target of rapamycin
MyD88	Myeloid differentiation primary response protein 88
NAC	N-acetyl-L-cysteine
NAD	Nicotinamide adenide dinucleotide
NF-κB	Nuclear factor κB
NLR	Nod-like-receptor
NO	Nitric oxide
NPAS2	Neuronal pas domain protein 2
NRF2	Nuclear factor (erythroid-derived 2)-like 2
OI	Octyl itaconate
OXPHOS	Oxidative phosphorylation
PAMP	Pathogen associated molecular pattern
PBS	Phosphate buffered saline
PCR	Polymerase chain reaction
PECs	Peritoneal cells
PER	Period
PHD	Prolyl hydroxylase domain-containing protein
PRR	Pattern recognition receptor
P/S	Penicillin/Streptomycin
PVDF	Polyvinylidene difluoride
qPCR	Quantitative PCR
REDOX	Reduction-oxidation
RNA	Ribonucleic acid
RNAi	RNA interference
ROR	RAR-related orphan receptor
RORE	Receptor-related orphan receptor response element
ROS	Reactive oxygen species
RPMI	Roswell Park Memorial Institute medium 1640

RT-PCR	Real time-PCR
S6K1	S6 kinase beta-1
SCN	Suprachiasmatic nucleus
SDH	Succinate dehydrogenase
SDS	Sodium dodecyl sulphate
S.E.M.	Standard error of the mean
tBHQ	tert-Butylhydroquinone
TBS	Tris buffered saline
TEMED	Tetramethylethylenediamine
TF-seq	Transcription factor sequencing
TIR	Toll/Interleukin-1 receptor
TIRAP	TIR domain containing adaptor protein
TLR	Toll-like receptor
TNF	Tumour necrosis factor
TRAF	TNF receptor associated
TRAM	TRIF- related adaptor molecule
TRIF	TIR-domain-containing adaptor protein inducing IFN-β
WT	Wild type
ZT	Zeitgeber

Abstract

The response of the innate immune system to an inflammatory insult is largely dependent on time-of-day, and many inflammatory conditions are associated with dysfunctional molecular clocks within immune cells. However, the mechanisms governing such responses have yet to be fully characterized. In this study, I have discovered a novel immunomodulatory role for the core molecular clock protein BMAL1.

I have demonstrated that BMAL1 drives expression of the major antioxidant transcription factor, NRF2, in macrophages. In doing so it promotes diurnal variation in anti-oxidant and oxidative stress/ROS regulation. Deletion of *Bmal1* in macrophages results in decreased NRF2 activity and antioxidant response, facilitating accumulation of oxidative stress.

Lack of BMAL1 may also facilitate increased ROS production via alterations to cellular metabolism. Deletion of *Bmal1* results in increased glycolysis and oxidative phosphorylation in response to LPS stimulation. The increased ROS in macrophages lacking BMAL1 is produced mainly from the mitochondria, supporting the theory of BMAL1 mediated regulation of metabolism as a regulator of oxidative stress.

NRF2 plays a critical role in the innate immune system, limiting inflammation via reactive oxygen species (ROS) suppression and direct repression of the pro-inflammatory cytokines IL-1β and IL-6. Lack of NRF2 in *Bmal1* deficient cells facilitates excess production of ROS, stabilising the hypoxic response protein HIF-1α. Increased ROS and HIF-1α levels, as well as decreased repressive activity of NRF2 in cells lacking BMAL1, results in increased production of the pro-inflammatory cytokine IL-1β. Deletion of *Bmal1* also increases cleavage of IL-1β

and cell death by the inflammasome, which appears to be at least partially mediated by oxidative stress.

In summary, I have uncovered novel roles for BMAL1 in macrophages, both as a regulator of metabolism and inflammation. These discoveries have implications in terms of treatment of inflammatory disorders that display circadian rhythmicity, and in the increasing number of inflammatory driven pathologies arising from our 24 hr modern society.

Chapter 1: Introduction

Much of the work presented in this chapter has been published in Seminars in Immunology as a review article titled "Immunometabolism, is it under the eye of the clock?" (Early J.O. and Curtis A.M. 2016) (1).

Inflammation is an umbrella term, describing the complex biological response to a multitude of stimuli, both endogenous and exogenous. While mostly considered a protective process, inflammation can also have harmful repercussions. Observations indicate a strong relationship between circadian rhythms and the innate immune response. However, our understanding of the mechanistic pathways linking the molecular clock and the immune response is lacking.

This project endeavours to uncover the impact of the molecular clock on inflammatory responses from macrophages. Under specific investigation is the relationship of the core molecular clock protein, Brain Muscle Arnt-Like Protein 1 (BMAL1), with the innate immune system and what role BMAL1 has following Toll-Like Receptor (TLR) 4 activation. Here I show that BMAL1 promotes expression of the nuclear factor (erythroid-derived 2)-like 2 (NRF2) mediated anti-oxidant defence pathway, limiting reactive oxygen species (ROS) induced inflammation following TLR4 activation. This study reveals a novel molecular mechanism to explain previously reported findings of the necessity of a functioning molecular clock in cells of the innate immune system to limit harmful levels of inflammation.

1.1 The circadian cycle

Life on earth follows a daily 24 hour (hr) rhythm due to the rotation of the earth on its axis and the daily cycle of light and temperature (1). The sleep-wake cycle in humans provides a clear example of our daily rhythmicity and connection to our 24 hr environment. Alterations in physiology that peak and trough in a 24 hr timescale are classified as circadian (2). The term circadian comes from the Latin word “circa” meaning "around" and *diēm*, meaning "day". Circadian rhythms are driven by oscillations in the proteins of the molecular circadian clock (2). This molecular clock allows an organism to track time of day, providing the means to anticipate and respond to the daily changes within the environment (3).

Nearly all organisms on this planet possess some form of molecular time keeping system (1), including single cell organisms such as the model cyanobacteria species, *Synechococcus elongates (4)*. The first observations of circadian rhythms in nature were noticed in the times of Alexander the Great, when daily leaf movement was seen in the leaves of the tamarind tree (5). The first recorded observations of endogenous circadian oscillation were recorded in 1729 by French scientist Jean-Jacques d’Ortous de Mairan (6). He noted that leaves of the *Mimosa pudica* opened in the morning and closed in the evening and that this 24 hr cyclical movement continued when the plants were kept in the dark. This was the first observation of an endogenous clock, separate from the exogenous influence of light. The term circadian was first coined in the 1950’s by Franz Halberg (7), who provided some of the first evidence of circadian control of immunity (8). Although clock mechanisms differ between organisms, conservation of a timer system throughout the evolutionary tree exemplifies its importance. In recent years significant advances have been made in our understanding of how the circadian cycle is controlled, and how this can in turn regulate many aspects of our physiology, including immune function (9).

1.1.1 Circadian rhythms

A circadian rhythm can largely be categorized as any biological process that exhibits an endogenous and entrainable oscillation within a 24 hr timescale (Figure 1.1) (1). Thus, they must continue to exhibit their respective oscillating pattern in the absence of any exogenous signals in order to provide an anticipatory function to the organism (10). However, these rhythms must also be entrainable by external sources, also termed zeitgebers, such as light, temperature and feeding. This facilitates adaption in the organism to alterations in the external environment, for example, alignment with changes in day length and temperature, or in crossing multiple time zones.

In summary, for a rhythm to be considered circadian it must meet three criteria:

1). The rhythm must be endogenous and have a free running rhythm that lasts 24 hrs. That is to say that in total darkness without exogenous input, the rhythms will continue to cycle. If not, it is now classified as an inducible, or diurnal rhythm.

2). The rhythm must be entrainable. Although the rhythm is endogenous, it must be able to be reset by external stimuli, such as light and heat. Given that the circadian clock is hypothesized to act as a predictor to exogenous stress, the cycle must be able to adapt to changes in the external environment such as seasonal alterations in day length or travelling between time zones. We term elements able to entrain rhythms “zeitgebers”, meaning time givers.

3). The rhythms must exhibit temperature compensation, i.e. the rhythms will persist across a range of physiological temperatures.

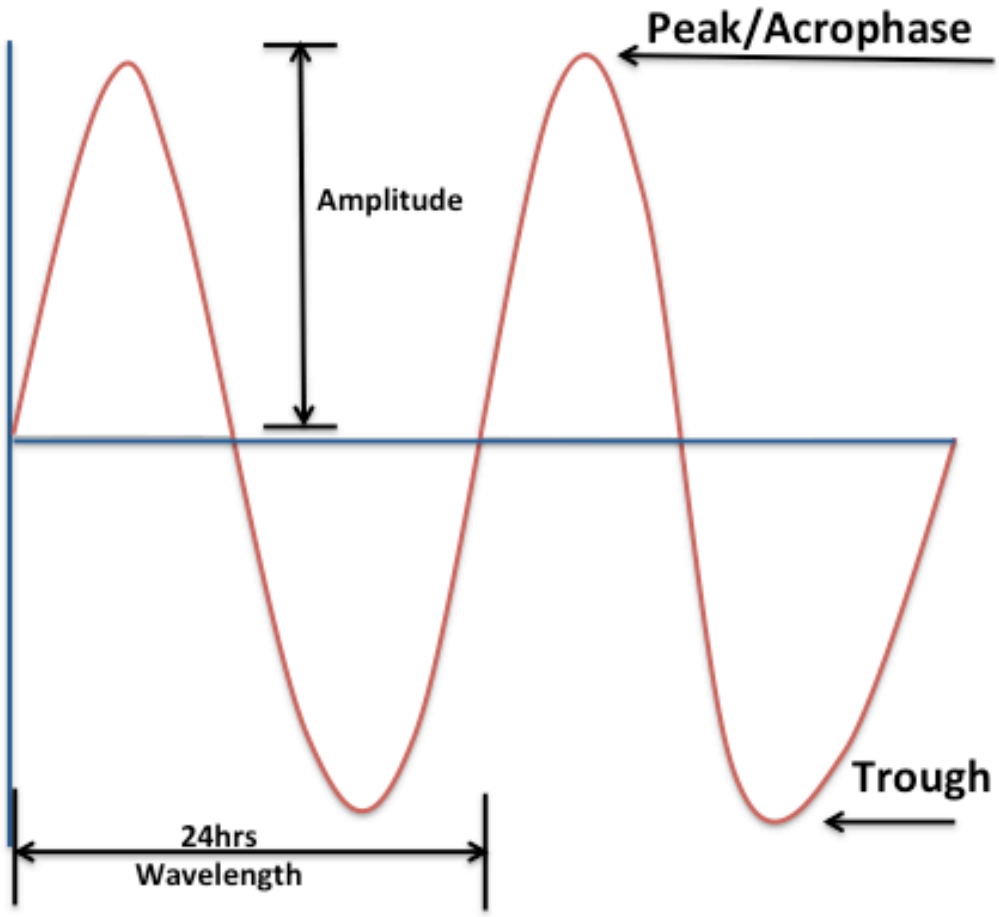

Figure 1.1 Properties of a circadian gene

For a gene to be considered circadian, it must peak and trough in expression within a 24 hr timescale. The gene must also continue to oscillate in this pattern in the absence of any external stimuli, termed zeitgebers or time givers. However, these zeitgebers may entrain a circadian rhythm to keep it cycling in time with external conditions. The amplitude refers to the difference between the peak or trough and the mean value of the wave. The period revers to the time elapsed for one complete cycle. The wavelength is the distance between two successive peaks or troughs.

1.1.2 Regulation of circadian rhythms

Nearly all organisms display genetically based 24 hr endogenous rhythms. While these clocks appear to be based on very similar genetic feedback loops, the specific genes involved in regulation of these rhythms are thought to have evolved independently in each kingdom (11). A "master clock" governs circadian rhythms in higher organisms. This master clock resides within the cells of the suprachiasmatic nucleus (SCN), in the anterior region of the hypothalamus in mammals (Figure 1.2) (12). The SCN coordinates all endogenous rhythms across the body and the rhythmicity of an organism is largely ablated if the SCN is destroyed (13). The SCN also serves to integrate exogenous zeitgebers, most notably light, to maximize coordination of endogenous rhythms with the external environment (14). Photosensitive melanopsin ganglion cells within the retina relay light input from the external world to the SCN (12). The neurons of the SCN are capable of firing with 24 hr rhythmicity, driven by a network of interlocking positive and negative feedback loops. The loops that drive 24 hr rhythms, or circadian rhythms comprise the molecular clock. Importantly, the clockwork machinery is present in virtually all cell types (15) including those of the immune system (16). The master clock of the SCN relays signals, which then synchronise molecular clocks found within central and peripheral tissues (17). While not entirely understood, synchronisation of peripheral clocks by the SCN appears to be largely orchestrated via the hypothalamus pituitary adrenal (HPA) axis and the autonomic nervous system (ANS) (18). Evidence of this axis is observed in the temporal release of Adrenocorticotropic hormone (ACTH), a hormone produced by the pituitary, which induces robust circadian rhythms in the release of corticosterone (19). It is also clearly observed in the levels of melatonin, the hormone of darkness. This hormone is released from the pineal gland in a rhythmic manner, accumulating when the light dims to facilitate sleep (20). The temporal release of hormonal and neuronal signals act as synchronizers and messengers from the SCN clock to the peripheral clocks

(21). The SCN's control over endocrine and autonomic outputs keeps the peripheral cells in synchrony with each other, allowing for strict coordination of tissue functions over the course of the day (22, 23).

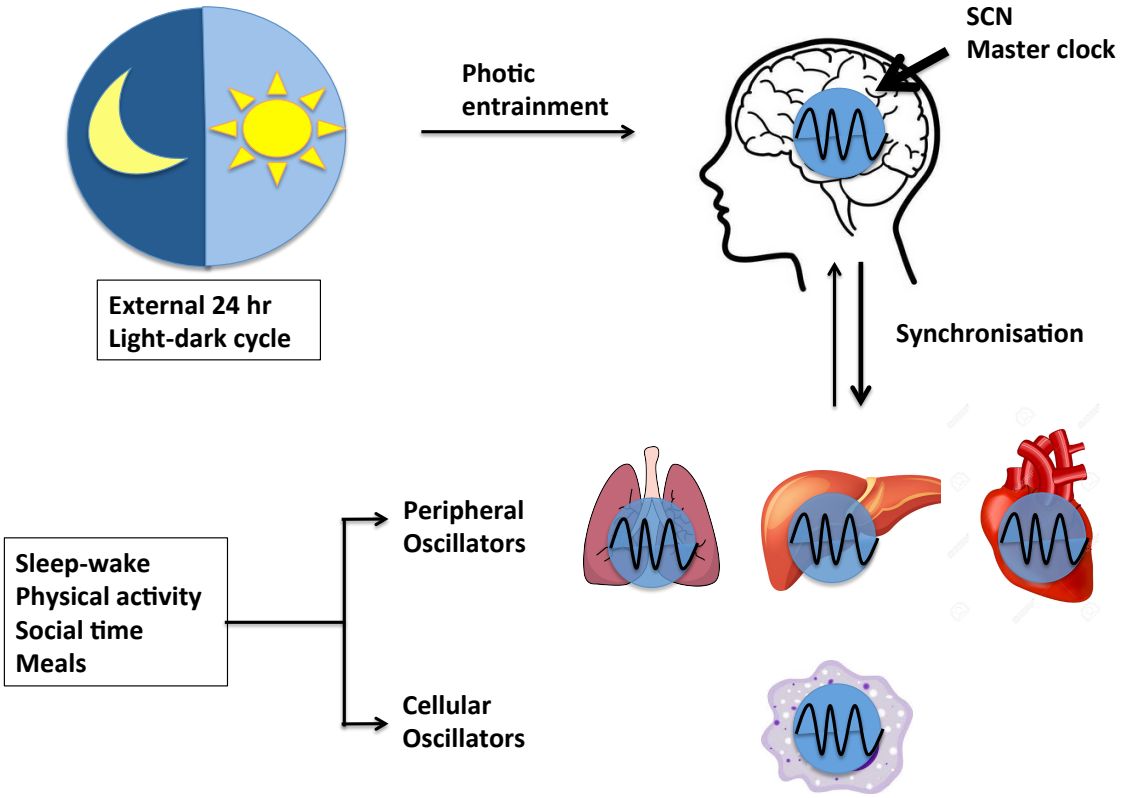

Figure 1.2 Regulation of mammalian circadian rhythms

Endogenous circadian rhythms are maintained in the SCN (master clock). These endogenous rhythms are entrained to the external environment by the photic period, which signals through the melanopsin ganglion cells and the retinohypothalmic tract. The SCN synchronizes the peripheral molecular clocks found in other bodily tissues via the HPA axis and the autonomic nervous system. The molecular clock is also sensitive to entrainment from other signals such as, feeding, social cues, sleep patterns and exercise.

1.1.3 The molecular clock

In 2017 the Nobel Prize for physiology and medicine was awarded to Prof. Jeffrey C. Hall, Prof. Michael Rosbash and Prof. Michael W. Young for their work in discovering the molecular mechanisms governing the circadian cycle in the fruit fly drosophila. They were able to isolate and identify the molecular components that make up the self-sustaining clockwork of the drosophila circadian cycle (24). With this discovery it became possible to identify similar mechanisms in mammals.

In mammals the molecular clock is powered by rhythmic localisation and activity of a number of clock proteins (Figure 1.3). BMAL1 is the main orchestrator of the molecular clock, as it is the only single clock gene deletion that leads to complete ablation of the molecular clock, resulting in a loss of all rhythmic behavioural activity (25). BMAL1 forms a heterodimeric partnership with Clock Locomotor Output Kaput (CLOCK), binding to E-box sites in the genome to induce gene expression (26). Neuronal PAS Domain Protein 2 (NPAS2), which is highly expressed in the brain, is also capable of dimerising to BMAL1 to induce expression of E-box controlled genes (27). The presence of E-boxes within the promoters of the clock repressors, period (PER1, 2 and 3) and cryptochrome (CRY1 and 2), generates a negative feedback loop. Following translation, PER and CRY cooperatively translocate back to the nucleus, inhibiting their own transcription by disrupting the BMAL1:CLOCK complex (28). The nuclear receptors RAR-related orphan receptor (ROR) (α, β, γ) AND REV-ERB (α, β) are also induced via E-box sites in their promoters and translocate back into the nucleus to bind receptor-related orphan receptor response elements (ROREs) in the promoter of *Bmal1* (23). REV-ERBs are capable of repressing *Bmal1* transcription (29), whereas RORs cause transcriptional activation of *Bmal1* (30). It is believed that posttranscriptional modifications, including control by miRNAs, provide another layer of organisation to this tightly regulated system (31, 32).

The BMAL1:CLOCK heterodimer can bind thousands of sites in the genome and it is the oscillation of this binding that leads to circadian expression of clock-controlled genes**.** However, mRNA expression is just one clock output. Protein modifications including epigenetics (33), subcellular localization (34), rates of translation (35, 36) reduction-oxidation (REDOX) (37) and ion concentrations (38) are some of the cellular functions that have been identified as clock regulated. The molecular clock exists within immune cells (15), including B cells (39) , T cells, (40) and macrophages (41), and appears to play a key role in each of these cell types.

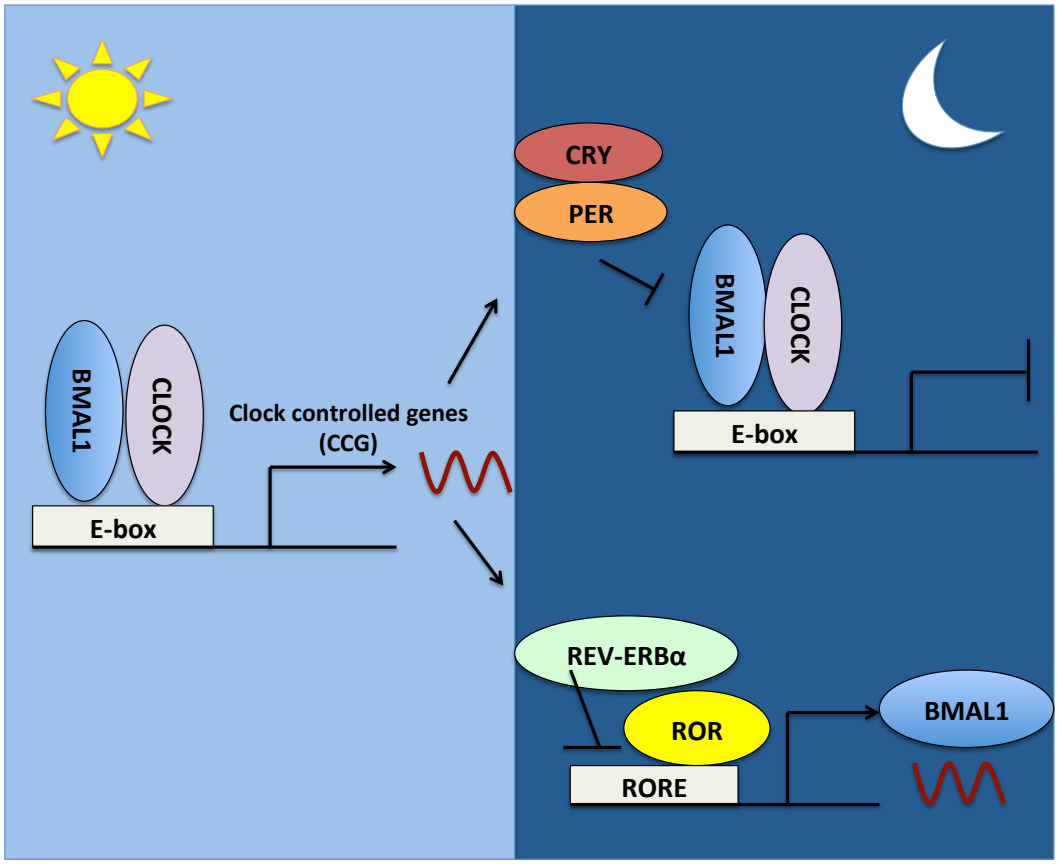

Figure 1.3 The oscillation of circadian clock proteins

During the day, the forward arm of the clock is active. Levels of BMAL1 are high facilitating heterodimerisation with CLOCK. In this partnership these proteins induce gene expression of clock-controlled genes (CCG) via E-box sites in their upstream promoter. This includes induction of the repressors period (PER) and cryptochrome (CRY), which peak in the night, translocate back to the nucleus and disrupt the BMAL1:CLOCK heterodimer. Similarly REVERB and ROR reach high levels during the night with REV-ERB transcriptionally repressing *Bmal1* and ROR transcriptionally activating *Bmal1*. The dynamic nature of these genes facilitates the rhythmic binding of BMAL1:CLOCK to E-box sites generating circadian rhythms in CCGs.

1.1.4 Models of clock study

Outside of genetic alterations to components of the molecular clock, it is possible to modify an organism's circadian cycle through introducing changes to its environment. This allows for dissemination of the various effects of different zeitgebers on the molecular clock, such as the light:dark cycle and food entrainment. For research purposes, time-of-day is denoted as zeitgebers time (ZT) 0-24. Hence, ZT0 refers to the time at which lights are turned on in the animal facility, and ZT12 is lights off. In mice ZT12 is the beginning of the active phase and ZT0 is their resting phase, given their status as a nocturnal species (42) (Figure 1.4). The circadian cycle of mice can be altered by adjusting the 12:12 light:dark cycle and waiting for the cycle to realign to the new setting. A light cabinet can make this adjustment easier. This apparatus generally has two or more sections, with their own independent light cycles, which can be adapted as necessary, meaning two or more different cycles can be investigated simultaneously (43). For investigation of whether rhythms are truly circadian or if they are light dependent, it is possible to house mice in complete darkness and to keep all other conditions constant. These mice will continue to follow an approximate 24 hr day, even in the absence of light, but rhythms that are dependent on light should now be absent (44). Overall these techniques, and many others provide powerful tools for disseminating the effect of circadian rhythms on certain aspects of physiology and on the effect of various zeitgebers on entrainment.

Cultured cells possess a molecular clock, however, the individual cell clocks are not in synchrony with surrounding cells due to lack of a coordinating mechanism (45). It was discovered that cells *in vitro* could be synchronized through addition of exogenous zeitgebers. A high concentration of serum for two hours followed by serum deprivation was shown to induce oscillations in gene expression (45). This technique was termed "serum shock" and opened up one of the most widely used

tools for study of circadian rhythms *in vitro*. Investigation in to the molecular basis of serum shock identified a novel role for glucocorticoids in cell synchronisation. Glucocorticoids are a class of corticosterioids that bind to glucocorticoid receptors (GRs), which are present in almost every vertebrate animal cell (46). They have been demonstrated to provide an important feedback mechanism on the immune system and are often used in medicine to treat overactive immune responses such as sepsis, asthma and autoimmune diseases (46). These hormones are highly abundant in serum and have been demonstrated to display clear rhythms over time-of-day (47). Interestingly, exogenous addition of glucocorticoids, specifically dexamethasone for 2 hours, has become another effective method of synchronising circadian rhythms *in vitro* (48).

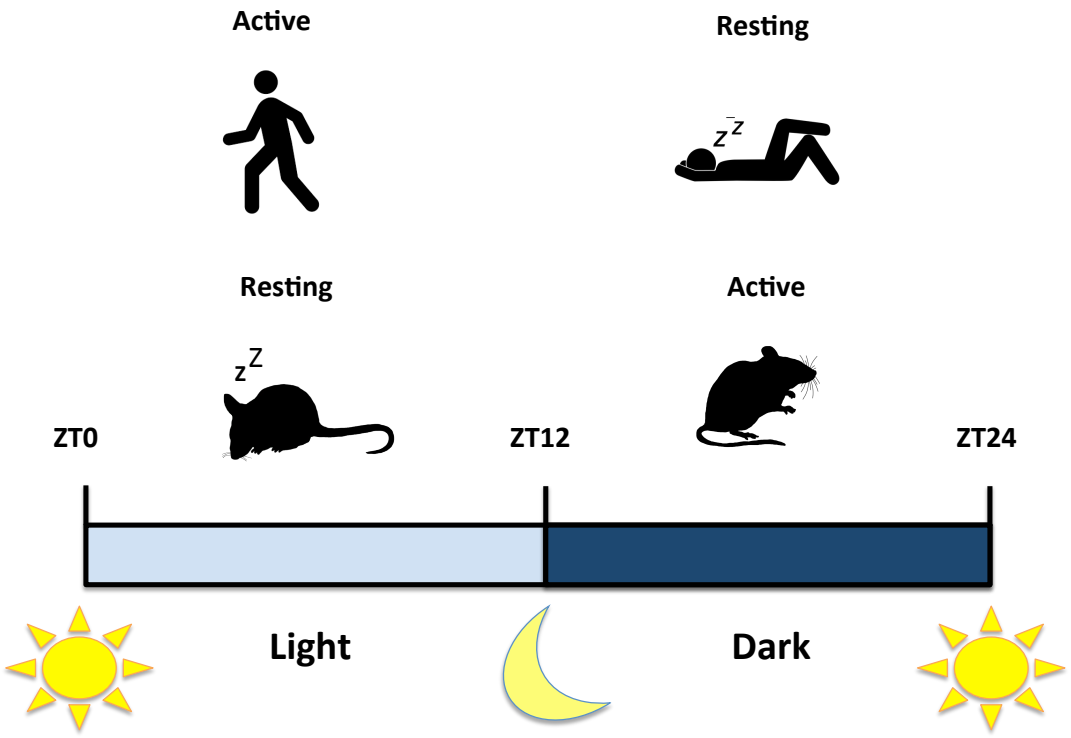

Figure 1.4 Light/Dark and activity

ZT0 refers to the beginning of the light period in an animal facility. During the light phase humans are generally active and laboratory mice are inactive. 12 hrs later ZT12 is reached and lights are shut off indicating the beginning of the dark phase. In general humans are inactive during the dark phase while laboratory mice are active. At ZT24, the lights are turned back on and a new cycle begins.

1.1.5 Circadian disruption in health and disease

While the circadian cycle functions to prepare us for daily oscillations in our external environment, it is not a perfect system. Evolution of the molecular clock did not factor the creation of long haul flight, shift work, or even full availability of food in first world societies. These processes leads to uncoupling of the master clock in the SCN to the clocks in peripheral tissue, resulting in desynchronisation of the circadian cycle (49). Thus, a mechanism that was originally intended to protect us from exogenous insult can in fact, result in endogenous harm in our modern society.

To appreciate the relationships between the environment, clocks, and physiology, one must only observe the consequences of perturbations in the sleep-wake cycle. Modern life and technology has seen us adopting lifestyles that remove us from the solar world in which we have evolved. Rather than rising upon first light and retiring upon its disappearance, light has become omnipresent in our lives, leading to circadian disturbances and alterations in our physiological responses. Non-traditional working hours has been linked to several metabolic and immune related disorders, including obesity (50), diabetes (51, 52) stroke (52), atherosclerosis (53) and coronary heart disease (54). Various cancers have been linked to disrupted circadian cycles, such as lymphatic (55), prostate (56, 57) and breast cancer (58). In 2007 the International Agency for Research on Cancer (IARC) claimed that shift work with circadian disruption is a highly probable human carcinogen (59).

Living at odds with our internal pacemaker may be a contributing factor in the current epidemic of obesity and obesity related disorders such as diabetes and heart disease (60). Our circadian clock serves to protect and prepare us for exogenous insults, however we are now living out of synchrony with our body clock. Social jetlag is a term used to describe how modern life is resulting in circadian misalignment (61). Mouse models of jet lag have been important in discerning this

fact. Alternating feeding patterns in mice, such as restricting feeding patterns to one time of day leads to uncoupling of the SCN from the peripheral clocks in the kidney, heart and pancreas (62). Mice fed a high fat diet during their inactive phase gain significantly more weight than those fed the same diet during their active phase (63). This phenomenon is recapitulated in humans, with people who preferentially eat their main meal later in the day, lose less weight than those who eat at an earlier stage (64). Indeed increased levels of social jetlag are associated with increased BMI in humans, as these people tend to eat outside of regular hours (61). Interestingly, the tendency to eat at later stages in the day correlates with frequency of a *Clock* gene mutation (64). In mice, mutations in *Clock* lead to obesity and metabolic disturbances (65). Outside of social jetlag, ageing is well documented to dampen the amplitude of circadian rhythms (66, 67). Circadian rhythms and sleep consolidation both begin to break down with normal ageing, and it is believed that these changes may be a factor for disorders such as Alzheimer's' disease (68) and other circadian and age associated pathologies such as diabetes and cancer (69).

The circadian cycle has been demonstrated to regulate both metabolism and inflammation, and in turn metabolism and inflammation may regulate the molecular clock (1, 23). Therefore, understanding the interplay between our endogenous rhythms and immunity will provide us with a more detailed understanding of immune cell activation

1.2 Innate immunity

The immune system in mammals is comprised of two elements, innate and adaptive immunity. While it was first assumed that the innate immune system was a form of non-specific defence, a more complex view has begun to emerge. The innate immune system is the first line of defence against infection, injury, and malignancy (70). Its roles range from pathogen clearance, damage limitation, and resolution of inflammation (70, 71). The innate immune system consists of a wide array of cell types and receptors, each of which provide a specific function to counteract infection and maintain tissue homeostasis (70).

Immune function is highly rhythmic in both mice and humans and thus the field has become of specific interest to circadian biologists. Immune cell trafficking has been clearly demonstrated to alter with time of day (72). In mice, the number of hematopoietic stem and progenitor cells and mature leukocytes peak during the resting phase (73). Similarly, leukocytes appear to be at their highest in blood during the resting phase but migrate to tissues during the active phase of mice (74). Similar rhythms are evident in humans, with circulating neutrophils and lymphocytes being highest between 16:00 to 24:00 and dropping between 04:00 to 12:00 (75). A recent study utilized humanized mice to demonstrate differences in temporal migration of mice and human immune cells. Mouse and human leukocytes were introduced to immunodeficient mice. The mouse leukocytes accumulated in circulation at ZT7 and reached a trough, when they migrated into tissues at ZT19 (76). Human leukocytes displayed the opposite rhythm to this, peaking at ZT19 and reaching a trough at ZT7 in blood (76). It was found that differential circadian regulation of C-X-C chemokine receptor type 4 (CXCR4) resulted in the differing phenotype between mice and human cells (76). Indeed, cytokines have previously been shown to display robust rhythms in mice and humans. (interleukin) IL-1β and

tumour necrosis factor (TNF)α have been shown to peak in circulation of mice during their active phase (72). Similar rhythms have been demonstrated in granulocyte-macrophage colony-stimulating-factor (GM-CSF) (75), IL-1β, and IL-6 in humans (77).

These changes in immune parameters have been shown to have clear effects on time-of-day variation in immune response. BMAL1 regulates diurnal oscillations in $Ly6C^{hi}$ monocytes and it is the time-of-day variation in infiltration of these cells that provides protection from *Listeria* (*L.) monocytogenes* infection (78). BMAL1 has also been shown to be crucial in regulating circadian mediated severity of a mouse model of multiple sclerosis, experimental autoimmune encephalomyelitis (EAE) (79). Initiation of EAE at ZT6 results in increased migration *of* IL-1β producing monocytes into the central nervous system (CNS), progressing disease severity (79). It is clear that circadian rhythms are present at all levels of innate immunity and understanding how the molecular clock regulates this system provides new therapeutic approaches.

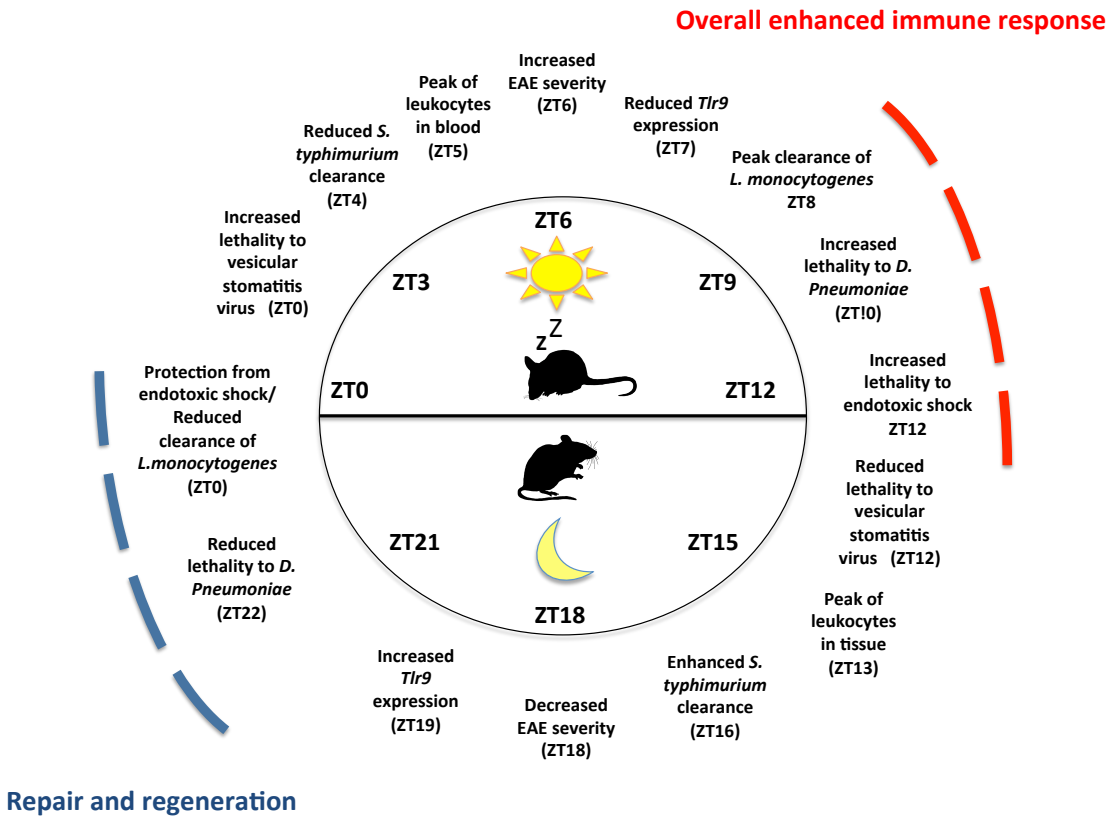

Figure 1.5 Circadian regulation of immune function

The circadian cycle appears to partition the immune response into two states. A state of anticipation and immune activity (red line) that appears to dominate during the active phase of mice, and a period of repair and regeneration (blue line) that seems to occur during the resting phase. It can be seen that mice are generally more susceptible to lethality from inflammatory signals during this active period, however there is increased clearance of pathogens during this state. The idea of a repair and regenerative phase remains largely speculative, however, it does coincide with reduced lethality and a decrease in inflammatory output.

1.2.1 Pattern recognition receptors and TLR signalling

The innate arm of the immune system consists of a wide repertoire of cell types, each with a specific array of functions (70). It provides the first line of defence against infection, limits damage after injury, and functions to remove dangerous cells and molecules (70). One aspect held in common by many cells is the expression of pattern recognition receptors (PRRs) to detect and respond to a plethora of common molecular signals (80). Inflammation inducing molecular signals can broadly be divided into two groups; danger-associated molecular patterns (DAMPs) and pathogen associated molecular patterns (PAMPs). DAMPs are generally endogenous molecules, often-released following cell death, cellular transformation, metabolic dysfunction, etc., which indicate deviation from homeostatic conditions (81). PAMPs are largely associated with pathogen invasion (82). Families of highly conserved PRRs have evolved, both extracellular and intracellular, to detect and initiate response to the multitude of aforementioned molecular patterns.

TLRs are localised on the plasma or endosomal membrane, sampling the extracellular space for bacterial and viral PAMPs, or endogenous DAMPs (83). The discovery of the Toll gene lead to a surge of interest in the field of innate immunity (84). TLRs are the most well documented family of PRRs and are often considered the archetypical PRR. The general method of activation of TLR signalling is quite well conserved with Toll/interleukin-1 receptor homology (TIR)-domain-containing adaptor proteins being recruited, inducing a response tailored to the particular activating ligand. The membrane bound TLRs and the endosomal TLRs 7, 8 and 9, potentiate their respective signal via myeloid differentiation primary response gene 88 (MyD88) (85). TLR2 and TLR4 utilise MyD88 adaptor-like (Mal) to facilitate interaction with MyD88 (85). Endocytosed TLR4 and endosomal TLR3 make use of TIR-domain-containing adapter-inducing interferon-β (TRIF) for signalling (86). In this case, TLR4 uses TRIF-related adaptor molecule (TRAM) as an accessory adaptor molecule (86). Bacterial PAMPs, such

as LPS, predominantly stimulate the MyD88 signalling pathway, activating nuclear factor (NF)-κB, mitogen-activated protein kinases (MAPK)-38 and c-Jun N-terminal kinases (JNKs) (87). Binding of lipopolysaccharide (LPS) to TLR4 induces this pathway, ultimately culminating in the production of pro-inflammatory cytokines, such as IL-1β, IL-6 and TNFα, promoting phagocytosis and the production of numerous antibacterial effectors (88) (Figure 1.5). In the case of viral PAMPs however, it is often the endosomal TLRs, such as TLR9, that are activated. In this case interferons are produced to generate an anti-viral response. It can be seen that MyD88 and TRIF signalling generated by endosomal TLRs signal via interferon regulatory factors (IRFs) to induce type 1 interferons, displaying the diversity of responses that can be generated by specific activating signals (83). However, it is important to note that the pathways are quite interconnected and can lead to cross activation (83).

Interestingly, some TLRs have been linked to the circadian cycle. Of particular interest is the circadian regulation evident in the viral sensing receptor TLR9. It has been demonstrated that both expression and activity of this receptor are dependent on the molecular clock (89). In a time-of-day vaccination model utilizing a TLR9 ligand as an adjuvant, mice immunized at the time of enhanced TLR9 responsiveness exhibited an improved adaptive immune response when tested weeks after vaccination (89). Also shown was a time-of-day dependent variation in lethality to TLR9 dependent sepsis, with lethality directly correlating with higher *Tlr9* expression and function (89). A similar phenotype of time of day dependent lethality to sepsis was shown in a TLR4 model. In the 1960's, Halberg was the first to observe a circadian variation in the susceptibility of mice to grams negative bacteria induced septic shock and death (8). Mice injected with components of gram-negative bacterial infection towards the end of the resting phase displayed greater lethality in comparison to any other time of day (8). It has also been shown that mice injected with LPS in early morning display 60% survival versus 0% survival when infected in the evening (31). It was further demonstrated that this

time of day response was due to the expression of *Bmal1* in the myeloid lineage. It was identified that BMAL1 can repress activity of NF-κB (90). Non-genetic disruption of the molecular clock has been shown to have similar effects on time-of-day sepsis phenotypes. Circadian disruption induced by acute jet-lag drives an exacerbated response to LPS induced death of mice (91). Mice subjected to 6-hour phase advances of the light/dark schedule over the course of 4 consecutive weeks displayed 81% mortality versus 21% mortality in control mice. The jet-lagged mice also produced significantly higher levels of pro-inflammatory cytokines including IL-1β (91). Altered expression of the core clock genes in the jet-lag mice was evident in the liver, thymus and peritoneal macrophages, however no loss in sleep or altered stress-response was evident. Therefore, circadian disruption, and not sleep loss leads to an increase in the innate immune response following experimentally induced jet-lag in mice (91), which may have relevance for the increased inflammatory conditions observed with shift work (92). Understanding this connection between circadian rhythms, pattern recognition receptors, and the innate immune response is crucial to uncovering disease mechanisms.

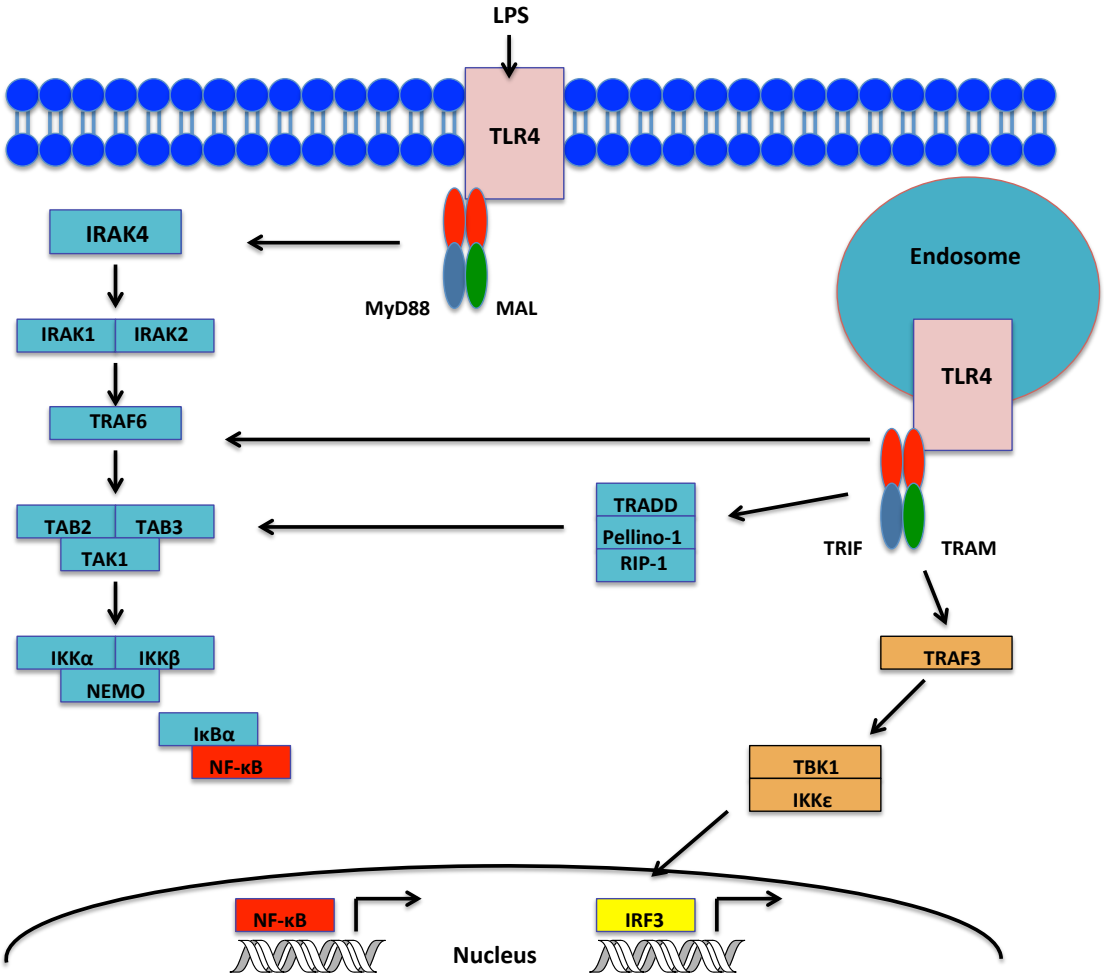

Figure 1.6 TLR4 signalling

LPS may bind to TLR4, which activates a number of intracellular signalling pathways. Adaptor proteins (MAL and MyD88) are recruited to TLR4 in the cell membrane, facilitating further signalling by kinases such as IRAKs. This cascade leads to the eventual activation of the transcription factor NF-κB, which may then enter the nucleus to induce expression of several pro-inflammatory cytokines. TLR4 can also be bound to the endosome, which requires different adaptors for potentiation of its signal. This activation can similarly activate the NF-κB pathway or it may activate the IRFs. TLR4 pathways originating from either the cell surface or endosome can interact with one another.

1.2.2 Clock proteins in immunity

Given the evidence for circadian influence on the functionality of the immune response, determining the specific functions that clock proteins play in these processes is important. While my work has mostly focused on BMAL1, a short summary on the impact of the other core individual clock proteins on immune function is detailed below.

CLOCK, like BMAL1, is also a bHLH PAS domain protein. However, unlike *Bmal1*, *Clock* transcript levels do not alter significantly across the day in tissues and cells including macrophages (41). CLOCK has important functions outside of its heterodimeric partnership with BMAL1. CLOCK also has histone acetyl transferase (HAT) activity, meaning it can add acetyl groups to certain lysine residues, including those in histone proteins, altering DNA confirmation and facilitating the transcription of a given gene (93).

Activation of NF-κB correlates positively with the circadian variation in lethality to LPS (90). CLOCK complexes with p65 causing increased acetylation and phosphorylation of p65 and enhancing the activity of the NF-κB complex (90). CLOCK mutant MEFs (94) and bone marrow derived macrophages (BMDMs) lacking CLOCK, are less responsive to LPS, and TNFα induced NF-κB activation (95). Therefore, CLOCK may drive, whereas BMAL1 may limit, pro-inflammatory responses in macrophages. Peritoneal macrophages lacking *Bmal1* show an increase in phosphorylated p65 (31). BMAL1 may exhibit some of its anti-inflammatory properties by sequestering CLOCK and preventing CLOCK-mediated activation of p65.

REV-ERBα is a potent transcriptional repressor both by recruitment of the NCoR-HDAC3 complex but also via modulation of enhancer RNAs (96). REV-ERBα has also been shown to impact on the inflammatory response. WT mice treated with LPS at

CT12 display greater levels of serum IL-6 versus mice treated at CT0. Deletion of *Rev-erbα* results in heightened levels of IL-6 at both time points (97) THP-1 cells treated with GSK4112 prior to LPS, decreased a range of pro-inflammatory cytokines and chemokines, including *Ccl2*. Interestingly, the repression of *Ccl2* by REV-ERBα is important in the onset, progression and resolution of vesicular stomatitis virus (VSV)-induced encephalitis (98). Mice infected at ZT0 with VSV had a significant decrease in survival rate versus those infected at ZT12. This increase in lethality at ZT0 was associated with higher levels of circulating CCL2, a greater number of peripherally derived immune cells accumulating in the olfactory bulb, and greater levels of pro-inflammatory cytokine production.

RORα and RORγ's role in the immune response has also been elucidated. Of particular note is their role in the differentiation of mature T helper17 (Th17) cells. These cells provide defence against extracellular and intracellular pathogens, however, they are also implicated as mediators of advancing autoimmune pathologies including experimental autoimmune encephalomyelitis (EAE), a model with features similar to multiple sclerosis, and collagen induced arthritis (CIA). Over-expression of RORγt (a RORγ isoform) drives the development of Th17 cells, where as *Rorγt* knockout mice display impaired Th17 development (99). Double knockout of RORα and RORγ leads to complete ablation of Th17 cells, making these mice resistant to EAE (100, 101)

The ROR proteins are also important in innate immune system as *Rorα sg/sg* mice are highly susceptible to LPS induced lethality (102). This could be in part due to less transcriptional activation of *Bmal1*, or via RORα's ability to induce transcription of IκBα, limiting translocation of NF-κB to the nucleus (103).

The PER proteins have also been linked to immune regulation. Global *Per2-/-* mice exhibit the opposite effect to LPS induced endotoxic shock than the effects seen in

myeloid-*Bmal1* deletion. *Per2-/-* mice are resistant to LPS-induced lethality at all time points analysed (104). Serum levels of IL-1β and IFNγ were significantly lower in *Per2-/-* mice following LPS injection, although IL-6, TNFα and IL-10 levels were comparable to controls (104). Increased levels of IFNγ were attributed to Natural Killer (NK) cell function, providing a role for PER2 in NK cells. *Tlr9* mRNA levels were diminished in the macrophages of *Per2-/-* mice and displayed a blunted response to CpG stimulation (89). It is possible that PER2 may drive inflammation by repressing BMAL1.

Similar to the effects of *Bmal1* deletion, complete clock disruption with *Cry1/Cry2* double knockout leads to enhanced inflammation. In a model of collagen induced arthritis (CIA), mice lacking CRY1 and CRY2 display greater levels of TNFα and have heightened inflammation in their joints versus wild-type mice (105). By ectopically expressing CRY1 in MEFs isolated from *Cry1/Cry2 –/-* mice, activation of a TNFα luciferase promoter was vastly decreased. This could possibly be due to CRY1 limiting NF-κB activation as has previously been demonstrated (106). Absence of CRY1 and CRY2 in fibroblasts and BMDMs leads to a basal increase in mRNA levels of *Cxcl1, Il-6 and Tnfα*. CRY1 is capable of binding to adenylate cyclase, subsequently limiting cyclic adenosine-monophosphate (cAMP) production, decreasing protein kinase A (PKA) activity, culminating in lower levels of p65 phosphorylation and NF-κB activation. With an emerging role of CRY in regulating NF-κB, a recently discovered activator of CRY could have potential in the treatment of inflammatory conditions revolving around the innate immune response. KL001 is capable of preventing ubiquitination of both CRY1 and CRY2, resulting in lengthening of the circadian period (107). This compound has been demonstrated to have an anti-inflammatory role in fibroblast-like synoviocytes (FLSs), a potential candidate for producing rhythmic inflammatory signals during collagen induced arthritis (108). KL001 and other clock compounds not only provide a tool for dissection of the molecular clock, but may also aid in the development of circadian based treatment

for inflammatory and metabolic diseases (107).

1.2.3 Inflammasomes

The term inflammasome was coined in 2002 in reference to the high molecular weight complex that forms in the cytosol of activated immune cells that facilitates the activation of inflammatory caspases (109). The field has since expanded rapidly and multiple inflammasomes have been identified, each of which is activated by specific PRRs and PAMPs or DAMPs. The core inflammasome receptor families are the NOD-like receptors (NLR), AIM2-like receptors (ALR) and RIG-I-like receptors (RIR), and these are expressed predominantly in myeloid cells (110). While the initiating receptor differs between inflammasomes, they mostly contain the apoptosis-associated speck-like protein (ASC) and the inactive zymogen pro-caspase-1 (110). Recognition of an inflammatory ligand results in oligomerisation of ASC, which consists of a pyrin domain and a caspase recruitment domain (CARD) (110). This facilitates binding of ASC to the upstream inflammasome receptor/sensor molecule and Caspase 1 (111). This results in proximity-induced auto processing of the Caspase 1 dimer (P10 and P20 subunits), allowing for tetramerisation of two P10 and two P20 subunits into an active zymogen (111). The newly formed tetramer can subsequently cleave pro-IL-1β and pro-IL-18 into their active forms, and induces pyroptosis through cleavage of gasdermin D (112). IL-1β, and IL-18 are released from the lysed cells, propagating the inflammatory response in a cascade like fashion (110, 113) (Figure 1.6).

A primary signal, often referred to as “signal 1”, such as LPS signalling through TLR4, initiates formation of the inflammasome (114). NLRP3 and AIM2 are two inflammasomes that may be stimulated in this manner (114, 115). The secondary signal, or “signal 2”, which leads to ASC oligomerisation, is highly specific to each

inflammasome receptor. For examples NLRP3 may respond to adenosine tri-phosphate (ATP), or nigericin (114), whereas AIM2 responds to double stranded DNA (115).

Inflammasomes have been described as being crucial to host defence. IL-1β is a well-established pyrogen critical in producing symptoms of fever and driving inflammation (116) by inducing the expression of downstream pro-inflammatory molecules such as cyclooxygenase type 2 (COX2) and nitric oxide (NO) (117), and promoting cellular proliferation and differentiation of immune cells (118, 119). However, aberrant inflammasome activation has also been linked to development of complications such as autoimmune diseases (120). IL-1β levels have been demonstrated to exhibit diurnal variation in the circulation of mice infected with *L.monocytogenes* (78), and in a mouse model of rheumatoid arthritis (108) . IL-1β is also associated with pathogenesis of several disorders, which have been linked to the circadian cycle, such as multiple sclerosis (79), sepsis (31), and rheumatoid arthritis (108).

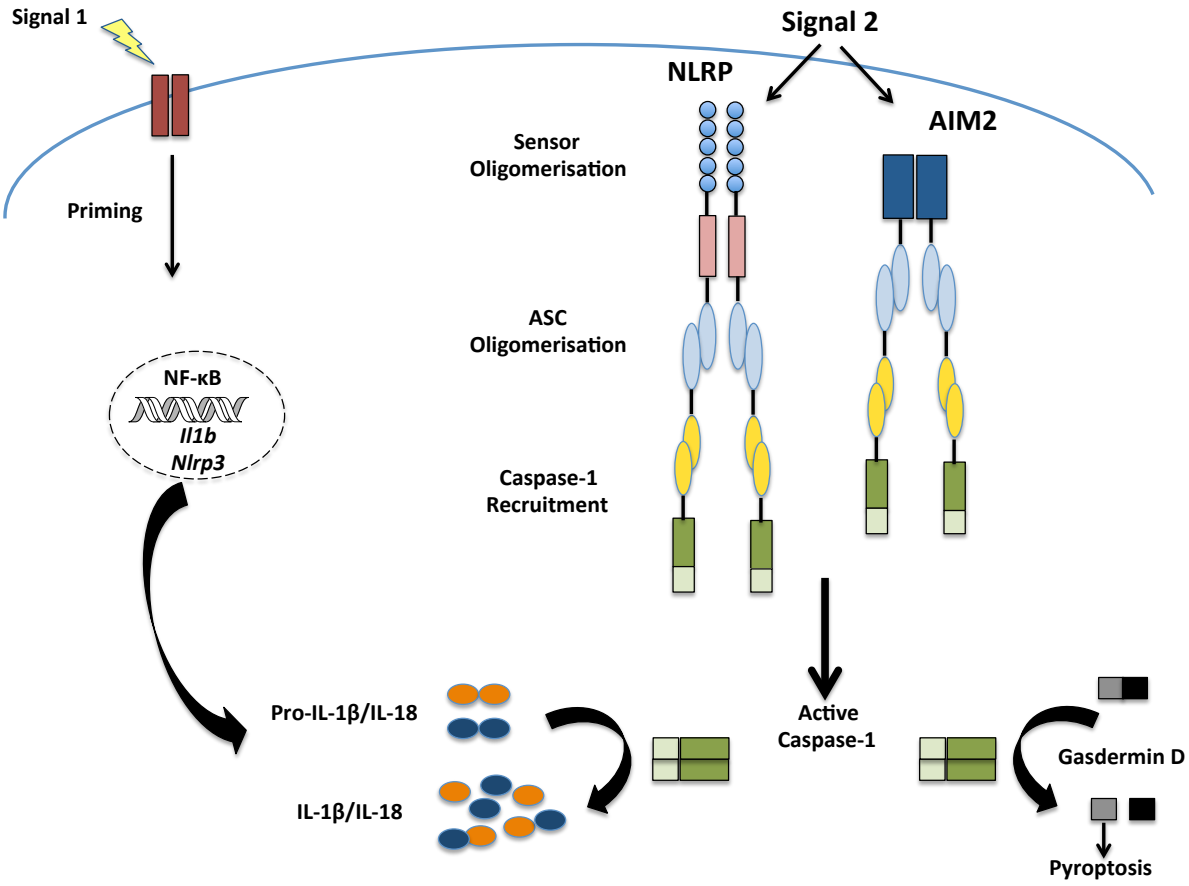

Figure 1.7 Activation of the NLRP3 and AIM2 inflammasomes

A number of circumstances can lead to priming and initiation of the NLRP3 and AIM2 inflammasome. Signal 1 can act through TLR receptors, allowing NF-κB to induce expression of *Il1b* and *Nlrp3*. Upon appearance of signal 2, inflammasome formation begins, which involves sensor oligomerisation, driving ASC oligomerisation and ultimately Caspase-1 recruitment. Once the complex is formed, procaspase-1 is cleaved into its active form, enabling it to cleave its substrates IL-1β and IL-18. Caspase-1 may also cleave Gasdermin D into its active form to initiate pyroptosis for propagation of the inflammatory signal.

1.2.4 Macrophages

Macrophages are a long-lived and tissue specific cell of the innate immune system that play a crucial role in host defence and tissue homeostasis (121). Macrophages display plasticity in their phenotype, which is governed largely by their respective microenvironment (122). These cells can function as phagocytes, detecting and engulfing foreign and endogenous substances, and can promote inflammation via the secretion of pro-inflammatory cytokines (123). However, macrophages can also become anti-inflammatory and promote tissue repair. This phenomenon has led to the sub-categorisation of activated macrophages into M1 and M2 phenotypes (Figure 1.7) (121). However, these terms have fallen out of favour in recent times, being replaced with the idea of a spectrum of activity dependent on the stimuli that activate them. Macrophages have a robust molecular clock with at least 8% of the peritoneal macrophage transcriptome demonstrating circadian gene expression (41). Given their status as a long-lived immune cell, known to exist in tissues for months at a time (124), it is likely that the endogenous clock is important in macrophage function. Indeed rhythms have been shown in several macrophage activities, such as cytokine output (97), and phagocytosis and bactericidal activity on *Salmonella (S.) typhimurium* (125). Therefore, macrophages are an excellent cell type in which to uncover how the clock directs the innate immune response.

1.2.5 Metabolic alterations in macrophages

While the activation of macrophages through PPRs is crucial in the generation of pro-inflammatory mediators, it also impacts on metabolic signalling within the cell. Recently these metabolic alterations have been linked to being important in potentiating and mediating the inflammatory output during the innate immune response (126). The ability of a cell to produce ATP for cellular function is essential to all cell types. Glycolysis

converts glucose to pyruvate within the cytoplasm, generating ATP by transferring phosphates from glycolytic intermediates to ADP. Under normoxic conditions this pyruvate is converted to acetyl-CoA, which is then shunted into the tricarboxylic acid (TCA) cycle, generating nicotinamide adenine dinucleotide (NADH) and flavin adenine dinucleotide (FADH2), fuelling oxidative phosphorylation (OXPHOS) and the generation of ATP via the electron transport chain. Under hypoxic conditions however, ATP can be generated solely by glycolysis. Interestingly, this phenomenon was noted to occur in tumour cells, even under normoxic conditions, leading to the coining of the term "the Warburg effect" (127). It was discovered that tumour cells forgo OXPHOS in favour of glycolysis for ATP production, with the pyruvate being converted to lactate. Interestingly, this event has now been demonstrated to occur in cells of the innate immune system following stimulation with LPS (127). In macrophages under LPS stimulation, the glycolytic enzymes hexokinase and glucose-6-phosphate dehydrogenase are up regulated, as are the overall rate of glycolysis and OXPHOS is decreased (128-130). The alterations to metabolic mediators during LPS induced TLR4 signalling has profound inflammatory potentiating effects on the cells with many of these mediators being directly linked to boosting reactive oxygen species (ROS) induced inflammation (130).

Of specific importance in the field of immunometabolism are the alterations in mitochondria function that occur during inflammation. Mitochondria are crucial for providing conditions necessary for OXPHOS (131). However, upon recognition of LPS, mitochondria have been discovered to undergo changes in function that appear to increase the pro-inflammatory state of the cell. For example, alterations to succinate dehydrogenase facilitate accumulation of succinate (130). This allows for increased production of ROS, which promotes hypoxia inducible factor (HIF-1α) accumulation (132). Under normoxic conditions HIF-1α is continually degraded by oxygen and α-ketoglutarate dependent hydroxylases (133). However, as its name suggests, HIF-1α accumulates under hypoxia and the hydroxylases that regulate its accumulation are

inhibited by ROS accumulation during inflammation (134). Therefore, ROS accumulation drives HIF-1a stabilisation in the cytoplasm. HIF-1α may then undergo nuclear translocation where it initiates transcription of target genes, such as that of the glycolytic machinery to up regulate glycolysis (132).

Another alteration in metabolism that occurs during inflammation is the production of a metabolite termed itaconate. Immune response gene 1 (I*rg1*) is rapidly up regulated following LPS stimulation of macrophages, promoting production of this metabolite (135). Itaconate has been linked to limiting SDH activity (135), preventing ROS accumulation, and limiting HIF-1α induced *Il1b* (135) (Ryan and Mills et.al. 2018 (in press)).

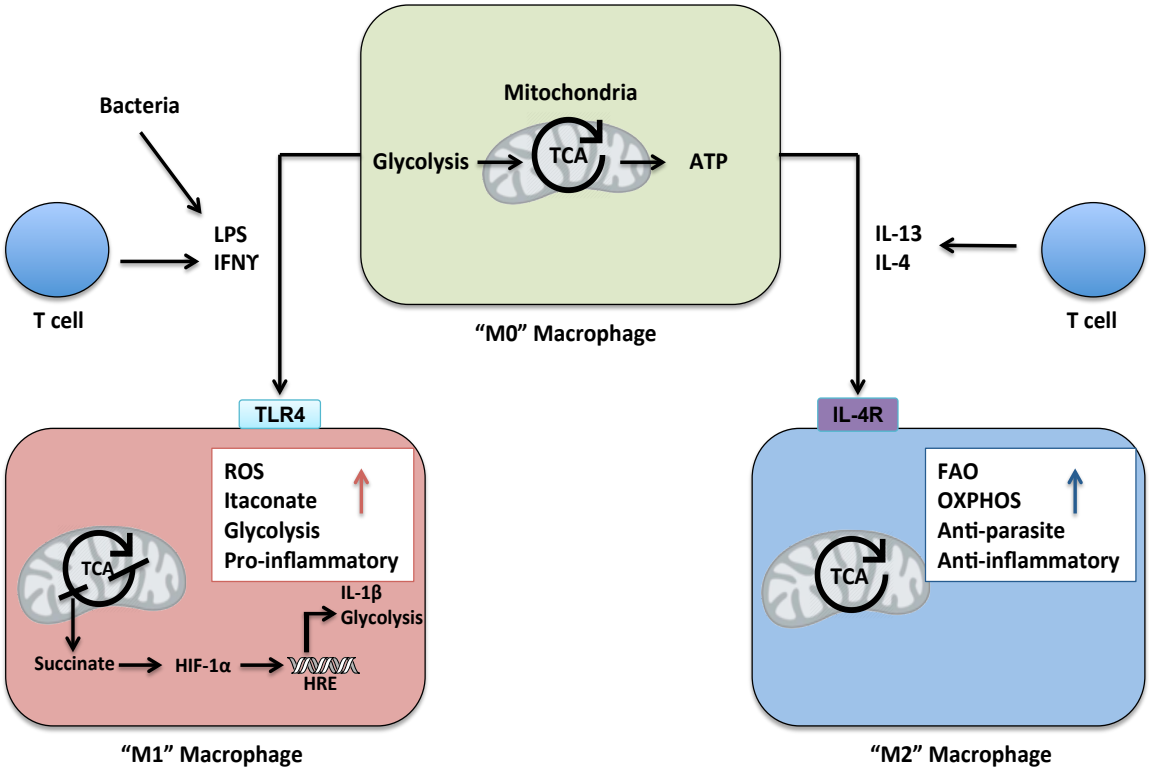

Figure 1.8 Metabolic reprogramming of macrophages

LPS and IFNγ are capable of driving M1 macrophage polarization. M1 polarisation is characterized by decreased utilization of the TCA cycle in favour of glycolysis. As a result, these cells present with increased ROS and inflammatory output. M2 polarisation can be driven by IL-4 or IL13. These cells have a higher reliance on the TCA cycle, thus utilize more oxygen, preventing ROS build up. These cells also exhibit higher levels of fatty acid oxidation (FAO) and have an overall anti-inflammatory phenotype.

1.2.6 Circadian regulation of metabolism

The circadian cycle has been linked to cellular metabolism in various cell types. Mouse embryonic fibroblasts (MEFs) lacking *Bmal1* exhibit a pro-glycolytic phenotype, evidenced by lower mitochondrial ATP production and higher production of lactate (136). Levels of the oxioreductase factor, nicotinamide adenine dinucleotide (NAD+) and FAO, which display a circadian rhythm in wild type mice, were diminished in cells lacking *Bmal1* (136). Deletion of both *Cry1* and *Cry2* produced the opposite effect on MEFs than *Bmal1* deletion, highlight the opposing nature of the forward and reverse limbs of the clock on metabolism regulation (136). It is believed that NAD+ shows rhythmicity due to circadian mediated regulation of *Nampt,* the rate-limiting enzyme in NAD+ synthesis (137). The fluctuations on NAD+ modulate the activity of certain deacetylase sirtuins, such as Sirtuin 1 (Sirt1) and Sirt3 (136, 137). Rhythms in Sirt3 activity regulate oxidative enzymes and respiration (136). Sirt1 has been shown to feedback on clock function by rhythmically deacetylating PER2, promoting its degradation (138). In a similar manner, AMP activated protein kinase (AMPK) phosphorylates CRY1, inducing destabilisation of the protein (139). The mTOR effector kinase, S6 protein kinase 1 (S6K1) has been demonstrated to rhythmically phosphorylate BMAL1 to facilitate association of BMAL1 with translational machinery and to promote protein synthesis (140). Collectively, these interactions between the clock and metabolism allow for feedback between nutrient sensing and the circadian cycle (141) (Figure 1.8).

Mitochondria form and functional changes are also documented to undergo alterations throughout the circadian day. Mitochondrial fission and fusion refers to two states of mitochondrial form. In the fissioned state mitochondria are more often in individual units and are associated with decreased OXPHOS and less efficient energy production (142). In their fusioned state, mitochondria can be seen to form interlinking networks, providing maximal efficiency for OXPHOS (142). The flux between fission and fusion has

been demonstrated to alter with circadian time-of-day, and rhythms are completely ablated in liver cells in which *Bmal1* is deleted (142). Mitochondrial morphology has previously been linked to function in immune cells such as T-cell fate (143) and phagocytosis in peritoneal macrophages (125). The mitochondrial electron transport chain provides an electro chemical gradient to drive ATP synthesis. This gradient generates mitochondrial membrane potential, a key indicator of mitochondrial health and function. Mitochondrial membrane potential was also demonstrated to have circadian rhythmicity, which was linked to phagocytosis in peritoneal macrophages (125). The alterations in morphology exhibited by mitochondria are likely to become an increasingly important topic in the field of circadian immunometabolism.

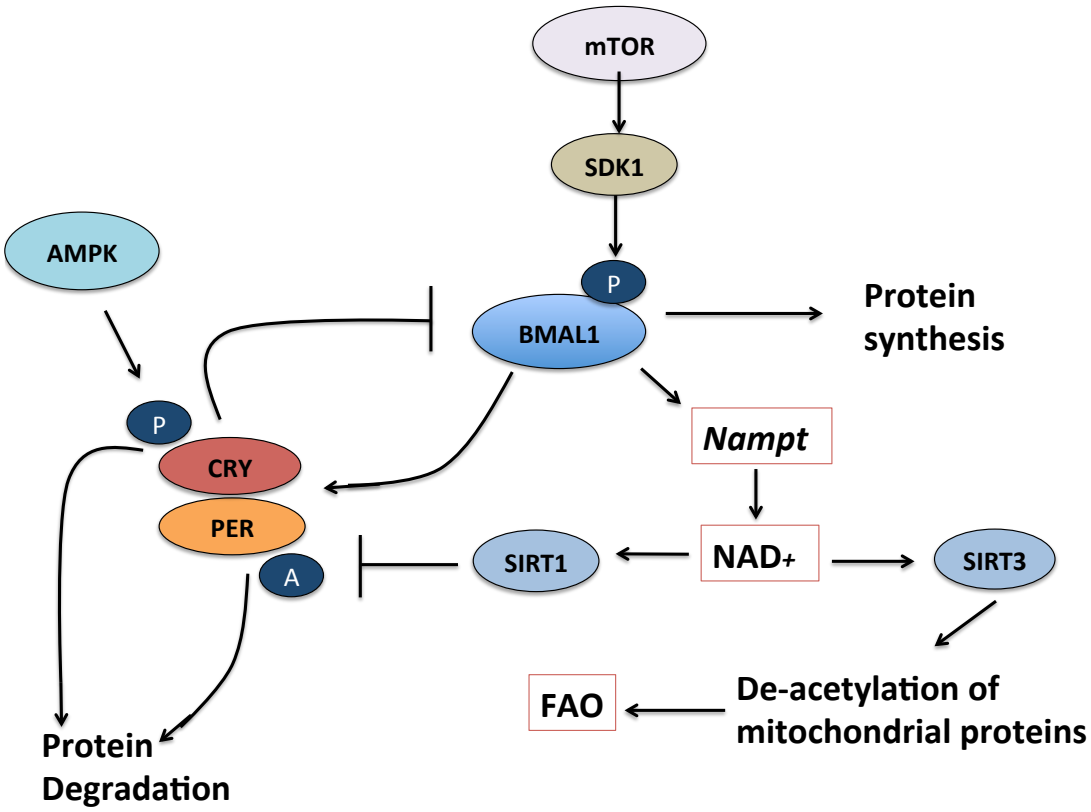

Figure 1.9 BMAL1 in cellular metabolism

The mTOR pathway acts through SDK1 to phosphorylate BMAL1, driving protein synthesis. BMAL1 drives expression of *Nampt,* the rate-limiting enzyme in NAD+ synthesis, and the cofactor for sirtuin de-acetylases. SIRT3 activity leads to de-acetylation of multiple mitochondrial proteins resulting in increased FAO. SIRT1 can feedback to promote BMAL1 activity by de-acetylating PER, reducing its ability to repress BMAL1:CLOCK. AMPK can similarly boost the activity of BMAL1 by phosphorylating CRY, inhibiting its activity.

1.3 Oxidative stress

A major alteration that occurs in macrophages during inflammation is the accumulation of ROS (144). This is largely facilitated by alterations to the electron transport chain within the mitochondria, which ultimately results in accumulation of free oxygen radicals such as peroxides and superoxides (145). To counteract this, antioxidants are produced to limit oxidative stress and maintain homeostasis within the cell (146).

1.3.1 ROS production

The original understanding of ROS was as an unwanted by-product of metabolism, which could act as a threat to cellular homeostasis through non-specific damage to biological molecules, or as a useful molecule for bacterial killing in the phagasome (147). However, in recent years a different picture has begun to emerge. What is now clear is that ROS can act as a signalling molecule, often as a secondary messenger (148). The function of ROS depends on the source and context of its release. Specifically, it has become clear that ROS promotes a pro-inflammatory phenotype in macrophages following TLR4 induction by LPS (149). However, the exact source of ROS during inflammation has long been debated.

There are multiple sources of ROS within the cell. The first and most well characterised are the NADPH oxidases, which are critical for host defence (150). NADPH oxidases are multi-protein complexes that can transfer electrons across biological membranes, generating superoxide in the process (147). This superoxide can then be transformed into ROS following downstream reactions, most commonly hydrogen peroxide. This enzyme family consists of seven members, NADPH oxidase (Nox) 1,2,3,4 and 5, and dual oxidase (Duox) 1 and 2 (147). These proteins display varied expression patterns depending on tissue type (147). While being involved in

host defence, many more roles of these proteins have been discovered, including regulation of gene expression, cellular signalling and post-translational processing of proteins (151, 152). Interestingly, while *Nox2* is crucial in phagocytes for bactericidal activity, it appears to play an anti-inflammatory role during response to sterile inflammation. Mice lacking components of the *Nox2* complex exhibit heightened neutrophil response during sterile peritonitis (153), develop spontaneous arthritis and produce more pro-inflammatory cytokines from $CD11b^{+}Gr\text{-}1^{+}$ myeloid cells (154). Whether ROS derived from NADPH activation is important during LPS induced inflammation is not well documented.

1.3.2 Mitochondrial ROS

ROS is also generated by metabolic processes, either mitochondrial or non-mitochondrial in origin (147). Many catabolic enzymes with oxidase activity generate ROS as part of their enzymatic activity, however the extent to which ROS produced from this source contributes to sterile inflammation is yet unclear (147). On the other hand, mitochondria as a source of inflammatory potentiating ROS has undergone an explosion of research in recent years (147).

As mentioned, it has become clear that during LPS induced activation of macrophages, a large boost in oxidative stress is observed. It is believed that a large portion of this oxidative stress is in fact mitochondrial ROS, which is generated as a consequence of a "leaky" oxidative phosphorylation process (145). Electrons move through the enzyme complexes of the electron transport chain, driving ATP production. Leak of electrons leads to one electron reduction of oxygen to produce superoxide. Most superoxide is efficiently converted to hydrogen peroxide (H_2O_2) by SOD2 (MnSOD) within the matrix of the mitochondria or by SOD1 (Cu/ZnSOD) in the intermembrane space. H_2O_2, unlike superoxide, can diffuse into the cytoplasm, acting as a redox signal from the mitochondria

to the rest of the cell (155). The generation and movement of ROS are tightly regulated within the mitochondria to preserve cellular integrity and to prevent damage induced by ROS dependent signalling and cellular damage (156). A multitude of protein complexes within the mitochondria are responsible for superoxide production (157). Within the electron transport chain (ETC), the prime ROS producers are complex 1 (mitochondrial matrix release) and complex 3 (mitochondrial matrix and intermembrane space release) (157). Interestingly, it has recently been demonstrated that mitochondrial ROS is particularly important during LPS induced inflammation, with activated macrophages repurposing mitochondria to switch from ATP production to ROS generation, facilitating production of HIF-1α induced IL-1β (132).

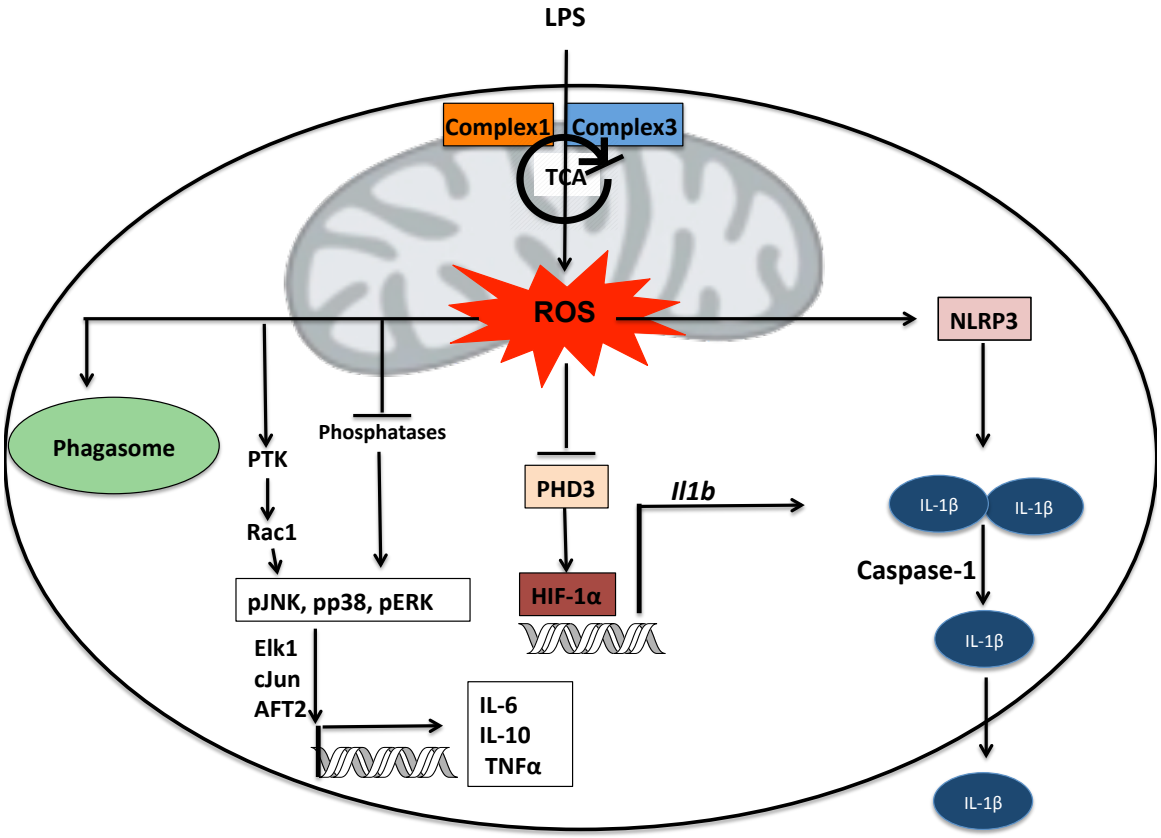

Figure 1.10 Mitochondrial ROS in immunity

LPS initiates changes in macrophage metabolism facilitating a switch from OXPHOS to primarily glycolysis. As a result, electron flow along the TCA cycle is impinged, generating ROS, largely from complex 1 and 3. The ROS from complex 1 may be used in the phagasome for bactericidal activity. It can also drive cytokine production. One mechanism for this is to sustain MAPK phosphorylation, either by inhibiting phosphatase activity or by directly inducing phosphorylation via protein tyrosine kinase (PTK) and Rac1. MAPK activates a host of transcription factors, such as E26 transformation-specific domain-containing protein (Elk1), cJzun and activator of iron transcription (AFT2). The other mechanism for cytokine production is inhibition of PHDs to facilitate HIF-1α mediated transcription of *Il1b.* Recent studies have hinted that mitochondrial ROS may drive NLRP3 inflammasome activation.

1.3.3 Circadian regulation of ROS

Several studies have linked ROS production to the molecular clock and BMAL1. Global deletion of *Bmal1* in mice leads to a plethora of pathologies including metabolic-circadian uncoupling, immune deregulation and accelerated ageing (158, 159). The ageing phenotype correlates positively with increased ROS production. Supplementing the diet of *Bmal1*$^{-/-}$ mice with N-acetyl L cysteine (NAC), a potent antioxidant, extends their lifespan (160). *Bmal1* deletion in pancreatic beta cells leads to extensive ROS induced oxidative damage and subsequent mitochondrial uncoupling, resulting in a loss of glucose stimulated insulin secretion and diabetes in these mice (161). Once again, it was possible to rescue this phenotype with administration of NAC. A third study links loss of *Bmal1* in the brain to astroglyosis and neurodegeneration (162). Loss of *Bmal1* results in suppressed antioxidant response, facilitating ROS induced damage and cell death. In the aforementioned study linking BMAL1 to mitochondrial dynamics, it was also discovered that cells lacking *Bmal1* produce greater levels of mitochondrial ROS in liver cells (142). It appears that in playing a role in mitochondrial architecture in the cell, BMAL1 also regulates mitochondrial ROS production.

Whether regulation of metabolism and ROS by the molecular clock is pertinent to inflammation is still largely unexplored. However, a recent study has linked circadian mediated regulation of immune cell trafficking to endogenous ROS levels (76). It was shown that rhythms in ROS levels promoted rhythms in HIF-1α stability in leukocytes (76). When HIF-1α was high it would bind to the BMAL1:CLOCK heterodimer, facilitating rhythms in *Cxcr4* production . Ultimately this leads to tissue migration at specific time-of-day that could be disrupted with NAC mediated scavenging of ROS (76). Whether this interaction between the circadian cycle, ROS and HIF-1α could have connotations in terms of the immune response is yet to be explored.

1.4 Antioxidants

It is one of the many paradoxes of life that while most organisms require oxygen for existence, this molecule can become highly reactive and is capable of causing damage to cells and tissues. For this reason antioxidants are produced to inhibit the oxidation of biological molecules and to provide balance to the oxidative state of cells via complex and often overlapping systems (163). In general, anti-oxidants serve as a counter balance to ROS, either preventing its formation, removing it before damage is caused, or, keeping certain ROS at optimum levels to act as signalling agents in cellular functions (146, 164).

1.4.1 NRF2 antioxidant defence pathway

Nuclear factor (erythroid-derived 2)-like 2 (NRF2) is a transcription factor that plays a major role in regulating the expression of anti-oxidant proteins. It functions to protect against oxidative damage that is triggered by ROS induced injury or inflammation (165). Importantly, NRF2 is expressed in macrophages and has a role in limiting ROS induced inflammation (166). Under basal conditions NRF2 is restricted to the cytoplasm by Kelch like-ECH-assoiciated protein 1 (KEAP1) which allows NRF2 to be continually targeted for ubiquitination and degradation by the proteasome (167). Upon initiation of oxidative stress, critical cysteine residues in KEAP1 are oxidised, preventing Cullin-3 assisted ubiquitination of NRF2 (168, 169). This facilitates accumulation of NRF2 in the cytoplasm leading to its translocation to the nucleus (Fig. 1.7). Within the nucleus NRF2 forms heterodimers with Maf proteins and binds to antioxidant response elements (AREs) upstream of several antioxidant genes, inducing their expression (170). NRF2 induces the expression of two key antioxidant genes, heme-oxygenase-1 (*Hmox-1*) (171) and NADPH:quinone oxidoreductase-1 (*Nqo1)* (172). HMOX-1 catalyses the breakdown of the pro-

oxidant heme into the antioxidant biliverdin, the anti-inflammatory agent carbon monoxide, and iron (173). NQO1 utilises NADPH to catalyse the reduction of oxidative quinones that lead to oxidative stress (172). In addition to direct regulation of antioxidant genes, NRF2 is crucial in the production and maintenance of the master redox molecule, glutathione (GSH). GSH is a potent antioxidant, capable of acting as an electron donor, reducing disulfide bonds in cytoplasmic proteins. In return GSH is oxidised to glutathione disulfide (GSSG). NRF2 induces expression of glutamate-cysteine ligase catalytic (*Gclc*) and glutamate-cysteine ligase modifier (*Gclm*), which form heterodimers providing the rate-limiting step of GSH synthesis (174). NRF2 is also capable of replenishing the GSH pool by inducing expression of glutathione reductase (*Gsr*), which converts GSSG to GSH (175). The ratio of GSH:GSSG is crucial to the oxidative state of cells.

A link has previously been established between the molecular clock and NRF2. The BMAL1:CLOCK heterodimer was demonstrated to be important in regulating anti-oxidant defence in the lung via rhythmic transcriptional activation of *Nrf2* via E-box binding sites (176). Disruption of the clock in mutant mice was shown to result in a loss of rhythmic transcription and expression of *Nrf2* mRNA and protein. Ultimately this resulted in reduced levels of total GSH and increased oxidative damage dealt to the lungs in a model of pulmonary fibrosis (176). Circadian regulation of NRF2 was also shown in the liver, with NRF2 targets genes and GSH shown to display diurnal rhythms (177). However, the molecular clock does not regulate NRF2 in all tissues. The BMAL1:CLOCK heterodimer was found to bind to the promoters of *Nqo1* and *Aldh2,* inducing their expression directly in the cerebral cortex, and not through the intermediate of NRF2 transcriptional regulation (162). Whether oxidative damage and inflammation in macrophages is under regulation of molecular clock mediated control of NRF2 has not yet been researched.

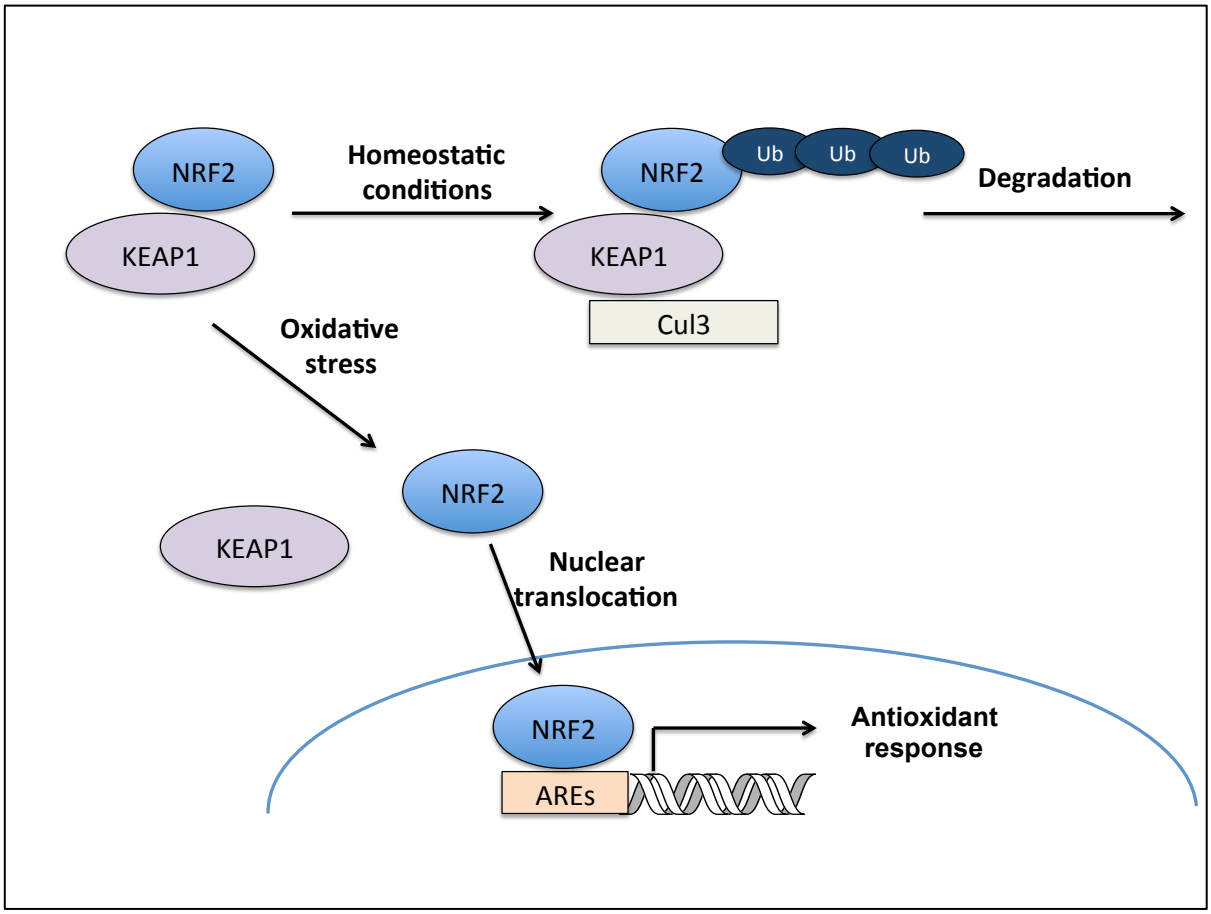

Figure 1.11 The NRF2 pathway

NRF2 is continually expressed in macrophages. Under homeostatic conditions, NRF2 remains bound in the cytoplasm by KEAP1. Cul3 assists in promoting ubiquitination and degradation of NRF2, facilitating constant turnover of the protein. Under oxidative stress conditions NRF2 is freed from KEAP1. Upon accumulation, NRF2 translocates to the nucleus where it may bind to antioxidant response elements in the promoters of certain genes, facilitating the initiation of the antioxidant defence response.

1.4.2 NRF2 in inflammation

In providing a role as a mediator of antioxidant defence, it is no surprise that NRF2 has been demonstrated to possess anti-inflammatory properties under numerous conditions. However, very little has been described on NRF2's specific role as an antioxidant to combat ROS induced inflammation. It has recently been discovered that itaconate is important in freeing NRF2 from KEAP1 mediated regulation following LPS stimulation (Dylan and Mills et.al. 2018 (in press)). Addition of exogenous octyl-Itaconate (OI), a synthetic cell permeable version of itaconate, boosts levels of NRF2 following LPS stimulation (Dylan and Mills et.al. 2018 (in press)). This boost in NRF2 decreases ROS induced HIF-1α, glycolysis, and overall results in reduced LPS induced IL-1β production (Dylan and Mills et.al. 2018 (in press)). This highlights a connection between antioxidant defence, metabolism, and regulation of IL-1β production.

NRF2 has previously been linked to regulation of both IL-1β and IL-6, independent of its role as an antioxidant mediator. NRF2 was found to bind to specific, non-antioxidant response elements, in the promoters of these cytokines, inhibiting RNA Polymerase II recruitment (166). Diethyl maleate (DEM), an NRF2 activator, but not NAC, was able to decrease levels of *Il1b* and *Il6* transcription, demonstrating that this effect was outside of ROS regulation (166). However, this study was carried out after acute LPS activation of macrophages (no later than 4 hrs treatment of LPS), at which ROS regulation is less critical. In later stages of macrophage activation (24 hrs treatment of LPS), ROS levels accumulate, leading to a stabilization of HIF-1α to drive IL-1β production (132). It is likely that at later time points following LPS stimulation that both the antioxidant effect of NRF2 and the direct binding activity to the *Il1b* promoter regulate IL-1β production.

Whether NRF2 plays a role in regulation of IL-1β processing by the NLRP3 inflammasome has been assessed in multiple studies, however, the literature on this topic is contradictory. Elevated ROS has previously been reported as being required for NLRP3 inflammasome activation (178-180). Activating NRF2 with tert-Butylhydroquinone (tBHQ) negatively regulates NLRP3 activation by inhibiting the priming step of activation (181). Dimethyl fumarate (DMF), another NRF2 activator, has been demonstrated to limit a mouse model of colitis by inhibiting NLRP3 inflammasome activity (182). Various other papers have linked synthetic NRF2 activation to a decrease in NLRP3 activity (183, 184). However, defective activation of NLRP3 and AIM2 has been demonstrated in mouse macrophages with genetic deletion of *Nrf2,* suggesting that NRF2 is crucial to effective inflammasome activation (185). Further study is required to fully discern the role of NRF2 in inflammasome regulation.

1.5 Aims

The overall aim of this project was to investigate the molecular mechanisms by which BMAL1 and the molecular clock may regulate inflammation in macrophages. Specifically, my focus was on regulation of the critical pro-inflammatory mediator IL-1β. The following specific aims were established:

1.) Determine the effect of BMAL1 on regulation of NRF2 in macrophages.
2.) Examine the role of BMAL1 in regulating oxidative stress in macrophages.
3.) Examine the effect of *Bmal1* deletion on metabolism in macrophages.
4.) Investigate the pro-inflammatory phenotype of cells with altered molecular clocks.
5.) To assess whether ROS scavenging and/or NRF2 activation could rescue the pro-inflammatory/IL-1β phenotype of *Bmal1* knockout macrophages.

This study has defined the role of *Bmal1* in regulation of LPS induced oxidative stress in macrophages and antioxidant regulation. Furthermore, I link this to regulation of metabolism and the pro-inflammatory cytokine IL-1β. I have also uncovered an interesting link between BMAL1 and regulation of cleaved IL-1β activation by the inflammasome that appears to be at least partially dependent on oxidative stress regulation. Overall, this study reveals a novel mechanism by which the circadian clock may regulate inflammation in macrophages.

Chapter 2: Materials and methods

2.1 Materials

2.1.1 Buffers

Buffer Name	Buffer Composition
Sample lysis buffer (5X)	10% (v/v) glycerol, 2% (w/v) sodium dodecyl sulphate (SDS), 200μg/ml bromophenol blue, 215mM Tris pH 6.8 50μl of 1M DTT (dithiothreitol) is added per ml of 5X sample lysis buffer
SDS-PAGE running buffer (10X)	30.3g 25mM Tris, 144g 192mM glycine, 10g 0.1% SDS. Made up to 1L with distilled H_2O
SDS-PAGE transfer buffer (10X)	0.25M Trizma base, 1.9M Glycine, 35mM SDS.
Tris-buffered saline (TBS) Tween (TBST) (10X)	12.11g Tris, 87.6g NaCl, 10ml Tween-20.
PBS	1.45M NaCl, 39mM NaH_2PO_4
ELISA wash buffer	0.05% Tween-20 in PBS, pH 7.2-7.4

Table 2.1 Buffer compositions

2.1.2 Reagents for cell culture

Dulbecco's modified Eagle medium (DMEM) and Roswell Park Memorial Institue medium 1640 (RPMI) were acquired from Gibco Biosciences. Foetal calf serum (FCS), Horse serum, penicillin/streptomycin (P/S), sterile PBS and Trypsin-ethylenediaminetetraacetic acid (Trypsin-EDTA) were obtained from Sigma-Aldrich. Lipofectamine RNAimax was purchased from Thermo Fisher Scientific,

2.1.3 Animals

All mice were maintained according to European Union regulations and the Irish Health Products Regulatory Authority. Experiments were performed under Health Products Regulatory Authority license with approval from the Trinity College Dublin BioResources Ethics Committee.

C57BL/6 wild-type mice (Harlan UK) were bred in house from established colonies. Mice with the gene *Bmal1* containing LoxP sites at either side of exon 8 were obtained from Jackson Labs (stock no. 007668). $Bmal1^{LoxP/LoxP}$ were crossed with $Lyz2^{Cre}$, which express Cre recombinase under the control of the Lyz2 promoter (which encodes LysozymeM) to produce progeny that have *Bmal1* excised in the myeloid lineage (monocytes, macrophages, and granulocytes). $Bmal1^{LoxP/LoxP}Lyz2^{Cre}$ ($Bmal1^{Myeloid-/-}$) mice where compared with control $Lyz2^{Cre}$ ($Bmal1^{Myeloid+/+}$). Offspring were genotyped to confirm the presence of LoxP sites and Cre recombinase.

All mice were housed under specific pathogen free conditions.

2.1.4 Primary cells and cell lines

All mice were euthanised humanely by carbon dioxide inhalation before extraction of Bone marrow derived macrophages (BMDMs) and peritoneal cells (PECs). L929 and RAW264.7 cells were purchased from Sigma-Aldrich.

2.1.5 Laboratory chemicals

NaCl, NaH_2PO_4, Na_2HPO_4, glycerol, SDS, DTT, glycine, Tris, Tween-20, BSA, diethyl maleate and N-acetyl-L-cysteine, GSK4112, SR9009, SR8278 and KL001 were purchased from Sigma-Aldrich.

2.1.6 Western blotting reagents

Sodium dodecyl sulphate (SDS), N, N, N', N' Tetramethylethylenediamine (TEMED), ammonium persulphate (APS), Tris, HCL and acrylamide:bisacrylamide were obtained from Sigma-Aldrich. ECL LumiGlow was purchased from Cell Signalling. Thermo Scientific Spectra multicolour marker was used. Polyvinylidene difluoride (PVDF) was sourced from Millipore. Marvel powdered milk was acquired from Tesco.

2.1.7 Antibodies

Antibody	Company	Dilution
Pro-IL-1β	R&D Systems	1:2000
Beta actin	Sigma-Aldrich	1:10,000
HIF-1α	Novus	1:1000
NRF2	Cell signalling	1:1000
BMAL1	Cell signalling	1:1000
KEAP1	Cell signalling	1:1000
Caspase 1	Adipogen Life Sciences	1:1000
Anti-Goat secondary	Jackson ImmunoResearch	1:2000
Anti-Mouse secondary	Jackson ImmunoResearch	1:2000
Anti-Rabbit secondary	Jackson ImmunoResearch	1:2000

Table 2.2 Antibodies

2.1.8 PCR

RNase-free H_20 and RNeasy plus mini kits were acquired from Qiagen. Reverse Transcription Kit was sourced from Applied Biosystems. SYBR primers were designed in house and ordered from MWG, see Table 2.3 for sequences. Taqman primers (*Bmal1, Nr1d1, Per2* and *18s)* were purchased from thermofischer. Kapa RT mastermix or Taqman master mix was used for real time qPCR. 8-strip PCR tubes, caps and plate seals were purchased from Fisher Ireland. qPCR 96 well plates were acquired from Applied Biosystems.

2.1.9 Enzyme-lined-immunoabsorbant assays (ELISA)

Mouse TNFα, IL-6, IL-10 and IL-1β Duoset ELISA kits were obtained from R&D Biosystems. 3,3',5,5'-tetramethylbenzidine (TMB) substrate were purchased from R&D Biosystems. Tween-20 and bovine serum albumin (BSA) were obtained from Sigma-Aldrich. HCL was purchased from Sigma-Aldrich.

2.1.10 GSH kit

GSH-Glow glutathione assay was purchased from Promega.

2.1.11 FACs and confocal reagents

CellROX deep red reagent and Aqua live/dead stains were obtained from molecular probes. Mitotracker red and green were purchased from Thermo Fisher.

2.1.12 Seahorse reagents

XF assay buffer, Seahorse cell culture plates, utility plates, calibrant solution, mitostress test and glycostress tests were obtained from Seahorse Biosciences. 2-deoxyglucose (2DG), glucose, glutamine and oligomycin were obtained from Sigma-Aldrich.

2.1.13 LDH assay kit

CytoTox 96 Non-Radioactive Cytotoxicity Assay was purchased from Promega.

2.1.14 BCA assay

Pierce BCA Protein Assay Kit was purchased from ThermoFisher Scientific

2.1.15 Subcellular frationation

Cytosolic and nuclear protein fractions were isolated using the Qproteome Cell Compartment Kit from Qiagen.

2.2 Methods

2.2.1 Culture of L929 cells

L929 cells were cultured in RPMI supplemented with 10 % FCS and 1 % P/S and maintained in a humidified incubator at 37 °C, 5 % CO_2. Cells were washed in PBS, removed from the flask using trypsin-EDTA, centrifuged, resuspended and seeded at $0.5x10^6$ cells/ml in T175 flasks. The cells were sub cultured every 7 days and the medium harvested, sterile filtered and stored at -20 °C. This supernatant was utilised as a source of MCSF for BMDM differentiation.

2.2.2 BMDM isolation

Mice were euthanized in a CO_2 chamber, followed by cervical dislocation to confirm death. The following procedures were then carried out aseptically in a laminar flow biosafety cabinet. An incision was made in the central abdomen, and the skin pulled down over the hind legs and removed. Bone was severed at the ankle and the feet were removed and discarded. An incision into the muscle was made close and parallel to the spine, and the tibia, femur and hipbone were removed. The muscle was removed from these bones and DMEM flushed through each using a 23 G syringe inserted into the exposed bone cavity. The flow through containing the bone marrow was collected in a sterile 50 ml tube. The bone marrow was centrifuged at 1500 rpm for 5 minutes and the supernatant discarded. The cell pellet was resuspended in 3 ml red cell lysis buffer, incubated for 5 minutes, and the reaction ended by the addition of 30 ml DMEM. The cells were then passed through a 70 μM cell strainer and centrifuged at 1500 RPM for 5 minutes prior to resuspension in 30 ml DMEM (plus 10 % FCS, 1 % P/S and 20 % L929 supernatant). 10 ml of the cell

suspension was plated per petri dish. The cells were cultured for 6 days, cells were then scraped, counted and replated in DMEM supplemented with 10 % FCS, 1 % P/S and 10 % L929 supernatant for experiments.

2.2.3 Peritoneal cell isolation

Mice were euthanized in a CO_2 chamber. The following procedures were then carried out aseptically in a laminar flow biosafety cabinet. An incision was made in the central abdomen, and the skin pulled down over the hind legs. A 23 G syringe was inserted into the peritoneal cavity and a lavage was carried out with 3 ml sterile PBS. The lavage was harvested using the same 23 G needle. The cells isolated were plated and allowed to settle for 30 minutes in DMEM supplemented with 10 % FCS and 1 % P/S. The media was removed and replaced to leave myeloid cell population adhered to the plate before experimental treatments were performed. For circadian experiments, the peritoneal cells (PECs) were allowed to settle for 30 minutes after extraction before lysis.

2.2.4 siRNA transfection

BMDMs were seeded at at $5x10^5$ cells/ml in a 12 well plate and incubated overnight at 37°C. 50 µM stock siRNA was diluted 1:10 in serum and P/S free media and pipetted up and down. Once this was done the larger volume was then diluted 1:50 in media (total dilution was now 1:500). For example, if carrying out transfection in 6 wells, 3 µl of 50 µM stock was diluted in 27 µl of media. This was then added to 1470 µl of serum and P/S free media and mixed. 2.5 µl of lipofectamine was used for each well in a transfection. For example, if carrying out transfection in 6 wells 15 µl of lipofectamine was added to 1485 µl of serum and P/S free media and mixed and allowed to sit for 5 minutes. The siRNA and lipofectamine were then combined (in

the above example this would give a final concentration of 50 nM siRNA in solution). This was pipetted up and down and allowed to incubate for 15 minutes. Media was then removed from the cells and 500 µl of the media containing 50 nM siRNA was added to each well. This was incubated for 24 hrs before treatments began. A negative control siRNA was used in each experiment.

Target	**Order code (Thermo Fisher Scientific)**
Bmal1	4390771/562620
Nrf2	4390771/570522
Keap1	4390771/578525
Scrambled Negative Control	4390843

Table 2.3 siRNA used

2.2.5 Western blotting

2.2.5.1 Lysis and denaturation

Media was removed from cells before addition of 50 µl SDS lysis buffer per well. Cells were scraped to ensure maximal harvest of lysate. Lysates were placed in 1.5 ml eppendorf tubes and heated to 95°C for 10 minutes to denature the proteins. These samples were stored at -20°C before use.

2.2.5.2 SDS polyacrylamide gel electrophoresis (SDS-PAGE)

SDS-PAGE was used to separate proteins by molecular weight. Samples were run at 25 mA/gel through a 5 % stacking gel, followed by a 10 or 12 % resolving gel.

Spectra pre-stained molecular markers were also run to reference band size. See table 2.4 for gel compositions.

	10% Resolving Gel	**12% Stacking Gel**	**5% Stacking Gel**
Distilled H_2O	5.9ml	4.9ml	4.1ml
Protogel	5.0ml	6ml	1ml
Tris pH 6.8	-	-	750ul
Tris pH 8.6	3.8	3.8	-
10% SDS	150ul	150ul	60ul
10% APS	150ul	150ul	60ul
TEMED	6ul	6ul	6ul

Table 2.4 Gel compositions

2.2.5.3 Electrophoretic transfer of proteins to membrane

Proteins were transferred from resolved gel to PVDF membrane by semi-dry or wet transfer. For semi-dry transfer, two pieces of filter paper were soaked in SDS-PAGE transfer bugger and place on the semi-dry transfer plate. A piece of PVDF was sprayed with 100% °minutes. For wet transfer the Atto wet transfer system (Atto) was used. The same transfer sandwich as in the semi dry transfer protocol was placed between two sponges. The sandwich was then placed into a transfer cassette with the gel on the black (cathode) side of the cassette, and the PVDF membrane on the white (anode) side of the cassette. The cassette was loaded into a transfer buffer filled tank and was run at 200 mA per box for 2 hours and 30 minutes.

2.2.5.4 Antibody incubation and visualisation

Following transfer, the PVDF membrane was blocked in 5 % (w/v) milk powder for 1 hour at room temperature. This was to prevent non-specific binding of antibody to the membrane. The membrane was then incubated at 4°C in primary antibody diluted in 5 % milk powder overnight. The membrane was washed 3 times in TBST, 5-10 minutes per wash, before incubating the membrane in secondary antibody dilute in 5 % milk powder for 1 hour. The membrane was washed 3 times in TBST again. Chemiluminescent substrate was added directly to the membrane before visualising the protein with the ChemiDoc MP gel imaging system (Biorad).

2.2.6 RNA extraction and analysis

2.2.6.1 RNA isolation

RNA extraction was carried out using a Qiagen Rneasy kit. Cells were lysed in 350 µl RLT lysis buffer and processed according to the manufacturer's instructions. RNA was quantified using a Nanodrop 2000 spectrophotometer and RNA was diluted to normalise concentrations accordingly. The RNA was then kept on ice and ustilised to make cDNA or was stored at -20°C.

2.2.6.2 Reverse transcription polymerase chain reaction (RT-PCT)

The RNA was converted to cDNA using the High-Capacity cDNA Reverse Transcription Kit (Applide Biosystems) according to manufacturers instructions. See table 2.5 for the reaction mix used. cDNA was dilted 1:5 in nuclease free H_2O and was stored at -20°C.

Reagent	Volume (μl)
10X RT Buffer	2.0
10X Random Primers	2.0
dNTPs	0.8
Multiscribe reverse transcribe enzyme	1.0
Nuclease-free H_2O	4.2
RNA	10.0

Table 2.5 RT-PCR Reaction mix

2.2.6.3 Quantification of mRNA targets

Quantitative PCR (qPCR) was carried out on cDNA using either specific custom designed primers (SYBR probes) or specific primers ordered from Thermo Fisher (Taqman probes). A list of SYBR primers used and their sequecnes can be found in table 2.6. Taqman primers used and order codes can be found in table 2.7.. The reaction mix for SYBR protocol can be found in table 2.5. The reaction mix for Taqman protocol can be found in table 2.6. The qPCR runs were done in a 96 well qPCR plate in an Applied Biosystems 7900 HT machine using a Fast PCR protocol. Relative expression was determined by ΔΔCt calculation for one internal control gene.

Target	Forward Sequence	Reverse sequence
Il-1b	GGAAGCAGCCCTTCATCTTT	TGGCAACTGTTCCTGAACTC
Rps18	GGATGTGAAGGATGGGAAGT	CCCTCTATGGGCTCGAATTT
Bmal1	TGCAATGTCCAGGAAGTTAGAT	GTTTGCTTCTGTGTATGGGTTG
Nrf2	CACATCCAGACAGACACCAG	ATGGGAATGTCTCTGCCAAA
Hmox1	GGAAGCAGCCCTTCATCTTT	TGGCAACTGTTCCTGAACTC
Gsr	GGAAGCAGCCCTTCATCTTT	TGGCAACTGTTCCTGAACTC
Nqo1	GCTGCAGACCTGGTGATATT	TGTAGGCAAATCCTGCTACG
Ldha	ATCTTGACCTACGTGGCTTGGA	CCATACAGGCACACTGGAATCTC
Hk2	TCGCCTGCTTATTCACGGAG	TCGCCTGCTTATTCACGGAG
Gapdh	TGTGTCCGTCGTGGATCTGA	CCTGCTTCACCACCTTCTTGAT
Phd3	TGCTGAAGAAAGGGCAGAAG	GCACACCACAGTCAGTCTTTA
Irg1	TGTTGCTGTTCACTCCATGGAT	TGTCTTTGGCTTCCTTGGAGAA
Gclm	TGGAGTTCCCAAATCAGCCC	TGCATGGGACATGGTGCATT
Nlrp3	CTCCCGCATCTCCATTTGT	CCCTCTATGGGCTCGAATTT

Table 2.6 SYBR primer sequences

Target	Assay ID ThermoFisher Scientific
Bmal1	Mm00500226_m1
Nr1d1	Mm00520708_m1
Per2	Mm00478113_m1
18s	Mm03928990_g1

Table 2.7 Taqman primer list

Reagent	Volume (µl)
SYBR Green FastMix	5
Specific Primer	0.3
Nuclease-free H_2O	0.7
cDNA	4

Table 2.8 SYBR PCR reaction mix

Reagent	Volume (µl)
Taqman mix	5
Specific Primer	0.25
Nuclease-free H_2O	0.75
cDNA	4

Table 2.9 Taqman PCR reaction mix

2.2.7 ELISA

Duoset ELISA kits for mouse IL-1β, IL-6, IL-10 and TNFα were utilised according to manufacturer's instructions to determine cytokine concentrations in appropriately diluted cell supernatants. TMB substrate and 1M H_2SO_4 stop solution were added before final measurement of absorbance at 450 nm using a FLUOstar Optima plate reader (BMG Labtech). Concentrations were determined from a standard range using a 4-parameter fit curve.

2.2.8 FACs analysis of cellular reactive oxygen species

BMDMs were cultured at $5x10^5$ cells per well. The following controls were used in each experiment: unstained cells, single stained cells (CellROX or Aqua Live/Dead stain alone), and dead cells (treated with 100% EtOH for 1 hour). After treatment, cells were stained with 5 μM CellROX (Invitrogen, US) for 30 minutes at 37°C and were protected from light. The media was then removed before adding 1 ml of PBS, containing 1:1000 Aqua Live/Dead stain, for 30 minutes at 37°C and were once again protected from light. Supernatants were removed before cells were washed in PBS three times. Cells were scraped in 1 ml PBS and transferred to polypropylene FACs tubes. The cells were analysed using a CyAn flow cytometer and FlowJo software. For circadian experiments, peritoneal cells were harvested and stained simultaneously with CellROX and $CD11b^+$ antibody. The same steps as listed above were then carried out.

2.2.9 Confocal imaging

BMDMs were cultured at $5x10^5$ cells per well. Cells were stained with 5 μM CellROX and 50 nM mitotracker green. The intracellular locus of ROS production was investigated by examining cells stained with CellROX using an epifluorescent live cell-imaging microscope (Zeiss ObserverZ1).

For assessment of mitochondrial membrane potential, cells were stained with 50 nM mitotracker red and 50 nM mitotracker green and were imaged using the x63 objective of a Zeiss LSM710 confocal microscope or for time-lapse microscopy images were acquired every 10 mins for 48 hrs using a wide-field epifluorescent microscope (Zeiss AxioObserver Z1) and a x63 oil immersion objective.

For quantification of ROS, Image J software was utilised. Images were converted to grey scale and an arbitrary threshold was determined, which was matched to the lowest intensity of CellROX staining. All pixels above this threshold were recoded as black and any below were set to background. The area of positive pixels per image was used as a semi-quantitative index of CellROX staining. At least 3 independent experiments would be combined to generate graphs.

2.2.10 Seahorse analysis

Cells were seeded overnight at $0.125x10^6$ cells/well in 250 µl DMEM supplemented with 10 % FCS and 1 % P/S and maintained in a humidified incubator at 37 °C, 5 % CO_2 in a specialised 24 well Seahorse cell plate. One well per row was left without cells in order to perform background measurements.

The following day, cells were treated with the required experimental conditions, and the volume of each well increased to 400 µl. The utility plate was prepared by addition of 1 ml of calibrant solution to each well and it was placed, along with the injector plate, in a CO_2-free incubator overnight. The Seahorse XF24 analyser was switched on to normalise system temperature and CO_2 concentration in advance of the run.

For testing initial glycolysis induction. One hr before the run, the medium was removed from the cells and replaced with 500 µL of prewarmed XF assay medium supplemented with glutamine. The cell plate was then placed in a CO_2-free incubator for one hr. LPS and 2DG were diluted in XF assay medium and added to the injector plate. The injector plate and utility plate were loaded into the Seahorse XF analyser for calibration. Following calibration, the utility plate was removed, the cell plate was loaded in its place and measurements commenced. LPS was injected into

selected wells following 30 minutes of recording. 2DG was later injected as a control to inhibit glycolysis.

For the glycostress test the same protocol was carried out except glucose, 2DG and oligomycin were loaded into the wells to be injected during the glycostress test protocol.

For mitostress test the same protocol was carried out except oligomycin, rotenone and antimycin A, and FCCP were loaded into the wells to be injected during the mitostress protocol.

2.2.11 Quantification of oxidative stress genes.

RT^2 Profiler Plates were used to screen for differences in Mouse Oxidative Stress pathways (Qiagen, Cat# PAMM-065ZC) between peritoneal cells isolated at ZT0 and ZT12 based on SYBR Green qPCR array. cDNA was generated from RNA samples using RT^2 First Strand Kit (Qiagen, Cat# 330401), and was mixed with SYBR Green qPCR Mastermix (Qiagen, Cat# 330520) and distributed to RT^2 Profiler plates which were preloaded with primer sets for pathway relevant genes. Amplification was then initiated in a real-time cycler 7900HT Fast (Applied Biosystems, Cat# 4351405) and data was analysed by the $\Delta\Delta C_T$ method.

2.2.12 Transcription factor sequencing

Transcription factor sequencing was performed as previously described by O'Connell et.al. (186). TF-seq lentiviral vectors were transfected into HEK293T cells. These vectors each contained a response element for a transcription factor of interest, a reporter gene, and a unique molecular identifier within their sequence. After 48 hrs the media containing a pool of lentiviral particles, which represented the TF-seq reporter library, were transfected into *Bmal1*$^{+/+}$ and *Bmal1*$^{-/-}$ BMDMs. After 72 hrs the BMDMs were re-plated into 96-well plates and left untreated or treated with LPS for 1 or 4 hrs before assay collection and assessment of transcription factor activity was carried out. Transcription factor activity was tested and separated on means of false discovery rate (FDR).

2.2.12.1 Serum shock

BMDMs were cultured at $5x10^5$ cells per well. Media was removed and cells were incubated in 50 % horse serum 50 % DMEM for 2 hours at 37°C. The supernatants were removed and the BMDMs were once again cultured in DMEM containing 10 % FCS and 1% P/S. RNA was extracted at indicated time points.

2.2.13 Glutathione assay

Free reduced glutathione was determined using the luminescence-based GSH-Glow glutathione assay (Promega) according to manufacturer's instructions**.** Luminescence measurements were performed in triplicates for each biological replicate and processed in a single run to aid comparative quantification. Relative luminescence units (RLUs) were corrected for background luminescence and converted to nanomoles per milligram of protein using a standard curve for reduced GSH. Values were normalised to cell number.

2.2.14 LDH assay

Cell death was determined using the CytoTox 96 Non-Radioactive cytotoxicity assay (Promega) according to manufacturers instructions. 30 minutes before completion of experiment 100 µl/ml of 10X lysis solution was added to a maximum LDH control well. Once experiment was completed 50 µl of each sample was taken and placed in a fresh 96 well plate. Plain media was used as a control for no LDH release. 50 µl of CytoTox 96 reagent was added to each well. The plate was covered in foil and incubated for 30 minutes at room temperature. 50 µl of stop solution was then added to each well and absorbance was read at 490 nm. LDH release was calculated relative to the maximum LDH release controls.

2.2.15 Inflammasome assays

BMDMs were cultured at $5x10^5$ cells per well. They were then primed with 100 ng/ml LPS for 3 hrs. For NLRP3 inflammasome stimulation, cells were treated with 5mM ATP for 1 hr before collection of supernatants and lysis of cells for protein or RNA extraction. For AIM2 inflammasome stimulation, cells were transfected with poly dA:dT for 3 hrs. 0.5 µg/ml poly dA:dT was mixed with 25 µl serum free media

per treatment. 1.5 µL Lipofectamine was mixed with 25 µL serum free media per treatment. The poly dA:dT and Lipofectamine were combined and allowed to rest for 20 minutes. 50 µl of the solution was then added to 450 µL serum free media in each well. After 3 hrs supernatants were collected and lysis of cells for protein or RNA was performed.

2.2.16 Subcellular fractionation

RAW264.7 cells were grown to confluence in T175 flasks and treated with 100 ng/ml LPS for 2, 4, 8 and 24 hrs. Cells were scraped and collected in PBS and centrifuged at 1000 x g for 5 minutes. Cytosolic and nuclear protein fractions were isolated using the Qproteome Cell Compartment Kit (Qiagen) according to manufacturers instructions.

2.2.17 BCA assay

Samples were lysed in lysis buffer without a colouring agent. 25 µl of each sample was placed into a well in a 96-well dish. Standards were generated from 0 µg/mL of protein (blank) to 250 µg/mL and 25 µl of each of these was added to the 96-well dish in technical replicate format. 200 µl of working reagent was added to each well and plate was incubated at 37°C for 30 minutes. Absorbance was then measured at 562 nm on plate reader.

2.2.18 Graphing of rhythms in peritoneal cells and serum shock

The data were plotted against time in hours and the presence of circadian patterns was assessed using multiple regression to fit a linearized cosinor model with a pre-

determined period of 24 hrs (187). Circadian patterns were indicated by statistical significance of the predicted cosinor (sine and cosine) regression coefficients. The cosinor model was defined by linear sine and cosine terms of transformations of the time variable in hours:

$$Y_i = M + \beta Cos(2\pi t_i / 24) + \gamma Sin(2\pi t_i / 24)$$

Where Y is time in hours, and M, b and g were predicted by regression (187). The cosinor curve provided a graphical representation of how closely the data approximated to the 24 hr periodicity of a circadian dataset, and the statistical significance of this was determined by testing the null hypothesis that the amplitude of the curve was equal to zero.

2.2.19 Statistical analysis

Data was evaluated on Prism5 and Stata 14 statistical software (StataCorp, College Station, TX). Differences were compared by using analysis of variance followed by tukey post-test analysis and/or paired or unpaired Student's *t* test, as appropriate. Results are presented as mean ± SEM from at least three independent experiments. Differences were considered significant at the values of $P < 0.05$ (*), $P < 0.01$ (**), and $P < 0.001$ (***).

Chapter 3: Results

BMAL1 mediated regulation of NRF2, oxidative stress, and metabolism

Much of the work presented in this chapter has been used in a publication that is currently being revised for PNAS titled "The Circadian Clock Protein BMAL1 Regulates IL-1β in Macrophages via NRF2" (Early J.O. et.al 2018).

3.1 Introduction

The molecular clock has been tightly linked with regulation of oxidative stress in multiple tissue types (1). Deletion of *Bmal1* was demonstrated to increase global levels of oxidative stress in mice, resulting in an advanced aging phenotype and tissue atrophy (158). This effect can be ameliorated by supplementation of antioxidants into the diet of these mice (160). Increases in oxidative stress were also shown with tissue specific deletion of *Bmal1*. In the pancreas, *Bmal1* deletion results in beta cell death and diabetes (161), whereas deletion in the brain results in astrogliosis and neurodegeneration (162). Oxidative stress is widely known as a driver of inflammation (188), especially within macrophages, thus examination of oxidative stress in macrophages lacking *Bmal1* was a crucial element of my studies.

The study demonstrating increased oxidative stress in pancreatic cells lacking *Bmal1,* showed that the NRF2 antioxidant defence pathway was also disrupted in these cells (161). This link between the circadian cycle and NRF2 has also been established in lung tissue, where the BMAL1:CLOCK heterodimer was shown to induce *Nrf2* expression in a circadian fashion (176). However, regulation of antioxidants by the molecular clock in the brain was previously shown to be independent of NRF2 (162). Therefore, a major element of my work was to uncover

whether *Nrf2* is under regulation of the circadian cycle in macrophages, and whether lack of this pathway in *Bmal1* deficient macrophages gives rise to increased oxidative stress. I also investigated whether there was any feedback mechanism linking oxidative stress and NRF2 to regulation of the circadian cycle.

Besides lack of antioxidant defence, alterations in metabolism are well established to alter the oxidative balance of a cell. Following LPS addition to macrophages, glycolysis is up regulated and mitochondrial oxidative phosphorylation is deregulated, giving rise to ROS production and HIF-1α stabilization (130, 132). The circadian cycle has previously been linked to metabolic regulation in liver cells (136), however its importance in regulating metabolism to dictate immune cell function has not previously been examined. For this reason, I investigated the extent of metabolic alterations in macrophages lacking BMAL1. I also began studies into alterations in mitochondria function across time-of-day. Mitochondria are a key source of ROS and have been shown to be critical in regulation of the innate immune response (132). Alterations to mitochondria in immune cells could explain circadian variation in a number of circadian associated immune pathologies.

3.2 Examining circadian mediated regulation of NRF2 in myeloid cells

3.2.1 *Nrf2* displays diurnal rhythms in myeloid cells

NRF2 is a master regulator of antioxidant response and a known regulator of inflammation in macrophages (166). BMAL1 mediated regulation of *Nrf2* has previously been demonstrated in both lung (189) and liver tissue (177). NRF2 has been shown to have E-box sites in its promoter that can be rhythmically bound by the BMAL1:CLOCK heterodimer, inducing circadian rhythms in its expression (189). However, molecular clock targets are known to differ greatly between cell types.

Given that NRF2 is known to respond to the oxidative stress induced by inflammatory stimuli such as LPS (190), I decided to investigate the level of circadian rhythmicity exhibited by NRF2 in myeloid cells.

I extracted peritoneal myeloid cells from mice every 4 hrs over a 24 hr period and extracted RNA for analysis of gene expression. Zeitgeber time (ZT) is defined as the time in hours following the onset of light in the animal facility. ZT0 corresponds to lights on and beginning of the resting phase, whereas ZT12 refers to lights off and beginning of the active phase. I first examined several clock genes expression levels to ensure circadian rhythms were present. I observed the expected rhythms in *Bmal1* (Figure 3.1A), *Nr1d1* (Figure 3.1B)*, and Per2* (Figure 3.1C) gene expression. A significant diurnal rhythm in *Nrf2* expression was then detected (Figure 3.1D), matching the expression pattern previously observed in lung tissue (189). This indicated that *Nrf2* mRNA is under circadian regulation in myeloid cells.

To further confirm rhythms in *Nrf2* expression, and to rule out the effects of light and/or cell extrinsic effect on the cycling of *Nrf2* mRNA, a serum shock experiment was performed. *Bmal1*$^{+/+}$ and *Bmal1*$^{-/-}$ BMDMs were synchronized with 50% horse serum and RNA was collected every 4 hrs for 36 hrs. Clear rhythms were observed in the expression of *Bmal1* (Figure 3.2A) and *Nrf2* (Fig. 3.2B) in *Bmal1*$^{+/+}$ BMDMs. However, *Nrf2* transcription was not rhythmic in *Bmal1*$^{-/-}$ BMDMs and its expression was constitutively lower. This result confirmed that circadian mediated regulation of *Nrf2* in macrophages is dependent on the presence of BMAL1.

3.2.2 Basal and induced levels of NRF2 are lower in *Bmal1 d*eficient macrophages

Given that NRF2 is induced in response to oxidative stress, which is often elevated in macrophages by immune stimuli such as LPS, I next examined the effects of LPS challenge on expression of *Nrf2* in unsynchronized *Bmal1*$^{-/-}$ BMDMs. It was found that the LPS induced boost in *Nrf2* transcription seen in *Bmal1*$^{+/+}$ BMDMs was largely absent in *Bmal1*$^{-/-}$ BMDMs (Figure 3.3A). At the protein level it was observed that NRF2 levels were decreased, both basally and following LPS stimulation, in *Bmal1*$^{-/-}$ BMDMs relative to *Bmal1*$^{+/+}$ BMDMs (Figure 3.3B). To exclude the possibility that deletion of *Bmal1* was impacting the differentiation of macrophages and thus leading to the observed alteration of *Nrf2* mRNA, I targeted *Bmal1* by siRNA in fully differentiated macrophages. Decreased expression of *Nrf2* mRNA was seen in response to LPS stimulation with siRNA knockdown of *Bmal1* (Figure 3.4A). Consistent with the effects observed in *Bmal1*$^{-/-}$ BMDMs, the protein level of NRF2 was severely decreased, both basally and following LPS stimulation with siRNA knockdown of *Bmal1* (Figure 3.4B). Where BMAL1 protein levels were low, NRF2 levels were similarly decreased. Thus, circadian and BMAL1 mediated regulation of NRF2, both basally and after LPS activation was demonstrated.

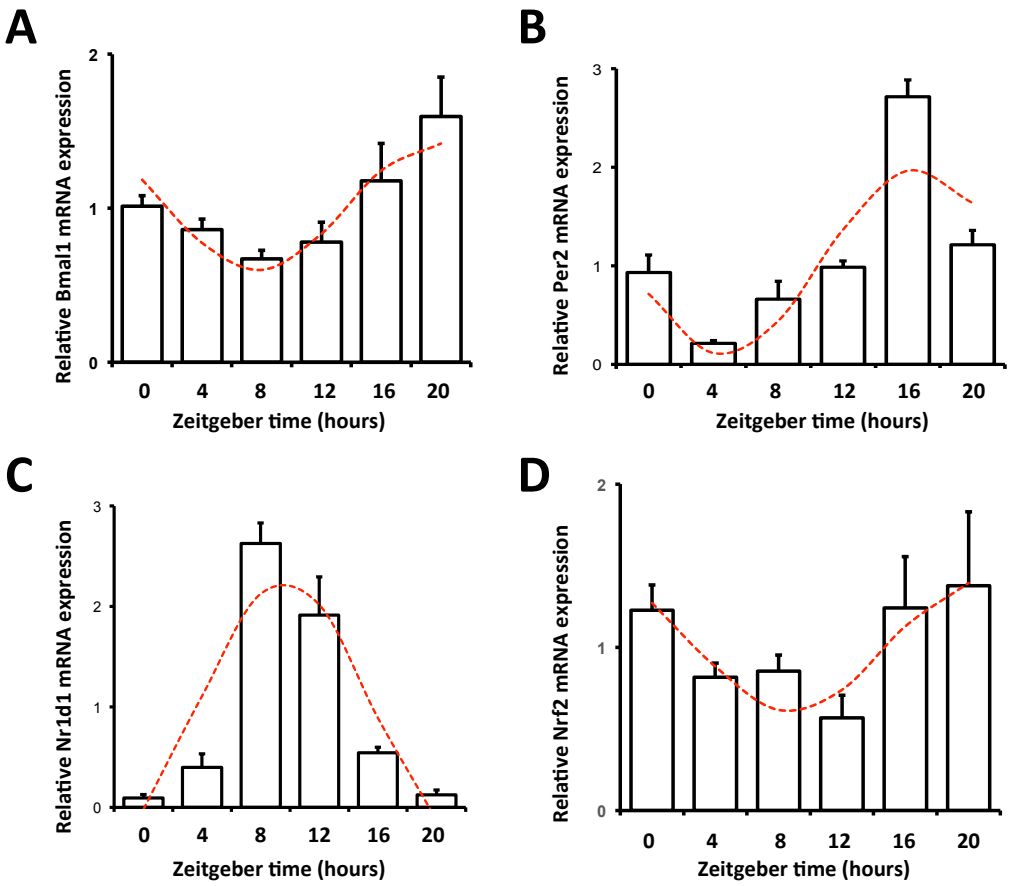

Figure 3.1. Dirunal rhythms are present in clock genes and *Nrf2* expression

Wild type mice were housed in a light cabinet for two weeks to adjust their circadian rhythms to a new cycle. These mice were subsequently culled at six different time points (ZT0, 4, 8, 12, 16 and 20) and their peritoneal cells were isolated and lysed in RLT RNA lysis buffer. mRNA was extracted and analysed using Taqman qPCR probes specific for murine (B) *Nr1d1* and (C) *Per2* and SYBR qPCR probes specific for murine (A) *Bmal1* and (D) *Nrf2*. Data was normalised to *18s* (Taqman) and *Rps18* (SYBR). Fold induction was calculated relative to a single time point. The presence of circadian patterns was assessed using multiple regression to fit a linearized cosinor model with a pre-determined period of 24 hrs. Data shown are the mean ± S.E.M., n=3-6.

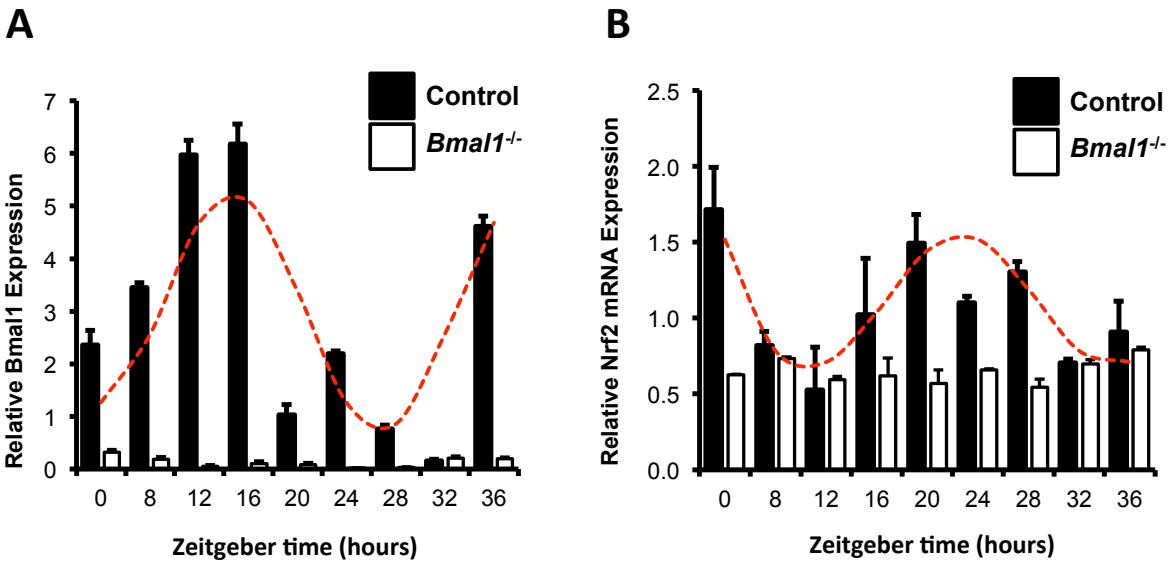

Figure 3.2 Rhythms in Nrf2 transcription are ablated with *Bmal1* deletion

Bmal1$^{+/+}$ and *Bmal1*$^{-/-}$ BMDMs were seeded at 5x10^5 cells/ml in a 12 well plate and incubated overnight at 37°C. Cells were then incubated in 50 % horse serum for 2 hrs to initiate serum shock. Media was replaced and RNA was collected at 0, 8, 12, 16, 20, 24, 28, 32 and 36 hrs post serum shock. mRNA was extracted and analysed using SYBR qPCR probes specific for murine (A) *Bmal1* and (B) *Nrf2*, Data was normalised to *Rps18*. The presence of circadian patterns was assessed using multiple regression to fit a linearized cosinor model with a pre-determined period of 24 hrs. Data shown are the mean ± S.E.M., n=3.

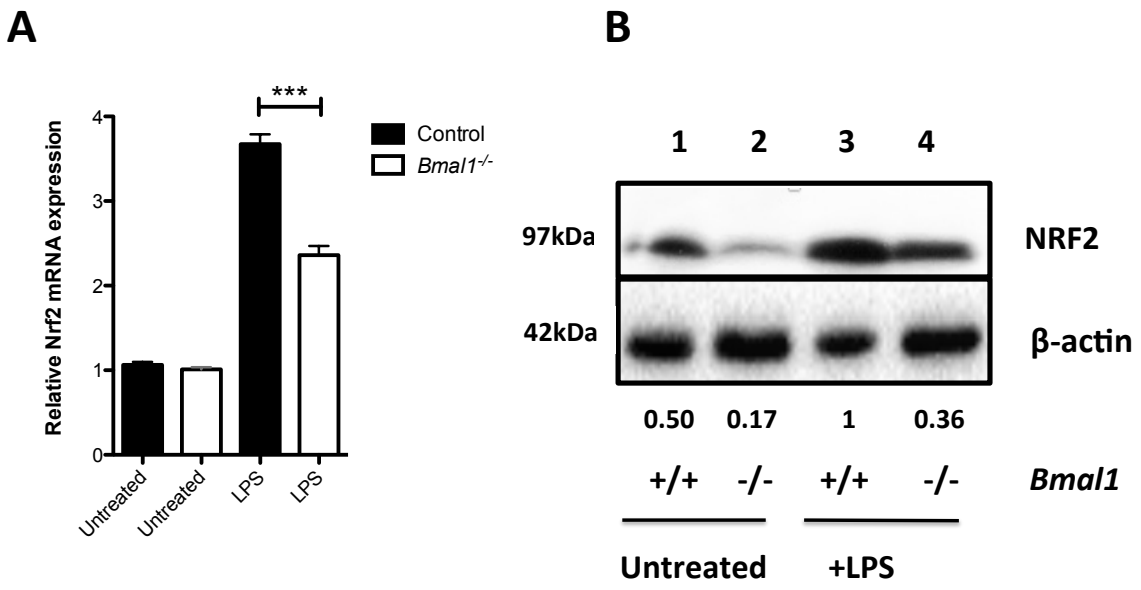

Figure 3.3 NRF2 transcript and protein is decreased in *Bmal1*$^{-/-}$ BMDMs

Bmal1$^{+/+}$ and *Bmal1*$^{-/-}$ BMDMs were seeded at 5x10^5 cells/ml in a 12 well plate and incubated overnight at 37°C. Cells were then left unstimulated or stimulated with 100 ng/ml LPS for 24 hrs. (A) Cells were lysed and mRNA was extracted and analysed using SYBR qPCR probes specific for murine *Nrf2.* Data was normalised to *Rps18.* Fold induction was calculated relative to untreated cells. Data shown are the mean ± S.E.M., n=4. (B) Cells were lysed in sample loading buffer and analysed by western blotting using anti-NRF2 and anti-β-actin antibodies. β-actin is presented as a loading control. Results are a representative of at least 3 independent experiments.

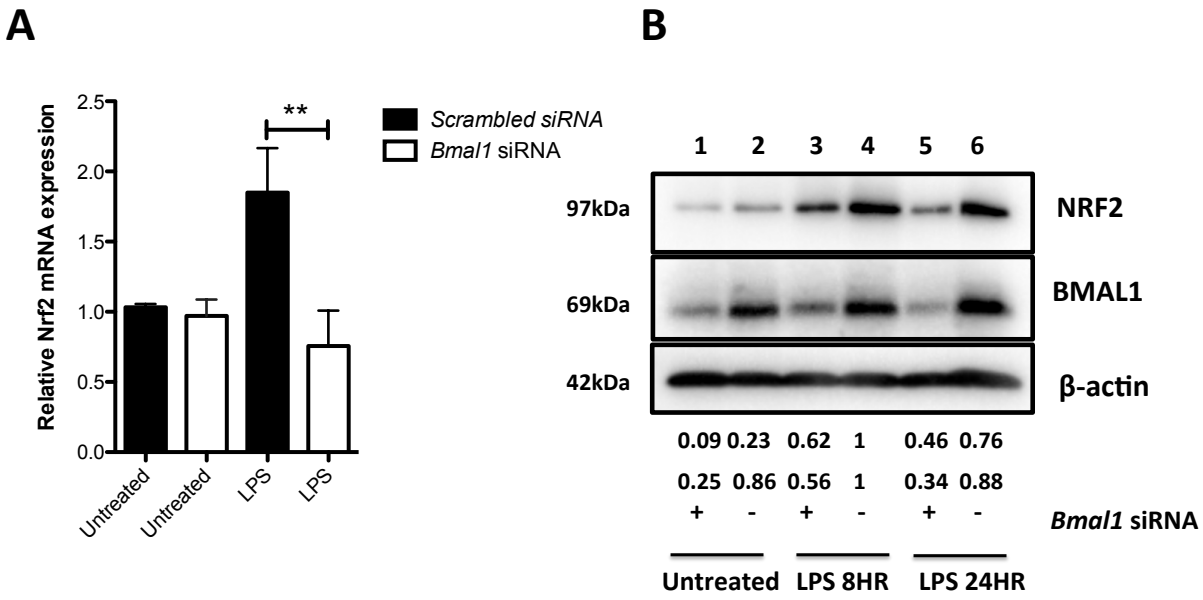

Figure 3.4 NRF2 transcript and protein is decreased in *Bmal*1 knockdown BMDMs

Wild type BMDMs were seeded at 5x10^5 cells/ml in a 12 well plate and incubated overnight at 37°C. BMDMs were then transfected with either a scrambled siRNA control or siRNA targeting *Bmal1.* The cells were then incubated overnight at 37°C. Cells were then left unstimulated or stimulated with 100 ng/ml LPS for 8 or 24 hrs. (A) Cells were lysed and mRNA was extracted and analysed using SYBR qPCR probes specific for murine *Nrf2.* Data was normalised to *Rps18.* Fold induction was calculated relative to untreated cells. Data shown are the mean ± S.E.M., n=6. (B) Cells were lysed in sample loading buffer and analysed by western blotting using anti-NRF2, anti-BMAL1 and anti-β-actin antibodies. β-actin is presented as a loading control. Results are a representative of at least 3 independent experiments.

3.3 Analysis of BMAL1 mediated regulation of NRF2 activity

3.3.1 Transcription factor sequencing uncovers decrease in NRF2 activity with deletion of *Bmal1*

To understand the impact of *Bmal1* deletion on the LPS response in macrophages, an unbiased screening approach of transcription factor activity, termed transcription factor sequencing (TF-Seq), was performed (186). The system utilizes 58 different lentiviral reporter vectors, which contain a response element for a transcription factor of interest. This response element is linked to a *Luc2p* promoter, facilitating expression of a reporter gene. Ultimately this allows for unbiased measurement of a specific transcription factors activity in a cell type of interest (186). Relative activity of the NRF2 transcription factor was found to be significantly decreased in *Bmal1*$^{-/-}$ macrophages following 1 (Figure 3.5A) and 4 hrs (Figure 3.5B) of LPS stimulation. The NRF2 pathway was the only signalling pathway in the screen to be significantly altered with *Bmal1* deletion (a full list of assayed transcription factors can be found in table 3.1). These results revealed that under acute exposure to LPS, the NRF2 pathway was uniquely suppressed by *Bmal1* deletion in macrophages.

3.3.2 Induction of NRF2 target antioxidant genes is decreased in *Bmal1* deficient macrophages

Upon initiation of oxidative stress, NRF2 mediates the induction of a panel of antioxidant genes that balance the oxidative state of the cell (167). Therefore, I next examined the impact of BMAL1 on NRF2-mediated antioxidant response genes. To

establish the effect of NRF2 loss on antioxidant gene regulation, I first targeted *Nrf2* by siRNA in fully differentiated macrophages. Knockdown of *Nrf2* was shown to decrease induction of three core NRF2 target genes, *Hmox1* (Figure 3.6A), *Gsr* (Figure 3.6B) and *Nqo1* (Figure 3.6C) in response to 24 hrs of LPS stimulation. *Hmox1* (Figure 3.7A), *Gsr* (Figure 3.7B) and *Nqo1* (Figure 3.7C) expression levels were also decreased in *Bmal1*$^{-/-}$ compared to *Bmal1*$^{+/+}$ BMDMs following LPS stimulation, further demonstrating that NRF2 activity was decreased with ablation of *Bmal1.* This effect was not restricted to LPS induction of *Nrf2* as the same phenotype was observed in *Hmox1* (Figure 3.8A)*, Gsr* (Figure 3.8B) and *Gclm* (Figure 3.8C) following 4 hrs of hydrogen peroxide stimulation. siRNA-mediated knockdown of *Bmal1* recapitulated the same effect on *Hmox1* (Figure 3.9A), *Gsr* (Figure 3.9B) and *Nqo1* (Figure 3.9C) expression following LPS stimulation. Ultimately it appeared that depletion of *Bmal1* phenocopies the antioxidant response of *Nrf2* silencing.

Reduced glutathione (GSH) synthesis is a downstream component of the NRF2 mediated anti-oxidant defence pathway. Glutathione reductase, the product of *Gsr,* which I determined was reduced with *Bmal1* deletion, catalyses the reduction of oxidized glutathione (GSSG) to the sulfhydryl GSH form (175). I found that total cell levels of GSH were decreased in *Bmal1*$^{-/-}$ BMDMs versus *Bmal1*$^{+/+}$ controls *(*Figure 3.10)*.* These results demonstrate that deletion or silencing of *Bmal1* results in the same suppression of the antioxidant response as direct silencing of *Nrf2,* suggesting that NRF2 activity in macrophages during inflammation is mediated by BMAL1.

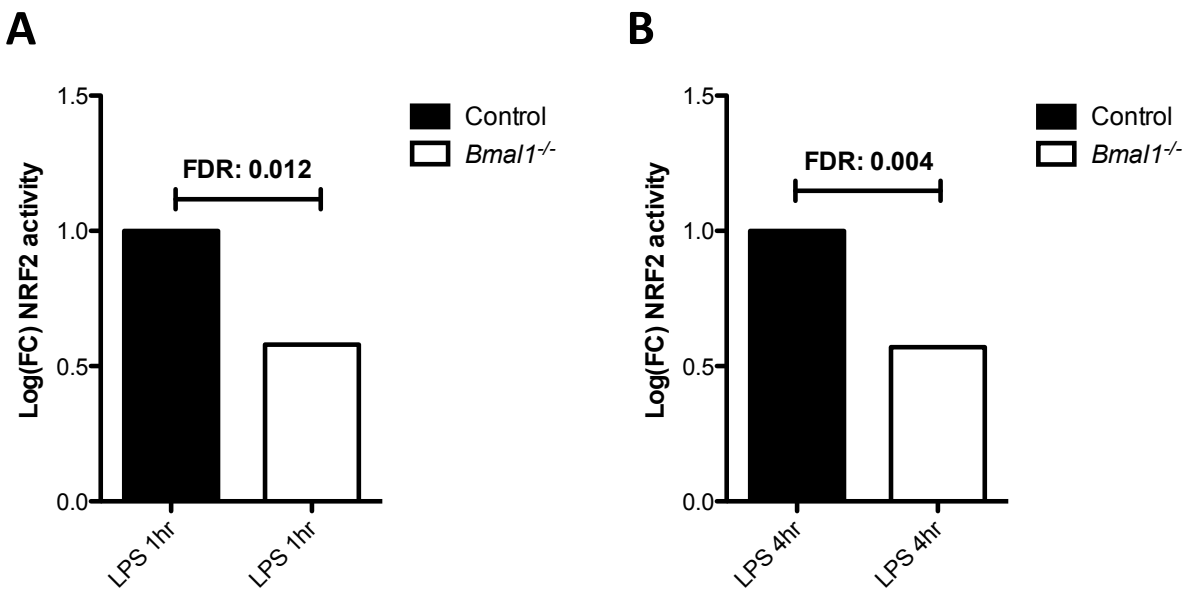

Figure 3.5 NRF2 activity is decreased in *Bmal1*$^{-/-}$ BMDMs determined by TF-seq

Bmal1$^{+/+}$ and *Bmal1*$^{-/-}$ BMDMs were transfected with separate lentiviral reporter vectors, each containing a specific response element for one of 58 transcription factors, with a downstream luciferase reporter construct. The cells were then left untreated or treated with 100 ng/ml LPS for 1 or 4 hrs. Relative activity of NRF2 in *Bmal1*$^{-/-}$ BMDMs was calculated relative to *Bmal1*$^{+/+}$ controls. The Log(FC) value following (A) 1 hr LPS, and (B) 4 hr LPS, was graphed and the FDR is shown.

Pathway	Transcription Factors
Aryl hydrocarbon receptor (AHR)	AHR
Amino acid deprivation (AARE)	ATF4
AP-1 (MAPK)	FOS, JUN
Apoptosis	TRP53
Antioxidant response element (ARE)	NFE2L2 (NRF2)
c-MAF	MAF
C-REL (alternative NF-κB)	REL
C/EBPα	CEBPA
C/EBPβ	CEBPB
Circadian cycle	CLOCK
Constitutive enhancer	NFYA
Constitutive enhancer	SP1
Cyclic AMP	CREB1
Early growth response	EGR1
ER stress element (ERSE)	XBP1
Farnesoid X receptor	NR1H4 (FXR)
GATA3	GATA3
Glucocorticoid receptor	NR3C1 (GR)
Hedgehog	GLI1
Hepatocyte nuclear factor 4	HNF4a
Hippo	TEAD1
Hypoxia	HIF1A
IFNβ	AP-1, IRF3, IRF7, NF-κB
Insulin (PI3K/AKT)	FOXO1
IRF1	IRF1
IRF3	IRF3
IRF3/IRF7	IRF3, IRF7
Liver X receptor	NR1H3 (LXR)
Lysosomal biogenesis	TFEB
MAPK	ELK1
NF-κB	NFKB1, RELA (p50, p65)
Notch	NICD, CBF1 (CSL, RBPJ)
PKC/Ca^{2+}	NFATC1
PPARg	PPARg, RXRA
RELB (alternative NF-κB)	RELB
Retinoic acid (RARE)	RARA
Retinoid-related orphan receptors (RORs)	RORC
RUNX	RUNX1
Serum response element	SRF
Sis-inducible element (SIE)	STAT3
STAT4	STAT4
STAT5	STAT5a, STAT5b
STAT6	STAT6
Sterol	SREBF1
TGF-β	SMAD2, SMAD3, SMAD4
Type I IFN	STAT1, STAT2
Type II IFN	STAT1, STAT1
Unfolded protein response element (UPRE)	ATF6
Vitamin D	VDR
Wnt	LEF1, TCF7, TCF7L1, TCF7L2
Minimal promoter only	single TATA promega pGL4 series

Table 3.1 Table of transcription factors and pathways analysed in TF-seq screen

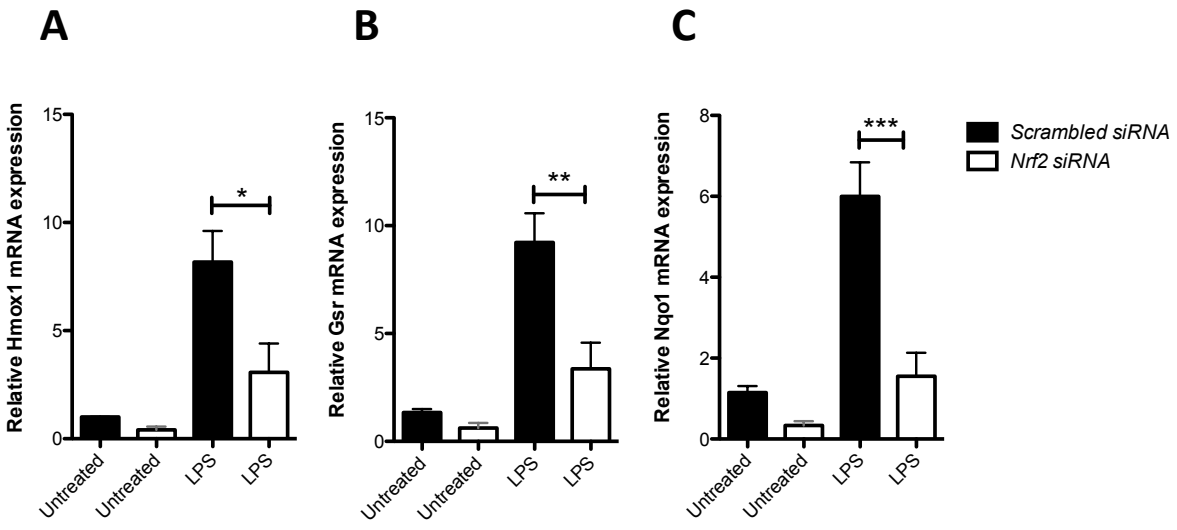

Figure 3.6 Antioxidant genes are decreased with LPS stimulation in *Nrf2* knockdown BMDMs

Wild type BMDMs were seeded at $5x10^5$ cells/ml in a 12 well plate and incubated overnight at 37°C. BMDMs were then transfected with either a scrambled siRNA control or siRNA targeting *Nrf2.* The cells were then incubated overnight at 37°C. Cells were then left unstimulated or stimulated with 100 ng/ml LPS for 24 hrs. Cells were lysed and mRNA was extracted and analysed using SYBR qPCR probes specific for murine (A) *Hmox1,* (B) *Gsr and* (C) *Nqo1.* Data was normalised to *Rps18.* Fold induction was calculated relative to untreated cells. Data shown are the mean ± S.E.M., n=4-6.

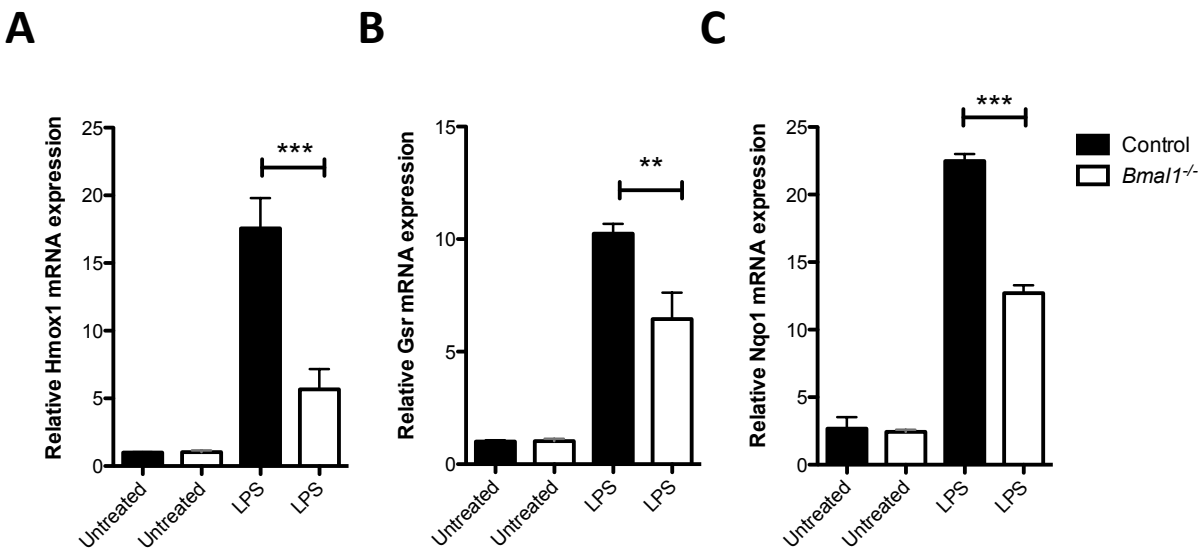

Figure 3.7 Antioxidant genes are decreased in *Bmal1*$^{-/-}$ BMDMs with LPS stimulation

Bmal1$^{+/+}$ and *Bmal1*$^{-/-}$ BMDMs were seeded at 5x10^5 cells/ml in a 12 well plate and incubated overnight at 37°C. Cells were then left unstimulated or stimulated with 100 ng/ml LPS for 24 hrs. Cells were lysed and mRNA was extracted and analysed using SYBR qPCR probes specific for murine (A) *Hmox1,* (B) *Gsr and* (C) *Nqo1.* Data was normalised to *Rps18.* Fold induction was calculated relative to untreated cells. Data shown are the mean ± S.E.M., n=4-6.

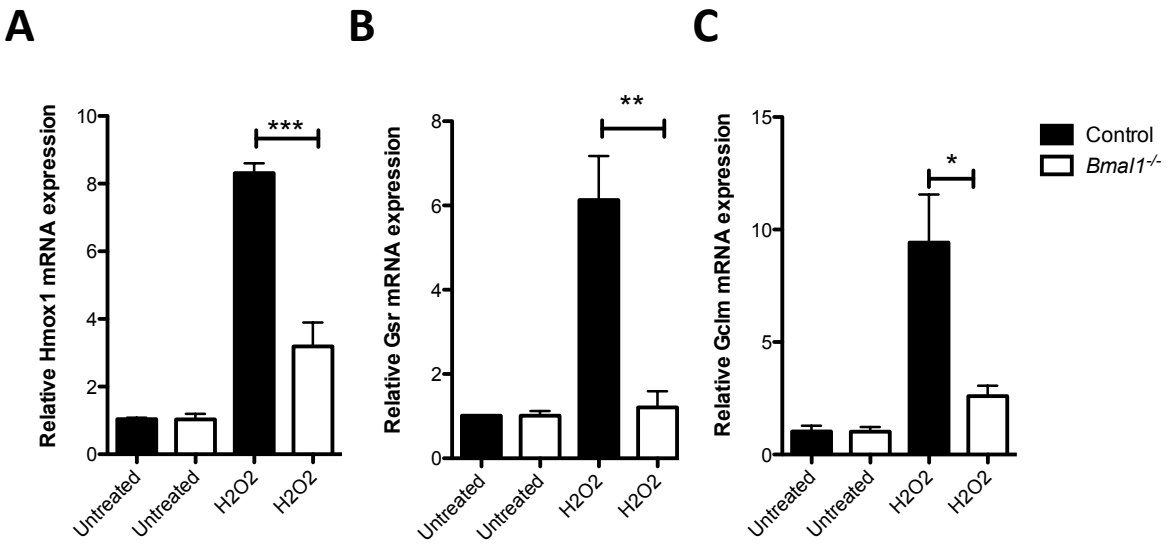

Figure 3.8 Antioxidant genes are decreased in *Bmal1-/-* BMDMs with H_2O_2 stimulation

Bmal1$^{+/+}$ and *Bmal1*$^{-/-}$ BMDMs were seeded at 5x10^5 cells/ml in a 12 well plate and incubated overnight at 37°C. Cells were then left unstimulated or stimulated with 50 μM H2O2 for 4 hrs. (A) Cells were lysed and mRNA was extracted and analysed using SYBR qPCR probes specific for murine (A) *Hmox1,* (B) *Gsr and* (C) *Gclm.* Data was normalised to *Rps18.* Fold induction was calculated relative to untreated cells. Data shown are the mean ± S.E.M., n=3.

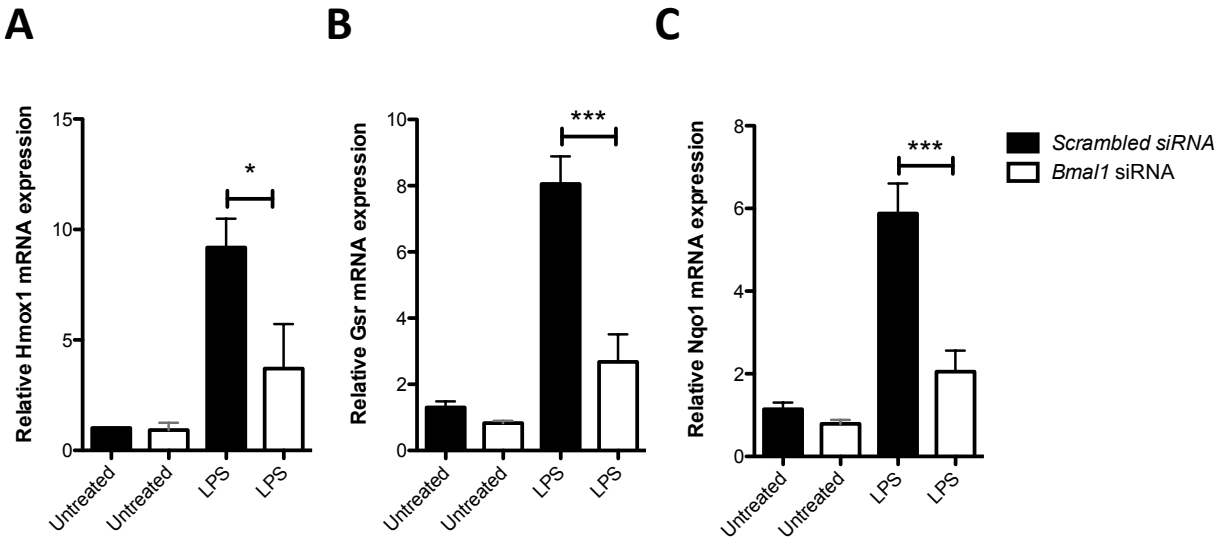

Figure 3.9 Antioxidant genes are decreased with LPS stimulation in *Bmal1* knockdown BMDMs

Wild type BMDMs were seeded at $5x10^5$ cells/ml in a 12 well plate and incubated overnight at 37°C. BMDMs were then transfected with either a scrambled siRNA control or siRNA targeting *Bmal1.* The cells were then incubated overnight at 37°C. Cells were then left unstimulated or stimulated with 100 ng/ml LPS for 24 hrs. Cells were lysed and mRNA was extracted and analysed using SYBR qPCR probes specific for murine (A) *Hmox1,* (B) *Gsr and* (C) *Nqo1.* Data was normalised to *Rps18.* Fold induction was calculated relative to untreated cells. Data shown are the mean ± S.E.M., n=4-6.

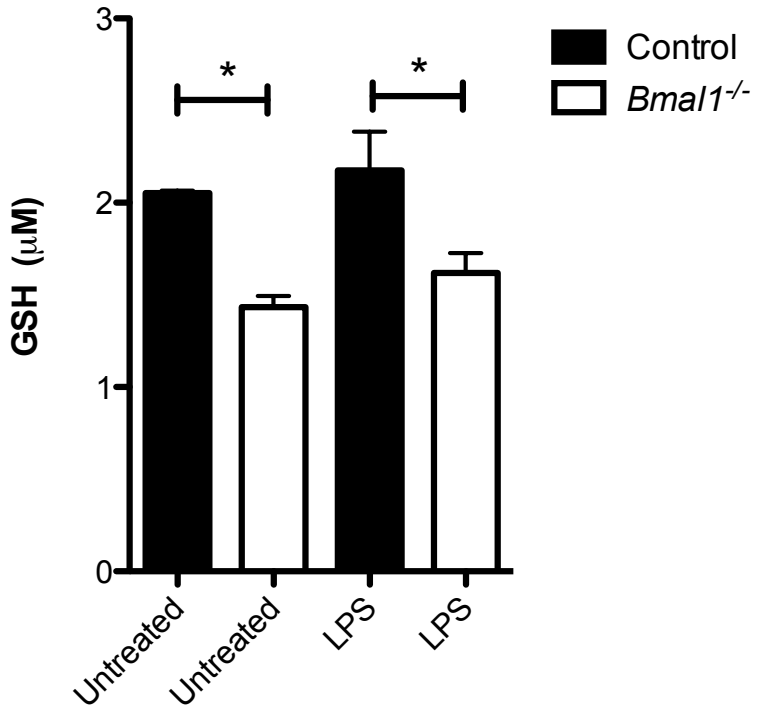

Figure 3.10 GSH is decreased in *Bmal1-/-* BMDMs

Bmal1$^{+/+}$ and *Bmal1*$^{-/-}$ BMDMs were seeded at 1x10^{6} cells/ml in an opaque 96 well plate and incubated overnight at 37°C. Cells were then left unstimulated or stimulated with 100 ng/ml LPS for 24 hrs. A luciferase-based assay was then carried out to determine total concentration of reduced glutathione according to the GSH-Glo promega kit protocol. Data was normalised to a standard curve of GSH. The data shown represents the mean ± S.E.M. of three independent biological replicates. Data shown are the mean ± S.E.M., n=3.

3.4 Examination of NRF2 mediated regulation of the circadian clock

While it has been established that the forward limb of the molecular clock can induce *Nrf2* expression, evidence is emerging that NRF2 can induce the opposite arm of the circadian cycle. It has been demonstrated that pharmacological activation of NRF2 activates expression of *Nr1d1* and *Cry2,* introducing a possible novel feedback loop between the molecular clock, NRF2, and oxidative stress (191). I utilised octyl-itaconate (OI), a cell permeable representative of the endogenous metabolite itaconate, to induce NRF2 activity in wild-type BMDMs (Ryan and Mills et.al. 2018 (in press)). OI induced the expression of *Clock* (Figure 3.11A)*, Nr1d1* (Figure 3.11B)*, and Cry2* (Figure 3.11C)*.* Addition of LPS to BMDMs has a similar effect on clock gene expression, with *Clock* (Figure 3.12A)*, Nr1d1* (Figure 3.12B)*, and Cry2* (Figure 3.12C) all showing boosted expression.

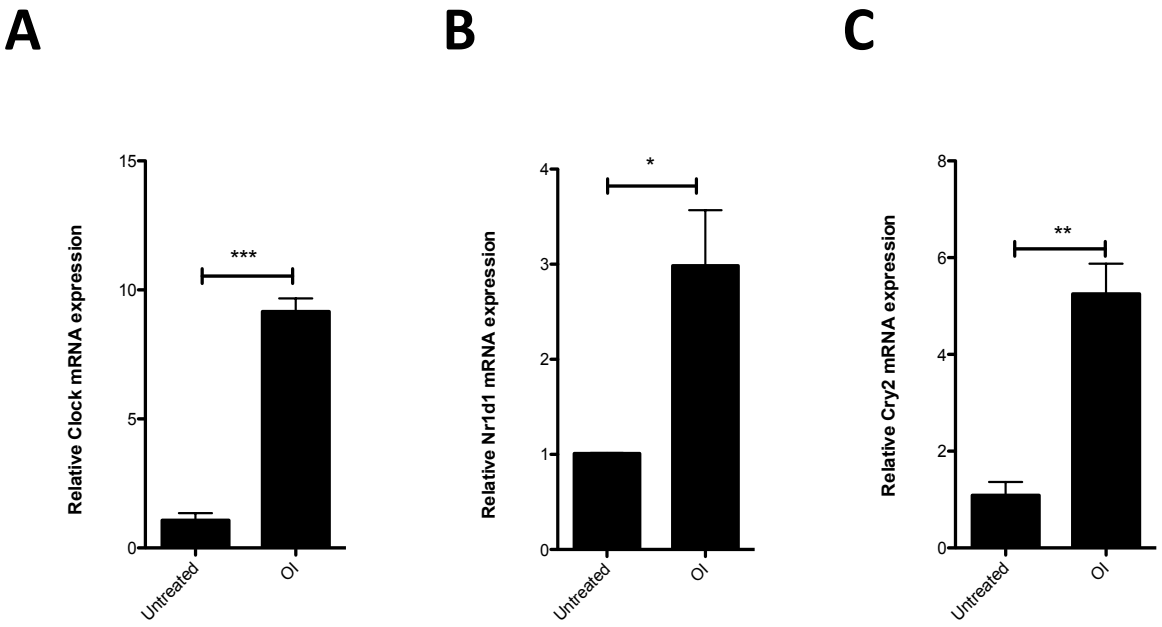

Figure 3.11 NRF2 activation alters expression of circadian clock genes

Wild type BMDMs were seeded at $5x10^5$ cells/ml in a 12 well plate and incubated overnight at 37°C. Cells were then left unstimulated stimulated with 125 μM OI for 24 hrs. Cells were lysed and mRNA was extracted and analysed using Taqman qPCR probes specific for murine (A) *Clock* (B) *Nr1d1 and* (C) *Cry2.* Data was normalised to *18s.* Fold induction was calculated relative to untreated cells. Data shown are the mean ± S.E.M., n=3.

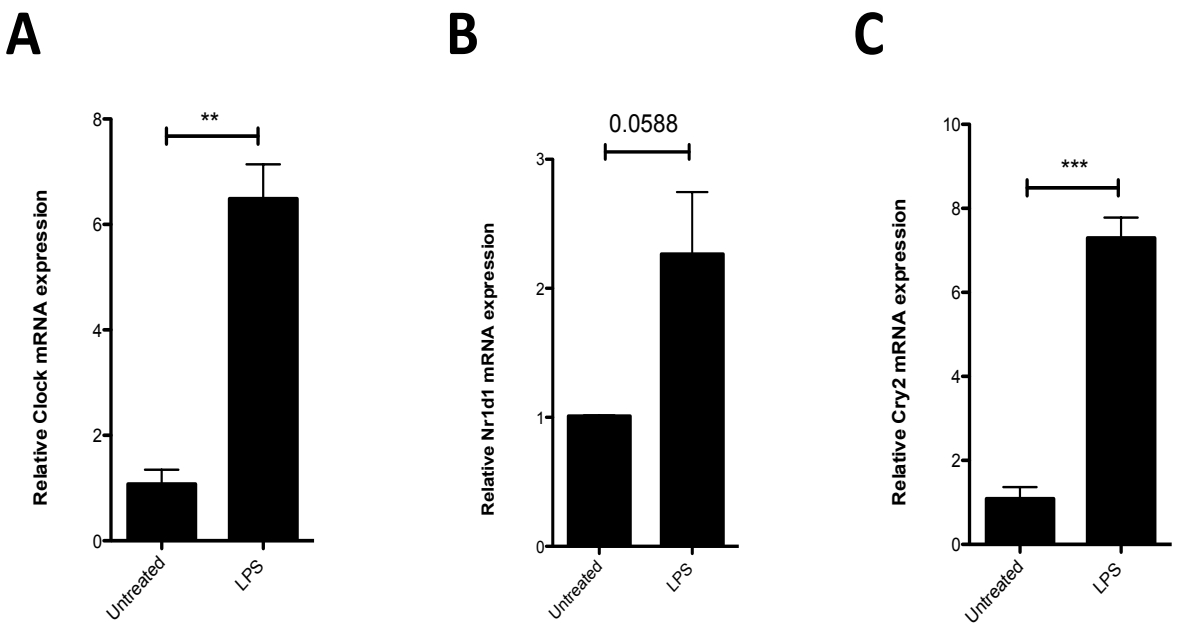

Figure 3.12 LPS stimulation alters expression of circadian clock genes

Wild type BMDMs were seeded at $5x10^5$ cells/ml in a 12 well plate and incubated overnight at 37°C. Cells were then left unstimulated or stimulated with 100 ng/ml LPS for 24 hrs. Cells were lysed and mRNA was extracted and analysed using Taqman qPCR probes specific for murine (A) *Clock* (B) *Nr1d1 and* (C) *Cry2.* Data was normalised to *18s.* Fold induction was calculated relative to untreated cells. Data shown are the mean ± S.E.M., n=3.

3.5 Analysis of BMAL1 mediated regulation of oxidative stress

3.5.1 ROS regulation displays diurnal rhythms

There have been several reports of BMAL1 mediated regulation of oxidative stress in various tissue types. The diurnal rhythm of *Nrf2* expression observed in myeloid cells suggests a diurnal rhythm in basal ROS regulation may be present in these cells. Both *Bmal1* (Figure 3.13A) and *Nrf2* (Figure 3.13B) displayed a trough in expression at ZT8 and a peak at ZT20 in peritoneal cells. This led me to investigate whether ROS levels showed similar diurnal variability. A significant increase in whole cell basal ROS levels was discovered in peritoneal myeloid cells at ZT8 versus ZT20 (Figure 3.13C), correlating negatively with the diurnal rhythm in *Bmal1* and *Nrf2* expression. Oxidative stress is well documented to induce inflammation in macrophages. Our lab previously reported on an increase in LPS induced inflammation at ZT12 relative to ZT0. Therefore, I next investigated whether there was differential expression in genes of the oxidative stress pathway at ZT0, when mice are protected from LPS induced lethality, and ZT12, when mice exhibited greater lethality. An enrichment of genes involved in ROS production and regulation was discovered at ZT12 versus ZT0 (Figure 3.14), providing further evidence for a rhythm in ROS regulation in peritoneal myeloid cells. A full list of these genes and their relative fold change at ZT12 relative to ZT0 can be found in table 3.2. Overall there was much greater relative expression of ROS production and regulation genes at ZT12, when mice are more pro-inflammatory.

3.5.2 ROS accumulation is increased in *Bmal1* deficient macrophages

To investigate whether BMAL1 has a direct effect on ROS regulation in macrophages, whole cell ROS levels were measured in macrophages lacking *Bmal1*. A substantial increase in the levels of ROS in *Bmal1*$^{-/-}$ BMDMs was detected both basally and with the addition of LPS in comparison to *Bmal1*$^{+/+}$ BMDMs (Figure 3.15). It appeared that BMAL1 was crucial to regulation of oxidative stress. This was further confirmed with siRNA-mediated knock down of *Bmal1* in wild-type BMDMs where the same phenotype of increased ROS was observed (Figure 3.16). I was also able to visualize this phenotype directly utilizing fluorescent imaging (Figure 3.17). Greater ROS was observed in *Bmal1* knockout macrophages both basally and following LPS stimulation, matching the previous results seen by flow cytometry. It also appeared that the ROS was largely being produced from the mitochondria of *Bmal1*$^{-/-}$ BMDMs given the co-localisation of the ROS and mitochondria stains. The relative fluorescence levels are graphed in Figure 3.18.

3.5.3 HIF-1α protein and activity increased in *Bmal1*$^{-/-}$ macrophages

HIF-1α is a hypoxic response protein that is activated in response to increased ROS levels (134). To assay whether HIF-1α accumulation was increased with deletion of *Bmal1*, I treated *Bmal1*$^{+/+}$ and *Bmal1*$^{-/-}$ BMDMs with LPS before measuring HIF-1α by western blot. I observed increased HIF-1α protein accumulation following LPS stimulation in *Bmal1*$^{-/-}$ BMDMs (Figure 3.19A). I also uncovered increased HIF-1α activity, as measured by increased *Phd3* expression, a direct target of HIF-1α (Figure 3.19B). It is likely that increased ROS facilitated increased HIF-1α accumulation.

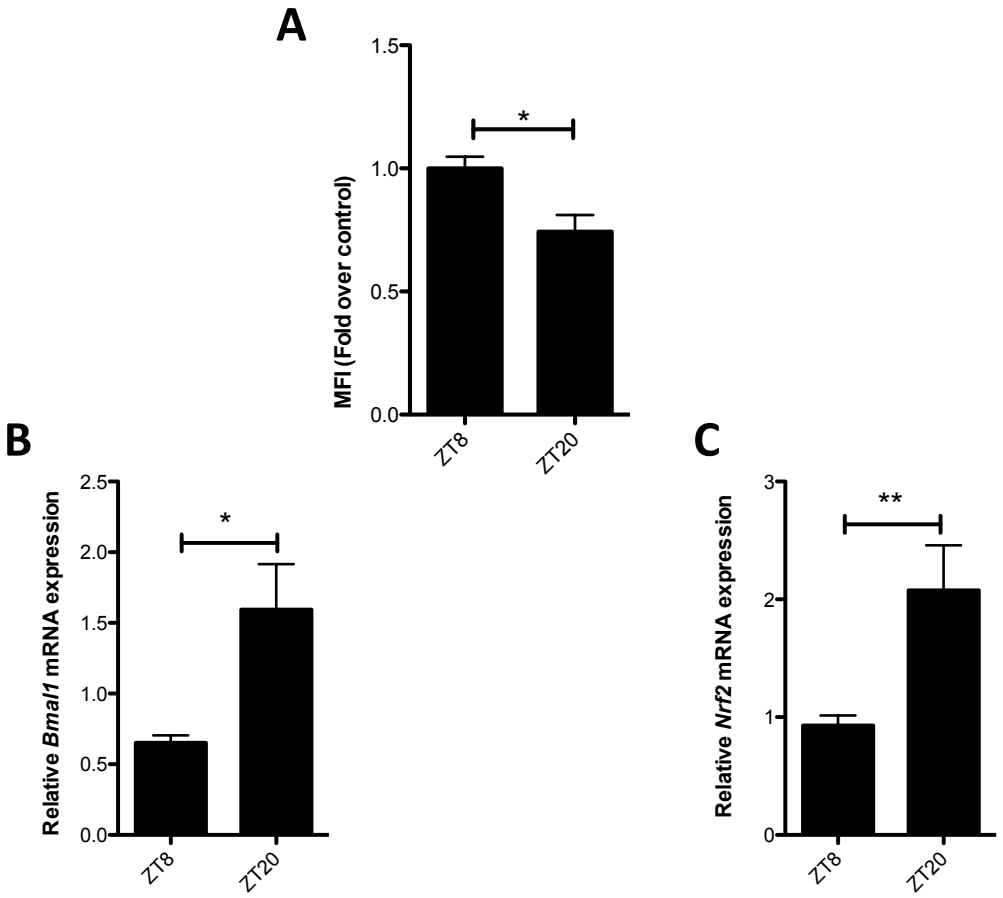

Figure 3.13 ROS displays variation in peritoneal myeloid cells

Wild type mice were housed in a light cabinet for two weeks to adjust their circadian rhythms to a new cycle. These mice were subsequently culled at ZT8 and ZT20 and their peritoneal cells were isolated. (A) These cells were stained with CellROX and an anti-CD11b^{+} antibody for 30 minutes. ROS in the myeloid cell population was measured by flow cytometry Fold induction of MFI was calculated relative to ZT8. Data shown are the mean ± S.E.M., n=4-6. Peritoneal cells were also isolated and lysed in RLT RNA lysis buffer. mRNA was extracted and analysed using SYBR qPCR probes specific for murine (B) *Bmal1* and (C) *Nrf2.* Data shown are the mean ± S.E.M., n=4-6.

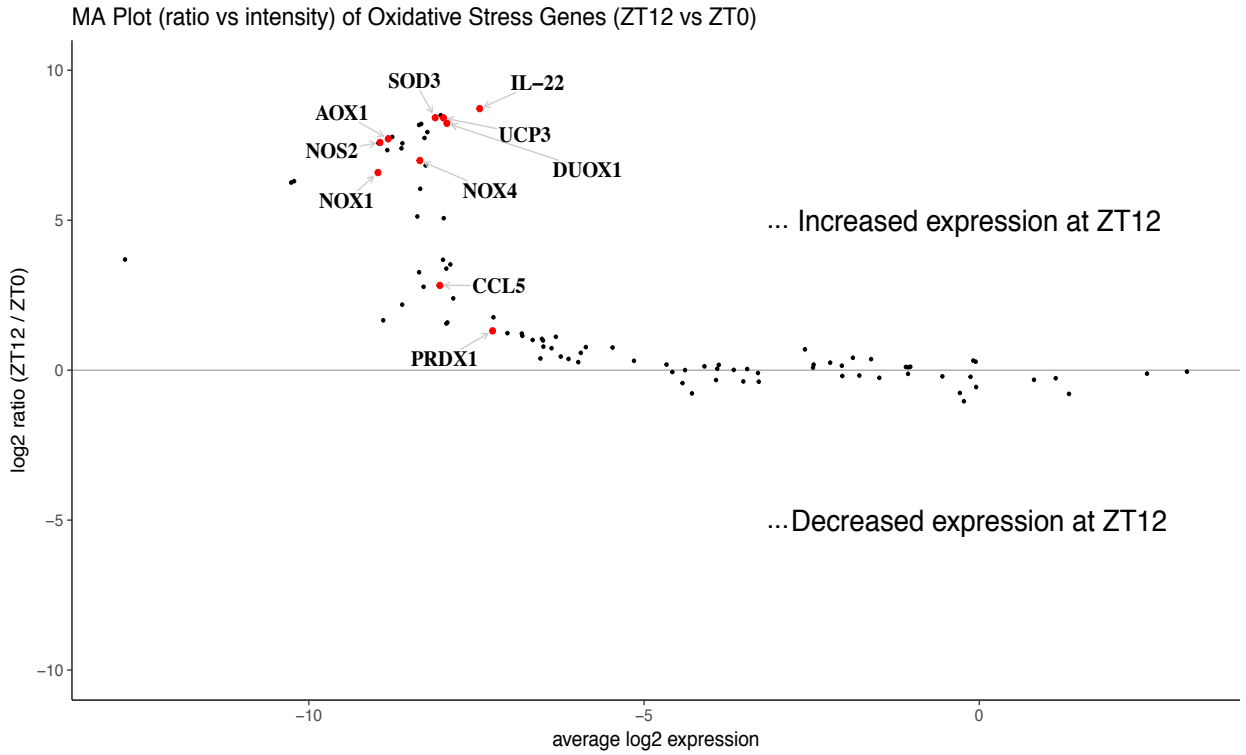

Figure 3.14 Diurnal regulation of oxidative stress genes is present in peritoneal cells

Wild type mice were culled at ZT0 and ZT12 and their peritoneal cells were isolated. cDNA was generated from RNA samples using RT^2 First Strand Kit and was mixed with SYBR Green qPCR Mastermix and distributed to RT^2 Profiler plates which were preloaded with primer sets for pathway relevant genes. Fold induction was calculated relative to ZT0 cells and the Log2 ratio was plotted on a graph where any gene above the X-axis was up regulated at ZT12 and below the X-axis was up regulated at ZT0. (n=3).

Gene	Log2-ratio
Alb	7.56
Als2	1.15
AOX1	7.72
Apc	0.79
Apoe	-0.05
Atr	1.66
Cat	0.00
CCL5	2.83
Ccs	0.76
Ctsb	-0.22
Cyba	-0.21
Cygb	7.78
Dnm2	0.19
DUOX1	8.23
Ehd2	1.56
Epx	6.83
Ercc2	1.04
Ercc6	1.76
Fancc	1.59
Fmo2	7.94
Fth1	-0.32
Gclc	0.39
Gclm	0.31
Gpx1	-0.79
Gpx2	7.74
Gpx3	0.58
Gpx4	-0.18
Gpx5	3.69
Gpx6	7.34
Gpx7	1.23
Gsr	-0.38

Gene	Log2-ratio
Gss	1.22
Gstk1	0.38
Gstp1	-0.33
Hmox1	-0.43
Hspa1a	-0.77
Idh1	0.15
Ift172	1.01
Il19	8.50
IL-22	8.72
Krt1	7.74
Lpo	7.40
Mb	8.18
Mpo	6.05
Ncf1	0.09
Ncf2	-0.19
Ngb	5.13
NOS2	7.59
NOX1	6.59
NOX4	6.99
Noxa1	6.26
Noxo1	3.68
Nqo1	5.07
Park7	0.01
PRDX1	1.31
Prdx2	-0.38
Prdx3	-0.06
Prdx4	-0.10
Prdx5	-0.25
Prdx6	0.05
Prnp	3.27
Psmb5	0.04

Gene	Log2-ratio
Ptgs1	0.25
Ptgs2	2.78
Rag2	7.57
Recql4	3.53
Scd1	2.19
Serpinb1b	0.45
Slc38a1	0.27
Sod1	0.69
Sod2	0.13
SOD3	8.42
Sqstm1	0.18
Srxn1	0.99
Tpo	8.21
Txn1	3.39
Txnip	0.37
Txnrd1	0.77
Txnrd2	0.73
Txnrd3	2.39
Ucp2	0.28
UCP3	8.41
Vim	0.41
Xpa	1.11
Actb	-0.11
B2m	-0.27
Gapdh	0.32
Gusb	0.19
Hsp90ab1	-0.12
MGDC	6.30

Table 3.2 Oxidative stress genes analysed and their Log2 ratios (ZT12/ZT0)

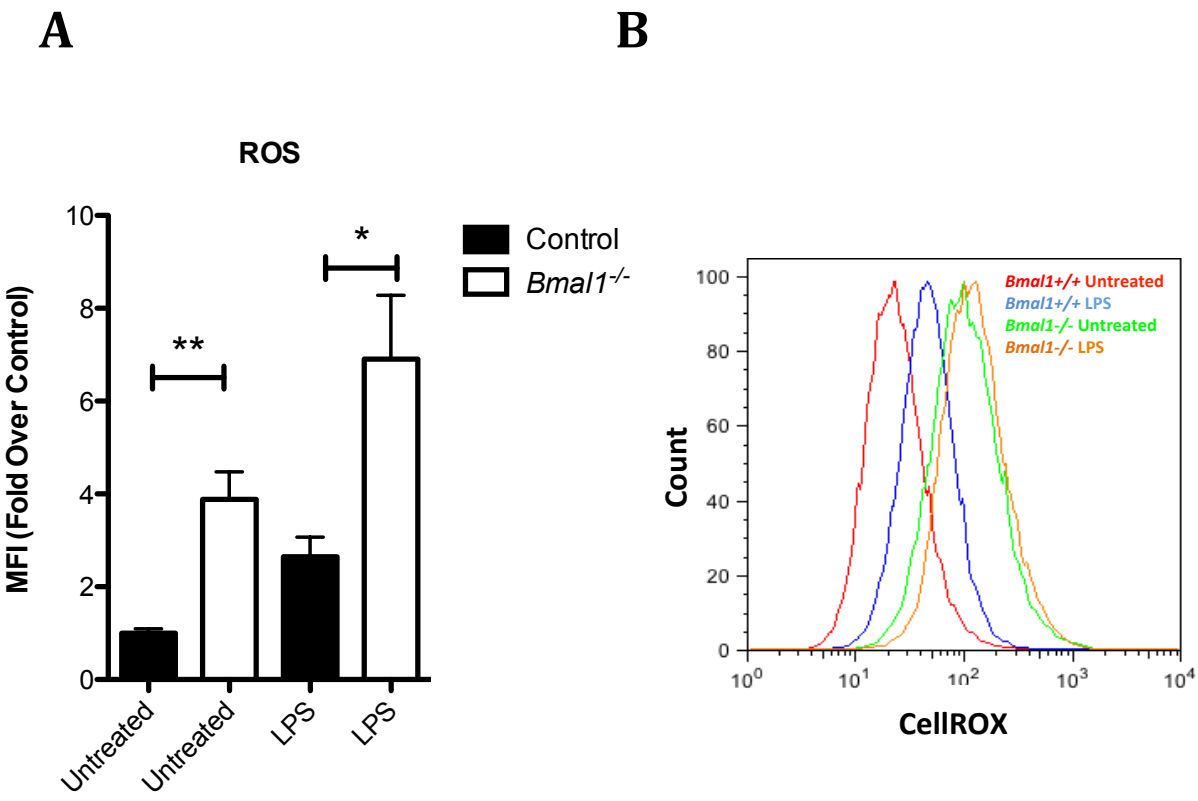

Figure 3.15 ROS levels are increased in *Bmal1*$^{-/-}$ BMDMs

Bmal1$^{+/+}$ and *Bmal1*$^{-/-}$ BMDMs were seeded at 5x10^5 cells/ml in a 12 well plate and incubated overnight at 37°C. Cells were then left unstimulated or stimulated with 100 ng/ml LPS for 24 hrs. These cells were stained with CellROX for 30 minutes before staining with Aqua Live/Dead stain for 30 minutes. ROS was measured by flow cytometry. (A) Fold induction of mean fluorescence intensity (MFI) was calculated relative to untreated wild type cells. Data shown are the mean ± S.E.M., n=4. (B) Representative histogram of ROS measured by flow cytometry.

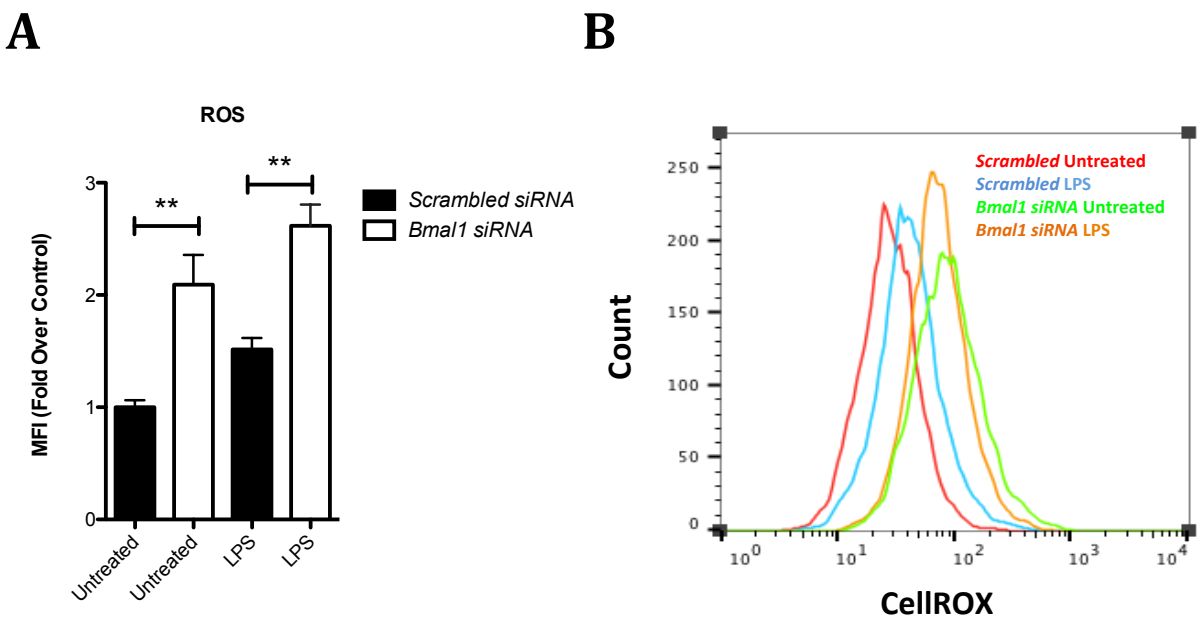

Figure 3.16 ROS levels are increased in *Bmal1* silenced BMDMs

Wild type BMDMs were seeded at 5x10^5 cells/ml in a 12 well plate and incubated overnight at 37°C. BMDMs were then transfected with either a scrambled siRNA control or siRNA targeting *Bmal1.* The cells were then incubated overnight at 37°C. Cells were then left unstimulated or stimulated with 100 ng/ml LPS for 24 hrs. These cells were stained with CellROX for 30 minutes before staining with Aqua Live/Dead stain for 30 minutes. ROS was measured by flow cytometry Fold induction of MFI was calculated relative to untreated wild type cells. Data shown are the mean ± S.E.M., n=5. (B) Representative histogram of ROS measured by flow cytometry.

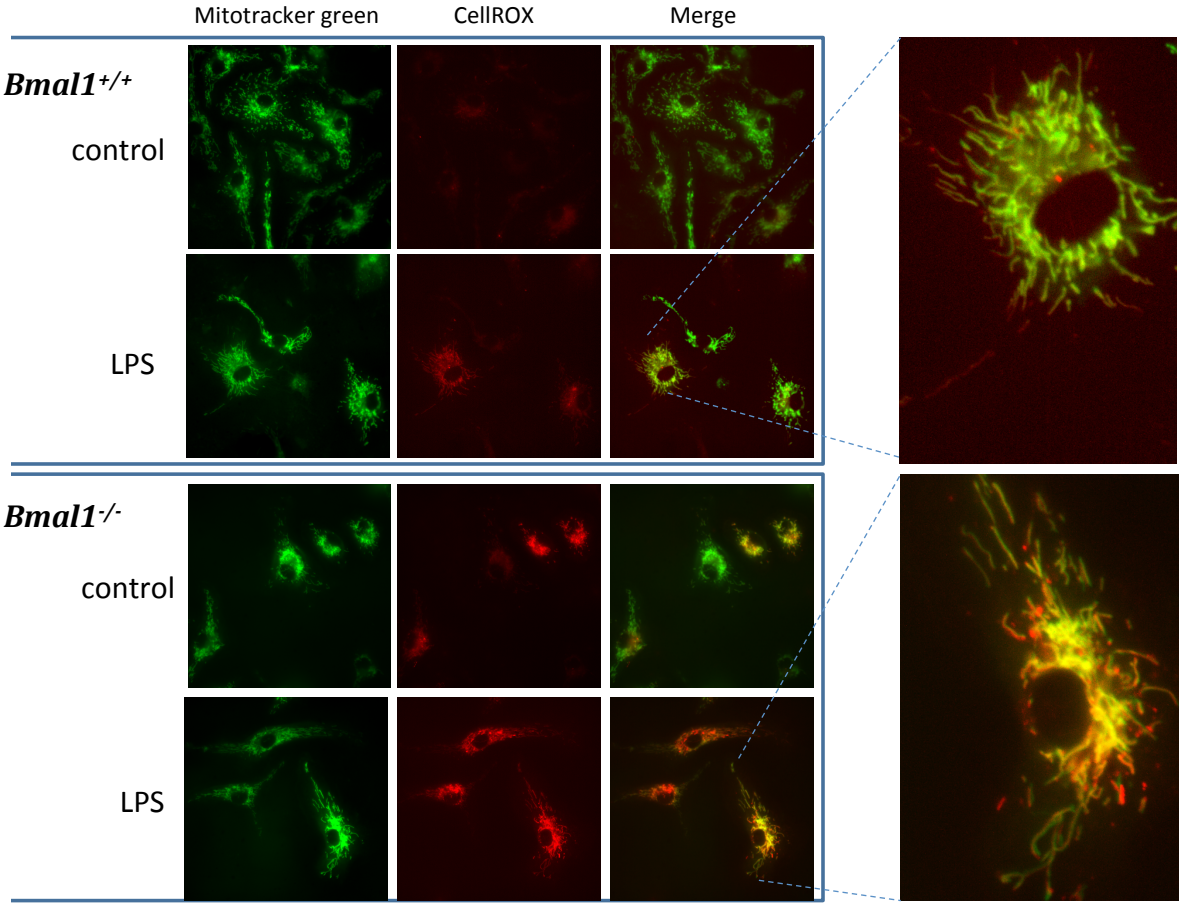

Figure 3.17 ROS levels are increased in *Bmal1*$^{-/-}$ BMDMs view by confocal

Bmal1$^{+/+}$ and *Bmal1*$^{-/-}$ BMDMs were seeded at 5x10^5 cells/ml in a µ dish and incubated overnight at 37°C. Cells were then left unstimulated or stimulated with 100 ng/ml LPS for 24 hrs. These cells were stained with CellROX and mitotracker green for 30 minutes before washing twice with PBS and replacing media. Cells were then imaged with a Zeiss LSM710 confocal microscope. Images shown are a representative of 3 separate experiments. Above image is a representative of n=3.

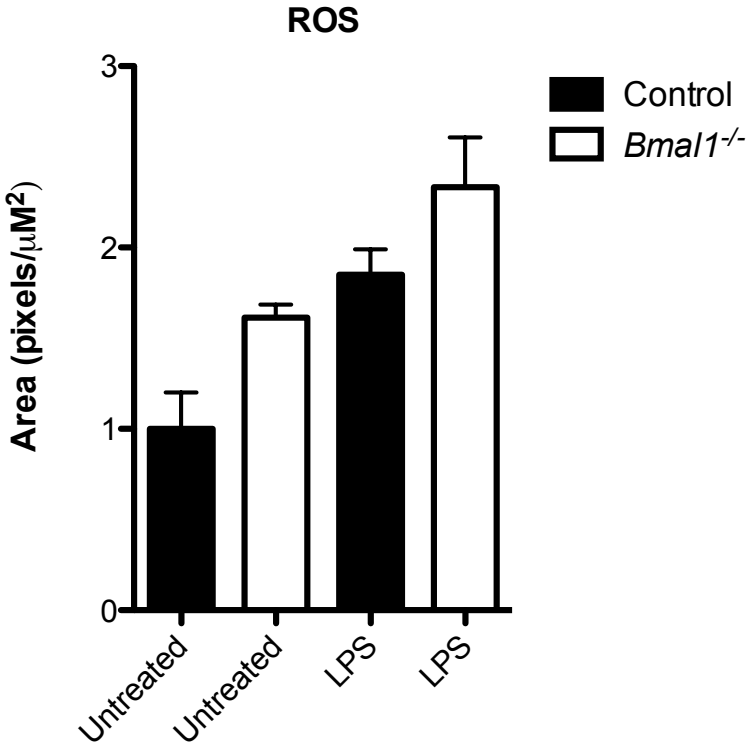

Figure 3.18 Quantification of ROS levels viewed by confocal

Quantification of fluorescence was carried out from three separate experiments and graphed. Data shown are the mean ± S.E.M., n=3.

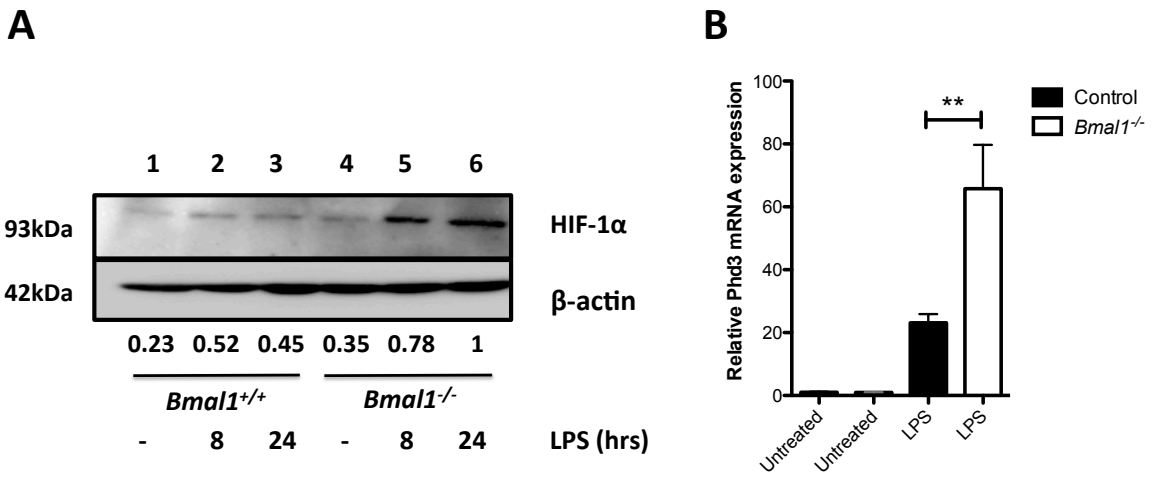

Figure 3.19 HIF-1α levels and activity are increased in *Bmal1*$^{-/-}$ BMDMs

Bmal1$^{+/+}$ and *Bmal1*$^{-/-}$ BMDMs were seeded at 5x10^5 cells/ml in a 12 well plate and incubated overnight at 37°C. Cells were then left unstimulated or stimulated with 100 ng/ml LPS for 24 hrs. (A) Cells were lysed in sample loading buffer and analysed by western blotting using anti-HIF-1α and anti-β-actin antibodies. β-actin is presented as a loading control. Results are a representative of at least 3 independent experiments. (B) Cells were lysed and mRNA was extracted and analysed using SYBR qPCR probes specific for murine *Phd3.* Data was normalised to *Rps18.* Fold induction was calculated relative to untreated cells. Data shown are the mean ± S.E.M., n=4.

3.6 Investigation into the effect of the circadian cycle on metabolism in macrophages

Previous reports have linked the circadian cycle to being important in metabolic regulation in various tissue types (136). However, the effect of *Bmal1* deletion on metabolism has never been measured in macrophages. For this reason, I carried out investigations into the metabolic state of *Bmal1*$^{-/-}$ BMDMs.

3.6.1 Glycolytic genes increased in *Bmal1*$^{-/-}$ macrophages

LPS stimulation leads to metabolic reshuffling in macrophages, promoting increased glycolysis in favour of oxidative phosphorylation (128). This increase in glycolysis is a HIF-1α dependent event and is marked by a significant increase in ROS (128). I measured several glycolytic genes between *Bmal1*$^{+/+}$ and *Bmal1*$^{-/-}$ BMDMs following LPS stimulation. *Hexokinase2 (Hk2)* (Figure 3.20A)*, Lactate dehydrogenase a (Ldha)* (a direct HIF-1α target) (Figure 3.20B) *and Glyceraldehyde 3-phosphate dehydrogenase (Gapdh)* (Figure 3.20C) were found to be increased in *Bmal1*$^{-/-}$ BMDMs following LPS stimulation indicating a potential increase in glycolysis in these cells.

3.6.2 Glycolysis and oxidative phosphorylation are increased in *Bmal1*$^{-/-}$ BMDMs

Given the increase in HIF-1α, glycolytic genes and ROS, I decided to carry out metabolic assays on *Bmal1*$^{+/+}$ and *Bmal1*$^{-/-}$ BMDMs. I first measured the initiation of glycolysis that occurs with LPS stimulation (192). *Bmal1*$^{+/+}$ and *Bmal1*$^{-/-}$ were seeded in seahorse plates and their basal ECAR was measured. LPS was then

injected into the wells and glycolysis was directly measured (Figure 3.21). I found that *Bmal1*$^{-/-}$ BMDMs exhibited increased glycolysis in response to LPS stimulation than their *Bmal1*$^{+/+}$ counterparts.

Given the above result I measured ECAR and OCR levels in *Bmal1*$^{+/+}$ and *Bmal1*$^{-/-}$ BMDMs following a longer period of LPS stimulation. In the glycolysis stress test, I found that *Bmal1*$^{-/-}$ BMDMs had greater levels of non-glycolytic acidification and higher glycolytic capacity, however their basal level of glycolysis was not increased relative to *Bmal1*$^{+/+}$ BMDMs (Figure 3.22A+B). Following addition of LPS however we see an overall increase in glycolysis in *Bmal1*$^{-/-}$ BMDMs and they retain their increased glycolytic capacity (Figure 3.22C+D). Interestingly, when measuring OCR utilising a mitostress test, no significant difference was found in basal differences between *Bmal1*$^{+/+}$ and *Bmal1*$^{-/-}$ BMDMs (Figure 3.23A+B). However, following LPS stimulation there was no decrease in basal and maximal respiration seen in *Bmal1*$^{-/-}$ BMDMs compared to the expected drop seen in *Bmal1*$^{+/+}$ BMDMs. A possible increase in proton leak and ATP production was also observed in *Bmal1*$^{-/-}$ BMDMs (Figure 3.23C+D). It appeared that while glycolysis was increased, mitochondrial respiration was not decreased in *Bmal1*$^{-/-}$ BMDMs.

3.6.3 *Irg1* expression is decreased in *Bmal1*$^{-/-}$ macrophages

Given my results on altered metabolism in *Bmal1*$^{-/-}$ BMDMs, I began investigating potential candidates that could be leading to the observed differences. Itaconate is a metabolite under regulation of the *Irg1* gene. Upon addition of LPS, *Irg1* is boosted facilitating production of itaconate (135). Itaconate has previously been attributed to decreasing OCR through SDH (complex 2) inhibition (135). It is also a recently discovered activator of NRF2 (Ryan and Mills et.al. 2018 (in press)). Addition of exogenous itaconate has been shown to boost NRF2 and lower ROS in macrophages

(Ryan and Mills et.al. 2018 (in press)). I measured *Irg1* gene expression between *Bmal1*$^{+/+}$ and *Bmal1*$^{-/-}$ BMDMs following LPS stimulation. *Irg1* transcription was significantly lower in *Bmal1*$^{-/-}$ BMDMs following LPS stimulation (Figure 3.24A). This was also found to be the case with siRNA targeting of *Bmal1* (Figure 3.24B).

3.6.4 Investigation of circadian rhythms in mitochondrial regulation

Given the alteration in mitochondrial respiration and the increase in ROS that appears to be co-localising with the mitochondria, I investigated whether there were endogenous rhythms in mitochondria membrane potential in macrophages. Wild type BMDMs were synchronized by serum shock before staining with mitotracker red, a stain for mitochondrial membrane potential. Fluoresence of these cells was measured over a 48 hr period and the results were normalized to mitotracker green, a control for mitochondrial number. Circadian rhythms were found in fluorescence over the course of 48 hrs, indicating clock mediated regulation of mitochondrial function (Figure 3.25).

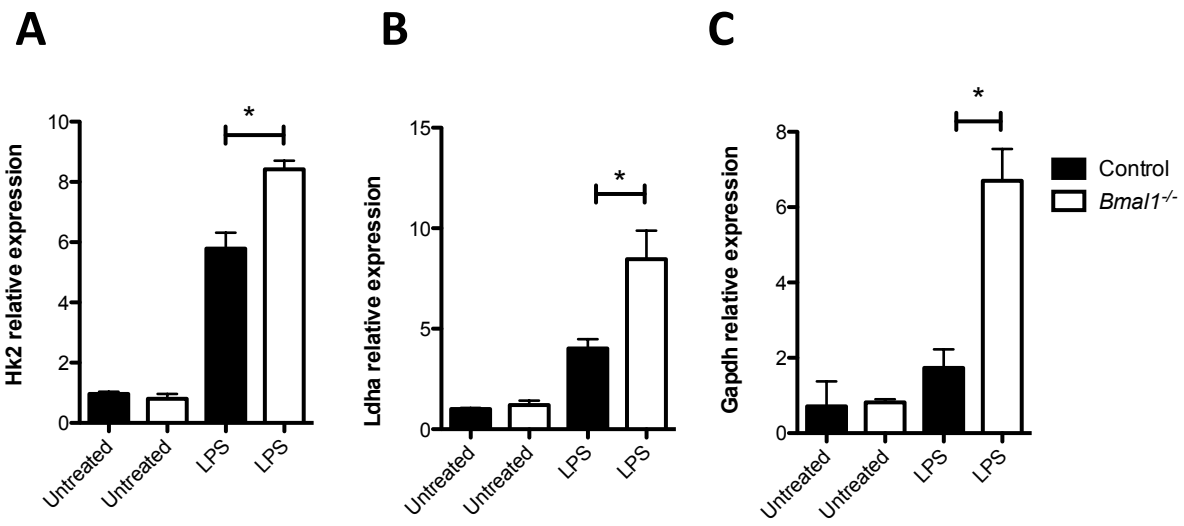

Figure 3.20 Glycolytic gene expression is increased in *Bmal1*$^{-/-}$ BMDMs following LPS stimulation

Bmal1$^{+/+}$ and *Bmal1*$^{-/-}$ BMDMs were seeded at 5x10^5 cells/ml in a 12 well plate and incubated overnight at 37°C. Cells were then left unstimulated or stimulated with 100 ng/ml LPS for 24 hrs. Cells were lysed and mRNA was extracted and analysed using SYBR qPCR probes specific for murine (A) *Hk2,* (B) *Ldha* and (C) *Gapdh.* Data was normalised to *Rps18.* Fold induction was calculated relative to untreated cells. Data shown are the mean ± S.E.M., n=3.

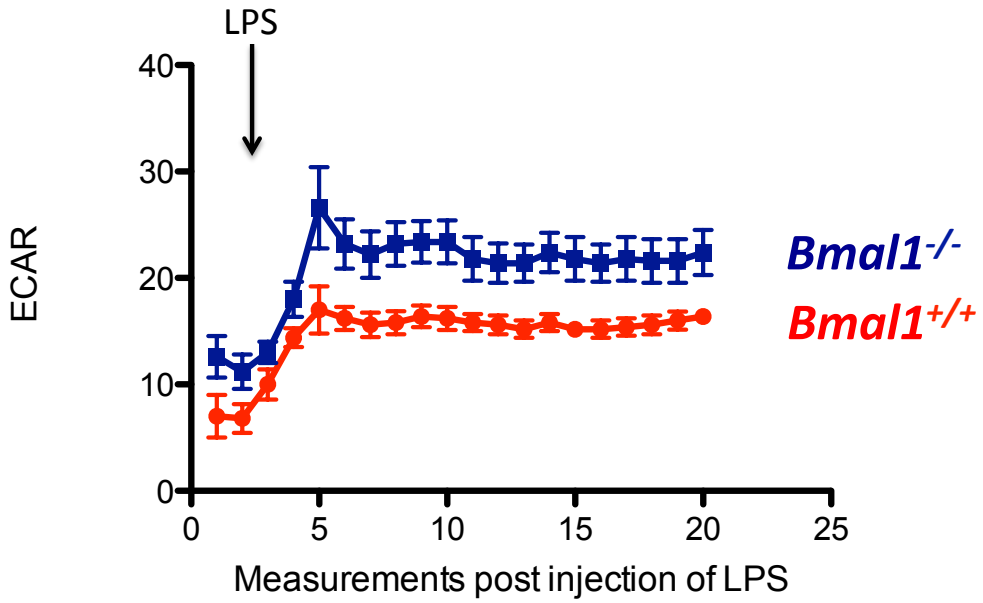

Figure 3.21 Initial glycolytic burst is increased in *Bmal1*$^{-/-}$ BMDMs following LPS stimulation

Bmal1$^{+/+}$ and *Bmal1*$^{-/-}$ BMDMs were seeded at 1.25x10^5 cells/well in a specialised 24 well Seahorse cell plate and incubated overnight at 37°C. One hr before the run, the medium was removed from the cells and replaced with 500 µL of prewarmed XF assay medium supplemented with glutamine. The cell plate was then placed loaded into the Seahorse XF analyser and measurements commenced. LPS was injected approximately 30 minutes after beginning of measurements and ECAR was measured. Data is a representative of 3 separate experiments. Data shown are the mean ± S.E.M. Data was normalised to protein levels as measured by BCA assay.

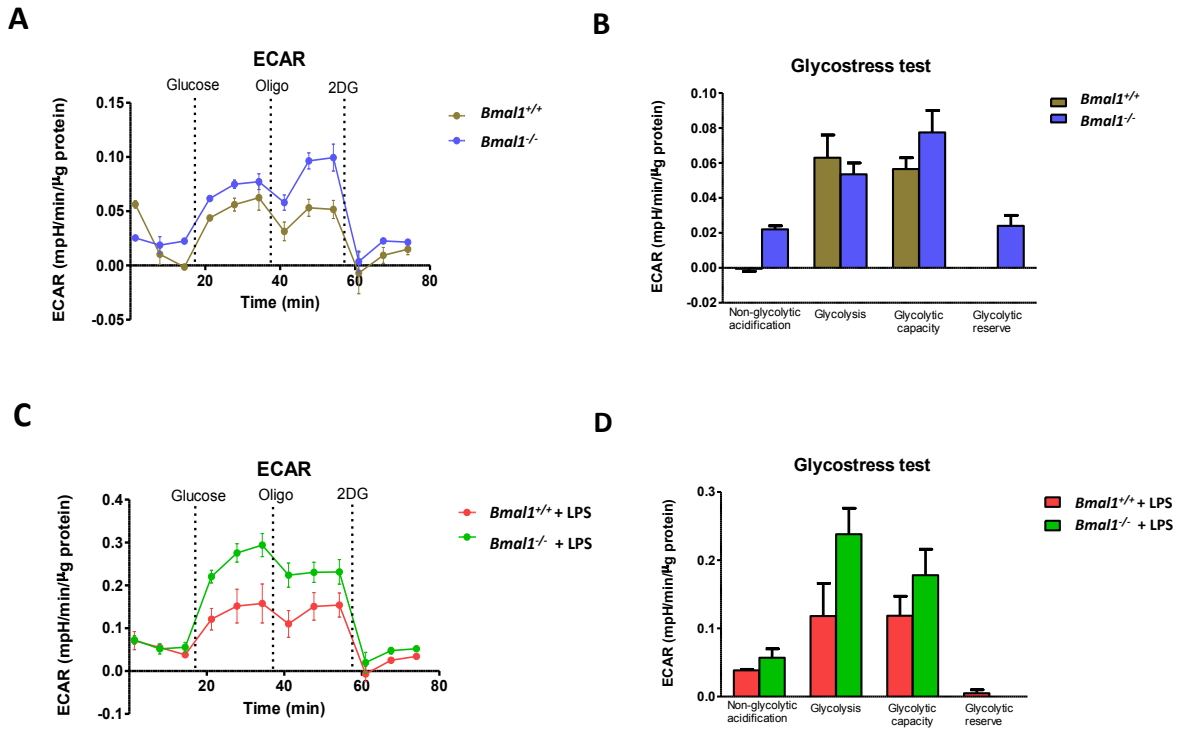

Figure 3.22 Glycolysis is increased in *Bmal1*$^{-/-}$ BMDMs

Bmal1$^{+/+}$ and *Bmal1*$^{-/-}$ BMDMs were seeded at 1.25x10^5 cells/well in a specialised 24 well Seahorse cell plate and incubated overnight at 37°C. Cells were then left unstimulated or stimulated with 100 ng/ml LPS for 24 hrs. One hr before the run, the medium was removed from the cells and replaced with 500 µL of prewarmed XF assay medium supplemented with glutamine. The cell plate was then placed loaded into the Seahorse XF analyser and glycolysis stress test was performed. (A) Trace graph showing glycolytic readouts in untreated *Bmal1*$^{+/+}$ and *Bmal1*$^{-/-}$ BMDMs. (B) Bar chart showing glycolytic readouts in untreated *Bmal1*$^{+/+}$ and *Bmal1*$^{-/-}$ BMDMs. Data shown are the mean ± S.E.M. (C) Trace graph showing glycolytic readouts in LPS treated *Bmal1*$^{+/+}$ and *Bmal1*$^{-/-}$ BMDMs. (D) Bar chart showing glycolytic readouts in LPS treated *Bmal1*$^{+/+}$ and *Bmal1*$^{-/-}$ BMDMs. Data is a representative of 3 separate experiments. Data was normalised to protein levels as measured by BCA assay.

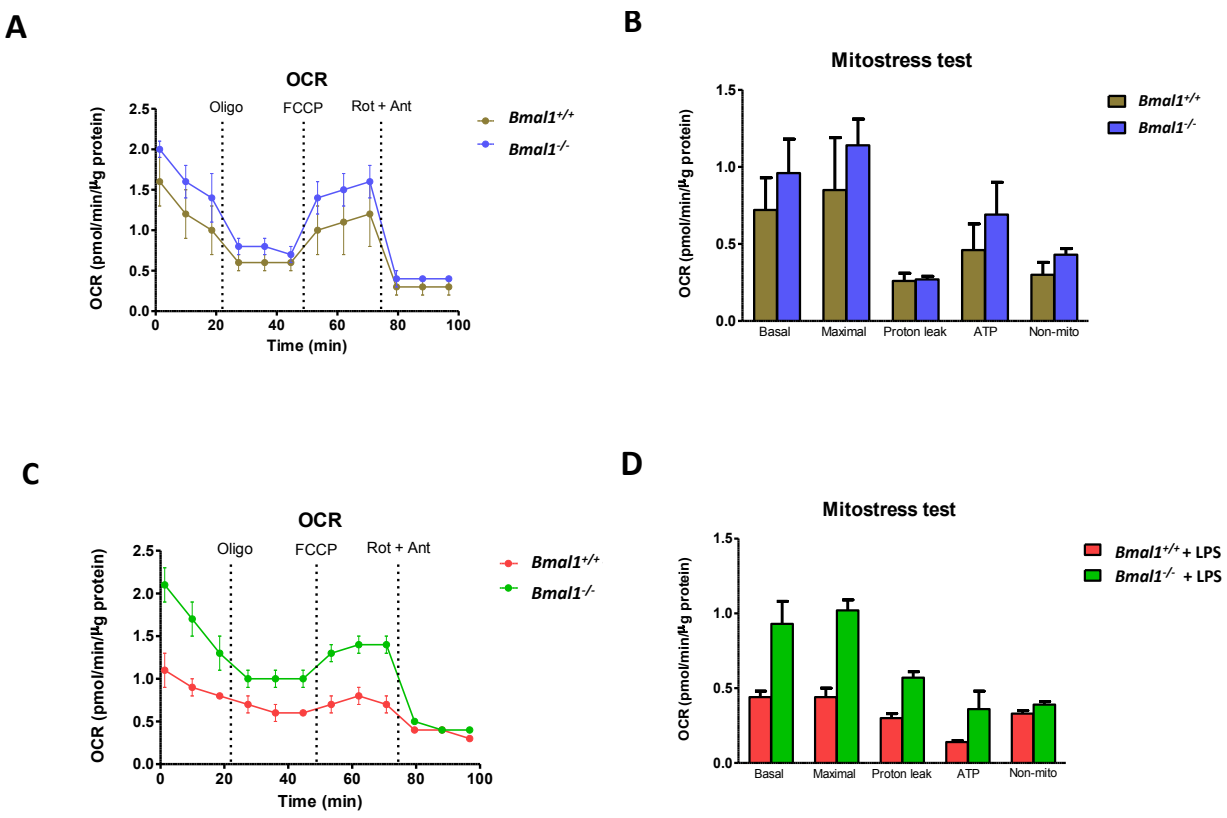

Figure 3.23 Oxidative phosphorylation is increased in *Bmal1*$^{-/-}$ BMDMs

Bmal1$^{+/+}$ and *Bmal1*$^{-/-}$ BMDMs were seeded at 1.25x10^5 cells/well in a specialised 24 well Seahorse cell plate and incubated overnight at 37°C. Cells were then left unstimulated or stimulated with 100 ng/ml LPS for 24 hrs. One hr before the run, the medium was removed from the cells and replaced with 500 µL of prewarmed XF assay medium supplemented with glutamine. The cell plate was then placed loaded into the Seahorse XF analyser and mitostress test was performed. (A) Trace graph showing mitochondrial metabolism readouts in untreated *Bmal1*$^{+/+}$ and *Bmal1*$^{-/-}$ BMDMs. (B) Bar chart showing mitochondrial metabolism readouts in untreated *Bmal1*$^{+/+}$ and *Bmal1*$^{-/-}$ BMDMs. (C) Trace graph showing mitochondrial metabolism readouts in LPS treated *Bmal1*$^{+/+}$ and *Bmal1*$^{-/-}$ BMDMs. (D) Bar chart showing mitochondrial metabolism readouts in LPS treated *Bmal1*$^{+/+}$ and *Bmal1*$^{-/-}$ BMDMs Data is a representative of 3 separate experiments. Data shown are the mean ± S.E.M. Data was normalised to protein levels as measured by BCA assay.

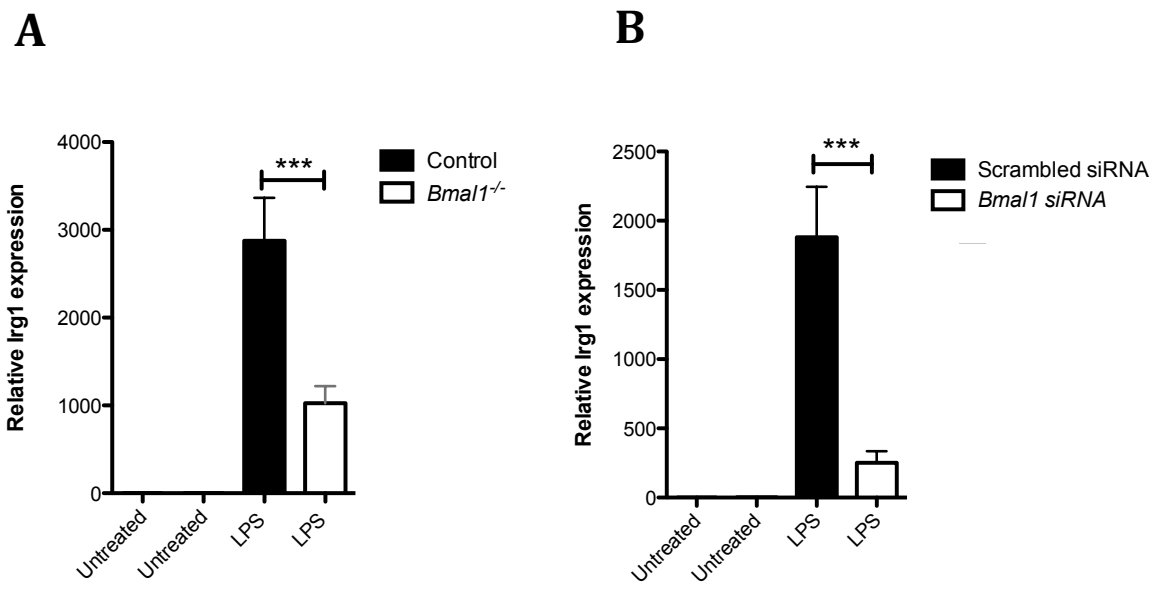

Figure 3.24 LPS induced *Irg1* transcription is decreased in both *Bmal1*$^{-/-}$ and *Bmal1* knockdown BMDMs

(A) *Bmal1*$^{+/+}$ and *Bmal1*$^{-/-}$ BMDMs were seeded at 5x10^5 cells/ml in a 12 well plate and incubated overnight at 37°C. Cells were then left unstimulated or stimulated with 100 ng/ml LPS for 24 hrs. Cells were lysed and mRNA was extracted and analysed using SYBR qPCR probes specific for murine *Irg1.* Data was normalised to *Rps18.* Fold induction was calculated relative to untreated cells. Data shown are the mean ± S.E.M., n=3. (B) Wild type BMDMs were seeded at 5x10^5 cells/ml in a 12 well plate and incubated overnight at 37°C. BMDMs were then transfected with either a scrambled siRNA control or siRNA targeting *Bmal1* Cells were then left unstimulated or stimulated with 100 ng/ml LPS for 24 hrs. Cells were lysed and mRNA was extracted and analysed using SYBR qPCR probes specific for murine *Irg1.* Data was normalised to *Rps18.* Fold induction was calculated relative to untreated cells. Data shown are the mean ± S.E.M., n=3.

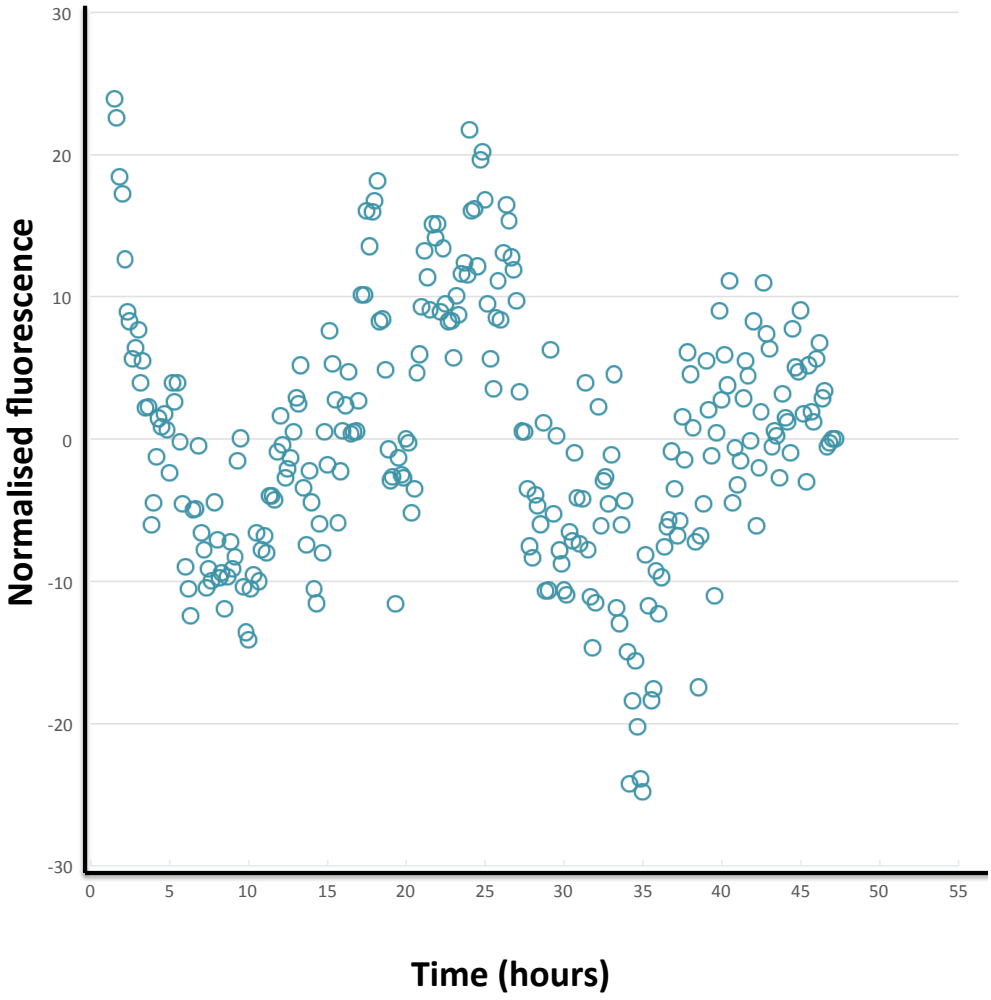

Figure 3.25 Mitochondrial membrane potential displays circadian rhythmicity

BMDMs were seeded at $5x10^5$ cells per well in a μ dish and incubated overnight at 37°C. Cells were then incubated in 50 % horse serum for 2 hrs to initiate serum shock. Media was then replaced. Cells were stained with Mitotracker red and were imaged using the x63 objective of a Zeiss LSM710 confocal microscope or for time-lapse microscopy images were acquired every 10 mins for 48 hrs using a wide-field epifluorescent microscope (Zeiss AxioObserver Z1) and a x63 oil immersion objective. Images shown are a representative of 3 separate experiments.

3.7 Discussion

3.7.1 Regulation of NRF2 by BMAL1

My results suggest that the NRF2 antioxidant defence pathway is under circadian mediated regulation in macrophages. Previous studies have accentuated the role of circadian rhythms in modulating *Nrf2* expression levels in various tissue types. Xu *et al.* (2016) demonstrated rhythms in *Nrf2* and its downstream targets expression levels in the liver (177). Binding of the BMAL1:CLOCK heterodimer to an E-box site within the *Nrf2* promoter has been demonstrated in lung tissue, providing time-of-day protection from pulmonary fibrosis (189). However, the molecular clock does not regulate NRF2 across all tissues. The BMAL1:CLOCK heterodimer was found to bind to the promoters of *Nqo1* and *Aldh2,* inducing their expression directly in the cerebral cortex, and not through the intermediate of NRF2 transcriptional regulation (162). In my study, I found diurnal rhythms in *Nrf2* in peritoneal myeloid cells across the circadian day. Interestingly, the trough and peak in *Nrf2* expression appeared to come just after the trough and peak in *Bmal1* expression, suggesting that BMAL1:CLOCK mediated induction of *Nrf2* occurs in myeloid cells. I further confirmed this with serum shock experiments in *Bmal1*$^{+/+}$ and *Bmal1*$^{-/-}$ BMDMs. Once again, a rhythm was found in *Nrf2* transcription, however, this rhythm was lost with *Bmal1* deletion and the levels of *Nrf2* were constitutively lower, matching patterns previously seen in lung tissue (176).

Upon activation of the immune response, oxidative stress builds in the cell, activating NRF2 (193). Transcription factor sequencing in LPS treated *Bmal1*$^{+/+}$ and *Bmal1*$^{-/-}$ BMDMs assessed the activity of 58 transcription factors associated with inflammatory pathways. This screen was limited by only examining macrophage response at 1 and 4 hrs of LPS and it is possible more would have been

achieved by measuring activity in later time points. Despite the limitations, the decrease in NRF2 activity in *Bmal1*$^{-/-}$ BMDMs strongly supported my hypothesis of a lack of NRF2 induction in these cells. This correlated well with my data demonstrating a basal decrease in NRF2 and a lack of LPS induced NRF2 accumulation in *Bmal1*$^{-/-}$ BMDMs. Ultimately, the lack of NRF2 activity with deletion of *Bmal1,* culminates in a lack of antioxidant response in these cells, matching the phenotype seen with *Nrf2* silencing. Interestingly, the same lack of NRF2 activity was seen following hydrogen peroxide stimulation, indicating that it is not simply LPS induced activation of NRF2 that is reduced in *Bmal1*$^{-/-}$ BMDMs, but all NRF2 induced activity as a whole.

Reduced glutathione (GSH) is a crucial mediator of detoxification in cells, mediating oxidative balance (163). Its synthesis is a downstream component of the NRF2 mediated anti-oxidant defence pathway (194). Glutathione reductase, the product of *Gsr,* which I determined was reduced with *Bmal1* deletion, catalyses the reduction of oxidized glutathione (GSSG) to the sulfhydryl GSH form (175). Glutamate cysteine ligase modifier subunit is encoded by *Gclm,* and is crucial in de novo synthesis of GSH (195). *Gclm* was also decreased with *Bmal1* deletion. I found that total cell levels of GSH were decreased in *Bmal1*$^{-/-}$ BMDMs versus *Bmal1*$^{+/+}$ controls, also confirming a decrease in NRF2 activity in these cells and insinuating an altered oxidative state in these cells. NAC primarily carries out its function as an antioxidant by acting as a precursor to glutathione synthesis. It is distinctly possible that the increased oxidative damage caused by *Bmal1* deletion in different tissues is due to GSH deficiency, explaining why NAC has been useful in removing deleterious effects of *Bmal1* deletion (160, 161).

While investigating regulation of NRF2 by BMAL1, I decided to assess whether there was a feedback loop evident between NRF2 and the circadian cycle. The molecular clock is built off of multiple intricate transcriptional, translational

feedback loops that allow for response to various cellular alterations and stresses (196). During the course of my studies, a study revealed that there was indeed a feedback loop of NRF2 on the circadian cycle (191). Ultimately, *Nrf2's* induction by the circadian cycle facilitates increased NRF2 activity. NRF2 may then bind elements in the promoter of *Nr1d1* and *Cry2,* allowing for inhibition of *Bmal1* transcription and activity (191). Indeed, when cells are treated with LPS we see alterations in transcription to components of the molecular clock. We previously reported that *Bmal1* transcription is decreased following LPS stimulation (31). We found this to be a result of boosted *Mir-155* expression (31). However, in this study I also found that LPS increased expression of both *Nr1d1* and *Cry2*, genes that have been demonstrated as being regulated by NRF2 (191). When wild type macrophages were treated with OI, a novel inducer of NRF2 activity (Ryan and Mills et.al. 2018 (in press)). I saw similar alterations to clock gene expression. *Nr1d1* and *Cry2* were both increased in a similar fashion to LPS induction. I hypothesise that there may exist a possible novel inflammatory feedback loop on the circadian cycle in macrophages. During inflammation, oxidative stress accumulates, facilitating NRF2 activity. NRF2 induces *Nr1d1* and *Cry2,* switching off the forward arm of the clock through BMAL1 inhibition. Decrease in BMAL1 activity facilitates a heightened inflammatory response, allowing for efficient pathogen clearance. However, with the forward arm of the clock disabled, *Nrf2* transcription decreases, lowering NRF2 activity. Ultimately this would allow for BMAL1 levels to accumulate once again facilitating resolution of inflammation and a return to homeostasis.

3.7.2 Regulation of oxidative stress by BMAL1 via NRF2

My results display a clear decrease in the NRF2 mediated antioxidant defence pathway in macrophages lacking *Bmal1.* The molecular clock has previously been

associated with regulation of oxidative stress in multiple tissue types (160, 162). In my studies I discovered a diurnal peak and trough in ROS in peritoneal myeloid cells. Interestingly, this matched the peak and trough in *Bmal1* and *Nrf2* expression. Given the importance of NRF2 in regulating oxidative stress, I hypothesise that BMAL1 mediated regulation of NRF2 is facilitating rhythms in ROS. While this mechanism prevents accumulation of ROS, it does not account for increased generation of oxidative stress. A diurnal peak and trough was clearly evident in ROS production and regulation genes between ZT0 and ZT12. For example, *Nox1,* which forms a catalytic subunit of NADPH oxidase, a major producer of ROS that is crucial to macrophage differentiation (197), was significantly up regulated at ZT12. Similarly, *Nos2*, an initiator of nitric oxide production and a marker of pro-inflammatory macrophage differentiation (198), was also increased. It is possible that increased ROS production as well as decreased ROS regulation could be leading to the circadian gating of LPS induced endotoxic shock seen in mice.

My results suggested an alteration to oxidative stress regulation with deletion of *Bmal1.* I confirmed this by measuring ROS directly by flow cytometry. *Bmal1* silencing or deletion resulted in a large increase in both basal and LPS induced ROS. This is most likely due to a lack of NRF2 induced antioxidant response in these cells and possibly also through increased ROS production. This conclusion was further supported when ROS levels in *Bmal1*$^{+/+}$ and *Bmal1*$^{-/-}$ BMDMs were examined by confocal. It was once again clear that oxidative stress was increased with *Bmal1* deletion. However, it was also clear that the ROS staining was co-localising with the mitochondrial stain, suggesting that the source of the increased ROS in *Bmal1*$^{-/-}$ BMDMs is the mitochondria. Mitochondrial ROS is emerging as a potent signal in driving inflammation (199), specifically it has been linked to facilitating accumulation of the hypoxic response protein HIF-1α (132). Further confirming the presence of increased oxidative stress and suggesting the source of this ROS as mitochondria, HIF-1α was largely increased with *Bmal1* deletion. Cumulatively,

these results highlight an altered oxidative landscape when the molecular clock is disrupted.

3.7.3 Regulation of metabolism by BMAL1

The presence of increased oxidative stress and HIF-1α are indicative of altered metabolism within a cell (130). Previous reports have detailed alterations in metabolism with *Bmal1* deletion in liver cells, both in metabolic phenotype (136) and mitochondrial dynamics (142). In the first instance, I investigated the overall metabolic status of *Bmal1*$^{-/-}$ BMDMs, both basally and with LPS stimulation. In line with the HIF-1α increase, other glycolytic genes were increased with *Bmal1* deletion. This correlated with an overall increase in glycolysis following LPS stimulation in these macrophages. Overall this phenotype matches with the held image of inflammation in macrophages. Increased glycolysis facilities increased oxidative stress and inflammation (128). However, OXPHOS was not decreased with *Bmal1* deletion following LPS stimulation, as was seen in control cells. This was confusing given the overall dogma of LPS resulting in decreased OXPHOS (128, 200). However, recent investigations have uncovered a role for the endogenous metabolite itaconate in regulation of OXPHOS (135). It appears that during inflammation, itaconate is induced to limit SDH (complex2), limiting OXPHOS. Macrophages lacking *Irg1* produce no itaconate. While there is increased OXPHOS in these cells, they also produce increased ROS and inflammation (135). I found a significant decrease in LPS induced *Irg1*, both in *Bmal1* knockout and knockdown BMDMs. I hypothesise that a lack of *Irg1* in *Bmal1*$^{-/-}$ BMDMs could be altering the metabolic state of these cells during inflammation, facilitating mitochondrial dysfunction and oxidative stress production. Interestingly, Itaconate has also recently been linked to boosting NRF2 activity and decreasing HIF-1α (Ryan and Mills et.al. 2018 (in press)). As well as this, circadian rhythms have previously been

linked to mitochondrial morphology and function (142). Specifically, rhythms were found in mitochondrial membrane potential across the circadian day. *Bmal1* deletion in liver cells has been shown to promote mitochondrial fission, a state in which they produce more ROS (142). Mitochondrial membrane potential has also been linked to the ability of a macrophage to perform phagocytosis (125) and is a known indicator of the metabolic health of a cell, being linked to energy and ATP production (201). Changes to mitochondrial membrane potential are also known to result in ROS production (201). It is possible that circadian rhythms in mitochondrial membrane potential and function could lead to oscillations in factors such as ROS, glycolysis and OXPHOS, and that deletion of *Bmal1* impacts these rhythms. I hypothesise that an accumulation of these factors, decreased antioxidant response, increased glycolysis and OXPHOS, altered mitochondrial morphology and function, are contributing to the increased inflammatory and oxidative state seen in *Bmal1* deficient or clock disrupted mice.

3.7.4 Final conclusions

In summary, regulation of oxidative stress appears to follow a diurnal rhythm in macrophages. Deletion of *Bmal1* facilitates disruption of this rhythm and promotes constitutively elevated levels of oxidative stress. The mechanisms resulting in this phenotype are outlined below:

First of all, these macrophages present with a lack of antioxidant defence due to dampening of the NRF2 mediated antioxidant defence pathway. Secondly, the metabolic state of these cells is vastly altered to wild type counterparts, with *Bmal1*$^{-/-}$ BMDMs displaying both increased levels of glycolysis and OXPHOS. It is possible these alterations are a result of altered mitochondrial physiology and function in these cells, and/or alterations in levels of the metabolite itaconate, a known post-translational regulator of NRF2. Given the emergence of the importance of oxidative stress and metabolism on the immune system, my results pave the way for understanding the mechanisms driving the inflammatory phenotype exhibited with disruption of the molecular clock.

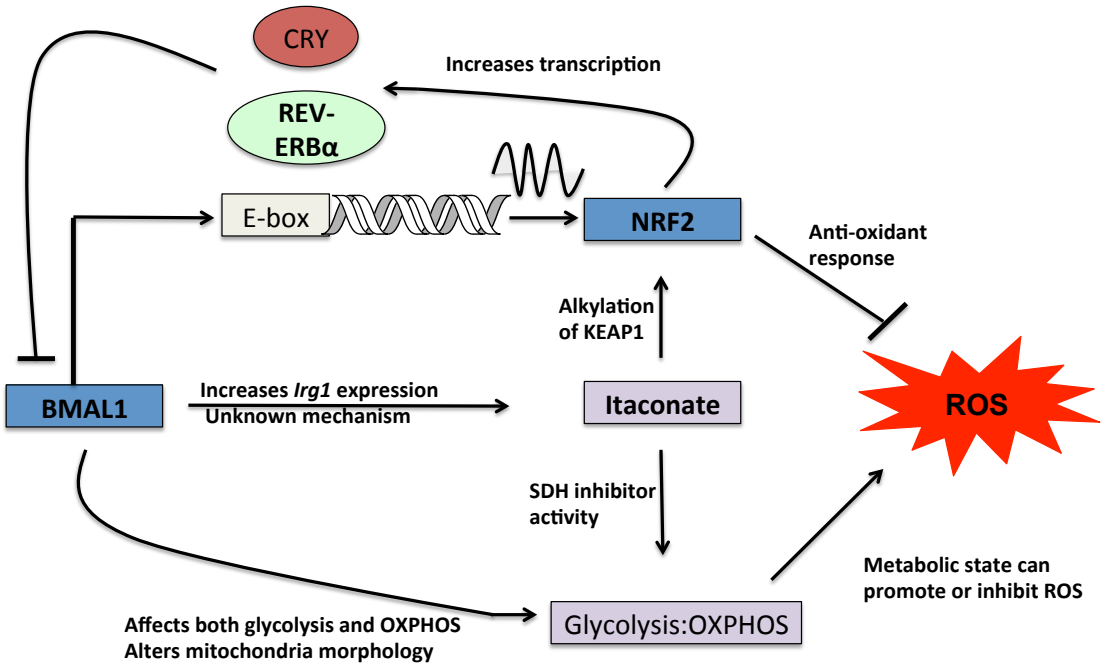

Figure 3.26 Current hypothesis for the role of BMAL1 in oxidative stress regulation

BMAL1 can induce circadian rhythms in the expression of *Nrf2* through direct binding to E-boxes in its promoter. NRF2 can feed back on clock function and phase by inducing clock repressors REV-ERBα and CRY2. BMAL1 also appears to be necessary for LPS induced *Irg1* expression. Itaconate is a positive regulator of NRF2 activity, freeing it from KEAP1 by alkylating certain cysteine residues. Itaconate also feeds back into metabolism and the TCA cycle by acting as an inhibitor of SDH activity. Deletion of BMAL1 results in altered glycolytic and OXPHOS phenotypes. Whether differences in itaconate plays a role is yet to be uncovered. However, alterations in metabolism and mitochondrial form and function would also alter ROS production in the cell.

Chapter 4: Results

BMAL1 regulates IL-1β in macrophages via NRF2

Much of the work presented in this chapter has been used in a publication that is currently being revised for PNAS titled "The Circadian Clock Protein BMAL1 Regulates IL-1β in Macrophages via NRF2" (Early J.O. et.al 2018).

4.1 Introduction

The molecular clock exists within immune cells (15), and recent reports have brought attention to the level of circadian rhythmicity displayed by the immune system. Daily oscillations in immune parameters have been demonstrated to significantly impact the type and magnitude of an immune response throughout the 24 hr day (1). In macrophages, ROS promote a pro-inflammatory response following LPS induced activation of TLR4, boosting production of the cytokine IL-1β via stabilization of HIF-1α (132). Given my previous results, which showed increased ROS and HIF-1α, I began to investigate whether IL-1β is under regulation of the molecular clock.

IL-1β is a well-established pyrogen critical in producing symptoms of fever and driving inflammation. It is also a major inducer of pathogenesis in multiple circadian associated disorders, such as sepsis (31), rheumatoid arthritis (108), and multiple sclerosis (79). Although IL-1β induction appears to be modulated by time of day (78, 108), the exact mechanisms underpinning time-of-day variation are unknown. I first investigated whether deletion of *Bmal1* had any effect on the regulation of IL-1β, or indeed other pro-inflammatory cytokines. I also tested whether several compounds that alter activity of REV-ERBα and CRY had any effect on cytokine production.

NRF2 is currently emerging in the literature as a novel regulator of inflammation. NRF2 can limit inflammation via suppression of oxidative stress (Dylan and Mills et.al. 2018 (in press)). However, NRF2 has been demonstrated to limit IL-6 and IL-1β production through direct binding of NRF2 to regulatory regions in their promoters, which inhibits RNA Pol II recruitment (166). I next endeavoured to assess whether the alterations in NRF2 levels and activity with deletion of *Bmal1* could impact the pro-inflammatory phenotype of these cells. This was followed by attempted rescue of inflammation via ROS scavenging and NRF2 activation.

4.2 BMAL1 localisation is dynamic following LPS stimulation

We have previously reported on LPS induced suppression of *Bmal1* transcription (31). However, localization of BMAL1 during LPS stimulation of macrophages has not previously been explored. BMAL1 nuclear (Figure 4.1A) and cytosolic (Figure 4.1B) translocation was examined in RAWs, a murine macrophage cell line, following 2, 4, 8 and 24 hrs of LPS stimulation. It was seen that BMAL1 was clearly present in the nucleus in untreated samples (lane 1). However, following LPS stimulation, BMAL1 was absent from the nuclear fraction and became present in the cytosolic fraction (lanes 2, 3 and 4). BMAL1 was present in the nucleus once again following 24 hrs of LPS (lane 5). It appears that BMAL1 localisation is spatially controlled following LPS stimulation in macrophages.

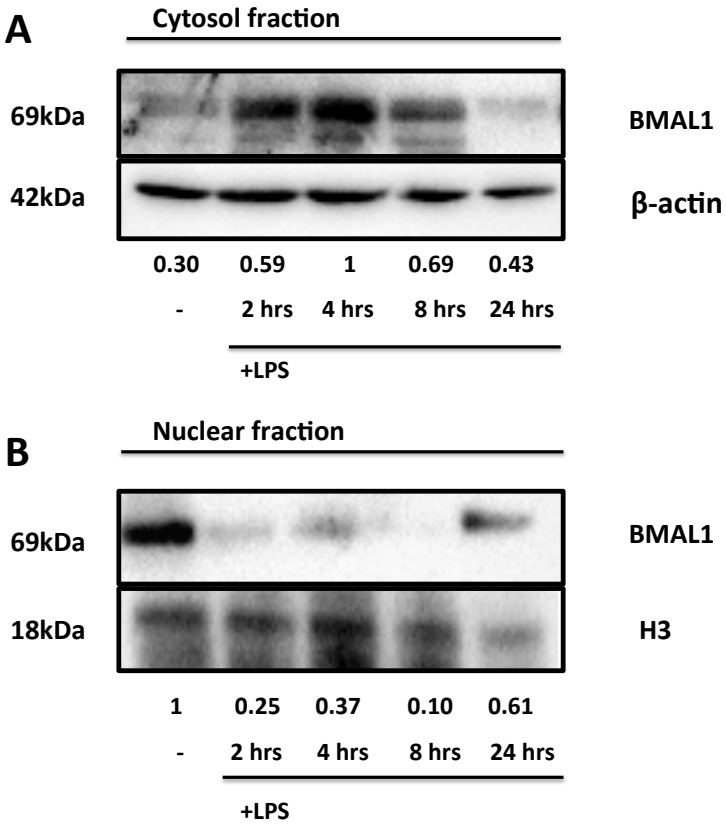

Figure 4.1 Localisation of BMAL1 is dynamic following LPS treatment

RAWs were grown until confluent in T175 flasks at 37°C in DMEM media supplemented with 10% FCS. Cells were left unstimulated or treated with 100ng/ml LPS for 2, 4, 8 or 24hrs. The samples were then fractionated isolating the nuclear and cytosolic fraction. The subsequent fractions were digested in RIPA protein lysis buffer and the level of protein was quantified by B.C.A. assay. The experiment shown is a representative of two independent experiments. (A) The cytosol fraction was analysed by western blotting using anti-BMAL1 and anti-β-actin antibodies. β-actin is presented as a loading control. (B) The nuclear fraction was analysed by western blotting using anti-BMAL1 and anti-Histone 3 (H3) antibodies. H3 is presented as a loading control.

4.3 *Bmal1* and *Nrf2* deficiency enhances IL-1β production

IL-1β levels demonstrate clear diurnal levels in circulation of mice following *L. monocytogenes* infection (78). In macrophages, ROS promote production of the cytokine IL-1β via stabilization of HIF-1α (130). NRF2 has been demonstrated to limit IL-1β, not only through suppression of ROS, but also through direct binding of NRF2 to regulatory regions in the *Il1b* promoter (166). Therefore, I next investigated whether BMAL1 mediated regulation of *Nrf2* would impact IL-1β production. Knockdown of *Nrf2* resulted in an increase in *Il1b* mRNA (Figure 4.2A) and protein (Figure 4.2B) following LPS stimulation, which confirmed previously reported findings of NRF2 mediated suppression of IL-1β (166) (Ryan and Mills et.al. 2018 (in press)). I next investigated the regulation of IL-1β in macrophages lacking *Bmal1*. LPS treatment of *Bmal1*$^{-/-}$ BMDMs revealed a boost in *Il1b* transcription relative to *Bmal1*$^{+/+}$ BMDMs at both 8 (Figure 4.3A) and 24 (Figure 4.3B) hrs following LPS stimulation. This effect was also observed at the protein level with a large increase in pro-IL-1β evident in *Bmal1*$^{-/-}$ BMDMs at 24 (Figure 4.4B), 48 (Figure 4.4C) and 72 (Figure 4.4D) hrs following LPS stimulation. However, an increase in pro-IL-1β was not evident in *Bmal1*$^{-/-}$ BMDMs following 4 hrs of LPS stimulation (Figure 4.4A). This phenotype was confirmed with siRNA-mediated knockdown of *Bmal1* in wild type BMDMs at the transcript (Figure 4.5A) and protein (Figure 4.5B) levels.

I extracted peritoneal cells (PECs) from *Bmal1*$^{+/+}$ and *Bmal1*$^{-/-}$ to assay whether the same phenotype was observed in these cells. The myeloid cells extracted from *Bmal1*$^{Myeloid-/-}$ mice produced no BMAL1 at the protein level (Figure 4.6A). I observed a similar phenotype to BMDMs, with greater production of pro-IL-1β observed in *Bmal1*$^{-/-}$ PECs relative to *Bmal1*$^{+/+}$ PECs (Figure 4.6B).

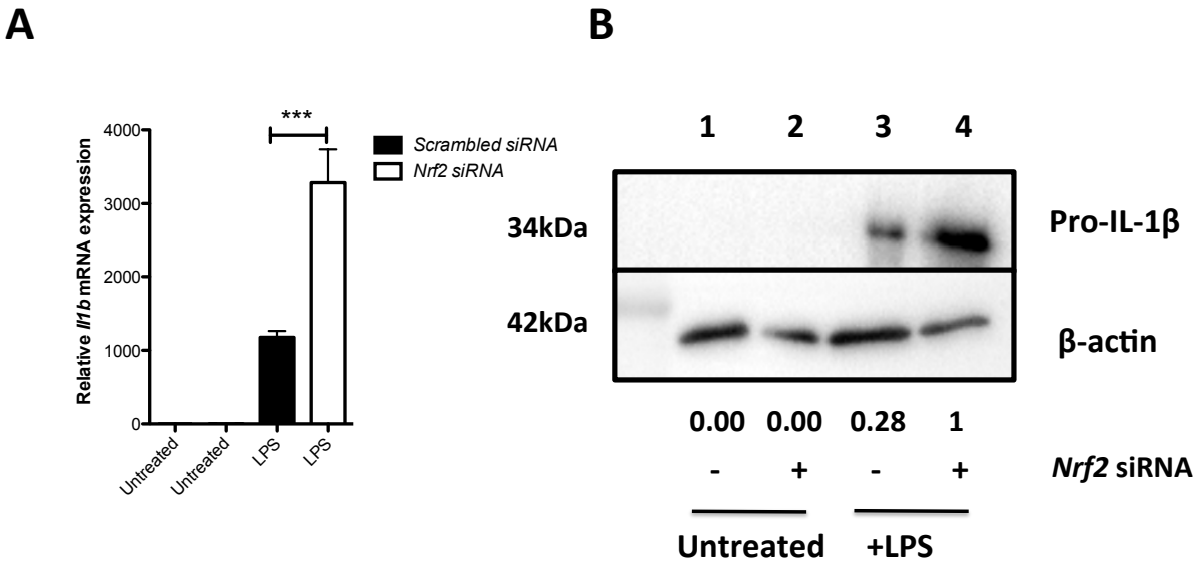

Figure 4.2 IL-1β transcript and protein are increased with *Nrf2* knockdown

Wild type BMDMs were seeded at 5x10^5 cells/ml in a 12 well plate and incubated overnight at 37°C. BMDMs were then transfected with either a scrambled siRNA control or siRNA targeting *Nrf2.* The cells were then incubated overnight at 37°C. Cells were then left unstimulated or stimulated with 100 ng/ml LPS for 24 hrs. (A) Cells were lysed and mRNA was extracted and analysed using SYBR qPCR probes specific for murine *Il1b.* Data was normalised to *Rps18.* Fold induction was calculated relative to untreated cells. Data shown are the mean ± S.E.M., n=3. (B) Cells were lysed in sample loading buffer and analysed by western blotting using anti-IL-1β and anti-β-actin antibodies. β-actin is presented as a loading control. Results are a representative of at least 3 independent experiments.

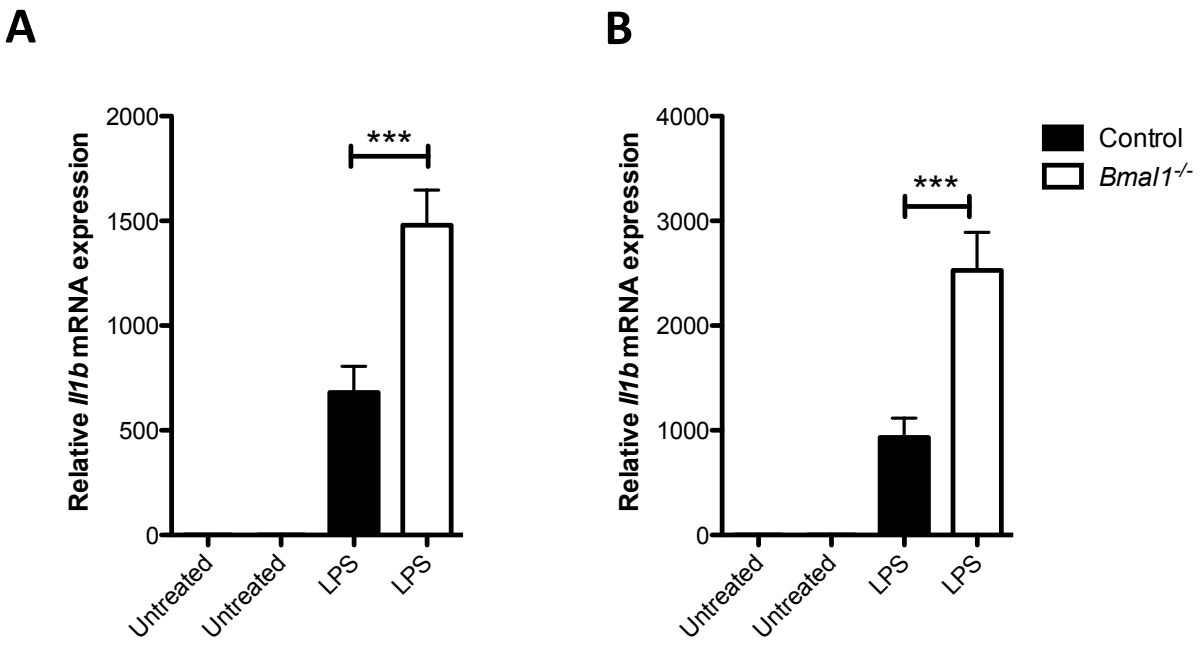

Figure 4.3 Increased *Il1b* transcription in *Bmal1*$^{-/-}$ BMDMs

Bmal1$^{+/+}$ and *Bmal1*$^{-/-}$ BMDMs were seeded at 5x10^5 cells/ml in a 12 well plate and incubated overnight at 37°C. Cells were then left unstimulated or stimulated with 100 ng/ml LPS for (A) 8 or (B) 24 hrs. Cells were lysed and mRNA was extracted and analysed using SYBR qPCR probes specific for murine *Il1b.* Data was normalised to *Rps18.* Fold induction was calculated relative to untreated cells. Data shown are the mean ± S.E.M., n=8.

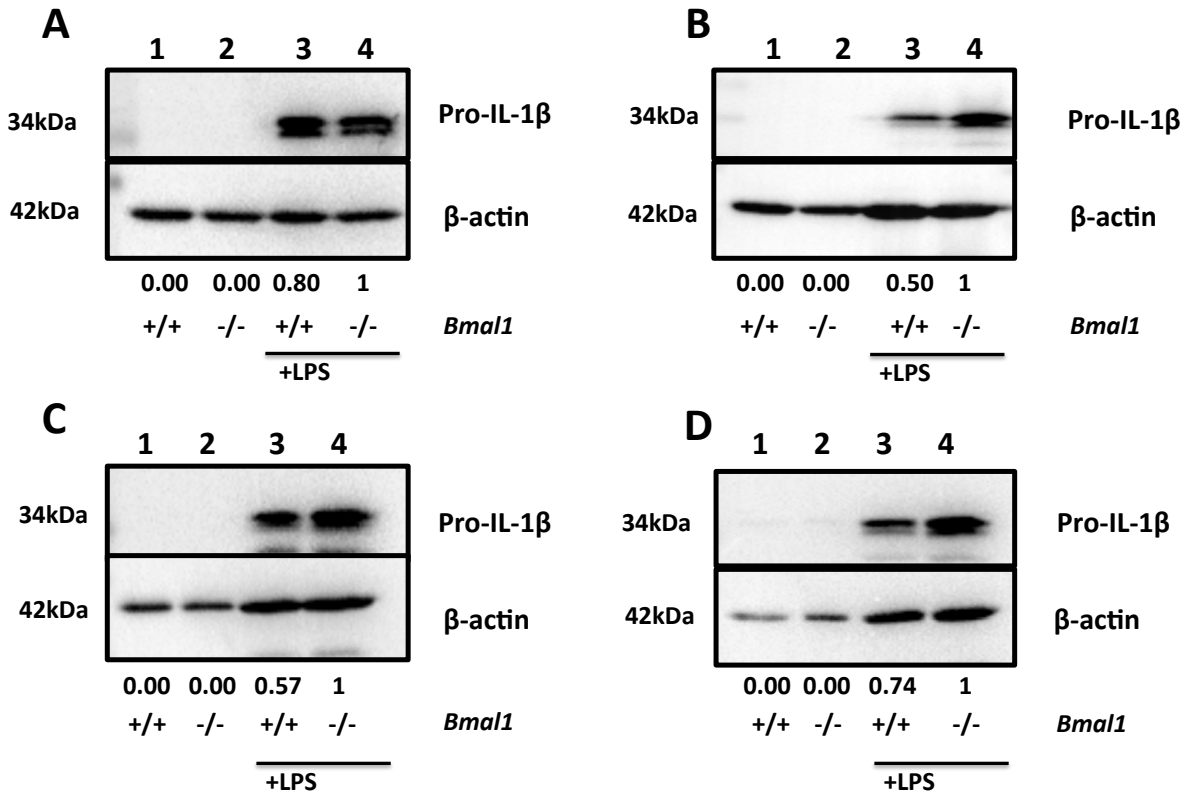

Figure 4.4 Increased Pro-IL-1β protein in *Bmal1*$^{-/-}$ BMDMs

Bmal1$^{+/+}$ and *Bmal1*$^{-/-}$ BMDMs were seeded at 5x10^5 cells/ml in a 12 well plate and incubated overnight at 37°C. Cells were then left unstimulated or stimulated with 100 ng/ml LPS for (A) 4, (B) 24 hrs, (C) 48 hrs or (D) 72 hrs. Cells were lysed in sample loading buffer and analysed by western blotting using anti-IL-1β and anti-β-actin antibodies. β-actin is presented as a loading control. Results are a representative of at least 3 independent experiments.

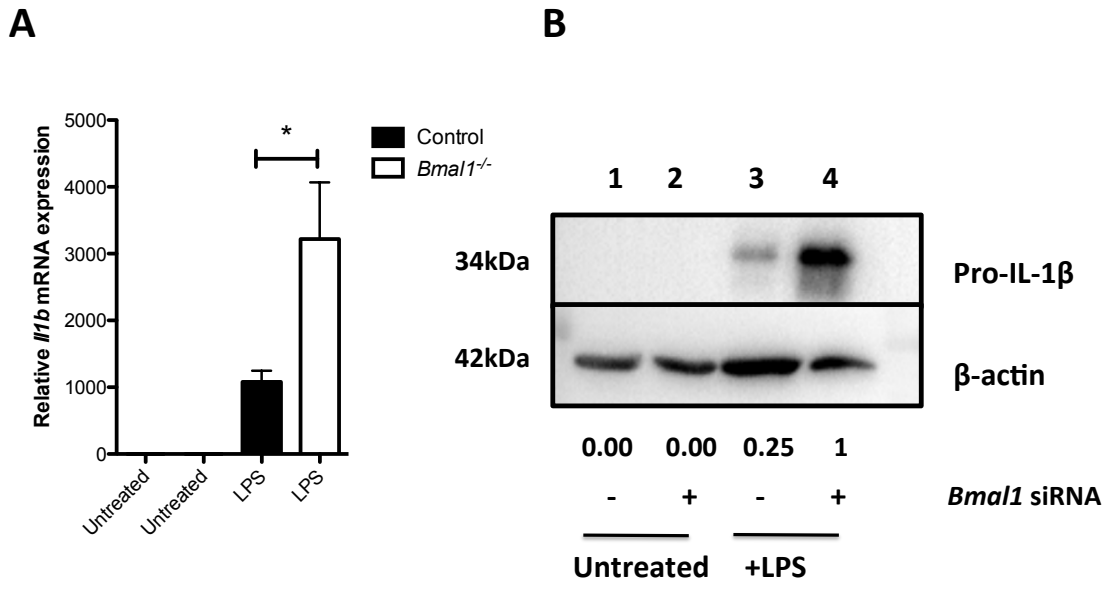

Figure 4.5 Increased IL-1β transcript and protein with *Bmal1* knockdown

Wild type BMDMs were seeded at 5x10^5 cells/ml in a 12 well plate and incubated overnight at 37°C. BMDMs were then transfected with either a scrambled siRNA control or siRNA targeting *Bmal1.* The cells were then incubated overnight at 37°C. Cells were then left unstimulated or stimulated with 100 ng/ml LPS for 24 hrs. (A) Cells were lysed and mRNA was extracted and analysed using SYBR qPCR probes specific for murine *Il1b.* Data was normalised to *Rps18.* Fold induction was calculated relative to untreated cells. Data shown are the mean ± S.E.M., n=6. (B) Cells were lysed in sample loading buffer and analysed by western blotting using anti-IL-1β and anti-β-actin antibodies. β-actin is presented as a loading control. Results are a representative of at least 3 independent experiments.

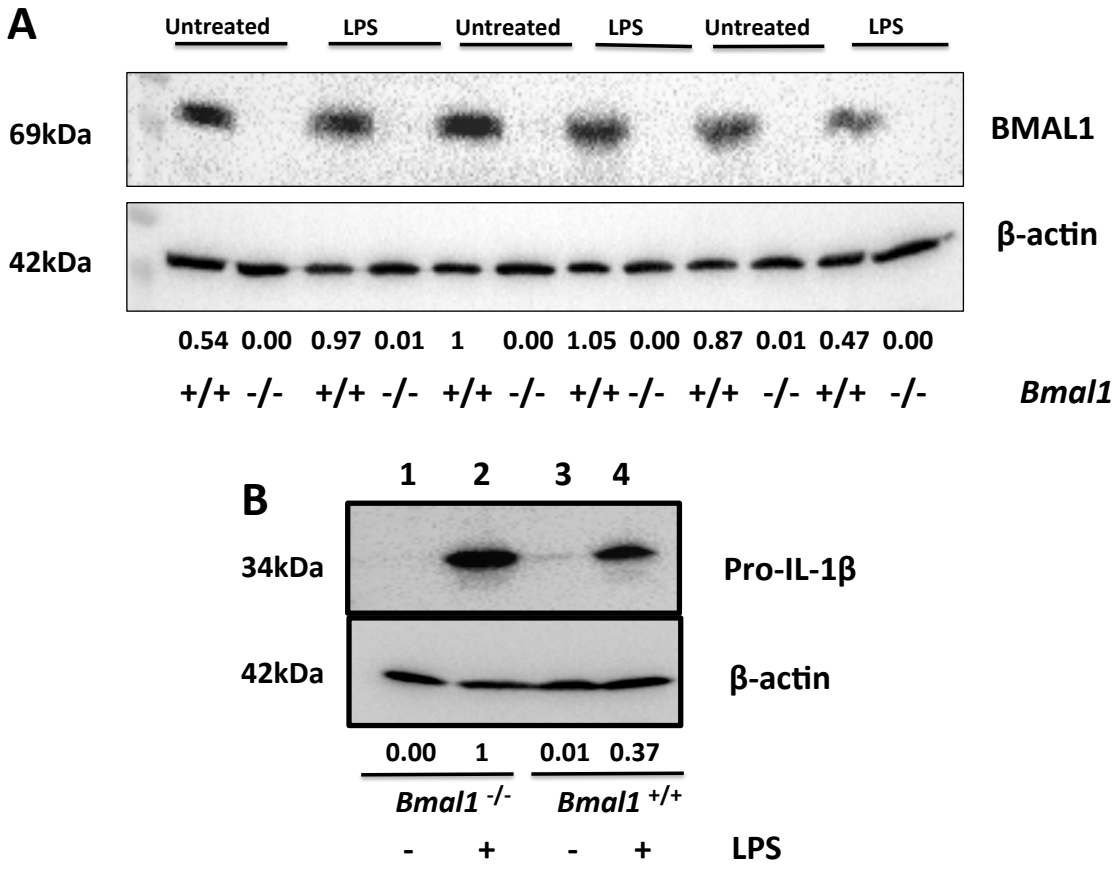

Figure 4.6 Increased Pro-IL-1β protein in *Bmal1*$^{-/-}$ PECs

PECs were isolated from *Bmal1*$^{+/+}$ and *Bmal1*$^{-/-}$ and plated at 5x10^5 cells/ml. Cells were then left unstimulated or stimulated with 100 ng/ml LPS for 24 hrs. Cells were lysed in sample loading buffer and analysed by western blotting using (A) anti-BMAL1 (B) anti-IL-1β and anti-β-actin antibodies. β-actin is presented as a loading control. Results are a representative of at least 3 independent experiments.

4.4 BMAL1 mediated regulation of pro-inflammatory cytokines

NF-κB has previously been demonstrated by our lab to be under regulation of the molecular clock (31). For this reason, I investigated other inflammatory cytokines in *Bmal1* deficient macrophages to assess the pattern of inflammation displayed by these cells. I measured the levels of IL-6 (Figure 4.7A), IL-10 (Figure 4.7B) and TNFα (Figure 4.7C) in *Bmal1*$^{-/-}$ BMDMs following LPS stimulation. An increase was observed in IL-6, a decrease in IL-10 and no change in TNFα relative to *Bmal1*$^{+/+}$ BMDMs. This phenotype in IL-6 (Figure 4.8A), IL-10 (Figure 4.8B) and TNFα (Figure 4.8C) was confirmed with siRNA-mediated knockdown of *Bmal1* in wild type BMDMs. When investigating these cytokines in peritoneal cells, a different pattern was observed. IL-6 (Figure 4.9A) exhibited no change, IL-10 (Figure 4.9B) was decreased and TNFα (Figure 4.9C) was increased in *Bmal1*$^{-/-}$ BMDMs following LPS stimulation.

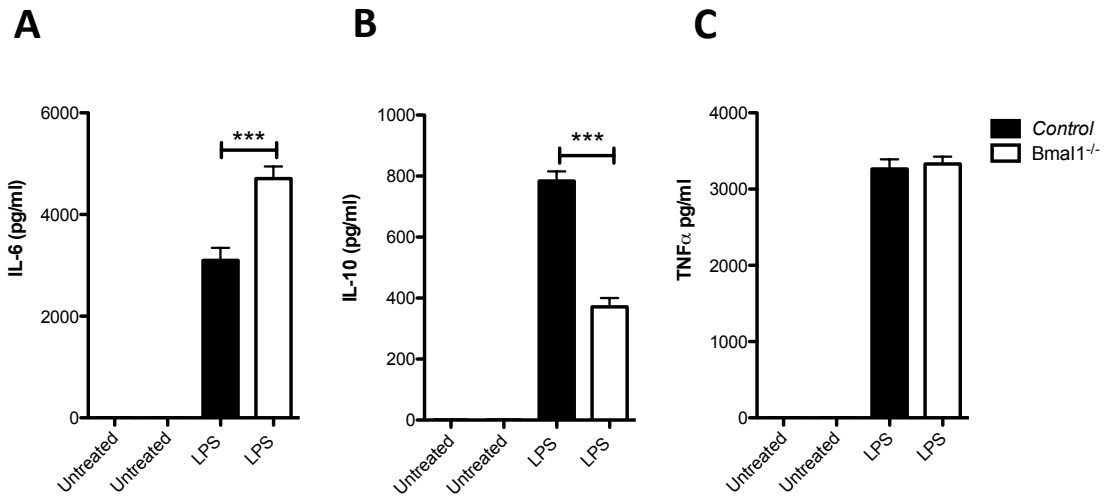

Figure 4.7 IL-6 increased, IL-10 decreased and no change in TNFα in *Bmal1*$^{-/-}$ BMDMs

Bmal1$^{+/+}$ and *Bmal1*$^{-/-}$ BMDMs were seeded at 5x10^5 cells/ml in a 12 well plate and incubated overnight at 37°C. Cells were then left unstimulated or stimulated with 100 ng/ml LPS for 24 hrs. Cell supernatants were removed and (A) IL-6, (B) IL-10 and (C) TNFα were quantified by ELISA. Data shown are the mean ± S.E.M., n=4.

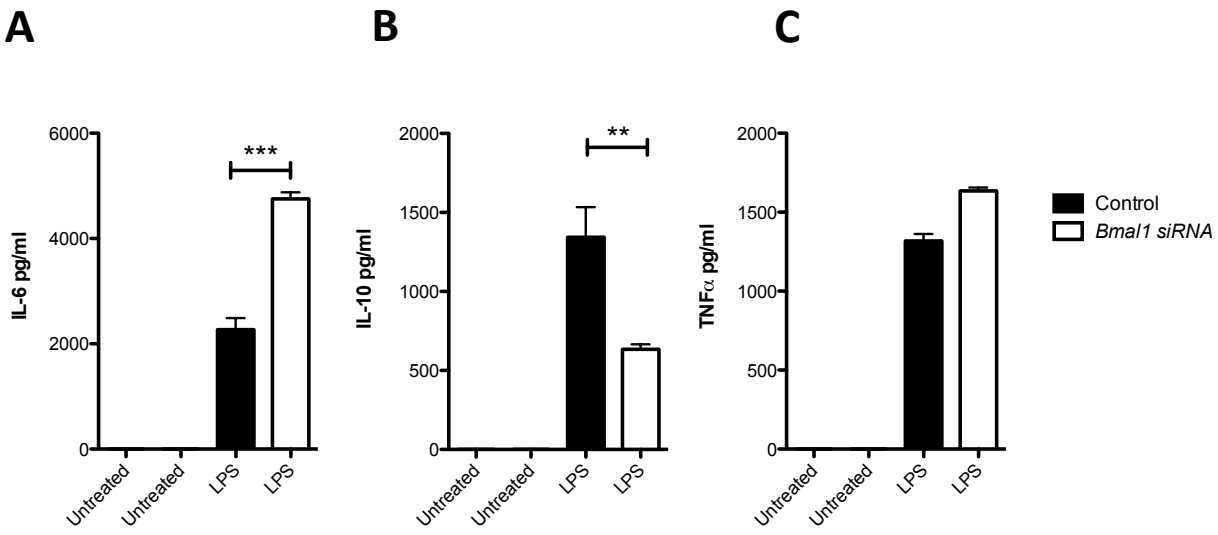

Figure 4.8 IL-6 increased, IL-10 decreased and no change in TNFα in *Bmal1* knockdown BMDMs

Wild type BMDMs were seeded at $5x10^5$ cells/ml in a 12 well plate and incubated overnight at 37°C. BMDMs were then transfected with either a scrambled siRNA control or siRNA targeting *Bmal1.* The cells were then incubated overnight at 37°C. Cells were then left unstimulated or stimulated with 100 ng/ml LPS for 24 hrs. Cell supernatants were removed and (A) IL-6, (B) IL-10 and (C) TNFα were quantified by ELISA. Data shown are the mean ± S.E.M., n=3.

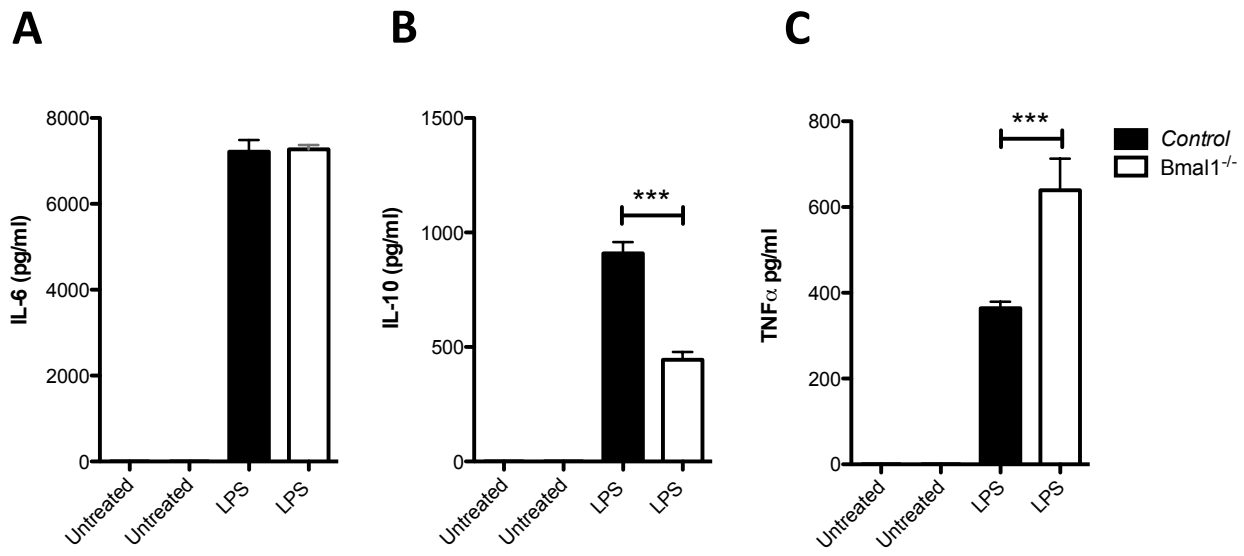

Figure 4.9 No change in IL-6, IL-10 decreased and TNFa increased in *Bmal1*$^{-/-}$ peritoneal cells

Peritoneal cells were isolated from *Bmal1*$^{+/+}$ and *Bmal1*$^{-/-}$and plated at 5x10^5 cells/ml. Cells were then left unstimulated or stimulated with 100 ng/ml LPS for 24 hrs. Cell supernatants were removed and (A) IL-6, (B) IL-10 and (C) TNFα were quantified by ELISA. Data shown are the mean ± S.E.M., n=3.

4.5 Examination of molecular clock agonists and antagonist on inflammatory cytokine production

To confirm the role of the molecular clock in cytokine regulation, a number of pharmaceutical agents were used to induce/repress various proteins of the molecular clock.

4.5.1 GSK4112 enhances production of pro-inflammatory cytokines

GSK4112 is a synthetic ligand and agonist for REV-ERBα, which has been documented to have an anti-inflammatory effect in human cells. Wild type BMDMs were pre-treated with 10, 25 and 50 μM GSK4112 before stimulation with LPS. These concentrations were decided on from observations in a previous publication (97). GSK4112 was found to boost LPS induced pro-IL-1β with all concentrations used (Figure 4.10A). Similar to *Bmal1*$^{-/-}$ BMDMs, GSK4112 boosted IL-6 at 50 μM (Figure 4.10B). It also produced a decrease in IL-10 (Figure 4.10C) and had no effect on TNFα (Figure 4.10D).

4.5.2 SR9009 decreases production of IL-10

SR9009 is another small molecule agonist that boosts REV-ERBα activity, but will also boost REV-ERBβ activity. Wild type BMDMs were pre-treated with 10 nM of SR9009 before stimulation with LPS. It has now come to light that this was not the optimal concentration as the IC50 for this compound has now been determined at 670 nm for REV-ERBα and 800 nm for REV-ERBβ (202). Unlike GSK4112, SR9009 produced no effect on pro-IL-1β (Figure 4.11A) levels. Similarly IL-6 was unaffected (Figure 4.11B). However, similar to GSK4112, SR9009 decreased IL-10 (Figure

4.11C) and had no effect on TNFα (Figure 4.11D). It is possible that increasing concentration of SR9009 would have produced an effect on pro-IL-1β and IL-6.

4.5.3 SR8278 decreases production of pro-IL-1β

SR8278 binds to REV-ERBα, inhibiting its activity. Wild type BMDMs were pre-treated with 10 and 25 μM SR8278 before stimulation with LPS. This concentration was used based on previous experiments with GSK4112. SR8278 was found to decrease LPS induced pro-IL-1β (Figure 4.12), which is interesting as it produced the opposite effect to GSK4112, the REV-ERBα agonist.

4.5.4 KL001 decreases production of pro-IL-1β

KL001 prevents ubiquitination of CRY, extending its period of activity and thus, increasing its activity. It has also been demonstrated to have an anti-inflammatory effect in a mouse model of rheumatoid arthritis (108). Wild type BMDMs were pre-treated with 10 and 25 μM KL001 before stimulation with LPS. These concentrations were decided on based on effects seen in a publication (108). KL001 was found to decrease LPS induced pro-IL-1β (Figure 4.13).

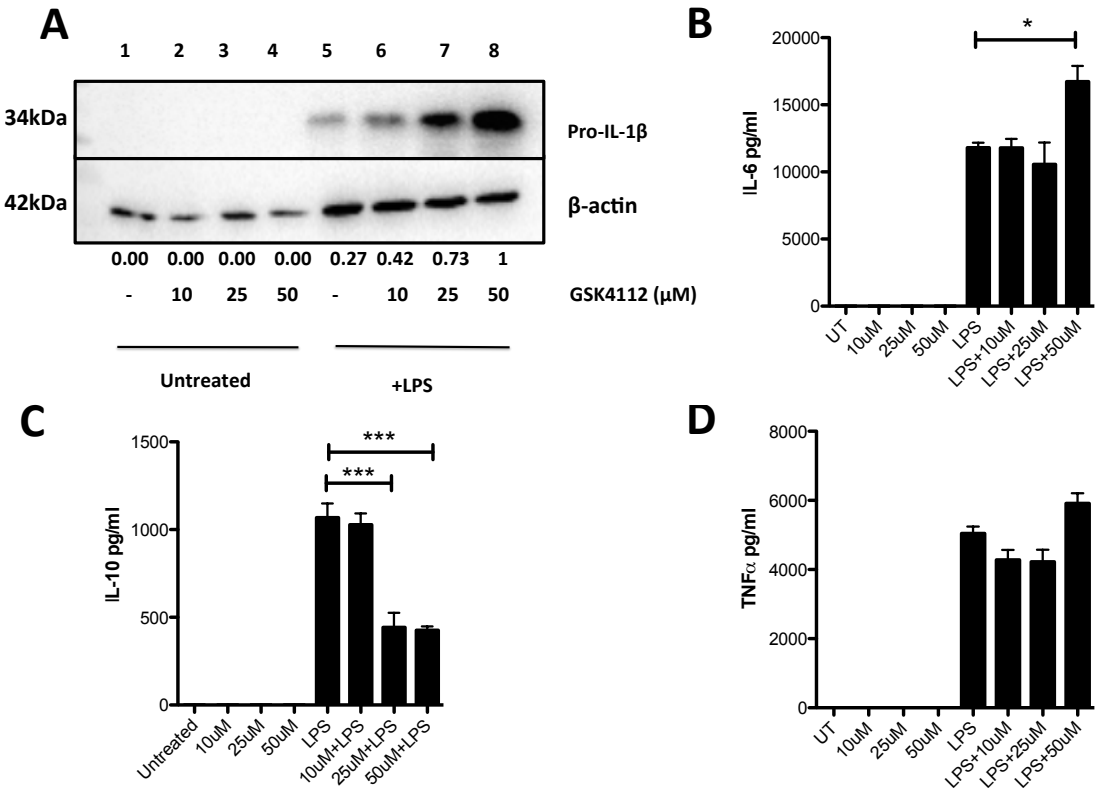

Figure 4.10 GSK4112 increases LPS induced Pro-IL-1B and IL-6, decreased IL-10 and has no effect on TNFα

Wild type BMDMs were seeded at $5x10^5$ cells/ml in a 12 well plate and incubated overnight at 37°C. Cells were left untreated or pretreated with 10, 25 or 50 μM GSK4112 for 1 hr before being left untreated or stimulated with 100 ng/ml LPS for 24 hrs. (A) Cells were lysed in sample loading buffer and analysed by western blotting using anti-IL-1β and anti-β-actin antibodies. β-actin is presented as a loading control. Results are a representative of at least 3 independent experiments. Cell supernatants were also removed and Cell supernatants were removed and (B) IL-6, (C) IL-10 and (D) TNFα were quantified by ELISA. Data shown are the mean ± S.E.M., n=3..

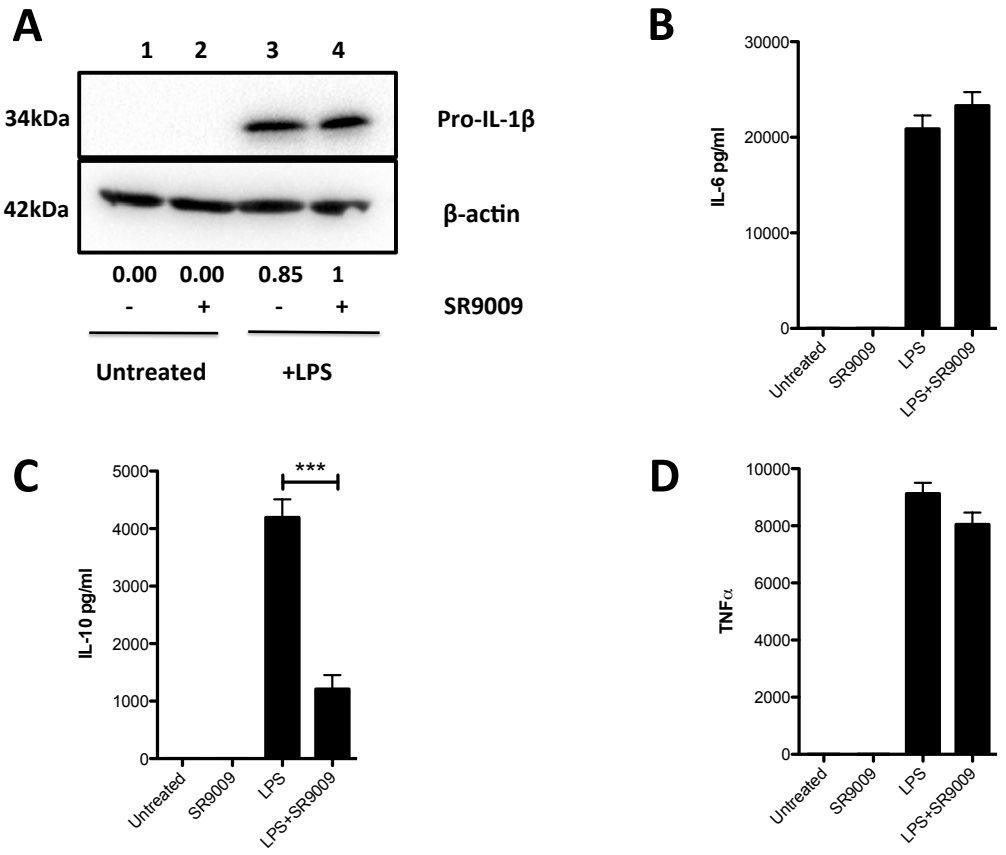

Figure 4.11 SR9009 decreases LPS induced IL-10 but has no effect on Pro-IL-1β, IL-6 or TNFα

Wild type BMDMs were seeded at $5x10^5$ cells/ml in a 12 well plate and incubated overnight at 37°C. Cells were left untreated or pretreated with 10 nM SR9009 for 1 hr before being left untreated or stimulated with 100 ng/ml LPS for 24 hrs. (A) Cells were lysed in sample loading buffer and analysed by western blotting using anti-IL-1β and anti-β-actin antibodies. β-actin is presented as a loading control. Results are a representative of at least 3 independent experiments. Cell supernatants were also removed and Cell supernatants were removed and (B) IL-6, (C) IL-10 and (D) TNFα were quantified by ELISA. Data shown are the mean ± S.E.M., n=3

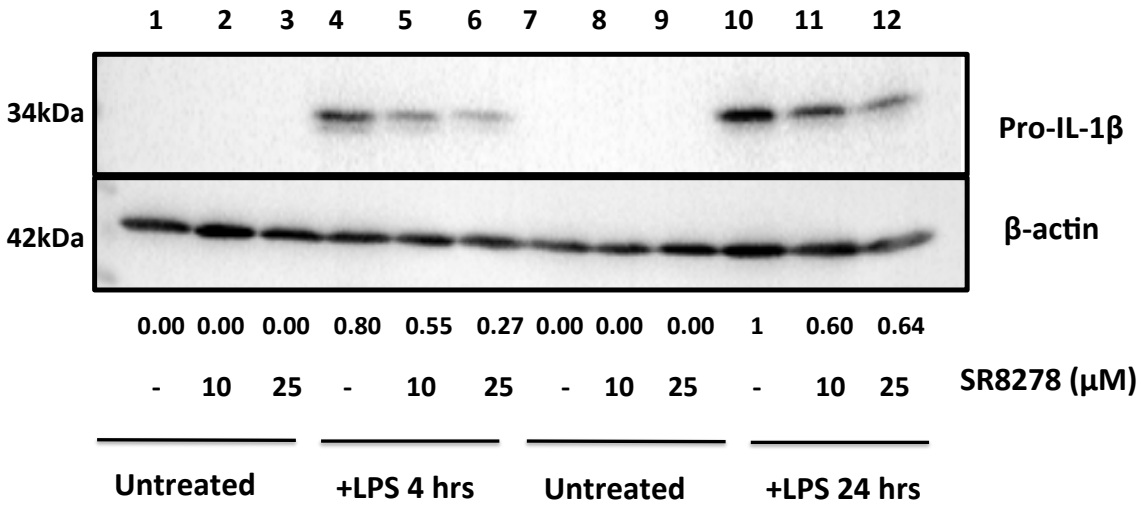

Figure 4.12 SR8278 decreases LPS induced Pro-IL-1β

Wild type BMDMs were seeded at $5x10^5$ cells/ml in a 12 well plate and incubated overnight at 37°C. Cells were left untreated or pretreated with 10 or 25 μM SR8278 for 1 hr before being left untreated or stimulated with 100 ng/ml LPS for 4 or 24 hrs. Cells were lysed in sample loading buffer and analysed by western blotting using anti-IL-1β and anti-β-actin antibodies. β-actin is presented as a loading control. Results are a representative of at least 3 independent experiments.

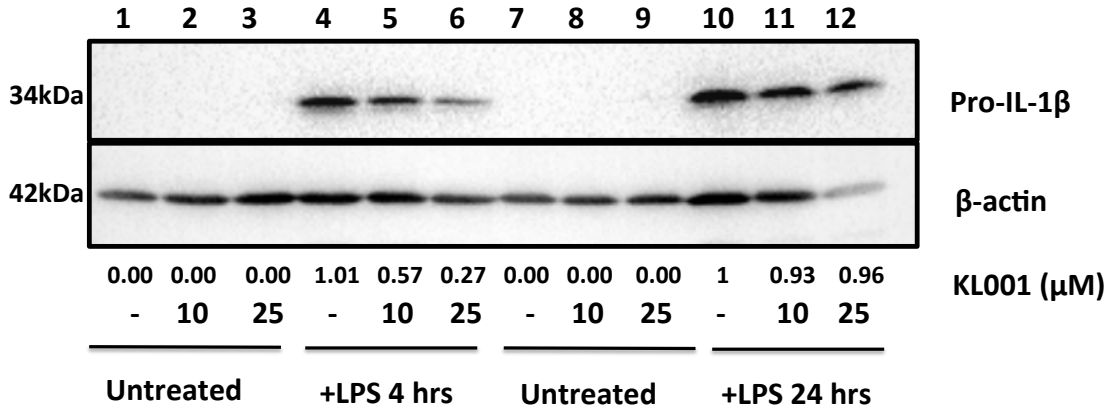

Figure 4.13 KL001 decreases LPS induced Pro-IL-1β

Wild type BMDMs were seeded at $5x10^5$ cells/ml in a 12 well plate and incubated overnight at 37°C. Cells were left untreated or pretreated with 10 or 25 μM KL001 for 1 hr before being left untreated or stimulated with 100 ng/ml LPS for 4 or 24 hrs. Cells were lysed in sample loading buffer and analysed by western blotting using anti-IL-1β and anti-β-actin antibodies. β-actin is presented as a loading control. Results are a representative of at least 3 independent experiments.

4.6 Investigation of BMAL1 mediated regulation of IL-1β processing

4.6.1 Increased IL-1β processing with deletion of *Bmal1*

Upon initiation of the inflammasome, pro-IL-1β is cleaved into the active IL-1β form (111). I investigated whether the increased pro-IL-1β production in *Bmal1*$^{-/-}$ BMDMs contributed to increased secretion of cleaved IL-1β. Cells were pre-treated with LPS for 3 hrs before addition of ATP to stimulate NLRP3 inflammasome formation. There was no significant difference in the levels of pro-IL-1β between *Bmal1*$^{+/+}$ and *Bmal1*$^{-/-}$ BMDMs following 4 hrs of LPS (Figure 4.14A). However following NLRP3 inflammasome activation there was a significant increase in cleaved IL-1β levels as measured by ELISA in the *Bmal1*$^{-/-}$ BMDMs (Figure 4.14B). This was also observed by western blotting of the supernatants, where a large increase in the levels of cleaved IL-1β was evident (Figure 4.14C).

Initiation of the inflammasome results in pyroptotic cell death, facilitating release of IL-1β, propagating the immune response (111). To test whether increased pyroptosis was evident in *Bmal1*$^{-/-}$ BMDMs, I measured cell death by LDH assay. Following NLRP3 activation *Bmal1*$^{-/-}$ BMDMs exhibited increased cell death relative to *Bmal1*$^{+/+}$ BMDMs (Figure 4.15).

4.6.2 Caspase 1, but not NLRP3 is increased in *Bmal1*$^{-/-}$ macrophages

To assess the mechanism of increased IL-1β cleavage in *Bmal1*$^{-/-}$ BMDMs, I measured the levels of NLRP3 in these cells. NLRP3 transcript and protein are basally produced in macrophages, but are further induced with LPS stimulation. I found no significant difference in transcript (Figure 4.16A) or protein (Figure 4.16B)

levels of NLRP3 between *Bmal1*$^{+/+}$ and *Bmal1*$^{-/-}$ BMDMs, either basally or following LPS stimulation. Upon initiation of NLRP3 inflammasome activity, pro-Caspase 1 is cleaved into its two active subunits, P10 and P20, to initiate processing of pro-IL-1β. I measured pro-Caspase 1, P20 and P10 in the supernatants of *Bmal1*$^{+/+}$ and *Bmal1*$^{-/-}$ BMDMs following NLRP3 inflammasome activation. Pro-Caspase 1 (Figure 4.17A), P20 (Figure 4.17A) and P10 (Figure 4.17B) were all increased in *Bmal1*$^{-/-}$ BMDMs relative to *Bmal1*$^{+/+}$ BMDMs, which would lead to increased pro-IL-1β cleavage.

4.6.3 Increased IL-1β processing in *Bmal1*$^{-/-}$ macrophages is not specific to NLRP3 inflammasome

Given the increase in pro-Caspase 1 cleavage but no significant increase in NLRP3 levels in *Bmal1*$^{-/-}$ BMDMs, I hypothesized that the increased cleavage of pro-IL-1β was not specific to the NLRP3 inflammasome. For this reason, I assayed AIM2 inflammasome activation in *Bmal1*$^{-/-}$ BMDMs. *Bmal1*$^{+/+}$ and *Bmal1*$^{-/-}$ BMDMs were stimulated with LPS before transfection of poly dA:dT into the cells. Measuring IL-1β by ELISA revealed a significant increase in *Bmal1*$^{-/-}$ BMDMs relative to *Bmal1*$^{+/+}$ BMDMs (Figure 4.18). This correlated with the result seen with NLRP3 activation.

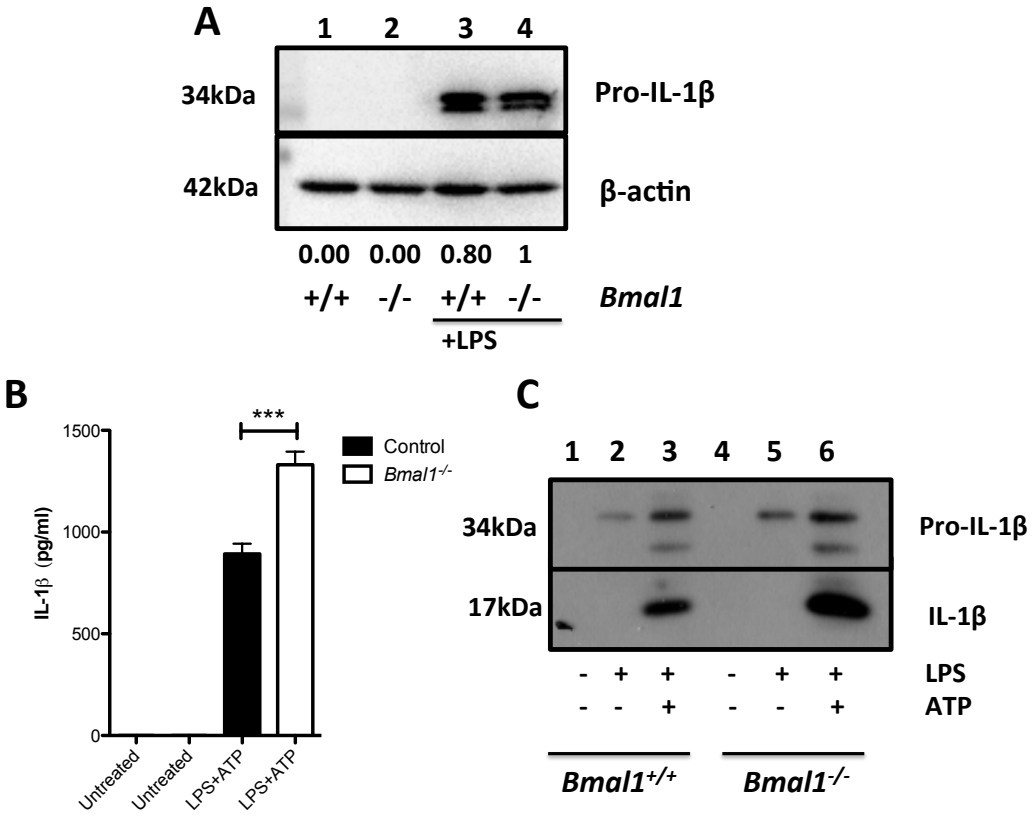

Figure 4.14 Increased IL-1β processing in *Bmal1*$^{-/-}$ BMDMs

Bmal1$^{+/+}$ and *Bmal1*$^{-/-}$ BMDMs were seeded at 5x10^5 cells/ml in a 12 well plate and incubated overnight at 37°C. (A) Cells were then left unstimulated or stimulated with 100 ng/ml LPS for 4 hrs. Cells were lysed in sample loading buffer and analysed by western blotting using anti-IL-1β and anti-β-actin antibodies. β-actin is presented as a loading control. Results are a representative of at least 3 independent experiments. (B) Cells were left unstimulated or stimulated with 100 ng/ml LPS for 3 hrs before addition of 5mM ATP to certain wells to activate the inflammasome. Cell supernatants were removed and IL-1β was quantified by ELISA. Data shown are the mean ± S.E.M., n=3. (C) Cell supernatants were removed and protein was concentrated with strata resin beads. Concentrated protein was denatured in sample loading buffer and analysed by western blotting using anti-IL-1β antibody to detect the pro and cleaved form.

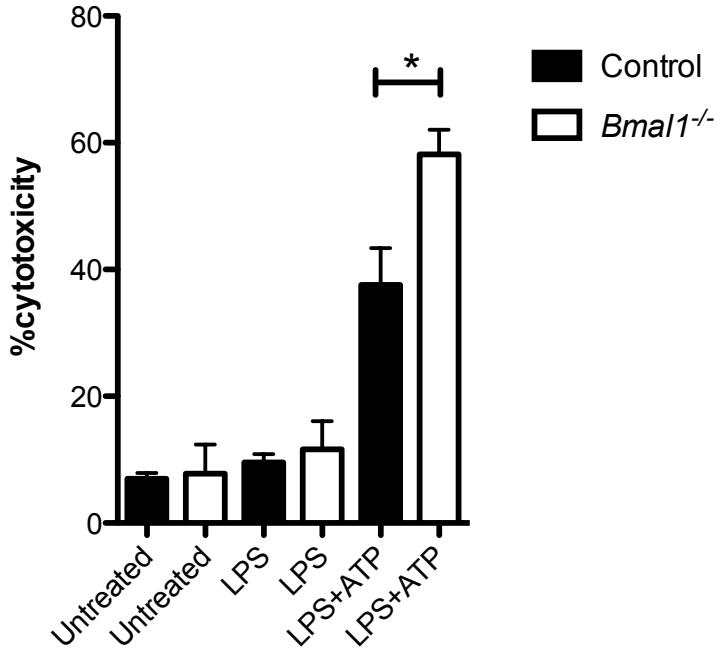

Figure 4.15 Increased cell death in *Bmal1*$^{-/-}$ BMDMs

Bmal1$^{+/+}$ and *Bmal1*$^{-/-}$ BMDMs were seeded at 5x10^5 cells/ml in a 12 well plate and incubated overnight at 37°C. Cells were left unstimulated or stimulated with 100 ng/ml LPS for 3 hrs before addition of 5mM ATP to certain wells to activate the inflammasome. A LDH assay was carried out with the cell supernatant to measure cell death differences following inflammasome stimulation. Data shown are the mean ± S.E.M., n=3

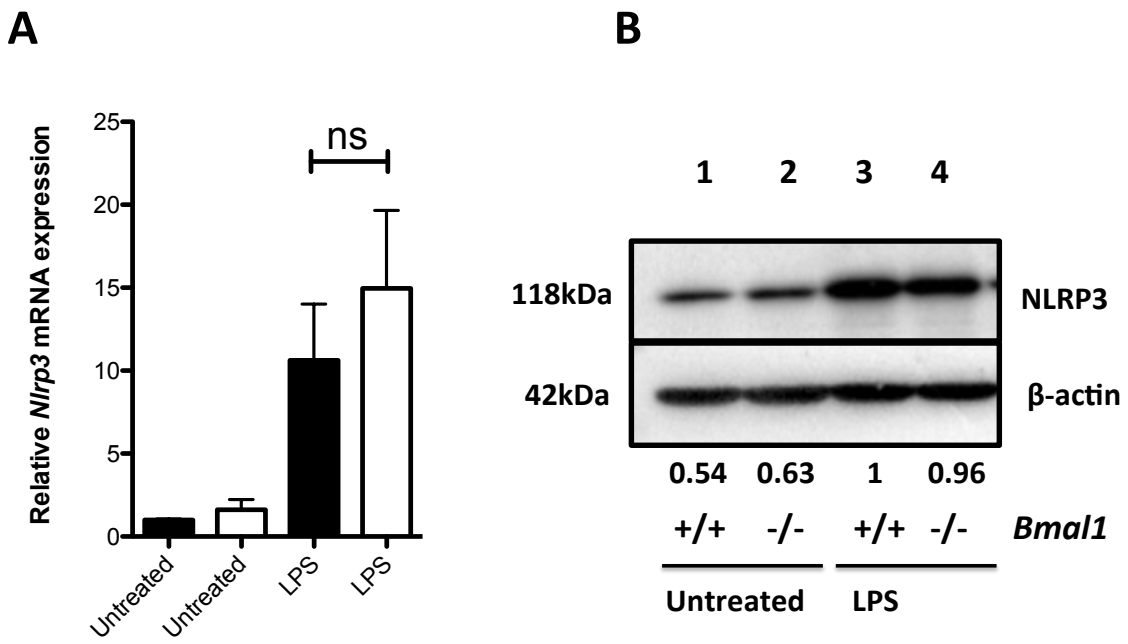

Figure 4.16 NLRP3 transcript and protein not increased in *Bmal1*$^{-/-}$ BMDMs

Bmal1$^{+/+}$ and *Bmal1*$^{-/-}$ BMDMs were seeded at 5x10^5 cells/ml in a 12 well plate and incubated overnight at 37°C. Cells were then left unstimulated or stimulated with 100 ng/ml LPS for 4 hrs. (A) Cells were lysed and mRNA was extracted and analysed using SYBR qPCR probes specific for murine *Nlrp3.* Data was normalised to *Rps18.* Fold induction was calculated relative to untreated cells. Data shown are the mean ± S.E.M., n=3. (B) Cells were lysed in sample loading buffer and analysed by western blotting using anti-NLRP3 and anti-β-actin antibodies. β-actin is presented as a loading control. Results are a representative of at least 3 independent experiments.

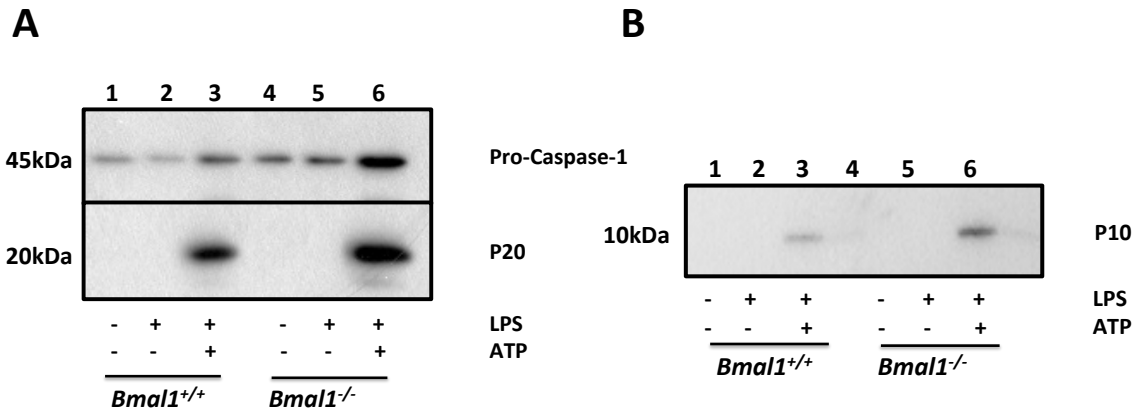

Figure 4.17 Caspase 1 levels increased in *Bmal1*$^{-/-}$ BMDMs

Bmal1$^{+/+}$ and *Bmal1*$^{-/-}$ BMDMs were seeded at 5x10^5 cells/ml in a 12 well plate and incubated overnight at 37°C. Cells were left unstimulated or stimulated with 100 ng/ml LPS for 3 hrs before addition of 5mM ATP to certain wells to activate the inflammasome. Cell supernatants were removed and protein was concentrated with strata resin beads. Concentrated protein was denatured in sample loading buffer and analysed by western blotting using (A) anti-Caspase 1 (P20) antibody and (B) anti-Caspase 1 (P!0) antibody to detect the pro and cleaved forms of Caspase 1.

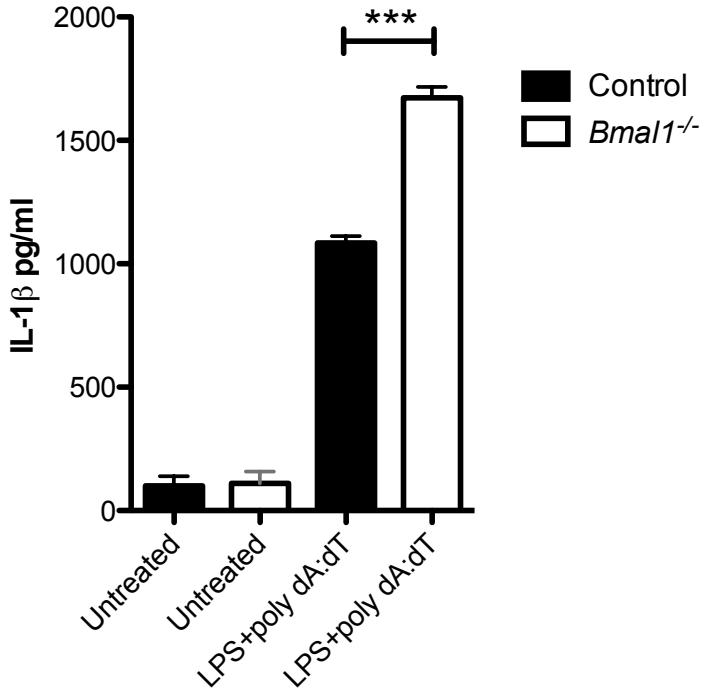

Figure 4.18 Increased IL-1β with AIM2 inflammasome activation in *Bmal1*$^{-/-}$ BMDMs

Bmal1$^{+/+}$ and *Bmal1*$^{-/-}$ BMDMs were seeded at 5x10^5 cells/ml in a 12 well plate and incubated overnight at 37°C. Cells were left unstimulated or stimulated with 100 ng/ml LPS for 3 hrs before transfecting certain wells with poly dA:dT to activate the AIM2 inflammasome. Cell supernatants were removed and IL-1β was quantified by ELISA. Data shown are the mean ± S.E.M., n=3.

4.7 Examination of *Keap1* knockdown in *Bmal1*$^{-/-}$ macrophages

My results demonstrate that depletion of the NRF2 pathway in *Bmal1*$^{-/-}$ BMDMs results in a pro-oxidant and pro-inflammatory phenotype. KEAP1 is a post-translational negative regulator of NRF2 accumulation and activity (167). I hypothesized that knockdown of *Keap1* in macrophages would facilitate NRF2 accumulation and allow for rescue of the pro-inflammatory phenotype of these cells.

4.7.1 *Keap1* knockdown decreases pro-inflammatory cytokine production in macrophages

To assess the role of KEAP1 and NRF2 on inflammatory cytokines, I knocked down *Keap1* in fully differentiated wild type BMDMs (Figure 4.19A). *Keap1* silencing reduced levels of pro-IL-1β protein relative to the scrambled siRNA control (Figure 4.19B), which was expected given the expected increase in NRF2 activity. I also measured levels of IL-6 (Figure 4.20A), IL-10 (Figure 4.20B) and TNFα (Figure 4.20C) by ELISA. IL-6 was decreased with *Keap1* knockdown, which was expected given the ability of NRF2 to limit *Il-6* transcription.

4.7.2 *Keap1* knockdown rescues NRF2 levels and activity in *Bmal1*$^{-/-}$ macrophages

Given that *Keap1* knockdown was efficient at lowering pro-inflammatory cytokine production in wild type BMDMs, I silenced *Keap1* in *Bmal1*$^{-/-}$ BMDMs. Measuring KEAP1 protein levels by Western blot revealed a possible increase in the levels of KEAP1 following LPS stimulation in *Bmal1*$^{-/-}$ BMDMs (Figure 4.21). However, KEAP1 appeared to be completely knocked down upon transfection with *Keap1* siRNA in

both *Bmal1*$^{+/+}$ and *Bmal1*$^{-/-}$ BMDMs. To assess the effect of *Keap1* silencing on NRF2 levels I measured transcript and protein of NRF2 in *Bmal1*$^{+/+}$ and *Bmal1*$^{-/-}$ BMDMs following *Keap1* siRNA transfection. The expected lack of response in *Nrf2* transcription in *Bmal1*$^{-/-}$ BMDMs was observed, however there was no difference between the scrambled and *Keap1* siRNA groups (Figure 4.22A). This was anticipated, as KEAP1 is a post-translational regulator of NRF2. Indeed, when investigating the protein levels of NRF2, a rescue in NRF2 protein levels was evident in *Bmal1*$^{-/-}$ BMDMs following *Keap1* siRNA (Figure 4.22B) (see lanes 1,2 and 3 versus 7, 8 and 9). This boost in NRF2 levels had a clear boost on NRF2 activity as demonstrated by measuring *Nqo1* mRNA transcription (Figure 4.23). *Keap1* siRNA transfection boosted *Nqo1* expression at both basal levels in both *Bmal1*$^{+/+}$ and *Bmal1*$^{-/-}$ BMDMs, rescuing the pro-oxidant phenotype of the *Bmal1*$^{-/-}$ BMDMs. This rescue was directly observed by measuring HIF-1α levels. *Bmal1*$^{+/+}$ and *Bmal1*$^{-/-}$ BMDMs were transfected with scrambled siRNA or siRNA targeting *Keap1.* The cells were then treated with LPS and HIF-1α was measured by western blot (Figure 4.24). The increased levels of HIF-1α in *Bmal1*$^{-/-}$ BMDMs relative to *Bmal1*$^{+/+}$ BMDMs, was ablated with *Keap1* knockdown (compare lanes 2 to 8 and 3 to 9). The boost in NRF2 levels with *Keap1* knockdown appeared to rescue the pro-oxidant effect of *Bmal1*$^{-/-}$ BMDMs on HIF-1α protein levels.

4.7.3 *Keap1* knockdown rescues IL-1β phenotype of *Bmal1*$^{-/-}$ macrophages

Given that *Keap1* silencing appeared to rescue the lack of antioxidant response in *Bmal1*$^{-/-}$ BMDMs, I investigated whether this rescued the IL-1β phenotype in these cells. I measured transcript levels of *Il1b* between *Bmal1*$^{+/+}$ and *Bmal1*$^{-/-}$ BMDMs following *Keap1* silencing. The significant increase in *Il1b* transcription in *Bmal1*$^{-/-}$ BMDMs relative to *Bmal1*$^{+/+}$ BMDMs was decreased following *Keap1* siRNA transfection (Figure 4.25A). This effect was also seen at the protein level, where the

large increase in pro-IL-1β in *Bmal1*$^{-/-}$ BMDMs was reduced following *Keap1* silencing (Figure 4.25B) (compare lanes 5 and 6 to 11 and 12).

NRF2 has previously been associated with both limiting, and being necessary for NLRP3 inflammasome activation (181, 185). Given previous results demonstrating an increase in pro-IL-1β cleavage and secretion in *Bmal1*$^{-/-}$ BMDMs, I measured whether boosting NRF2 activity through *Keap1* knockdown had an effect on IL-1β release. *Bmal1*$^{+/+}$ and *Bmal1*$^{-/-}$ BMDMs were transfected with scrambled or *Keap1* siRNA before carrying out an NLRP3 inflammasome assay and measuring IL-1β by ELISA (Figure 4.26). Similar to pro-IL-1β levels, *Keap1* silencing reduced the increased levels of cleaved IL-1β seen in *Bmal1*$^{-/-}$ BMDMs.

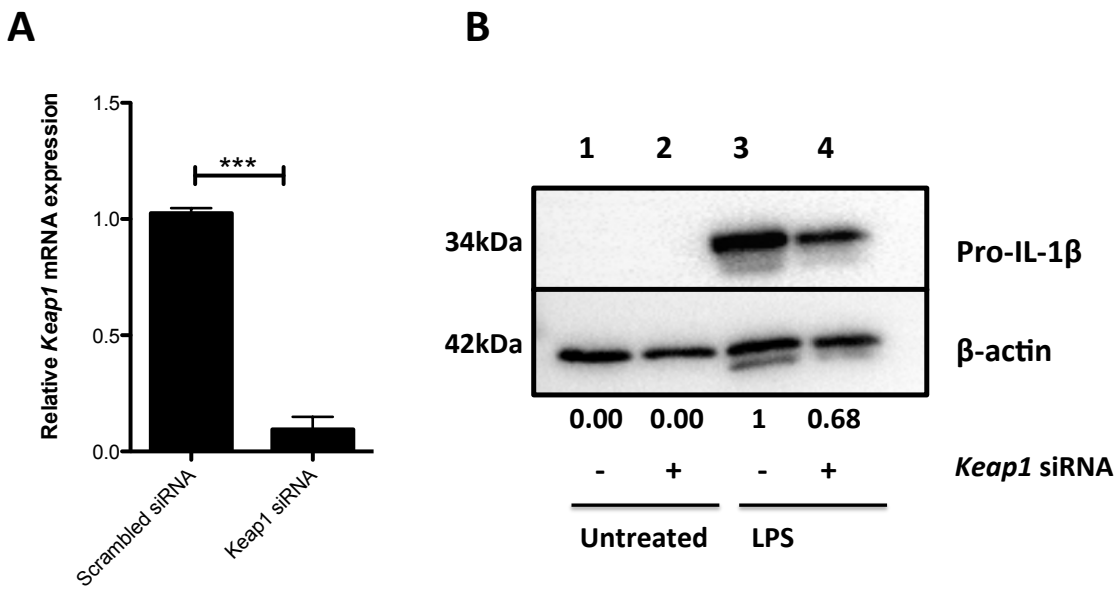

Figure 4.19 *Keap1* knockdown decreases Pro-IL-1β

Wild type BMDMs were seeded at $5x10^5$ cells/ml in a 12 well plate and incubated overnight at 37°C. BMDMs were then transfected with either a scrambled siRNA control or siRNA targeting *Keap1.* The cells were then incubated overnight at 37°C (A) Cells were lysed and mRNA was extracted and analysed using SYBR qPCR probes specific for murine *Keap1.* Data was normalised to *Rps18.* Fold induction was calculated relative to untreated cells. Data shown are the mean ± S.E.M., n=4. (B) Cells were left unstimulated or stimulated with 100 ng/ml LPS for 24 hrs. Cells were lysed in sample loading buffer and analysed by western blotting using anti-IL-1β and anti-β-actin antibodies. β-actin is presented as a loading control. Results are a representative of at least 3 independent experiments.

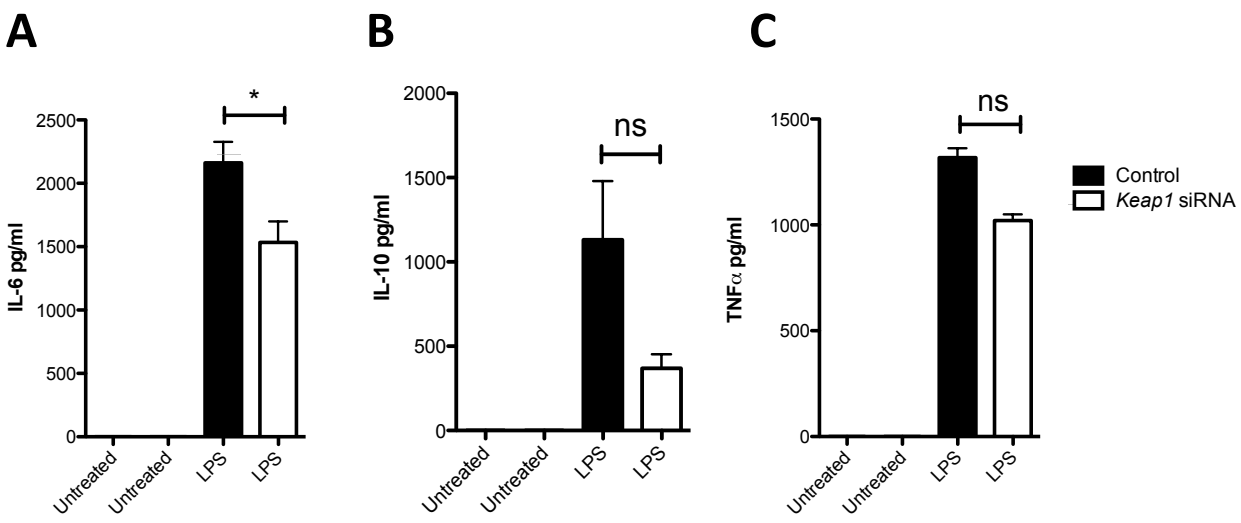

Figure 4.20 *Keap1* knockdown decreases IL-6 but has no effect on IL-10 and TNFα

Wild type BMDMs were seeded at $5x10^5$ cells/ml in a 12 well plate and incubated overnight at 37°C. BMDMs were then transfected with either a scrambled siRNA control or siRNA targeting *Keap1.* Cells were left unstimulated or stimulated with 100 ng/ml LPS for 24 hrs. Cell supernatants were removed and (A) IL-6, (B) IL-10 and (C) TNFα were quantified by ELISA. Data shown are the mean ± S.E.M., n=3.

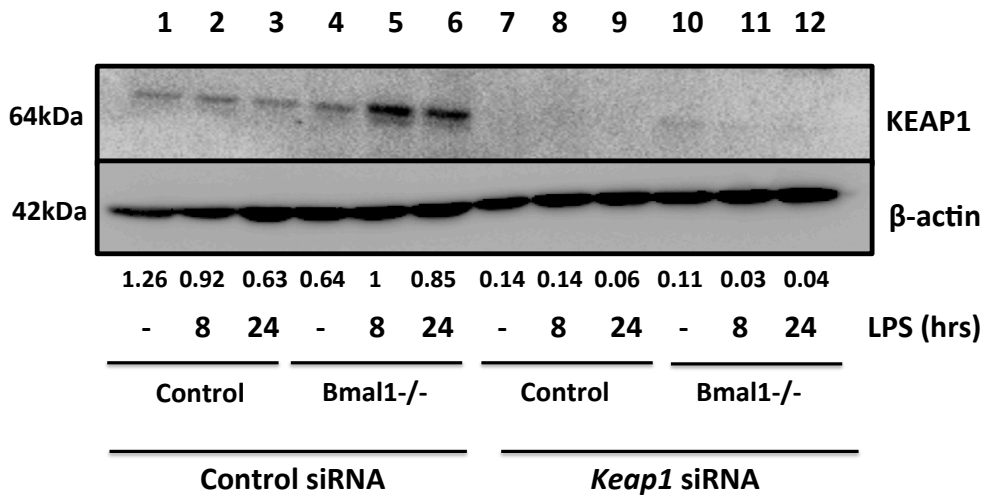

Figure 4.21 *Keap1* knockdown depletes KEAP1 protein in *Bmal1*$^{+/+}$ and *Bmal1*$^{-/-}$ BMDMs

Bmal1$^{+/+}$ and *Bmal1*$^{-/-}$ BMDMs were seeded at 5x10^5 cells/ml in a 12 well plate and incubated overnight at 37°C. BMDMs were then transfected with either a scrambled siRNA control or siRNA targeting *Keap1.* Cells were left unstimulated or stimulated with 100 ng/ml LPS for 8 or 24 hrs. Cells were lysed in sample loading buffer and analysed by western blotting using anti-KEAP1 and anti-β-actin antibodies. β-actin is presented as a loading control. Results are a representative of at least 3 independent experiments.

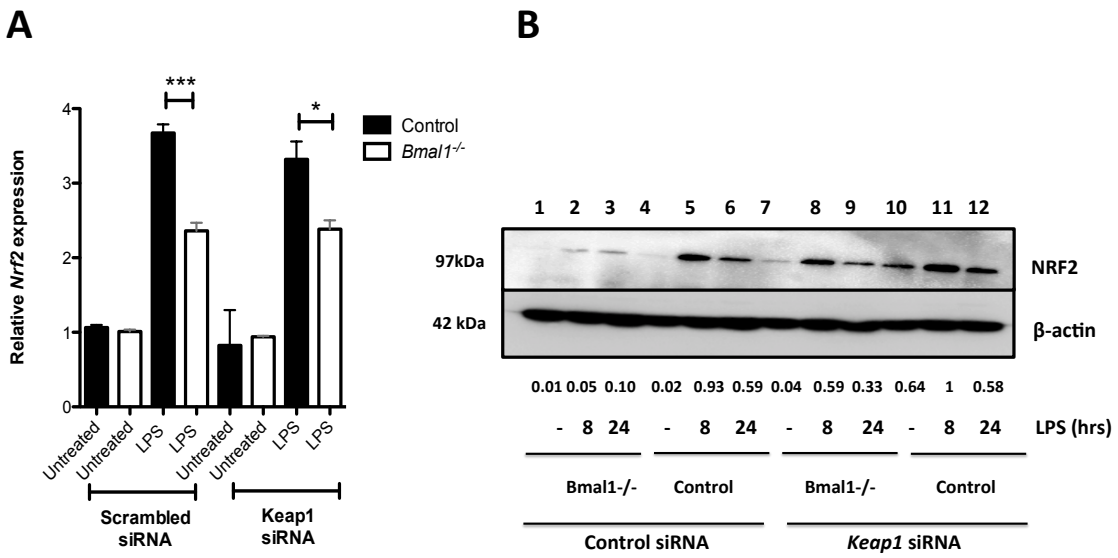

Figure 4.22 *Keap1* knockdown has no effect on *Nrf2* transcription but increases NRF2 protein in *Bmal1*$^{-/-}$ BMDMs

Bmal1$^{+/+}$ and *Bmal1*$^{-/-}$ BMDMs were seeded at 5x10^5 cells/ml in a 12 well plate and incubated overnight at 37°C. BMDMs were then transfected with either a scrambled siRNA control or siRNA targeting *Keap1.* (A) Cells were left unstimulated or stimulated with 100 ng/ml LPS for 8 or 24 hrs. Cells were lysed and mRNA was extracted and analysed using SYBR qPCR probes specific for murine *Nrf2.* Data was normalised to *Rps18.* Fold induction was calculated relative to untreated cells. Data shown are the mean ± S.E.M., n=4. (B) Cells were left unstimulated or stimulated with 100 ng/ml LPS for 8 or 24 hrs. Cells were lysed in sample loading buffer and analysed by western blotting using anti-NRF2 and anti-β-actin antibodies. β-actin is presented as a loading control. Results are a representative of at least 3 independent experiments.

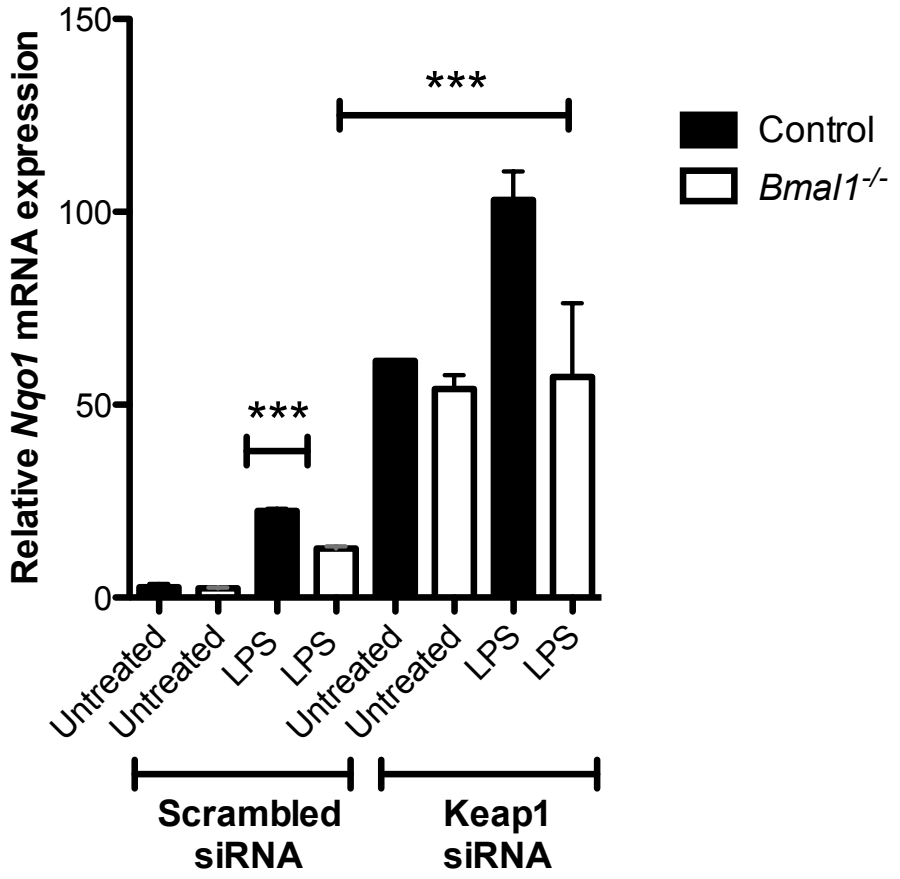

Figure 4.23 *Nqo1* transcription is increased with *Keap1* knockdown in *Bmal1*$^{+/+}$ and *Bmal1*$^{-/-}$ BMDMs

Bmal1$^{+/+}$ and *Bmal1*$^{-/-}$ BMDMs were seeded at 5x10^5 cells/ml in a 12 well plate and incubated overnight at 37°C. BMDMs were then transfected with either a scrambled siRNA control or siRNA targeting *Keap1.* Cells were left unstimulated or stimulated with 100 ng/ml LPS for 24 hrs. Cells were lysed and mRNA was extracted and analysed using SYBR qPCR probes specific for murine *Nqo1.* Data was normalised to *Rps18.* Fold induction was calculated relative to untreated cells. Data shown are the mean ± S.E.M., n=4.

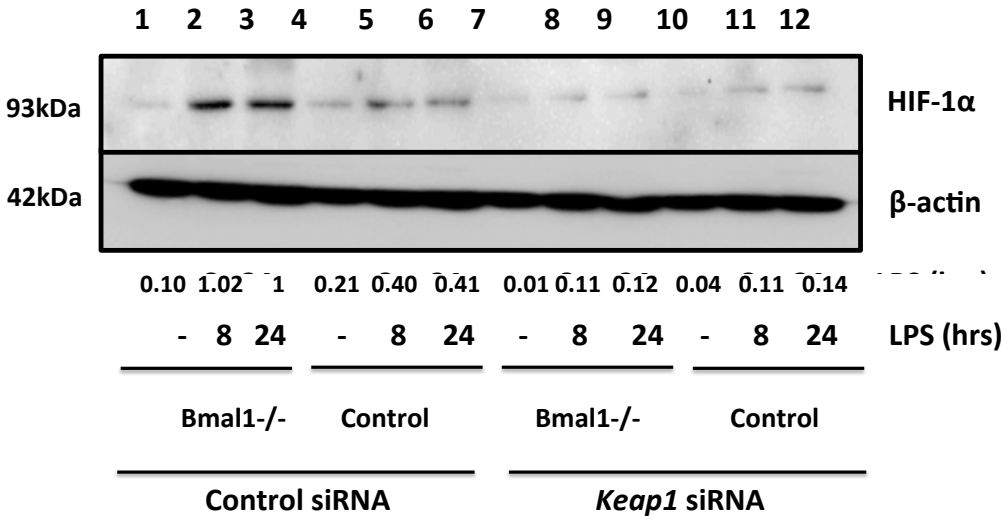

Figure 4.24 Increased HIF-1α levels *in Bmal1*$^{-/-}$ BMDMs decreased with *Keap1* knockdown

Bmal1$^{+/+}$ and *Bmal1*$^{-/-}$ BMDMs were seeded at 5x10^5 cells/ml in a 12 well plate and incubated overnight at 37°C. BMDMs were then transfected with either a scrambled siRNA control or siRNA targeting *Keap1.* Cells were left unstimulated or stimulated with 100 ng/ml LPS for 8 or 24 hrs. Cells were lysed in sample loading buffer and analysed by western blotting using anti-HIF-1α and anti-β-actin antibodies. β-actin is presented as a loading control. Results are a representative of at least 3 independent experiments.

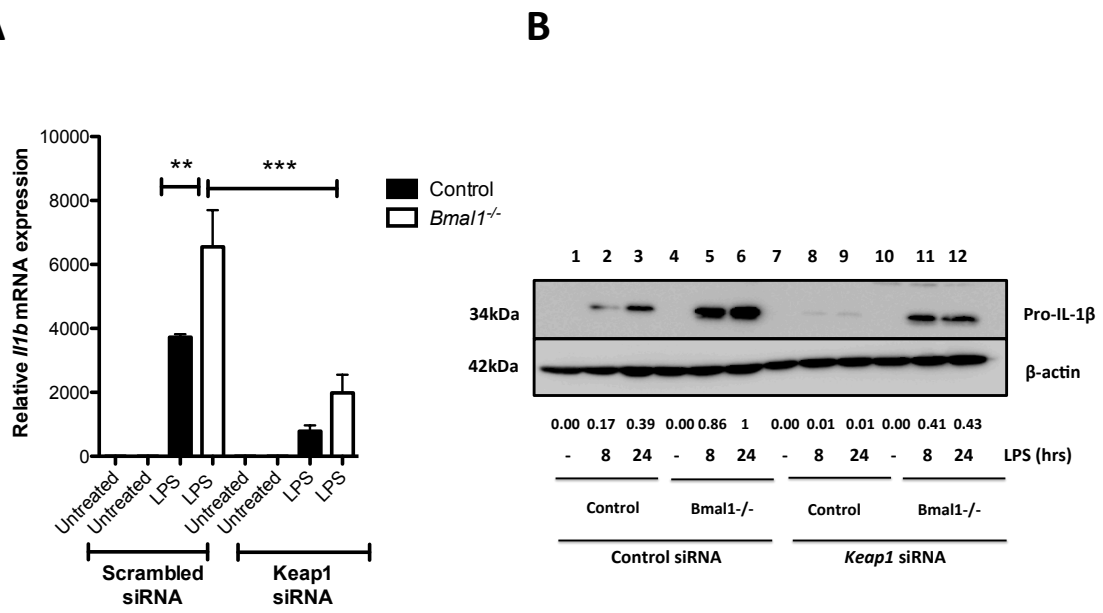

Figure 4.25 Keap1 knockdown decreases IL-1B transcription and protein in *Bmal1*$^{-/-}$ BMDMs

Bmal1$^{+/+}$ and *Bmal1*$^{-/-}$ BMDMs were seeded at 5x10^5 cells/ml in a 12 well plate and incubated overnight at 37°C. BMDMs were then transfected with either a scrambled siRNA control or siRNA targeting *Keap1.* (A) Cells were left unstimulated or stimulated with 100 ng/ml LPS for 24 hrs. Cells were lysed and mRNA was extracted and analysed using SYBR qPCR probes specific for murine *Il1b.* Data was normalised to *Rps18.* Fold induction was calculated relative to untreated cells. Data shown are the mean ± S.E.M., n=3. (B) Cells were left unstimulated or stimulated with 100 ng/ml LPS for 8 or 24 hrs. Cells were lysed in sample loading buffer and analysed by western blotting using anti-IL-1β and anti-β-actin antibodies. β-actin is presented as a loading control. Results are a representative of at least 3 independent experiments.

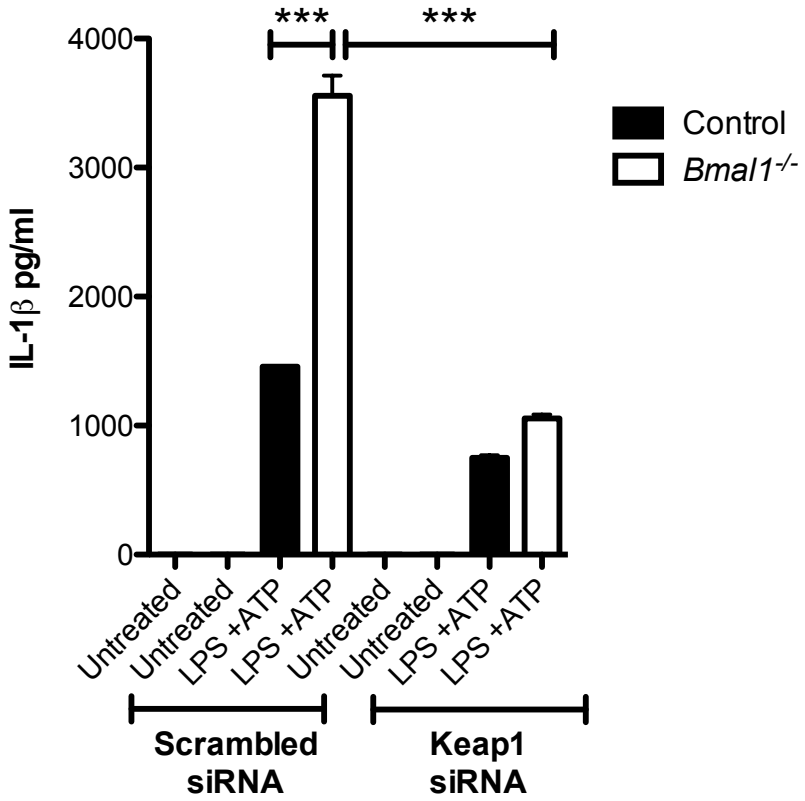

Figure 4.26 *Keap1* knockdown decreases IL-1β activation in *Bmal1*$^{-/-}$ BMDMs

Bmal1$^{+/+}$ and *Bmal1*$^{-/-}$ BMDMs were seeded at 5x10^5 cells/ml in a 12 well plate and incubated overnight at 37°C. BMDMs were then transfected with either a scrambled siRNA control or siRNA targeting *Keap1.* Cells were left unstimulated or stimulated with 100 ng/ml LPS for 24 hrs before addition of 5mM ATP to certain wells to activate the inflammasome. Cell supernatants were removed and IL-1β was quantified by ELISA. Data shown are the mean ± S.E.M., n=3.

4.8 Investigation into the effects of pharamcological activation of NRF2 and ROS scavenging on *Bmal1*$^{-/-}$ macrophages

ROS is a well-documented driver of IL-1β production through HIF-1α (132). NRF2 is known to decrease ROS through promoting an antioxidant response to antagonise oxidative stress. However, NRF2 has also been found to bind specific inhibitory sites in the promoter of the pro-inflammatory cytokines, allowing it to inhibit IL-1β independent of ROS regulation (166). To determine whether the reduction in IL-1β levels was due to direct inhibition of *Il1b* expression by NRF2, or if ROS and HIF-1α decrease, mediated by the antioxidant defence pathway, also played a role, I treated *Bmal1*$^{+/+}$ and *Bmal1*$^{-/-}$ BMDMs with DEM and NAC. DEM activates NRF2 through depletion of glutathione and through direct modification of KEAP1. NAC suppresses ROS by increasing intracellular GSH levels

4.8.1 NAC and DEM treatment decreases pro-inflammatory cytokine production in macrophages

To assess the effect of NAC and DEM on inflammatory cytokine production, wild type BMDMs were pre-treated with both NAC and DEM before LPS stimulation. NAC and DEM were shown to reduce levels of LPS induced pro-IL-1β protein levels in wild type BMDMs (Figure 4.27). DEM appeared to inhibit pro-IL-1β to a greater level than NAC, possibly indicating that both NRF2's activity as an antioxidant and a transcriptional repressor of IL-1β play a role.

I next assessed the effect of NAC and DEM on LPS induced IL-6 (Figure 4.28A), IL-10 (Figure 4.28B) and TNFα (Figure 4.28C) between *Bmal1*$^{+/+}$ and *Bmal1*$^{-/-}$ BMDMs. NAC appeared to partially increase levels of IL-6, whereas DEM completely inhibited IL-6 production in both *Bmal1*$^{+/+}$ and *Bmal1*$^{-/-}$ BMDMs. Both NAC and DEM appeared

to inhibit LPS induced IL-10 in both *Bmal1*$^{+/+}$ and *Bmal1*$^{-/-}$ BMDMs. NAC has a large inhibitory effect on TNFα whereas DEM had minimal effect on this cytokine in both *Bmal1*$^{+/+}$ and *Bmal1*$^{-/-}$ BMDMs. Ultimately pharmacological scavenging of ROS and induction of NRF2 shared some effects on inflammatory cytokines but also exhibited differences, most notably in IL-6 and TNFα repression. The rescue of the increased IL-6 in *Bmal1*$^{-/-}$ BMDMs is particularly interesting given that IL-6 is a direct NRF2 target.

4.8.2 DEM but not NAC rescues NRF2 activity in *Bmal1*$^{-/-}$ macrophages

Nqo1 transcription was measured in *Bmal1*$^{+/+}$ and *Bmal1*$^{-/-}$ BMDMs following NAC and DEM to assess NRF2 activity (Figure 4.29). DEM significantly boosted levels of *Nqo1* expression in both *Bmal1*$^{+/+}$ and *Bmal1*$^{-/-}$ BMDMs, rescuing the lack of antioxidant response in *Bmal1*$^{-/-}$ BMDMs in a similar manner to *Keap1* knockdown. NAC had no boosting effect on *Nqo1* expression, even lowering its transcription in *Bmal1*$^{+/+}$ BMDMs.

4.8.3 DEM and NAC rescue IL-1β activity in *Bmal1*$^{-/-}$ macrophages

Given that both NAC and DEM have been reported to lower ROS, and DEM also facilitates increased NRF2s transcriptional activity, I measured whether these compounds could rescue the pro-inflammatory phenotype of *Bmal1*$^{-/-}$ macrophages. Both NAC and DEM reduced the increased levels of *Il1b* transcription in *Bmal1*$^{-/-}$ macrophages (Figure 4.30A). A greater decrease with DEM treatment was seen. This phenotype was also observed at the protein level, where both NAC and DEM had an inhibitory effect on pro-IL-1β in both *Bmal1*$^{+/+}$ and *Bmal1*$^{-/-}$ BMDMs (Figure 4.30B). Once again DEM had a greater inhibitory effect than NAC.

4.8.4 OI decreases pro-IL-1β in *Bmal1*$^{-/-}$ macrophages

Previous results have shown alterations to the metabolic landscape of macrophages lacking a molecular clock. Of particular interest was the lack of *Irg1* expression in response to LPS stimulation in *Bmal1*$^{-/-}$ macrophages. Itaconate is a known regulator of both metabolism and activates NRF2 in a similar manner to DEM. For this reason I supplemented *Bmal1*$^{+/+}$ and *Bmal1*$^{-/-}$ BMDMs with OI before treating with LPS to measure pro-IL-1β levels. Much like DEM, OI had an inhibitory effect on pro-IL-1β in both *Bmal1*$^{+/+}$ and *Bmal1*$^{-/-}$ BMDMs (Figure 4.31).

4.8.5 NAC and DEM partially rescue cleaved IL-1β phenotype in *Bmal1*$^{-/-}$ macrophages

Given that *Keap1* siRNA appeared to rescue the increased cleavage of pro-IL-1β to its active form, I assayed whether NAC and DEM had an effect on this phenotype I treated *Bmal1*$^{+/+}$ and *Bmal1*$^{-/-}$ BMDMs with NAC and DEM before carrying out an NLRP3 inflammasome assay. Both NAC and DEM appeared to suppress levels of IL-1β activation in both *Bmal1*$^{+/+}$ and *Bmal1*$^{-/-}$ BMDMs (Figure 4.32). However, only NAC reduced cell death levels in *Bmal1*$^{-/-}$ BMDMs (Figure 4.33).

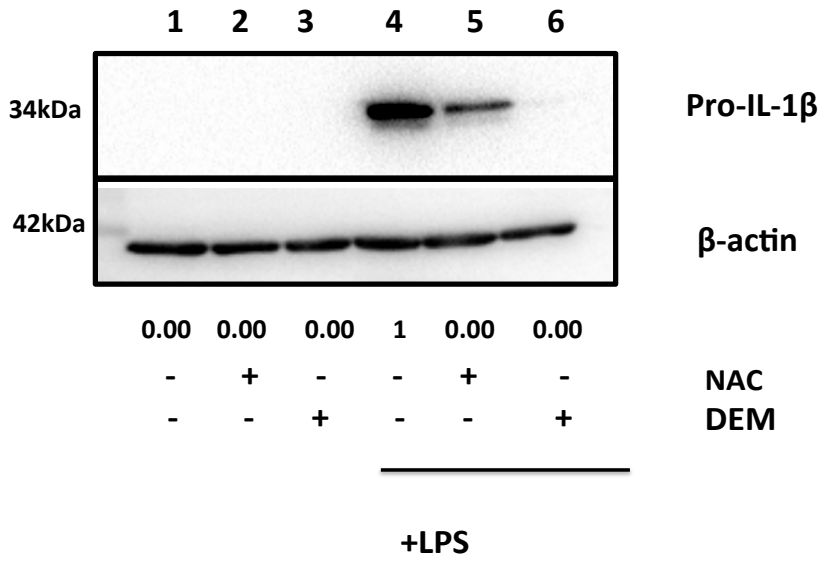

Figure 4.27 NAC and DEM decrease Pro-IL-1β levels

Wild type BMDMs were seeded at $5x10^5$ cells/ml in a 12 well plate and incubated overnight at 37°C. Cells were then left untreated or pre-treated with 10mM NAC or 100 μM DEM for 3 hrs. Cells were left unstimulated or stimulated with 100 ng/ml LPS for 24 hrs. Cells were lysed in sample loading buffer and analysed by western blotting using anti-IL-1β and anti-β-actin antibodies. β-actin is presented as a loading control. Results are a representative of at least 3 independent experiments.

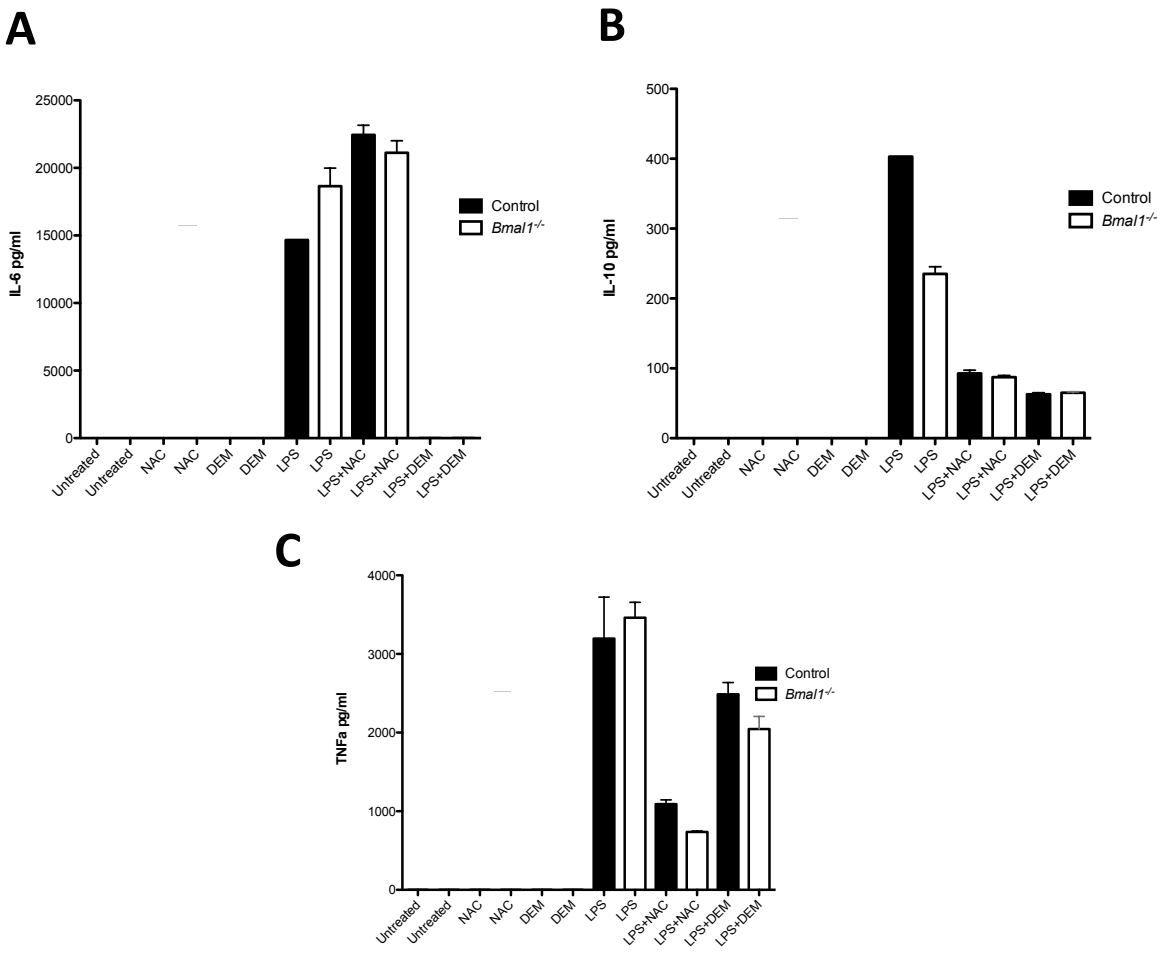

Figure 4.28 NAC and DEM affect inflammatory cytokine levels in *Bmal1*$^{+/+}$ and *Bmal1*$^{-/-}$ BMDMs

Bmal1$^{+/+}$ and *Bmal1*$^{-/-}$ BMDMs were seeded at 5x10^5 cells/ml in a 12 well plate and incubated overnight at 37°C. Cells were then left untreated or pre-treated with 10mM NAC or 100 μM DEM for 3 hrs. Cells were left unstimulated or stimulated with 100 ng/ml LPS for 24 hrs. Cell supernatants were removed and (A) IL-6, (B) IL-10 and (C) TNFα were quantified by ELISA. Data shown are the mean ± S.E.M., n=2.

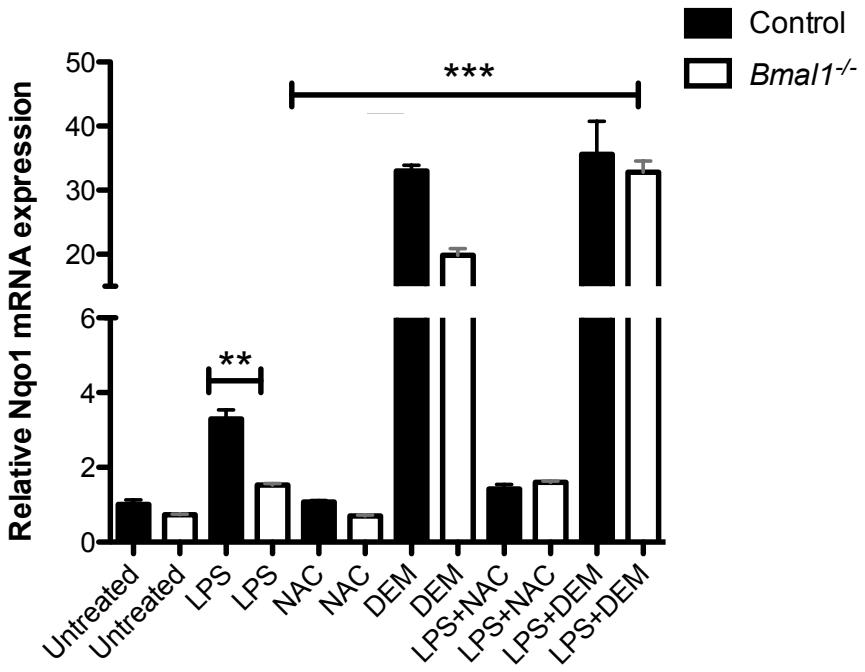

Figure 4.29 DEM but not NAC increases Nqo1 expression in *Bmal1*$^{+/+}$ and *Bmal1*$^{-/-}$ BMDMs

Bmal1$^{+/+}$ and *Bmal1*$^{-/-}$ BMDMs were seeded at 5x10^5 cells/ml in a 12 well plate and incubated overnight at 37°C. Cells were then left untreated or pre-treated with 10mM NAC or 100 μM DEM for 3 hrs. Cells were left unstimulated or stimulated with 100 ng/ml LPS for 24 hrs. Cells were lysed and mRNA was extracted and analysed using SYBR qPCR probes specific for murine *Nqo1.* Data was normalised to *Rps18.* Fold induction was calculated relative to untreated cells. Data shown are the mean ± S.E.M., n=3

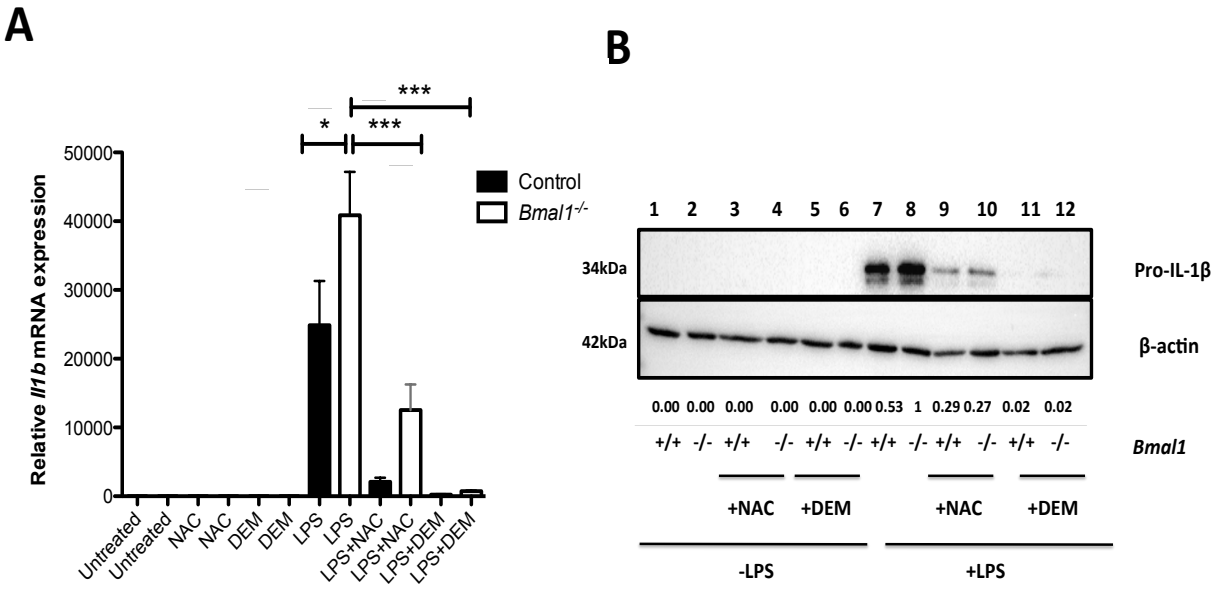

Figure 4.30 DEM and NAC decrease IL-1β transcript and protein in *Bmal1*$^{+/+}$ and *Bmal1*$^{-/-}$ BMDMs

Bmal1$^{+/+}$ and *Bmal1*$^{-/-}$ BMDMs were seeded at 5x10^5 cells/ml in a 12 well plate and incubated overnight at 37°C. Cells were then left untreated or pre-treated with 10mM NAC or 100 μM DEM for 3 hrs. Cells were left unstimulated or stimulated with 100 ng/ml LPS for 24 hrs. (A) Cells were lysed and mRNA was extracted and analysed using SYBR qPCR probes specific for murine *Il1b.* Data was normalised to *Rps18.* Fold induction was calculated relative to untreated cells. Data shown are the mean ± S.E.M., n=3 (B) Cells were lysed in sample loading buffer and analysed by western blotting using anti-IL-1β and anti-β-actin antibodies. β-actin is presented as a loading control. Results are a representative of at least 3 independent experiments.

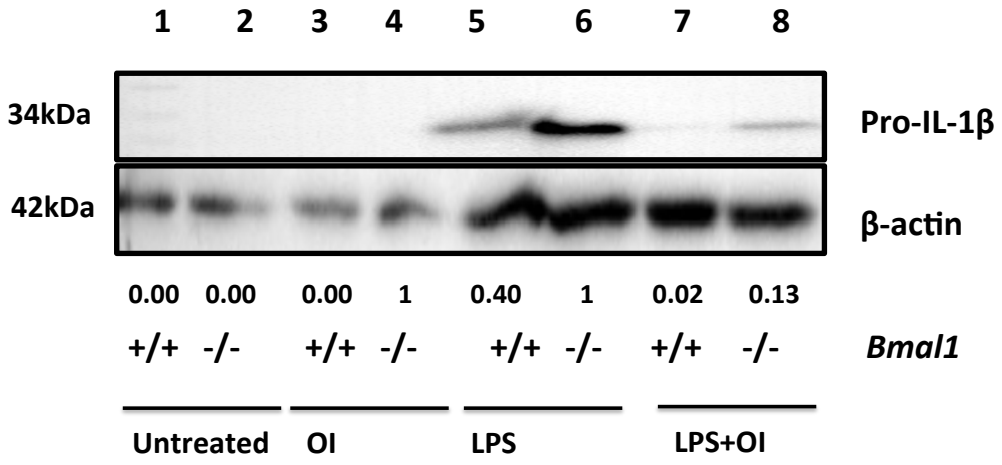

Figure 4.31 OI decreases Pro-IL-1β protein in *Bmal1*$^{-/-}$ BMDMs

Bmal1$^{+/+}$ and *Bmal1*$^{-/-}$ BMDMs were seeded at 5x10^5 cells/ml in a 12 well plate and incubated overnight at 37°C. Cells were then left untreated or pre-treated with 125 μM OI for 3 hrs. Cells were left unstimulated or stimulated with 100 ng/ml LPS for 24 hrs. Cells were lysed in sample loading buffer and analysed by western blotting using anti-IL-1β and anti-β-actin antibodies. β-actin is presented as a loading control. Results are a representative of at least 3 independent experiments.

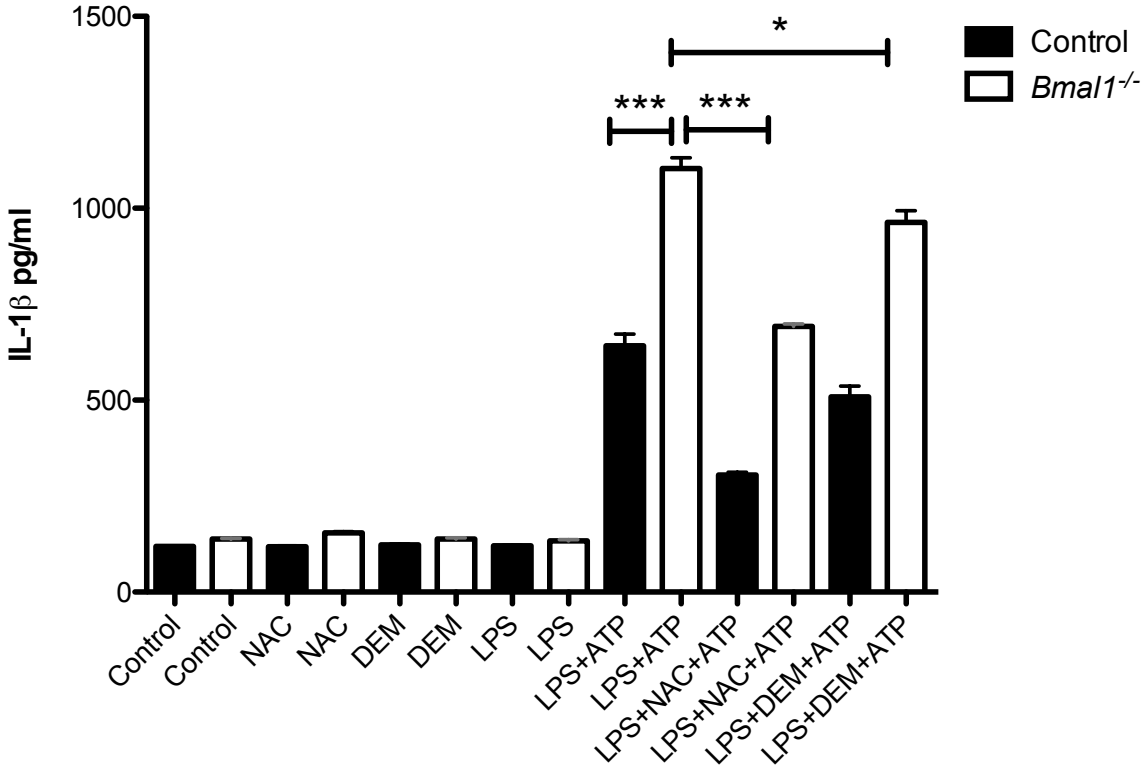

Figure 4.32 NAC and DEM decrease IL-1β activation in *Bmal1*$^{-/-}$ BMDMs

Bmal1$^{+/+}$ and *Bmal1*$^{-/-}$ BMDMs were seeded at 5x10^5 cells/ml in a 12 well plate and incubated overnight at 37°C. Cells were left unstimulated or stimulated with 100 ng/ml LPS for 3 hrs. Cells were then left untreated or pre-treated with 10mM NAC or 100 μM DEM for 1 hr before addition of 5mM ATP to certain wells to activate the inflammasome. Cell supernatants were removed and IL-1β was quantified by ELISA. Data shown are the mean ± S.E.M., n=3.

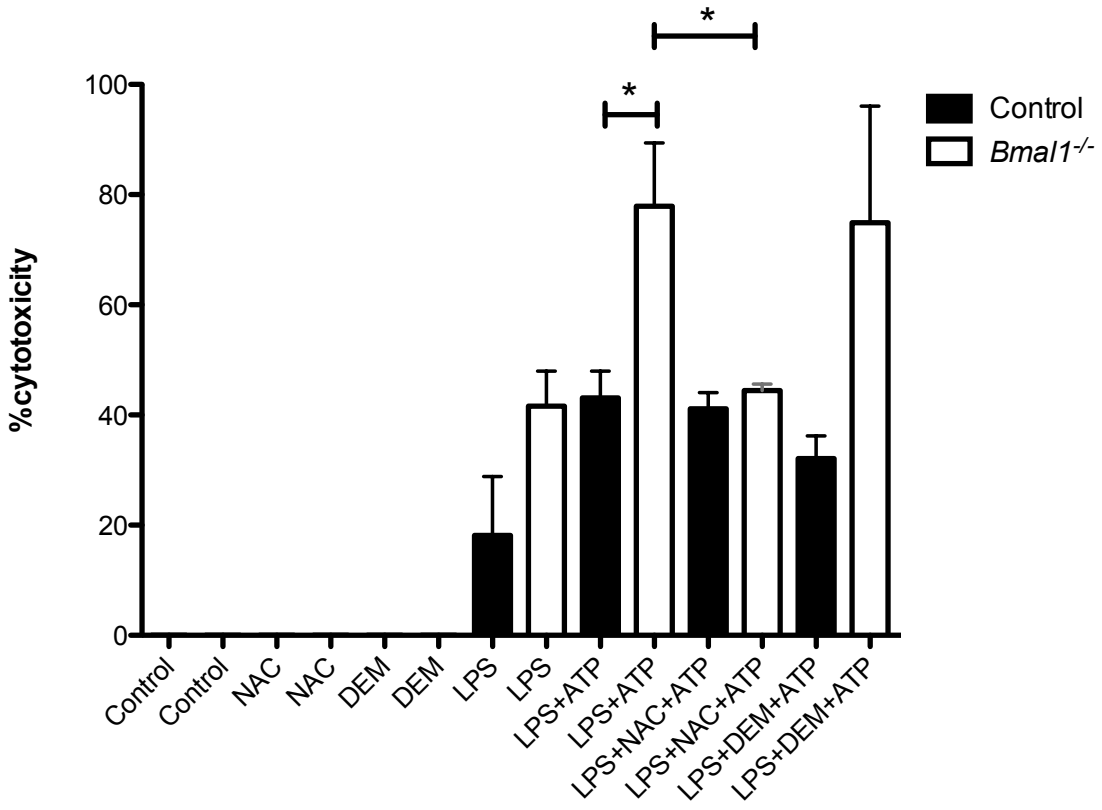

Figure 4.33 NAC but not DEM decreases NLRP3 induced cell death in *Bmal1*$^{-/-}$ BMDMs

Bmal1$^{+/+}$ and *Bmal1*$^{-/-}$ BMDMs were seeded at 5x10^5 cells/ml in a 12 well plate and incubated overnight at 37°C. Cells were left unstimulated or stimulated with 100 ng/ml LPS for 3 hrs. Cells were then left untreated or pre-treated with 10mM NAC or 100 μM DEM for 1 hr before addition of 5mM ATP to certain wells to activate the inflammasome. A LDH assay was carried out with the cell supernatant to measure cell death differences following inflammasome stimulation. Data shown are the mean ± S.E.M., n=3.

4.9 Discussion

Over the past number of years, evidence for circadian rhythmicity in various components of the innate immune has emerged. These variations range from timed molecular alterations within innate immune cells (31), to coordination of immune cell trafficking across the circadian day (76) and response to pathogen infection (78). Ultimately the molecular clock has been demonstrated to impact on a range of diseases and has become an important target for timed administration of various therapies and vaccinations.

4.9.1 Regulation of BMAL1 during inflammation

Previous work from our lab has demonstrated dynamic regulation of components of the molecular clock following onset of inflammation. Transcription and translation of BMAL1 in macrophages was shown to decrease following LPS stimulation, resulting in increased inflammatory output from these cells (31). This effect is seen at the whole organism level, as when BMAL1 levels are low at ZT12, mice are more susceptible to LPS induced lethality. Similarly, mice lacking BMAL1 in the myeloid lineage lose this circadian mediated protection (31). However, while we know that BMAL1 is important during inflammation, it remains uncertain whether the protein plays an active role following initiation of the immune response. In fractionation experiments I uncovered that BMAL1 is not simply blocked in activity following LPS stimulation, but migrates from the nucleus to the cytoplasm. What processes underlie this event and the reason for its occurrence are yet unknown. Interestingly, the reappearance of BMAL1 in the nucleus at 24 hrs post LPS stimulation could have some significance in terms of inflammatory output of the macrophage. It could be that the stark variation in phenotype to LPS induced endotoxic shock between myeloid specific *Bmal1*$^{+/+}$ and *Bmal1*$^{-/-}$ mice is partially due to the localisation of

BMAL1 within the macrophage. In wild type macrophages BMAL1 may induce anti-inflammatory pathways once it reappears within the nucleus after 24hrs of LPS, or, there could be a possible anti-inflammatory role for BMAL1 in the cytoplasm of macrophages during shorter exposure to LPS. Both these events would be non-existent in *Bmal1*$^{-/-}$ macrophages thus rendering animals with myeloid deletion of *Bmal1* susceptible to LPS induced lethality.

4.9.2 BMAL1 mediated regulation of IL-1β

My investigations into the pro-inflammatory cytokine IL-1β began for several reasons. First of all, it is a potent regulator of innate immunity, being linked to several disorders that are circadian in nature, such as sepsis (203), rheumatoid arthritis (204), and asthma (205). Secondly IL-1β is tightly linked to regulation by metabolism (130) and oxidative stress (132) in macrophages, both of which I have shown to be altered in *Bmal1* deficient macrophages. It was my belief that linking BMAL1 to molecular mediated regulation of IL-1β could explain the circadian variation seen in multiple immune parameters and diseases.

NRF2 has been linked to regulation of pro-inflammatory cytokines, both through regulation of oxidative stress (Dylan and Mills et.al. 2018 (in press)), and through direct repression of their transcription (166). Indeed, I showed this through *Nrf2* knockdown in fully differentiated macrophages, which revealed a significant increase in both transcription and translation of IL-1β. Interestingly, the same effect was noted in macrophages in which *Bmal1* was silenced or deleted. BMAL1 has previously been shown to limit NF-κB activity in peritoneal myeloid cells, limiting production of pro-inflammatory cytokines (31). Deletion of *Bmal1* could result in increased IL-1β through this mechanism, given that *Il1b* transcription is regulated by this pathway (206). However, I have uncovered several lines of evidence that

would show that this is not the case in BMDMs. First of all, pro-IL-1β protein levels were not increased in *Bmal1*$^{-/-}$ BMDMs following 4 hrs of LPS stimulation. NF-κB mediated transcription of pro-inflammatory cytokines begins shortly after LPS stimulation, therefore if NF-κB activity was responsible for increased IL-1β in *Bmal1*$^{-/-}$ BMDMs we would see an increase in protein at this time. Further demonstrating this fact, is the lack of difference between *Bmal1*$^{+/+}$ and *Bmal1*$^{-/-}$ BMDMs in terms of TNFα levels, as TNFα is a classic target of NF-κB. NRF2 on the other hand peaks in protein accumulation following 8 to 24 hrs of LPS stimulation. Our lab previously demonstrated an increase in TNFα production from *Bmal1*$^{-/-}$ peritoneal myeloid cells. I myself showed this result in peritoneal cells. However, there is no difference in TNFα production in *Bmal1*$^{-/-}$ BMDMs. TNFα is not a documented NRF2 target. We see also that while IL-10 is decreased in both *Bmal1*$^{-/-}$ PECs and BMDMs, IL-6 shows no increase in *Bmal1*$^{-/-}$ PECs, but is significantly increased in BMDMs. This is interesting given that IL-6 is another target of NRF2 transcriptional repression (166). Silencing of *Bmal1* in mature BMDMs resulted in the same inflammatory phenotype as *Bmal1*$^{-/-}$ BMDMs. It is well established that the effect of the molecular clock differs vastly between different cell types. It is distinctly possible that different pathways are utilized in different myeloid cells to regulate pro-inflammatroy cytokines. It should also be noted that the BMDMs utilised in these studies were unsynchronised, but the PECs would have been synchronised when being extracted from the peritoneum. Therefore time-of-day differences in the components of the molecular clock of these cells could have altered the inflammatory output, causing this variation seen between BMDMs and PECs. Given the increase in IL-1β and IL-6 in BMDMs lacking *Bmal1,* but no change in TNFα, I hypothesized that lack of NRF2 may be at least partly responsible for the increased inflammation in BMDMs.

While NRF2 is known to directly regulate IL-1β via transcriptional regulation, it may also regulate HIF-1α via attenuation of oxidative stress. I saw a clear increase in HIF-

1α protein levels in *Bmal1*$^{-/-}$ BMDMs, which I hypothesise is due to increased oxidative stress in these cells. Accumulation of HIF-1α facilitates transcription of *Il1b*. Glycolysis was increased in *Bmal1*$^{-/-}$ BMDMs. Inhibition of glycolysis with 2DG is known to inhibit IL-1β (130). Also, staining of ROS and mitochondria revealed co-localisation of the two stains. Mitochondrial ROS is a well-known driver of IL-1β (132). It is distinctly possible that both increased mitochondrial ROS production and lack of antioxidant regulation are facilitating increased IL-1β with deletion of *Bmal1.*

4.9.3 Pharmacological manipulation of the clock regulates IL-1β

To further link the molecular clock to regulation of IL-1β in macrophages, I utilized several compounds targeting the molecular clock. GSK4112 has previously been shown to have anti-inflammatory effects in human monocytes, limiting production of IL-6 (97). Interestingly, treating BMDMs with GSK4112 resulted in increased IL-6 at higher doses. It also decreased IL-10 and had no effect on TNFα, phenocopying *Bmal1*$^{-/-}$ BMDMs. This was interesting given the role of REV-ERBα as an inhibitor of *Bmal1* transcription. The difference in effect on IL-6 between mouse and human cells could possibly be explained by different functions of these proteins between species, or the difference between the human myeloid cell line and primary mouse macrophages. Use of another REV-ERBα agonist, which is also an agonist for REV-ERBβ, SR9009, did not recapitulate the IL-1β or IL-6 phenotype of GSK4112. However, IL-10 was decreased and there was no difference in TNFα. Whether this was a concentration issue or whether the two drugs have different efficiencies in boosting REV-ERBα activity or off target effects is unknown. However, it has now come to light that the IC50 of SR9009 is much higher than the concentration used, 670 nm for REV-ERBα and 800 nm for REV-ERBβ. This compound also affects REV-ERBβ, which GSK4112 does not. Also unsure is whether these drugs affect the NRF2 antioxidant defence pathway, as is the case in *Bmal1-/-* BMDMs. Interestingly,

SR8278, a REV-ERBα antagonist (207), has the opposite effect of GSK4112, limiting pro-IL-1β production following LPS stimulation. Given this result, it is highly probable that REV-ERBα is involved in regulation of IL-1β in mouse macrophages. However, whether this is a result of direct REV-ERBα activity, or due to REV-ERBα mediated inhibition of *Bmal1* requires further investigation. Further experiments are required with more careful consideration of the effective dosages of these compounds.

Further confirming a role for the molecular clock in IL-1β regulation was use of the cryptochrome agonist KL001. KL001 was previously demonstrated to be effective in limiting symptoms of rheumatoid arthritis in mice and human fibroblast like synoviocytes, decreasing TNFα induced TNFα, IL-6 and IL-1β (108). I have shown that KL001 limits LPS induced IL-1β in BMDMs, further linking the clock to regulation of inflammation. Given that IL-1β and IL-6 are both impacted by this drug, it is possible that KL001 is regulating NRF2 in some manner. However, further experimentation would be required to state this definitively.

4.9.4 Boosting NRF2 activity and limiting ROS confirms role of BMAL1 in IL-1β production

Given the emerging proof of NRF2 regulation impacting on the pro-inflammatory state of *Bmal1-/-* macrophages, I began researching ways in which to boost NRF2 activity and pursued a genetic approach. *Keap1* knockdown has previously been demonstrated to boost NRF2 activity, limiting oxidative stress within different cell types (208, 209). Knockdown of *Keap1* in BMDMs was effective and I showed that it had the desired effect by limiting levels of LPS induced IL-1β. *Keap1* knockdown also decreased IL-6 in wild type BMDMs but had no significant effect on IL-10 or TNFα, which was expected as NRF2 has been linked to IL-6 but not TNFα or IL-10 in

My experiments utilizing *Keap1* knockdown exhibited that dysfunction of NRF2 was responsible for the increased IL-1β phenotype in *Bmal1*$^{-/-}$ BMDMs. However, whether this was due to NRF2's role as an antioxidant or a direct anti-inflammatory agent was still unclear. It was previously shown that NRF2 limited IL-1β independently of ROS. However, this study was carried out after acute LPS activation of macrophages (no later than 4 hrs treatment of LPS) (166). In later stages of macrophage activation (24 hrs treatment of LPS), ROS levels accumulate, leading to a pseudo-hypoxic state to stabilize HIF-1α and drive IL-1β production (130, 210). Pharmacologically reducing ROS has previously been demonstrated to rescue the damage to various tissues inflicted by *Bmal1* deletion (160). Similarly specific pharmacological activation of NRF2 by sulforophane was shown to rescue the pulmonary fibrosis mediated by clock disruption (189). I utilized NAC to directly limit LPS induced ROS, while using DEM to boost NRF2 levels and activity. If the increased oxidative stress in *Bmal1*$^{-/-}$ BMDMs was not relevant in the context of IL-1β release, we would expect no rescuing effect with NAC. DEM operated as a form of positive control, given that it would both boost NRF2 activity and limit ROS.

It was found that both NAC and DEM limited pro-IL-1β production following 24 hrs of LPS stimulation in wild type BMDMs. However, I saw that there was a further decrease with DEM over NAC treatment. This was possibly due to the dual action of NRF2 as an anti-oxidant and anti-inflammatory. The effect of NAC and DEM on other cytokines between *Bmal1*$^{+/+}$ and *Bmal1*$^{-/-}$ BMDMs yielded some interesting results, with NAC and DEM being shown to have alternating effects on different cytokines, showing that some of the roles of NRF2 may be independent of ROS, such as the drop in IL-6 production with DEM that is not evident with NAC.

In my studies NAC did not boost NRF2 target genes. If anything, there was a clear decrease in NRF2 target genes following NAC stimulation, as seen in *Nqo1*

expression levels. I hypothesise this is due to NAC fulfilling the role of an antioxidant in the cell, limiting oxidative stress and thus removing the activating signal for NRF2 activation. Whether this has connotations in the clinic given the frequent use of NAC as an anti-toxicity agent, has not been investigated and would be an interesting avenue of research. On the other hand, DEM substantially boosted *Nqo1* expression in both *Bmal1*$^{+/+}$ and *Bmal1*$^{-/-}$ BMDMs, matching the effects seen in *Keap1* knockdown. Once again like *Keap1* knockdown, NAC and DEM both decrease LPS induced IL-1β transcript and protein. As was seen in wild type BMDMs, I saw greater inhibition of IL-1β with DEM. It can be clearly seen that both oxidative stress and NRF2 deregulation play a role in the enhanced production of IL-1β in *Bmal1*$^{-/-}$ BMDMs. Further advancing this concept was the reduction of LPS induced pro-IL-1β seen with addition of OI. This was interesting given itaconate's ability to limit IL-1β through three separate mechanisms. Boosting NRF2, activity (Ryan and Mills et.al. 2018 (in press)), decrease of ROS (135), and limiting of SDH activity (135). Given the lack of LPS induced *Irg1* expression in *Bmal1*$^{-/-}$ BMDMs, this could be another possible mechanism for increased inflammation in these cells. Decreased itaconate production following LPS stimulation could facilitate KEAP1 stability, preventing NRF2 activation. This has been shown in *Irg1* knockout macrophages, which produce greater HIF-1α and IL-1β levels.

While my work has clearly demonstrated BMAL1 at the forefront of NRF2 regulation in macrophages, there is more to uncover on the exact mechanism for this regulation. Be it completely transcriptional, as has previously been described, or is there a new mechanism for post translational modifications of KEAP1 through metabolic regulation such as through itaconate.

4.9.5 BMAL1 regulates inflammasome activation

The inflammasome is required to cleave the inactive pro-IL-1β into its active form, so it may be released from the cell and propagate the inflammatory cascade (211). While the inflammasome is crucial to host defence (212) and auto-immune disorders (120), very little has been discovered regarding molecular clock mediated regulation of the inflammasome. Given the nature of my project in which I delve into the molecular regulation of IL-1β by the molecular clock, it seemed sensible to look at the next step, that is processing of pro- IL-1β into its mature form.

The infllammasome protocols I utilized required short time points of LPS stimulation. As was previously seen, pro-IL-1β is not significantly increased in *Bmal1*$^{-/-}$ BMDMs at these times. However, there was a large boost in cleaved IL-1β production in *Bmal1*$^{-/-}$ BMDMs following NLRP3 initiation. This indicated that it was not simply increased production of pro-IL-1β facilitating increased cleavage, but must in fact be greater processing of the protein. It was found this was not due to increased NLRP3 as the transcript and protein levels were not increased in *Bmal1*$^{-/-}$ BMDMs. Also, stimulation of the AIM2 inflammasome recapitulated the increased IL-1β phenotype, therefore indicating that the effect was downstream of the inflammasome sensors.

Given the lack of specificity of inflammasome activation, two other candidates presented themselves as possible mechanisms for increased IL-1β release, increased cell death, or increased cleavage by Caspase 1. The increase in cell death could be facilitating greater release of IL-1β in *Bmal1*$^{-/-}$ BMDMs. But I also uncovered greater levels of Caspase 1in the supernatants of these cells. The increased presence of Caspase 1 in the supernatants could be due to increased cell death in *Bmal1*$^{-/-}$ BMDMs, however there was overall more cleaved Caspase 1 in these cells. The mechanism for this increase requires further investigation, however NRF2 has previously been linked to Caspase 1 regulation, although in this case *Nrf2* knockout resulted in decreased Caspase 1 activation (185). Given my previous results on

NRF2 mediated regulation of IL-1β, it seemed pertinent to assess whether this would play a role in inflammasome regulation. The literature on NRF2 and NLRP3 is confusing at best, with differing reports on the effect of pharmacological versus genetic alterations to NRF2 activity (181, 183-185). My results hinted at a decrease in NLRP3 induced IL-1β with *Keap1* knockdown. However, this inflammasome assay was carried out after *Keap1* had been knocked down, thus NRF2 would have been activated previous to LPS stimulation and would decrease *Il1b* transcription. Therefore, the decrease may have been evident, not because of decreased cleavage of pro-IL-1β, but decreased transcription of *Il1b* t To this end I primed cells with LPS for 3 hrs, to facilitate *Il1b* transcription, followed by 1 hr of DEM to activate NRF2, or NAC to supress ROS. Both NAC and DEM limited NLRP3 induced IL-1β in *Bmal1*$^{+/+}$ and *Bmal1*$^{-/-}$ BMDMs. The relative decrease was similar, however NAC had a much more potent effect in suppressing IL-1β. I hypothesise that this may be due to the short duration of the inflammasome protocol. In previous experiments cells were pre-treated with DEM for 3 hrs before treating with LPS giving the cells adequate time to boost NRF2 levels. However, in the inflammasome experiments cells were only pre-treated with DEM for 1 hr before stimulation with ATP, which may not allow enough time for NRF2 to accumulate and have an effect. NAC on the other hand would instantly begin reducing ROS. A similar case can be made for the cell death phenotype. The increased cell death seen in *Bmal1*$^{-/-}$ BMDMs is completely rescued to wild type levels with NAC, however there is no effect with DEM. Whether NRF2 plays a direct role in NLRP3 inflammasome activation or whether it is ROS mediated requires further investigation. Also, while ROS appears to play a clear role in NLRP3 induced death in *Bmal1*$^{-/-}$ BMDMs, it had no effect on *Bmal1*$^{+/+}$ BMDMs. It may be that the increased ROS in *Bmal1*$^{-/-}$ BMDMs is leading to increased death with NLRP3 activation, but that ROS itself does not have much contribution in a wild type setting.

4.9.6 Final conclusions

In summary, it appears that regulation of pro-inflammatory cytokines is under the regulation of the molecular clock in macrophages. Specifically, BMAL1 appears to be crucial in regulation of the pyrogenic cytokine IL-1β. In fact, any form of modulation of the molecular clock components by pharmacological means appears to affect the balance of LPS induced IL-1β production. This extends to processing of the cleaved form of IL-1β, which does not appear to be specific to inflammasome, but instead is linked to increased Caspase 1 and cell death.

Certainly, the IL-1β phenotype of cells lacking *Bmal1* appears to be largely dependent on alterations to oxidative stress and NRF2 in these cells. Rescue experiments recover the pro-inflammatory phenotype of these cells, and open exciting avenues of research for people who experience inflammatory disorders due to circadian disruption such as shift workers. Whether the altered metabolism of the *Bmal1*$^{-/-}$ BMDMs also contributes to the IL-1β phenotype is yet to be concluded. However, given the interconnection between metabolism, oxidative stress, and NRF2, it can be safely assumed that this is the case.

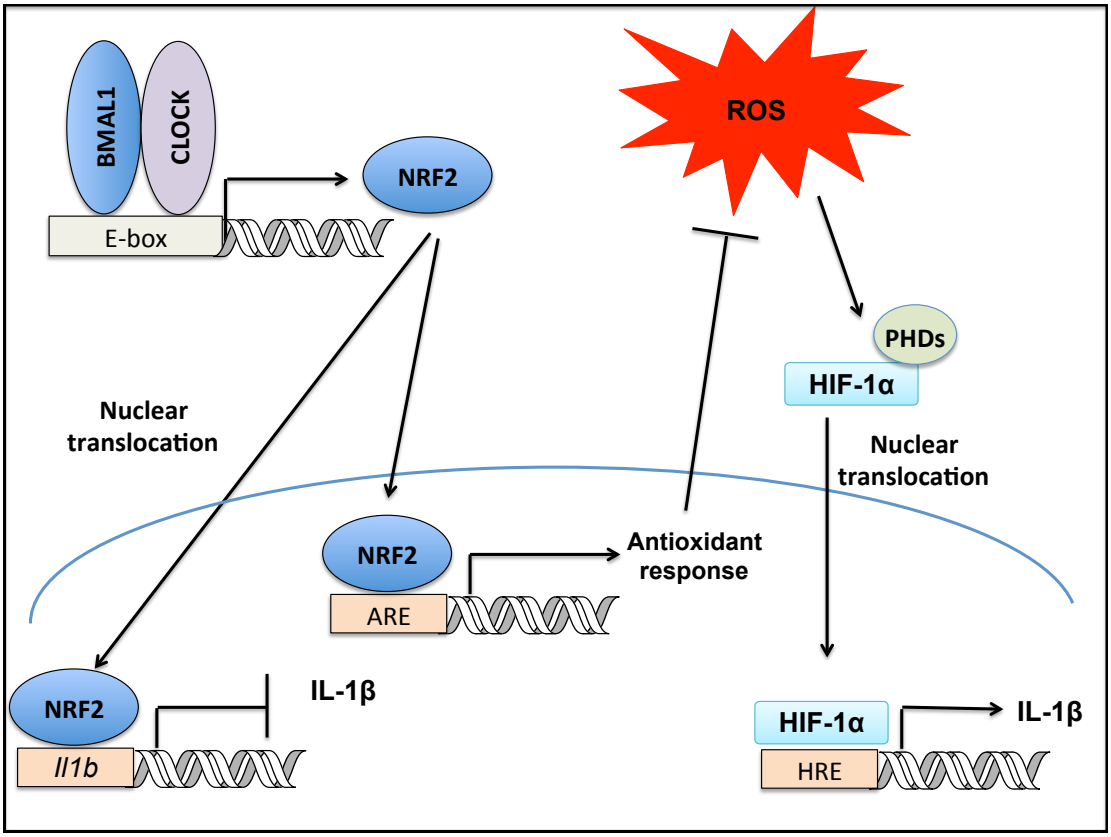

Figure 4.34 Current hypothesis for BMAL1 mediated regulation of IL-1β

BMAL1 in a heterodimeric partnership with CLOCK can induce rhythmic expression of NRF2. This leads to basal rhythms in homeostatic ROS regulation. Under conditions of inflammatory stress, the "timed" state of the cell is important. High levels of NRF2 at a given time of day facilitate a greater anti-inflammatory response versus low levels of NRF2. NRF2 can limit IL-1β through two mechanisms. Direct limitation of *Il1b* transcription and suppression of ROS induced HIF-1α.

Chapter 5: General Discussion

Over the course of my studies, I have uncovered that the molecular clock protein, BMAL1, is involved in regulating LPS induced IL-1β in murine macrophages. Specifically, I uncovered in macrophages that the activity of NRF2 over time-of-day and under LPS induction is directly mediated by BMAL1. Furthermore, I have shown that reduction of NRF2 activity leads to a loss of redox homeostasis, resulting in the aberrant production of the pro-inflammatory cytokine IL-1β, providing a mechanism as to why macrophages lacking BMAL1 are highly pro-inflammatory in response to LPS. A further investigation into the effect of the molecular clock on other aspects of immunometabolism has also elucidated some interesting results, tying the molecular clock to metabolism, oxidative stress and cytokine release in macrophages.

5.1 Circadian rhythms: Linking metabolism and immunity

In the not so distant past, the fields of metabolism and immunology were widely separated. As scientists we all learned the various metabolic pathways as part of an enforced undergraduate regime. The idea that the fuel utilized by an immune cell, or indeed the way it is broken down, could result in varying phenotypes of pathology was unheard of. Similarly, the reverse is true. The idea that the output of an immune cell could impact on metabolic disorders such as diabetes and obesity went largely unexplored. In the past 5-10 years there has been a rediscovery of metabolism by immunologists, aided and abetted by the emergence of new high throughput, highly sensitive techniques. Ultimately this has led to a merging of the two into a hybrid field, immunometabolism, where neither the biochemists nor immunologists are comfortable, but the area is clearly a new and important frontier in science.

Given the pervasiveness of the molecular clock into nearly all aspects of biological life, one interested in circadian rhythms can throw a dart at a chart of biological processes, and more than likely uncover that this process is in some way influenced by the circadian cycle. This leads to some very interesting discussions at circadian biology conferences, as the field is so diverse, ranging from ornithology to intensive biochemistry. Circadian rhythms have long been associated with direct control over immunity and metabolism as individual subjects, however my study is one of the first to investigate directly the role of the circadian cycle in immunometabolism.

5.2 Circadian misalignment: A malady of modern society

Humans living in built up towns or cities may consider themselves well removed from the influence of nature. However, we are much more tied to our external environment than we realise. Even small changes, such as those imposed by daylight saving time have been linked to consequences in terms of health. There is some evidence of an increased risk of myocardial infarction (213, 214) and stroke (215) following the one-hour phase advance by which we set the clocks forward in spring. The greatest risk is experienced within the first one or two days following the time shift. Given the problems that arise with such small insults to our circadian rhythms, the variety of health problems that arise with larger disruptions to our circadian cycles, such as with jet lag or shift work, come as no surprise. This is still omitting the ever presence of light in our society and also social pressures that keep us from living to our own chronotype (our individual propensity to sleep at certain times of the day according to our own rhythms).

My research was based on the fact that most of the conditions associated with clock disruption are diseases mediated by alterations to inflammation and metabolism, for example diabetes, cardiovascular disease and cancer. Cancer is particularly

interesting in this regard as it was within tumour cells that Warburg metabolism, the shift to aerobic glycolysis, was first discovered (216). Also, certain classes of tumour often utilise immune evasion as a technique to prevent detection and destruction by the innate immune system (217). Over the last number of years circadian cycle disruption has been linked to breast (58), lymphatic (55) and prostate cancers (56). Shift work has been labelled a highly probable carcinogen by the IARC (59). Uncovering the molecular mechanisms linking the molecular clock to such pathologies is crucial to understanding the impact of clock disruption on our health and wellbeing.

5.3 IL-1β: The missing link

While being known as a potent regulator of innate immunity, IL-1β is now placed at the crossroads between metabolism and immunity. Over the past number of years, it has become clear that regulation of IL-1β production appears to be largely under the influence of cellular metabolism. This regulation ranges from mitochondrial bioenergetics (130) to fatty acid metabolism (218). Of note is the potent effect of mitochondrial ROS mediated regulation of HIF-1α on IL-1β production (132). It is my belief that this axis, ROS-HIF-1a-IL1β, is pivotal to the influence of the circadian cycle on innate immunity.

Our lab has previously linked the deletion of *Bmal1* in the myeloid lineage with an increase in IL-1β producing myeloid cells in the CNS, driving disease severity in a mouse model of multiple sclerosis (79). Other studies have shown diurnal fluctuations in the levels of IL-1β in serum. Mice treated with *L. monocytogenes* at ZT8 (the time at which I show lower *Nrf2* and *Bmal1* but higher ROS in peritoneal myeloid cells) have higher concentrations of IL-1β in their serum than mice treated at ZT0 (78) The molecular mechanisms of circadian mediated regulation of IL-1β

have not previously been described, however, mechanisms have been described for many of the components that regulate IL-1β. HIF-1α was shown to be under circadian regulation to direct leukocyte migration (76). This effect was largely due to oscillations in ROS in these cells. Increased glycolysis, a known marker of increased IL-1β, is seen in liver cells lacking *Bmal1 (136).* Mitochondrial ROS is also increased in liver cells lacking a functioning molecular clock (142). NRF2 is under circadian regulation in lung (189), liver (177) and pancreatic cells (161). In these examples we see a clear correlation with my own research, of altered metabolism and oxidative stress regulation in macrophages, furthering proof that circadian mediated regulation of ROS and NRF2 may be driving rhythms in IL-1β regulation. This may have ramifications in terms of treatment of conditions in which IL-1β, immunometabolism and the clock intersect.

5.4 Clinical relevance

Of all the cytokine families, the IL-1 family of ligands is primarily associated with acute and chronic levels of inflammation. IL-1β has been identified as a target for therapeutic intervention in multiple disorders such as type 2 diabetes, gout, muckle-wells syndrome and rheumatoid arthritis. Recent discoveries from the CANTOS study have revealed fascinating results utilising canakinumab, a monoclonal antibody targeting IL-1β (219). It was found that this antibody drastically reduced the risks of a secondary cardiovascular event in patients with high levels of C-reactive protein. The cardiovascular system is well documented to be under regulation of the circadian cycle (220) and shift workers are more prone to heart conditions (221) . Given the critical role that macrophages play in atherosclerotic plaque formation (222), it is distinctly possible that circadian disruption leading to altered IL-1β regulation from macrophages could be leading to the increased prevalence of heart conditions in people with disrupted circadian rhythms.

NRF2 was also a major component of my studies and has itself become a major target of therapeutic interest in the last number of years. Many drugs have been developed with the goal of boosting NRF2 activity, some of which are in use or are undergoing clinical trials, such as dimethalfumarate (DMF) (223), resveratrol (224) and sulphoraphane (225). DMF is utilised in the treatment of multiple sclerosis (226, 227). Resveratrol has been tested in multiple inflammatory conditions (228). Sulphoraphane, derived from the extract of broccoli, was shown to limit mouse models of bleomycin induced lung fibrosis in a circadian study (189). Whether sulfuophane would have any effect on the fibrotic damage caused by bleomycin in chemotherapy for lung cancer has not yet been investigated, however sulphorphane is under investigation as an anti-cancer agent (229). However, antioxidants present themselves as something of a double-edged sword in terms of cancer research. While antioxidants in some studies prevent cancer (230-232), other studies demonstrate that antioxidants may actually aid tumour growth following onset of cancer (233, 234). It is possible antioxidant regulation and immune regulation by the molecular clock are two sides of the same coin. A delicate balance between inflammatory and anti-inflammatory signals exist for a reason, to protect us from outside influence and to protect our bodies from our own immune system. It is likely that the circadian cycle oversees this balance.

Of course, the field of immunometabolism presents itself as a promising therapeutic target given the range of metabolites that are seen to alter under different stages of inflammation. Of specific note is the HIF-1α pathway given its pivotal role in regulating Warburg metabolism in both tumour (235) and immune cells (128), and its role in IL-1β production (132). Increased levels of HIF-1α in solid tumours is associated with poor prognosis (236). Pathogenesis of rheumatoid arthritis is largely associated with deregulation of the hypoxic pathway (237). However, while multiple HIF inhibitors have been generated, difficulties have arisen in utilising

these therapeutically. HIF is crucial for homeostatic control in multiple tissue types, and therefore inhibiting this pathway often leads to off target effects. While HIF appears to be difficult to target due to its pleitrophic role as a transcription factor, identifying HIF downstream targets and the roles they play may open more successful avenues of research.

Despite the prevalence of circadian rhythms in our physiology, relatively little has been done to target it at a molecular level in humans. Small molecule activators and inhibitors have begun to emerge, but it appears that these compounds have struggled to advance through pharmaceutical clinical development. I have demonstrated that these compounds appear to be potent in regulating inflammation in macrophages. Other publications have similarly displayed this fact (97, 108), however, their use *in vivo* is still lacking with the exception of SR9009, which has been directly demonstrated to reduce the body fat of mice (202). Obviously, this makes SR9009 of huge commercial value in terms of weight loss and I have seen a presence online of bodybuilders attaining the drug for personal use. This is worrying, as we do not fully understand the impact of this drug or how it might impact the circadian cycle of humans. Similar to HIF signalling, it may be the case that the molecular clock itself regulates far too many targets to make it amenable for direct modulation with small molecule inhibitors. Therefore, understanding the downstream targets of the clock is key. However, some of the biggest studies with regard to the circadian cycle in health revolve around “chronotherapies”. This field is open to a lot of advancement given the potent differences that are observed in time-of-day variation in disease severity. It has also been discovered that the majority of best-selling drugs and World Health Organization essential medicines directly target the products of genes showing rhythmicity (238). Many of these drugs display short half-lives and could benefit from timed administration. (238). This is especially relevant in terms of cancer treatment where circadian timing has been demonstrated to modify the tolerability of anticancer medications by 2- to 10-

fold in both experimental models and cancer patients (239). Given the links between the clock and IL-1β production, and our data showing that the intermediary is NRF2, it may be useful to start to consider timed administration of NRF2 activators for inflammatory conditions.

Many disorders of the circadian cycle could be attenuated through awareness and prevention, rather than through modulation by pharmaceutical agents. A greater understanding of the damage that shift work exerts on our bodies is needed. Even for non-shift workers, sleep hygiene and sleep duration is very important. Televisions and screens populate our bedrooms and streetlights shine through our windows. The presence of these subtle light sources is disrupting our natural rhythms and disturbing sleep, both of which are linked to multiple pathologies. Steps can be taken to limit the effect of modern society on our endogenous clock, but only if people are aware of the situation.

5.5 Thesis conclusions

While circadian rhythms are well documented in innate immunity, the molecular mechanisms governing this connection are lacking. This thesis has given a definitive role to the molecular clock in regulating oxidative stress in macrophages via NRF2, thus providing a mechanism for time-of-day variation in a range of inflammatory condition that can be mediated by oxidative stress and IL-1β. Moreover, this thesis has highlighted some interesting avenues of research, establishing a connection between the molecular clock, metabolism, and inflammation in macrophages.

The specific conclusions from my research are as follows:

- This thesis has successfully shown that the molecular clock is important in regulating the NRF2 antioxidant defence pathway in macrophages. Specifically, it appears that NRF2 is under direct control of BMAL1 and that circadian fluctuations in the molecular clock give rise to patterns in NRF2 levels. Disruption of the molecular clock disrupts this regulation resulting in a dampened antioxidant response and increased levels of ROS accumulation.

- Oxidative stress appears to exhibit diurnal variation in macrophages and is greatly increased in macrophages lacking a functional molecular clock. While dampening of the NRF2 antioxidant defence pathway is definitely contributing to increased ROS, it is yet unsure if there is also greater ROS production in these cells. The altered metabolic state of these cells and the co-localisation of ROS with mitochondria would suggest that *Bmal1*$^{-/-}$ macrophages are not only exhibiting ROS accumulation, but are also exhibiting increased production of oxidative stress.

- The decreased levels of NRF2 in macrophages lacking a functional molecular clock gives rise to increased inflammatory output from these cells following stimulation. Specifically, IL-1β levels are increased drastically with deletion of *Bmal1,* and this appears to be at least partially mediated by increased levels of HIF-1α in these cells. It is possible to rescue the increased IL-1β phenotype of these cells by re-establishing NRF2 activity or limiting oxidative stress, providing a mechanistic link for *Bmal1* deletion and inflammation.

- Increased processing of pro-IL-1β into its active form in macrophages lacking *Bmal1* appears to be non-specific to a given inflammasome, but is more likely mediated by increased levels of Caspase 1 in these cells. However, the exact mechanism for this remains elusive. Preliminary results indicate a possible

role for oxidative stress in promoting increased inflammasome induced pyroptosis in these cells.

5.6 Closing remarks

The circadian cycle remains one of the most important coordinators of our physiological functions across the 24 hr day. Further understanding of the molecular mechanisms linking the circadian cycle to biological processes opens up multiple avenues of research for understanding our own bodies, and in developing targets for therapeutic interventions. My work has uncovered a novel role for the molecular clock in promoting antioxidant response to limit inflammation in macrophages. Severity of circadian inflammatory conditions involving oxidative stress and IL-1β such as asthma (240), sepsis (241), rheumatoid arthritis (108), osteoarthritis (242) and multiple sclerosis (79), could very well be mediated at the molecular level by this BMAL1-NRF2-IL-1β axis. Further understanding of how the clock intersects with NRF2 function and activity may reveal new chronotherapies for treating circadian gated inflammatory disorders.

Chapter 6: References

1. Early JO & Curtis AM (2016) Immunometabolism: Is it under the eye of the clock? *Semin Immunol* 28(5):478-490.
2. Buhr ED & Takahashi JS (2013) Molecular components of the Mammalian circadian clock. *Handbook of experimental pharmacology* (217):3-27.
3. Partch CL, Green CB, & Takahashi JS (2014) Molecular architecture of the mammalian circadian clock. *Trends in cell biology* 24(2):90-99.
4. Pattanayak GK, Lambert G, Bernat K, & Rust MJ (2015) Controlling the Cyanobacterial Clock by Synthetically Rewiring Metabolism. *Cell reports* 13(11):2362-2367.
5. H B (1903) *Botanische Forschungen des Alexanderzuges.*
6. Gardner MJ, Hubbard KE, Hotta CT, Dodd AN, & Webb AA (2006) How plants tell the time. *Biochem J* 397(1):15-24.
7. Halberg F*, et al.* (2003) Transdisciplinary unifying implications of circadian findings in the 1950s. *Journal of Circadian Rhythms* 1:2-2.
8. Halberg F, Johnson EA, Brown BW, & Bittner JJ (1960) Susceptibility rhythm to E. coli endotoxin and bioassay. *Proc Soc Exp Biol Med* 103:142-144.
9. Dumbell R, Matveeva O, & Oster H (2016) Circadian Clocks, Stress, and Immunity. *Frontiers in endocrinology* 7:37.
10. Wever RA (1986) Characteristics of circadian rhythms in human functions. *Journal of neural transmission. Supplementum* 21:323-373.
11. Meuti ME & Denlinger DL (2013) Evolutionary links between circadian clocks and photoperiodic diapause in insects. *Integrative and comparative biology* 53(1):131-143.
12. Gooley JJ, Lu J, Chou TC, Scammell TE, & Saper CB (2001) Melanopsin in cells of origin of the retinohypothalamic tract. *Nat Neurosci* 4(12):1165-1165.
13. Abe K, Kroning J, Greer MA, & Critchlow V (1979) Effects of destruction of the suprachiasmatic nuclei on the circadian rhythms in plasma corticosterone, body temperature, feeding and plasma thyrotropin. *Neuroendocrinology* 29(2):119-131.
14. Welsh DK, Takahashi JS, & Kay SA (2010) Suprachiasmatic nucleus: cell autonomy and network properties. *Annual review of physiology* 72:551-577.
15. Schibler U & Sassone-Corsi P (2002) A Web of Circadian Pacemakers. *Cell* 111(7):919-922.
16. Boivin DB*, et al.* (2003) Circadian clock genes oscillate in human peripheral blood mononuclear cells. *Blood* 102(12):4143-4145.
17. Barclay JL, Tsang AH, & Oster H (2012) Chapter 10 - Interaction of central and peripheral clocks in physiological regulation. *Progress in brain research*, eds Andries Kalsbeek MMTR & Russell GF (Elsevier), Vol Volume 199, pp 163-181.

18. Nader N, Chrousos GP, & Kino T (2010) Interactions of the Circadian CLOCK System and the HPA Axis. *Trends in endocrinology and metabolism: TEM* 21(5):277-286.
19. Mohawk JA, Pargament JM, & Lee TM (2007) Circadian Dependence of Corticosterone Release to Light Exposure in the Rat. *Physiol Behav* 92(5):800-806.
20. Cajochen C, Krauchi K, & Wirz-Justice A (2003) Role of melatonin in the regulation of human circadian rhythms and sleep. *J Neuroendocrinol* 15(4):432-437.
21. Kalsbeek A*, et al.* (2012) Circadian rhythms in the hypothalamo–pituitary–adrenal (HPA) axis. *Molecular and Cellular Endocrinology* 349(1):20-29.
22. Guo H, Brewer JM, Lehman MN, & Bittman EL (2006) Suprachiasmatic regulation of circadian rhythms of gene expression in hamster peripheral organs: effects of transplanting the pacemaker. *J Neurosci* 26(24):6406-6412.
23. Curtis Anne M, Bellet Marina M, Sassone-Corsi P, & O'Neill Luke AJ (2014) Circadian Clock Proteins and Immunity. *Immunity* 40(2):178-186.
24. Tataroglu O & Emery P (2015) The molecular ticks of the Drosophila circadian clock. *Current opinion in insect science* 7:51-57.
25. Bunger MK*, et al.* (Mop3 Is an Essential Component of the Master Circadian Pacemaker in Mammals. *Cell* 103(7):1009-1017.
26. Ripperger JA & Schibler U (2006) Rhythmic CLOCK-BMAL1 binding to multiple E-box motifs drives circadian Dbp transcription and chromatin transitions. *Nat Genet* 38(3):369-374.
27. DeBruyne JP, Weaver DR, & Reppert SM (2007) CLOCK and NPAS2 have overlapping roles in the suprachiasmatic circadian clock. *Nat Neurosci* 10(5):543-545.
28. Ye R*, et al.* (2014) Dual modes of CLOCK:BMAL1 inhibition mediated by Cryptochrome and Period proteins in the mammalian circadian clock. *Genes & Development* 28(18):1989-1998.
29. Preitner N*, et al.* (2002) The Orphan Nuclear Receptor REV-ERB α Controls Circadian Transcription within the Positive Limb of the Mammalian Circadian Oscillator. *Cell* 110(2):251-260.
30. Sato TK*, et al.* (2004) A Functional Genomics Strategy Reveals Rora as a Component of the Mammalian Circadian Clock. *Neuron* 43(4):527-537.
31. Curtis AM*, et al.* (2015) Circadian control of innate immunity in macrophages by miR-155 targeting Bmal1. *Proceedings of the National Academy of Sciences* 112(23):7231-7236.
32. Hansen KF, Sakamoto K, & Obrietan K (2011) MicroRNAs: a potential interface between the circadian clock and human health. *Genome Medicine* 3(2):10-10.
33. Gallego M & Virshup DM (2007) Post-translational modifications regulate the ticking of the circadian clock. *Nat Rev Mol Cell Biol* 8(2):139-148.

34. Miyazaki K, Wakabayashi M, Chikahisa S, Sei H, & Ishida N (2007) PER2 controls circadian periods through nuclear localization in the suprachiasmatic nucleus. *Genes Cells* 12(11):1225-1234.
35. Missra A*, et al.* (2015) The Circadian Clock Modulates Global Daily Cycles of mRNA Ribosome Loading. *The Plant Cell* 27(9):2582-2599.
36. Kojima S, Sher-Chen EL, & Green CB (2012) Circadian control of mRNA polyadenylation dynamics regulates rhythmic protein expression. *Genes & Development* 26(24):2724-2736.
37. Putker M & O'Neill JS (2016) Reciprocal Control of the Circadian Clock and Cellular Redox State - a Critical Appraisal. *Molecules and Cells* 39(1):6-19.
38. Ko GYP, Shi L, & Ko ML (2009) Circadian regulation of ion channels and their functions. *Journal of neurochemistry* 110(4):1150.
39. Silver AC, Arjona A, Hughes ME, Nitabach MN, & Fikrig E (2012) Circadian expression of clock genes in mouse macrophages, dendritic cells, and B cells. *Brain, behavior, and immunity* 26(3):407-413.
40. Bollinger T*, et al.* (2011) Circadian Clocks in Mouse and Human CD4+ T Cells. *PLoS ONE* 6(12):e29801.
41. Keller M*, et al.* (2009) A circadian clock in macrophages controls inflammatory immune responses. *Proceedings of the National Academy of Sciences* 106(50):21407-21412.
42. Eckel-Mahan K & Sassone-Corsi P (2015) Phenotyping Circadian Rhythms in Mice. *Current protocols in mouse biology* 5(3):271-281.
43. Bains RS*, et al.* (2017) Assessing mouse behaviour throughout the light/dark cycle using automated in-cage analysis tools. *Journal of Neuroscience Methods*.
44. LeGates TA & Altimus CM (2011) Measuring Circadian and Acute Light Responses in Mice using Wheel Running Activity. *Journal of Visualized Experiments : JoVE* (48):2463.
45. Balsalobre A, Damiola F, & Schibler U (1998) A serum shock induces circadian gene expression in mammalian tissue culture cells. *Cell* 93(6):929-937.
46. Cain DW & Cidlowski JA (2017) Immune regulation by glucocorticoids. *Nat Rev Immunol* 17(4):233-247.
47. Dickmeis T (2009) Glucocorticoids and the circadian clock. *The Journal of endocrinology* 200(1):3-22.
48. Nagoshi E*, et al.* (2004) Circadian gene expression in individual fibroblasts: cell-autonomous and self-sustained oscillators pass time to daughter cells. *Cell* 119(5):693-705.
49. Baron KG & Reid KJ (2014) Circadian misalignment and health. *Int Rev Psychiatry* 26(2):139-154.
50. Karlsson B, Knutsson A, & Lindahl B (2001) Is there an association between shift work and having a metabolic syndrome? Results from a population based study of 27 485 people. *Occupational and Environmental Medicine* 58(11):747-752.

51. Morikawa Y, *et al.* (2005) Shift work and the risk of diabetes mellitus among Japanese male factory workers. *Scand J Work Environ Health* 31(3):179-183.
52. Karlsson B, Alfredsson L, Knutsson A, Andersson E, & Toren K (2005) Total mortality and cause-specific mortality of Swedish shift- and dayworkers in the pulp and paper industry in 1952-2001. *Scand J Work Environ Health* 31(1):30-35.
53. Haupt CM, *et al.* (2008) The relation of exposure to shift work with atherosclerosis and myocardial infarction in a general population. *Atherosclerosis* 201(1):205-211.
54. Tenkanen L, Sjoblom T, & Harma M (1998) Joint effect of shift work and adverse life-style factors on the risk of coronary heart disease. *Scand J Work Environ Health* 24(5):351-357.
55. Lahti TA, Partonen T, Kyyronen P, Kauppinen T, & Pukkala E (2008) Night-time work predisposes to non-Hodgkin lymphoma. *Int J Cancer* 123(9):2148-2151.
56. Kubo T, *et al.* (2006) Prospective cohort study of the risk of prostate cancer among rotating-shift workers: findings from the Japan collaborative cohort study. *Am J Epidemiol* 164(6):549-555.
57. Conlon M, Lightfoot N, & Kreiger N (2007) Rotating shift work and risk of prostate cancer. *Epidemiology* 18(1):182-183.
58. Schernhammer ES, Kroenke CH, Laden F, & Hankinson SE (2006) Night work and risk of breast cancer. *Epidemiology* 17(1):108-111.
59. Straif K, *et al.* (2007) Carcinogenicity of shift-work, painting, and fire-fighting. *The Lancet. Oncology* 8(12):1065-1066.
60. Pi-Sunyer X (2009) The Medical Risks of Obesity. *Postgraduate medicine* 121(6):21-33.
61. Roenneberg T, Allebrandt Karla V, Merrow M, & Vetter C (2012) Social Jetlag and Obesity. *Current Biology* 22(10):939-943.
62. Schibler U, Ripperger J, & Brown SA (2003) Peripheral circadian oscillators in mammals: time and food. *J Biol Rhythms* 18(3):250-260.
63. Arble Dm, Bass J, Laposky Ad, Vitaterna Mh, & Turek Fw (2009) Circadian timing of food intake contributes to weight gain. *Obesity (Silver Spring)* 17(11):2100-2102.
64. Garaulet M, *et al.* (2013) Timing of food intake predicts weight loss effectiveness. *Int J Obes* 37(4):604-611.
65. Turek Fw, *et al.* (2005) Obesity and metabolic syndrome in circadian Clock mutant mice. *Science* 308(5724):1043-1045.
66. Duffy JF, Zitting KM, & Chinoy ED (2015) Aging and Circadian Rhythms. *Sleep medicine clinics* 10(4):423-434.
67. Schmidt C, Peigneux P, & Cajochen C (2012) Age-related changes in sleep and circadian rhythms: impact on cognitive performance and underlying neuroanatomical networks. *Frontiers in neurology* 3:118.

68. Chauhan R, Chen K-F, Kent BA, & Crowther DC (2017) Central and peripheral circadian clocks and their role in Alzheimer's disease. *Disease Models & Mechanisms* 10(10):1187-1199.
69. Cao Y & Wang R-H (2017) Associations among Metabolism, Circadian Rhythm and Age-Associated Diseases. *Aging and Disease* 8(3):314-333.
70. Hato T & Dagher PC (2014) How the Innate Immune System Senses Trouble and Causes Trouble. *Clinical Journal of the American Society of Nephrology*.
71. Albiger B, Dahlberg S, Henriques-Normark B, & Normark S (2007) Role of the innate immune system in host defence against bacterial infections: focus on the Toll-like receptors. *Journal of internal medicine* 261(6):511-528.
72. Haus E & Smolensky MH (1999) Biologic rhythms in the immune system. *Chronobiol Int* 16(5):581-622.
73. Mendez-Ferrer S, Lucas D, Battista M, & Frenette PS (2008) Haematopoietic stem cell release is regulated by circadian oscillations. *Nature* 452(7186):442-447.
74. Scheiermann C*, et al.* (2012) Adrenergic nerves govern circadian leukocyte recruitment to tissues. *Immunity* 37(2):290-301.
75. Akbulut H, Icli F, Büyükcelik A, Akbulut KG, & Demirci S (1999) The role of granulocyte‐macrophage‐colony stimulating factor, cortisol, and melatonin in the regulation of the circadian rhythms of peripheral blood cells in healthy volunteers and patients with breast cancer. *Journal of Pineal Research* 26(1):1-8.
76. Zhao Y*, et al.* (2017) Uncovering the mystery of opposite circadian rhythms between mouse and human leukocytes in humanized mice. *Blood*.
77. Gudewill S*, et al.* (1992) Nocturnal plasma levels of cytokines in healthy men. *European Archives of Psychiatry and Clinical Neuroscience* 242(1):53-56.
78. Nguyen KD*, et al.* (2013) Circadian gene Bmal1 regulates diurnal oscillations of Ly6C(hi) inflammatory monocytes. *Science* 341(6153):1483-1488.
79. Sutton CE*, et al.* (2017) Loss of the molecular clock in myeloid cells exacerbates T cell-mediated CNS autoimmune disease. *Nature communications* 8(1):1923.
80. Takeuchi O & Akira S (2010) Pattern Recognition Receptors and Inflammation. *Cell* 140(6):805-820.
81. Chen GY & Nunez G (2010) Sterile inflammation: sensing and reacting to damage. *Nat Rev Immunol* 10(12):826-837.
82. Janeway CA, Jr. & Medzhitov R (2002) Innate immune recognition. *Annual review of immunology* 20:197-216.
83. O'Neill LA, Golenbock D, & Bowie AG (2013) The history of Toll-like receptors - redefining innate immunity. *Nat Rev Immunol* 13(6):453-460.
84. Vogel SN (2012) How Discovery of Toll-Mediated Innate Immunity in Drosophila Impacted Our Understanding of TLR Signaling (and Vice Versa). *The Journal of Immunology* 188(11):5207-5209.

85. O'Neill LAJ, Golenbock D, & Bowie AG (2013) The history of Toll-like receptors [mdash] redefining innate immunity. *Nat Rev Immunol* 13(6):453-460.
86. Kawai T & Akira S (Toll-like Receptors and Their Crosstalk with Other Innate Receptors in Infection and Immunity. *Immunity* 34(5):637-650.
87. Kawasaki T & Kawai T (2014) Toll-Like Receptor Signaling Pathways. *Frontiers in immunology* 5(461):00461.
88. Lu YC, Yeh WC, & Ohashi PS (2008) LPS/TLR4 signal transduction pathway. *Cytokine* 42(2):145-151.
89. Silver Adam C, Arjona A, Walker Wendy E, & Fikrig E (2012) The Circadian Clock Controls Toll-like Receptor 9-Mediated Innate and Adaptive Immunity. *Immunity* 36(2):251-261.
90. Spengler ML, *et al.* (2012) Core circadian protein CLOCK is a positive regulator of NF-κB–mediated transcription. *Proceedings of the National Academy of Sciences* 109(37):E2457-E2465.
91. Castanon-Cervantes O, *et al.* (2010) Disregulation of inflammatory responses by chronic circadian disruption. *Journal of immunology (Baltimore, Md. : 1950)* 185(10):5796-5805.
92. Puttonen S, Viitasalo K, & Harma M (2011) Effect of shiftwork on systemic markers of inflammation. *Chronobiol Int* 28(6):528-535.
93. Doi M, Hirayama J, & Sassone-Corsi P (2006) Circadian regulator CLOCK is a histone acetyltransferase. *Cell* 125(3):497-508.
94. Bellet MM, Zocchi L, & Sassone-Corsi P (2012) The RelB subunit of NFκB acts as a negative regulator of circadian gene expression. *Cell Cycle* 11(17):3304-3311.
95. Bellet MM, *et al.* (2013) Circadian clock regulates the host response to Salmonella. *Proc Natl Acad Sci U S A* 110(24):9897-9902.
96. Lam MT, *et al.* (2013) Rev-Erbs repress macrophage gene expression by inhibiting enhancer-directed transcription. *Nature* 498(7455):511-515.
97. Gibbs JE, *et al.* (2012) The nuclear receptor REV-ERBalpha mediates circadian regulation of innate immunity through selective regulation of inflammatory cytokines. *Proc Natl Acad Sci U S A* 109(2):582-587.
98. Gagnidze K, *et al.* (2016) Nuclear receptor REV-ERBα mediates circadian sensitivity to mortality in murine vesicular stomatitis virus-induced encephalitis. *Proceedings of the National Academy of Sciences* 113(20):5730-5735.
99. Ivanov, II, *et al.* (2006) The orphan nuclear receptor RORgammat directs the differentiation program of proinflammatory IL-17+ T helper cells. *Cell* 126(6):1121-1133.
100. Yang XO, *et al.* (2008) TH17 lineage differentiation is programmed by orphan nuclear receptors RORα and RORγ. *Immunity* 28(1):29-39.
101. Dang EV, *et al.* (2011) Control of T(H)17/T(reg) Balance by Hypoxia-inducible Factor 1. *Cell* 146(5):772-784.

102. Stapleton CM, *et al.* (2005) Enhanced susceptibility of staggerer (RORalphasg/sg) mice to lipopolysaccharide-induced lung inflammation. *Am J Physiol Lung Cell Mol Physiol* 289(1):18.
103. Delerive P, *et al.* (2001) The orphan nuclear receptor ROR alpha is a negative regulator of the inflammatory response. *EMBO Rep* 2(1):42-48.
104. Liu J, *et al.* (2006) The circadian clock Period 2 gene regulates gamma interferon production of NK cells in host response to lipopolysaccharide-induced endotoxic shock. *Infect Immun* 74(8):4750-4756.
105. Hashiramoto A, *et al.* (2010) Mammalian clock gene Cryptochrome regulates arthritis via proinflammatory cytokine TNF-alpha. *J Immunol* 184(3):1560-1565.
106. Narasimamurthy R, *et al.* (2012) Circadian clock protein cryptochrome regulates the expression of proinflammatory cytokines. *Proc Natl Acad Sci U S A* 109(31):12662-12667.
107. Hirota T, *et al.* (2012) Identification of small molecule activators of cryptochrome. *Science* 337(6098):1094-1097.
108. Hand LE, *et al.* (2016) The circadian clock regulates inflammatory arthritis. *Faseb J*.
109. Martinon F, Burns K, & Tschopp J (2002) The inflammasome: a molecular platform triggering activation of inflammatory caspases and processing of proIL-beta. *Mol Cell* 10(2):417-426.
110. Broz P & Dixit VM (2016) Inflammasomes: mechanism of assembly, regulation and signalling. *Nat Rev Immunol* 16(7):407-420.
111. Latz E, Xiao TS, & Stutz A (2013) Activation and regulation of the inflammasomes. *Nat Rev Immunol* 13(6):397-411.
112. Liu X, *et al.* (2016) Inflammasome-activated gasdermin D causes pyroptosis by forming membrane pores. *Nature* 535(7610):153-158.
113. Schroder K & Tschopp J (2010) The inflammasomes. *Cell* 140(6):821-832.
114. Jo EK, Kim JK, Shin DM, & Sasakawa C (2016) Molecular mechanisms regulating NLRP3 inflammasome activation. *Cellular & molecular immunology* 13(2):148-159.
115. Di Micco A, *et al.* (2016) AIM2 inflammasome is activated by pharmacological disruption of nuclear envelope integrity. *Proceedings of the National Academy of Sciences* 113(32):E4671-E4680.
116. Dinarello CA (2015) The history of fever, leukocytic pyrogen and interleukin-1. *Temperature (Austin)* 2(1):8-16.
117. Dinarello CA (2009) Immunological and inflammatory functions of the interleukin-1 family. *Annual review of immunology* 27:519-550.
118. Burger D, Molnarfi N, Gruaz L, & Dayer JM (2004) Differential induction of IL-1beta and TNF by CD40 ligand or cellular contact with stimulated T cells depends on the maturation stage of human monocytes. *J Immunol* 173(2):1292-1297.
119. Freedman AS, *et al.* (1988) Pre-exposure of human B cells to recombinant IL-1 enhances subsequent proliferation. *J Immunol* 141(10):3398-3404.

120. Shaw PJ, McDermott MF, & Kanneganti TD (2011) Inflammasomes and autoimmunity. *Trends in molecular medicine* 17(2):57-64.
121. Galván-Peña S & O'Neill LAJ (2014) Metabolic Reprograming in Macrophage Polarization. *Frontiers in immunology* 5(420):00420.
122. Stout RD*, et al.* (2005) Macrophages Sequentially Change Their Functional Phenotype in Response to Changes in Microenvironmental Influences. *The Journal of Immunology* 175(1):342-349.
123. Arango Duque G & Descoteaux A (2014) Macrophage cytokines: involvement in immunity and infectious diseases. *Frontiers in immunology* 5:491.
124. Gonzalez-Mejia ME & Doseff AI (2009) Regulation of monocytes and macrophages cell fate. *Front Biosci (Landmark Ed)* 14:2413-2431.
125. Oliva-Ramirez J, Moreno-Altamirano MM, Pineda-Olvera B, Cauich-Sanchez P, & Sanchez-Garcia FJ (2014) Crosstalk between circadian rhythmicity, mitochondrial dynamics and macrophage bactericidal activity. *Immunology* 143(3):490-497.
126. O'Neill LAJ & Pearce EJ (2016) Immunometabolism governs dendritic cell and macrophage function. *The Journal of Experimental Medicine* 213(1):15-23.
127. Palsson-McDermott EM & O'Neill LAJ (2013) The Warburg effect then and now: From cancer to inflammatory diseases. *BioEssays* 35(11):965-973.
128. Kelly B & O'Neill LA (2015) Metabolic reprogramming in macrophages and dendritic cells in innate immunity. *Cell research* 25(7):771-784.
129. Newsholme P, Curi R, Gordon S, & Newsholme EA (1986) Metabolism of glucose, glutamine, long-chain fatty acids and ketone bodies by murine macrophages. *Biochem J* 239(1):121-125.
130. Tannahill GM*, et al.* (2013) Succinate is an inflammatory signal that induces IL-1[bgr] through HIF-1[agr]. *Nature* 496(7444):238-242.
131. Chaban Y, Boekema EJ, & Dudkina NV (2014) Structures of mitochondrial oxidative phosphorylation supercomplexes and mechanisms for their stabilisation. *Biochimica et Biophysica Acta (BBA) - Bioenergetics* 1837(4):418-426.
132. Mills EL*, et al.* (2016) Succinate Dehydrogenase Supports Metabolic Repurposing of Mitochondria to Drive Inflammatory Macrophages. *Cell* 167(2):457-470 e413.
133. Marxsen JH*, et al.* (2004) Hypoxia-inducible factor-1 (HIF-1) promotes its degradation by induction of HIF-alpha-prolyl-4-hydroxylases. *Biochem J* 381(Pt 3):761-767.
134. Nishi K*, et al.* (2008) LPS induces hypoxia-inducible factor 1 activation in macrophage-differentiated cells in a reactive oxygen species-dependent manner. *Antioxidants & redox signaling* 10(5):983-995.
135. Lampropoulou V*, et al.* (2016) Itaconate Links Inhibition of Succinate Dehydrogenase with Macrophage Metabolic Remodeling and Regulation of Inflammation. *Cell Metab* 24(1):158-166.

136. Peek CB, *et al.* (2013) Circadian Clock NAD(+) Cycle Drives Mitochondrial Oxidative Metabolism in Mice. *Science (New York, N.Y.)* 342(6158):1243417-1243417.
137. Ramsey KM, *et al.* (2009) Circadian Clock Feedback Cycle Through NAMPT-Mediated NAD(+) Biosynthesis. *Science (New York, N.Y.)* 324(5927):651-654.
138. Asher G, *et al.* (SIRT1 Regulates Circadian Clock Gene Expression through PER2 Deacetylation. *Cell* 134(2):317-328.
139. Lamia KA, *et al.* (2009) AMPK regulates the circadian clock by cryptochrome phosphorylation and degradation. *Science* 326(5951):437-440.
140. Lipton JO, *et al.* (2015) The Circadian Protein BMAL1 Regulates Translation in Response to S6K1-Mediated Phosphorylation. *Cell* 161(5):1138-1151.
141. Peek CB, Ramsey KM, Marcheva B, & Bass J (2012) Nutrient sensing and the circadian clock. *Trends Endocrinol Metab* 23(7):312-318.
142. Jacobi D, *et al.* (2015) Hepatic Bmal1 Regulates Rhythmic Mitochondrial Dynamics and Promotes Metabolic Fitness. *Cell Metabolism* 22(4):709-720.
143. Buck MD, *et al.* (2016) Mitochondrial Dynamics Controls T Cell Fate through Metabolic Programming. *Cell* 166(1):63-76.
144. Mittal M, Siddiqui MR, Tran K, Reddy SP, & Malik AB (2014) Reactive oxygen species in inflammation and tissue injury. *Antioxidants & redox signaling* 20(7):1126-1167.
145. Murphy MP (2009) How mitochondria produce reactive oxygen species. *Biochem J* 417(1):1-13.
146. Sies H (1997) Oxidative stress: oxidants and antioxidants. *Experimental physiology* 82(2):291-295.
147. Pelletier M, Lepow TS, Billingham LK, Murphy MP, & Siegel RM (2012) New Tricks From an Old Dog: Mitochondrial Redox Signaling in Cellular Inflammation. *Seminars in immunology* 24(6):384-392.
148. Finkel T (2011) Signal transduction by reactive oxygen species. *J Cell Biol* 194(1):7-15.
149. Asehnoune K, Strassheim D, Mitra S, Kim JY, & Abraham E (2004) Involvement of reactive oxygen species in Toll-like receptor 4-dependent activation of NF-kappa B. *J Immunol* 172(4):2522-2529.
150. Leto TL & Geiszt M (2006) Role of Nox family NADPH oxidases in host defense. *Antioxidants & redox signaling* 8(9-10):1549-1561.
151. Bedard K & Krause KH (2007) The NOX family of ROS-generating NADPH oxidases: physiology and pathophysiology. *Physiol Rev* 87(1):245-313.
152. Lambeth JD (2004) NOX enzymes and the biology of reactive oxygen. *Nat Rev Immunol* 4(3):181-189.
153. Pollock JD, *et al.* (1995) Mouse model of X-linked chronic granulomatous disease, an inherited defect in phagocyte superoxide production. *Nat Genet* 9(2):202-209.
154. Lee K, Won HY, Bae MA, Hong JH, & Hwang ES (2011) Spontaneous and aging-dependent development of arthritis in NADPH oxidase 2 deficiency

through altered differentiation of CD11b+ and Th/Treg cells. *Proc Natl Acad Sci U S A* 108(23):9548-9553.
155. Collins Y, *et al.* (2012) Mitochondrial redox signalling at a glance. *J Cell Sci* 125(Pt 4):801-806.
156. Zorov DB, Juhaszova M, & Sollott SJ (2014) Mitochondrial reactive oxygen species (ROS) and ROS-induced ROS release. *Physiol Rev* 94(3):909-950.
157. Brand MD (2010) The sites and topology of mitochondrial superoxide production. *Experimental gerontology* 45(7-8):466-472.
158. Kondratov RV, Kondratova AA, Gorbacheva VY, Vykhovanets OV, & Antoch MP (2006) Early aging and age-related pathologies in mice deficient in BMAL1, the core componentof the circadian clock. *Genes & Development* 20(14):1868-1873.
159. Rudic RD*, et al.* (2004) BMAL1 and CLOCK, Two Essential Components of the Circadian Clock, Are Involved in Glucose Homeostasis. *PLoS Biology* 2(11):e377.
160. Kondratov RV, Vykhovanets O, Kondratova AA, & Antoch MP (2009) Antioxidant N-acetyl-L-cysteine ameliorates symptoms of premature aging associated with the deficiency of the circadian protein BMAL1. *Aging (Albany NY)* 1(12):979-987.
161. Lee J*, et al.* (2013) Bmal1 and β-Cell Clock Are Required for Adaptation to Circadian Disruption, and Their Loss of Function Leads to Oxidative Stress-Induced β-Cell Failure in Mice. *Molecular and Cellular Biology* 33(11):2327-2338.
162. Musiek ES*, et al.* (2013) Circadian clock proteins regulate neuronal redox homeostasis and neurodegeneration. *J Clin Invest* 123(12):5389-5400.
163. Birben E, Sahiner UM, Sackesen C, Erzurum S, & Kalayci O (2012) Oxidative stress and antioxidant defense. *The World Allergy Organization journal* 5(1):9-19.
164. Davies KJ (1995) Oxidative stress: the paradox of aerobic life. *Biochemical Society symposium* 61:1-31.
165. Hayes JD & Dinkova-Kostova AT (2014) The Nrf2 regulatory network provides an interface between redox and intermediary metabolism. *Trends in biochemical sciences* 39(4):199-218.
166. Kobayashi EH*, et al.* (2016) Nrf2 suppresses macrophage inflammatory response by blocking proinflammatory cytokine transcription. *Nature communications* 7:11624.
167. Itoh K*, et al.* (1999) Keap1 represses nuclear activation of antioxidant responsive elements by Nrf2 through binding to the amino-terminal Neh2 domain. *Genes Dev* 13(1):76-86.
168. Yamamoto T*, et al.* (2008) Physiological significance of reactive cysteine residues of Keap1 in determining Nrf2 activity. *Mol Cell Biol* 28(8):2758-2770.

169. Sekhar KR, Rachakonda G, & Freeman ML (2010) Cysteine-based regulation of the CUL3 adaptor protein Keap1. *Toxicology and applied pharmacology* 244(1):21-26.
170. Itoh K, *et al.* (1997) An Nrf2/Small Maf Heterodimer Mediates the Induction of Phase II Detoxifying Enzyme Genes through Antioxidant Response Elements. *Biochemical and Biophysical Research Communications* 236(2):313-322.
171. Reichard JF, Motz GT, & Puga A (2007) Heme oxygenase-1 induction by NRF2 requires inactivation of the transcriptional repressor BACH1. *Nucleic acids research* 35(21):7074-7086.
172. Venugopal R & Jaiswal AK (1996) Nrf1 and Nrf2 positively and c-Fos and Fra1 negatively regulate the human antioxidant response element-mediated expression of NAD(P)H:quinone oxidoreductase1 gene. *Proc Natl Acad Sci U S A* 93(25):14960-14965.
173. Bonkovsky HL, *et al.* (2013) Porphyrin and heme metabolism and the porphyrias. *Comprehensive Physiology* 3(1):365-401.
174. Solis WA, *et al.* (2002) Glutamate-cysteine ligase modifier subunit: mouse Gclm gene structure and regulation by agents that cause oxidative stress. *Biochem Pharmacol 2002* 63(9):1739-1754.
175. Deponte M (2013) Glutathione catalysis and the reaction mechanisms of glutathione-dependent enzymes. *Biochimica et biophysica acta* 1830(5):3217-3266.
176. Pekovic-Vaughan V, *et al.* (2014) The circadian clock regulates rhythmic activation of the NRF2/glutathione-mediated antioxidant defense pathway to modulate pulmonary fibrosis. *Genes Dev* 28(6):548-560.
177. Xu YQ, *et al.* (2012) Diurnal variation of hepatic antioxidant gene expression in mice. *PLoS ONE* 7(8):e44237.
178. Cruz CM, *et al.* (2007) ATP activates a reactive oxygen species-dependent oxidative stress response and secretion of proinflammatory cytokines in macrophages. *J Biol Chem* 282(5):2871-2879.
179. Heid ME, *et al.* (2013) Mitochondrial reactive oxygen species induces NLRP3-dependent lysosomal damage and inflammasome activation. *J Immunol* 191(10):5230-5238.
180. Sorbara MT & Girardin SE (2011) Mitochondrial ROS fuel the inflammasome. *Cell research* 21(4):558-560.
181. Liu X, *et al.* (2017) Nuclear Factor E2-Related Factor-2 Negatively Regulates NLRP3 Inflammasome Activity by Inhibiting Reactive Oxygen Species-Induced NLRP3 Priming. *Antioxidants & redox signaling* 26(1):28-43.
182. Liu X, *et al.* (2016) Dimethyl fumarate ameliorates dextran sulfate sodium-induced murine experimental colitis by activating Nrf2 and suppressing NLRP3 inflammasome activation. *Biochemical pharmacology* 112:37-49.
183. Hou Y, *et al.* (2018) Nrf2 inhibits NLRP3 inflammasome activation through regulating Trx1/TXNIP complex in cerebral ischemia reperfusion injury. *Behavioural brain research* 336:32-39.

184. Xu X, *et al.* (2018) Nrf2/ARE pathway inhibits ROS-induced NLRP3 inflammasome activation in BV2 cells after cerebral ischemia reperfusion. *Inflammation research : official journal of the European Histamine Research Society ... [et al.]* 67(1):57-65.
185. Zhao C, Gillette DD, Li X, Zhang Z, & Wen H (2014) Nuclear factor E2-related factor-2 (Nrf2) is required for NLRP3 and AIM2 inflammasome activation. *J Biol Chem* 289(24):17020-17029.
186. O'Connell DJ, *et al.* (2016) Simultaneous Pathway Activity Inference and Gene Expression Analysis Using RNA Sequencing. *Cell systems* 2(5):323-334.
187. Cornelissen G (2014) Cosinor-based rhythmometry. *Theoretical biology & medical modelling* 11:16.
188. Mills EL & O'Neill LA (2016) Reprogramming mitochondrial metabolism in macrophages as an anti-inflammatory signal. *European journal of immunology* 46(1):13-21.
189. Pekovic-Vaughan V, *et al.* (2014) The circadian clock regulates rhythmic activation of the NRF2/glutathione-mediated antioxidant defense pathway to modulate pulmonary fibrosis. *Genes & Development* 28(6):548-560.
190. Yin S & Cao W (2015) Toll-Like Receptor Signaling Induces Nrf2 Pathway Activation through p62-Triggered Keap1 Degradation. *Mol Cell Biol* 35(15):2673-2683.
191. Wible RS, *et al.* (2018) NRF2 regulates core and stabilizing circadian clock loops, coupling redox and timekeeping in Mus musculus. *eLife* 7.
192. Everts B, *et al.* (2014) TLR-driven early glycolytic reprogramming via the kinases TBK1-IKKvarepsilon supports the anabolic demands of dendritic cell activation. *Nat Immunol* 15(4):323-332.
193. Ma Q (2013) Role of nrf2 in oxidative stress and toxicity. *Annual review of pharmacology and toxicology* 53:401-426.
194. Ha KN, Chen Y, Cai J, & Sternberg P, Jr. (2006) Increased glutathione synthesis through an ARE-Nrf2-dependent pathway by zinc in the RPE: implication for protection against oxidative stress. *Investigative ophthalmology & visual science* 47(6):2709-2715.
195. Yang Y, *et al.* (2002) Initial characterization of the glutamate-cysteine ligase modifier subunit Gclm(-/-) knockout mouse. Novel model system for a severely compromised oxidative stress response. *J Biol Chem* 277(51):49446-49452.
196. Wilking M, Ndiaye M, Mukhtar H, & Ahmad N (2013) Circadian rhythm connections to oxidative stress: implications for human health. *Antioxidants & redox signaling* 19(2):192-208.
197. Xu Q, *et al.* (2016) NADPH Oxidases Are Essential for Macrophage Differentiation. *J Biol Chem* 291(38):20030-20041.
198. Jablonski KA, *et al.* (2015) Novel Markers to Delineate Murine M1 and M2 Macrophages. *PLoS ONE* 10(12):e0145342.
199. Naik E & Dixit VM (2011) Mitochondrial reactive oxygen species drive proinflammatory cytokine production. *J Exp Med* 208(3):417-420.

200. McGettrick AF & O'Neill LAJ (2013) How Metabolism Generates Signals during Innate Immunity and Inflammation. *Journal of Biological Chemistry* 288(32):22893-22898.
201. Bagkos G, Koufopoulos K, & Piperi C (2014) A new model for mitochondrial membrane potential production and storage. *Medical hypotheses* 83(2):175-181.
202. Solt LA*, et al.* (2012) Regulation of Circadian Behavior and Metabolism by Synthetic REV-ERB Agonists. *Nature* 485(7396):62-68.
203. Chaudhry H*, et al.* (2013) Role of Cytokines as a Double-edged Sword in Sepsis. *In Vivo* 27(6):669-684.
204. Kay J & Calabrese L (2004) The role of interleukin-1 in the pathogenesis of rheumatoid arthritis. *Rheumatology (Oxford)* 43 Suppl 3:iii2-iii9.
205. Whelan R*, et al.* (2004) Role and regulation of interleukin-1 molecules in pro-asthmatic sensitised airway smooth muscle. *The European respiratory journal* 24(4):559-567.
206. Bonizzi G & Karin M (The two NF-κB activation pathways and their role in innate and adaptive immunity. *Trends in Immunology* 25(6):280-288.
207. Kojetin D, Wang Y, Kamenecka TM, & Burris TP (2011) Identification of SR8278, a synthetic antagonist of the nuclear heme receptor REV-ERB. *ACS Chem Biol* 6(2):131-134.
208. Kim JY*, et al.* (2017) Keap1 knockdown in melanocytes induces cell proliferation and survival via HO-1-associated beta-catenin signaling. *Journal of dermatological science* 88(1):85-95.
209. More VR*, et al.* (2013) Keap1 knockdown increases markers of metabolic syndrome after long-term high fat diet feeding. *Free Radic Biol Med* 61:85-94.
210. Palazon A, Goldrath AW, Nizet V, & Johnson RS (2014) HIF transcription factors, inflammation, and immunity. *Immunity* 41(4):518-528.
211. He Y, Hara H, & Nunez G (2016) Mechanism and Regulation of NLRP3 Inflammasome Activation. *Trends in biochemical sciences* 41(12):1012-1021.
212. Chen G & Pedra JH (2010) The inflammasome in host defense. *Sensors (Basel)* 10(1):97-111.
213. Janszky I*, et al.* (2012) Daylight saving time shifts and incidence of acute myocardial infarction--Swedish Register of Information and Knowledge About Swedish Heart Intensive Care Admissions (RIKS-HIA). *Sleep medicine* 13(3):237-242.
214. Janszky I & Ljung R (2008) Shifts to and from daylight saving time and incidence of myocardial infarction. *The New England journal of medicine* 359(18):1966-1968.
215. Foerch C, Korf HW, Steinmetz H, & Sitzer M (2008) Abrupt shift of the pattern of diurnal variation in stroke onset with daylight saving time transitions. *Circulation* 118(3):284-290.
216. Liberti MV & Locasale JW (2016) The Warburg Effect: How Does it Benefit Cancer Cells? *Trends in biochemical sciences* 41(3):211-218.

217. Vinay DS, *et al.* (2015) Immune evasion in cancer: Mechanistic basis and therapeutic strategies. *Seminars in cancer biology* 35 Suppl:S185-S198.
218. Carroll RG, *et al.* (2018) An unexpected link between fatty acid synthase and cholesterol synthesis in proinflammatory macrophage activation. *Journal of Biological Chemistry*.
219. Ridker PM, *et al.* (2017) Antiinflammatory Therapy with Canakinumab for Atherosclerotic Disease. *The New England journal of medicine* 377(12):1119-1131.
220. Van Laake LW, Luscher TF, & Young ME (2017) The circadian clock in cardiovascular regulation and disease: Lessons from the Nobel Prize in Physiology or Medicine 2017. *European heart journal*.
221. Wyse CA, *et al.* (2017) Adverse metabolic and mental health outcomes associated with shiftwork in a population-based study of 277,168 workers in UK biobank(). *Annals of medicine* 49(5):411-420.
222. Libby P (2016) Assisted Living in the Atheroma: Elderly Macrophages Promote Plaques. *Cell Metab* 24(6):779-781.
223. Hoffmann C, *et al.* (2017) Dimethyl Fumarate Induces Glutathione Recycling by Upregulation of Glutathione Reductase. *Oxidative medicine and cellular longevity* 2017:6093903.
224. Kode A, *et al.* (2008) Resveratrol induces glutathione synthesis by activation of Nrf2 and protects against cigarette smoke-mediated oxidative stress in human lung epithelial cells. *Am J Physiol Lung Cell Mol Physiol* 294(3):L478-488.
225. Townsend BE & Johnson RW (2016) Sulforaphane induces Nrf2 target genes and attenuates inflammatory gene expression in microglia from brain of young adult and aged mice. *Experimental gerontology* 73:42-48.
226. Scannevin RH, *et al.* (2012) Fumarates promote cytoprotection of central nervous system cells against oxidative stress via the nuclear factor (erythroid-derived 2)-like 2 pathway. *The Journal of pharmacology and experimental therapeutics* 341(1):274-284.
227. Linker RA, *et al.* (2011) Fumaric acid esters exert neuroprotective effects in neuroinflammation via activation of the Nrf2 antioxidant pathway. *Brain : a journal of neurology* 134(Pt 3):678-692.
228. Palsamy P & Subramanian S (2011) Resveratrol protects diabetic kidney by attenuating hyperglycemia-mediated oxidative stress and renal inflammatory cytokines via Nrf2-Keap1 signaling. *Biochimica et biophysica acta* 1812(7):719-731.
229. Kensler TW, *et al.* (2012) Modulation of the metabolism of airborne pollutants by glucoraphanin-rich and sulforaphane-rich broccoli sprout beverages in Qidong, China. *Carcinogenesis* 33(1):101-107.
230. Nishino H, *et al.* (2004) Cancer prevention by antioxidants. *Biofactors* 22(1-4):57-61.
231. Sylvester PW & Shah S (2002) Antioxidants in dietary oils: their potential role in breast cancer prevention. *Malaysian journal of nutrition* 8(1):1-11.

232. Wang XD & Russell RM (2000) Antioxidants and lung cancer prevention. *Nestle Nutrition workshop series. Clinical & performance programme* 4:39-53; discussion 53-34.
233. Le Gal K*, et al.* (2015) Antioxidants can increase melanoma metastasis in mice. *Science translational medicine* 7(308):308re308-308re308.
234. Sayin VI*, et al.* (2014) Antioxidants accelerate lung cancer progression in mice. *Science translational medicine* 6(221):221ra215.
235. Courtnay R*, et al.* (2015) Cancer metabolism and the Warburg effect: the role of HIF-1 and PI3K. *Molecular biology reports* 42(4):841-851.
236. Muz B, de la Puente P, Azab F, & Azab AK (2015) The role of hypoxia in cancer progression, angiogenesis, metastasis, and resistance to therapy. *Hypoxia (Auckl)* 3:83-92.
237. Biddlestone J, Bandarra D, & Rocha S (2015) The role of hypoxia in inflammatory disease (review). *International journal of molecular medicine* 35(4):859-869.
238. Zhang R, Lahens NF, Ballance HI, Hughes ME, & Hogenesch JB (2014) A circadian gene expression atlas in mammals: implications for biology and medicine. *Proc Natl Acad Sci U S A* 111(45):16219-16224.
239. Levi F, Okyar A, Dulong S, Innominato PF, & Clairambault J (2010) Circadian timing in cancer treatments. *Annual review of pharmacology and toxicology* 50:377-421.
240. Zaslona Z*, et al.* (2017) The circadian protein BMAL1 in myeloid cells is a negative regulator of allergic asthma. *Am J Physiol Lung Cell Mol Physiol*:ajplung 00072 02017.
241. Curtis AM*, et al.* (2015) Circadian control of innate immunity in macrophages by miR-155 targeting Bmal1. *Proc Natl Acad Sci U S A* 112(23):7231-7236.
242. Gossan N, Boot-Handford R, & Meng QJ (2015) Ageing and osteoarthritis: a circadian rhythm connection. *Biogerontology* 16(2):209-219.

Chapter 7: Appendix